A THESIS

FOR THE DEGREE OF DOCTOR OF PHILOSOPHY

Development of Functional Cosmetic Materials Using the Bioactive Compounds from Brown Seaweeds

Soo-Jin Heo

Department of Marine Biotechnology

GRADUATE SCHOOL

CHEJU NATIONAL UNIVERSITY

2008. 02

Development of Functional Cosmetic Materials Using the Bioactive Compounds from Brown Seaweeds

Soo-Jin Heo

(Supervised by Professor You-Jin Jeon)

A thesis submitted in partial fulfillment of the requirement for the degree of

DOCTOR OF PHILOSOPHY

2008. 02.

This thesis has been examined and approved by

Thesis director, Ki-Wan Lee, Professor of Marine Life Science

---

Jehee Lee, Professor of Marine Biotechnoloy

Youngheun Jee, Professor of Veterinary Medicine

Soo-Hyun Kim, Professor of Food Bioengineering

You-Jin Jeon, Professor of Marine Biotechnology

Date

Department of Marine Biotechnology

GRADUATE SCHOOL

CHEJU NATIONAL UNIVERSITY

CONTENTS

Part Ⅲ. Isolation of cosmetic materials from *Ishige okamurae*

국문초록

오늘날 고도의 산업 발달은 심각한 환경오염을 초래하였고 이로 인한 오존층 파괴는 지표면에 도달하는 자외선 양을 증가시켜 환경에 부정적인 영향을 끼치고 있다. 또한 경제성장이 국민소득을 증가시키면서 삶의 질을 높이려는 노력이 지속되었고, 이로 인해 다양한 레저활동을 즐기려는 인구가 빠르게 증가되어 자외선 노출시간에 비례한 피부 흑화 현상이 증가하는 추세이다. 인간의 피부는 인체와 외부 환경과 경계를 이루는 기관으로서 체온 조절과 외부로부터 내부 장기를 보호하는 등 생명유지를 위한 주요 기능을 수행하며 부수적으로 피부 호흡, 특정 물질에 대한 선택적 흡수, 피부색 형성 등의 기능이 있다.

인체를 청결 또는 미화하고 피부 또는 모발을 건강하게 유지하기 위해 사용되는 화장품은 현대에 들어 약진하는 산업중의 하나이다. 이러한 산업에는 자외선 차단, 미백, 주름방지, 항산화, 항균 등 다수의 분야가 포함되며, 이에 관련된 제품들을 만들 수 있는 천연물에 대한 관심이 증가하는 추세이지만 실질적으로 산업에 응용되고 있는 천연물은 많지 않다.

이 연구에서는 다양한 천연물의 보고인 해양으로부터 새로운 기능성 화장품소재를 개발하기 위하여 제주연안에 서식하고 있는 40종의 해조류들을 대상으로 라디칼 소거활성과 tyrosinase억제 활성을 검정하였다. 스크리닝 결과 갈조류인 꽈배기 모자반 (*Sargassum siliquastrum*), 패 (*Ishige okamurae*), 그리고 감태 (*Ecklonia cava*)에서 다른 해조류들에 비해 우수한 효과를 나타내는 것을 확인하였고, 이에 따라 이들 세 종의 갈조류를 대

상으로 활성물질을 분리하여 항산화, 미백 및 자외선 차단 효과를 검증하였다.

그 결과 꽈배기 모자반으로부터 우수한 DPPH 라디칼 소거효과를 나타내는 chromene계열의 물질인 sargachromanol series와 세포보호 및 자외선 차단 효과가 우수한 carotenoid계열의 물질인 fucoxanthin이 분리되었다. 또한 패 와 감태 에서 우수한 항산화효과와 미백, 그리고 자외선 차단효과를 갖는 phlorotannin계열의 물질인 diphlorethohydroxycarmalol과 dieckol이 분리되었다. 이들 중 dieckol은 동물실험을 통해 자외선 차단 효과를 확인한 결과에서도 우수한 홍반 감소효과와 부종 억제효과가 검증되었다.

따라서 이 연구에서 분리된 dieckol은 *in vitro*와 *in vivo* 모두에서 상기한 효과가 우수하게 나타나 새로운 기능성 화장품소재로의 이용이 유망할 것으로 판단된다.

LIST OF FIGURES

organic solvents. Experiments were performed in triplicate and the data are expressed as mean ± SE.

b, 150 μM; c, 300 μM; d, 450 μM.

Fig. 2-39B. ESR spectrum obtained in an ethanol solution of 30 μmol/l DPPH at various concentrations of sargachromanol D isolated from *S. siliquastrum*. a, control; b, 10 μM; c, 20 μM; d, 40 μM.

Fig. 2-39C. ESR spectrum obtained in an ethanol solution of 30 μmol/l DPPH at various concentrations of sargachromanol E isolated from *S. siliquastrum*. a, control; b, 10 μM; c, 20 μM; d, 40 μM.

Fig. 2-39D. ESR spectrum obtained in an ethanol solution of 30 μmol/l DPPH at various concentrations of sargachromanol G isolated from *S. siliquastrum*. a, control; b, 10 μM; c, 20 μM; d, 40 μM.

Fig. 2-39E. ESR spectrum obtained in an ethanol solution of 30 μmol/l DPPH at various concentrations of sargachromanol I isolated from *S. siliquastrum*. a, control; b, 30 μM; c, 60 μM; d, 90 μM.

Fig. 2-39F. ESR spectrum obtained in an ethanol solution of 30 μmol/l DPPH at various concentrations of sargachromanol O isolated from *S. siliquastrum*. a, control; b, 30 μM; c, 60 μM; d, 90 μM.

Fig. 2-39G. ESR spectrum obtained in an ethanol solution of 30 μmol/l DPPH at various concentrations of sargachromanol V isolated from *S. siliquastrum*. a, control; b, 30 μM; c, 60 μM; d, 90 μM.

Fig. 2-40. Hydroxyl radical scavenging activity of the active compounds isolated from *S. siliquastrum*. ◆, sargachromanol D; ◇, sargachromanol E; ■, sargachromanol I; □, sargachromanol O; ▲, sargachromanol G; △, sargachromanol V. Experiments were performed in triplicate and the data are expressed as mean ± SE.

Fig. 2-41. Hydrogen peroxide scavenging activity of the active compounds isolated from *S. siliquastrum*. ◆, sargachromanol D; ◇, sargachromanol E; ■,

sargachromanol G; □, sargachromanol I; ▲, sargachromanol O; △, sargachromanol V. Experiments were performed in triplicate and the data are expressed as mean ± SE.

Fig. 2-42. Effect of the active compounds isolated from *S. siliquastrum* on scavenging reactive oxygen species. The intracellular reactive oxygen species generated was detected by DCF-DA method. ◆, sargachromanol D; ◇, sargachromanol E; ■, sargachromanol G; □, sargachromanol I; ▲, sargachromanol O; △, sargachromanol V; ●, fucoxanthin. Experiments were performed in triplicate and the data are expressed as mean ± SE.

Fig. 2-43. Protective effect of fucoxanthin isolated from *S. siliquastrum* on H_2O_2 induced oxidative damage of vero cells. The viability of vero cells on H_2O_2 treatment was determined by MTT assay. Experiments were performed in triplicate and the data are expressed as mean ± SE. Statistical evaluation was performed to compare the experimental groups and corresponding control groups. *, $p < 0.001$

Fig. 2-44. Inhibitory effect of different concentrations of fucoxanthin isolated from *S. siliquastrum* on H_2O_2 induced DNA damages. The damaged cells on H_2O_2 treatment was determined by comet assay. ■, % Fluorescence in tail; ●, Inhibitory effect of cell damage. Experiments were performed in triplicate and the data are expressed as mean ± SE. Statistical evaluation was performed to compare the experimental groups and corresponding control groups. *, $p < 0.001$

Fig. 2-45. Photomicrographs of DNA damage and migration observed under fucoxanthin isolated from *S. siliquastrum* where the tail moments were decreased. A, control; B, cells treated with 50 μM H_2O_2; C, cells treated with 5 μM compound + 50 μM H_2O_2; D, cells treated with 50 μM compound + 50 μM H_2O_2; E, cells treated with 250 μM compound + 50 μM H_2O_2.

Fig. 2-46. Protective effect of fucoxanthin isolated from *S. siliquastrum* against H_2O_2-

induced apoptosis in vero cells. Cellular morphological changes were observed under a fluorescence microscope after Hoechst 33342 staining. A, untreated; B, 500 μM H_2O_2; C, 5 μM compound + 500 μM H_2O_2; D, 50 μM compound + 500 μM H_2O_2; E, 250 μM compound + 500 μM H_2O_2. Apoptotic bodies are indicated by arrows.

Fig. 2-47. Effect of fucoxanthin isolated from *S. siliquastrum* on scavenging intracellular ROS generated by UV-B radiation. The fibroblasts were treated with various concentrations of fucoxanthin and after 1h later, UV-B radiation at 50 mJ/cm^2 was applied to the cells. The intracellular ROS was detected using fluorescence spectrophotometer after DCF-DA staining. Experiments were performed in triplicate and the data are expressed as mean ± SE. Statistical evaluation was performed to compare the experimental groups and corresponding control groups. *, $p < 0.005$, **, $p < 0.001$

Fig. 2-48. Protective effect of fucoxanthin isolated from *S. siliquastrum* on UV-B radiation-induced cell damage of fibroblasts. The fibroblasts were treated with various concentrations of fucoxanthin and after 1h later, UV-B radiation at 50 mJ/cm^2 was applied to the cells. The viability of fibroblasts on UV-B radiation was determined by MTT assay. Experiments were performed in triplicate and the data are expressed as mean ± SE. Statistical evaluation was performed to compare the experimental groups and corresponding control groups. *, $p < 0.005$, **, $p < 0.001$

Fig. 2-49. Inhibitory effect of different concentrations of fucoxanthin isolated from *S. siliquastrum* on UV-B radiation induced DNA damages. The damaged cells on UV-B radiation was determined by comet assay. ■, % Fluorescence in tail; ●, Inhibitory effect of cell damage. Experiments were performed in triplicate and the data are expressed as mean ± SE. Statistical evaluation was performed to compare the

generated was detected by DCF-DA method. Experiments were performed in triplicate and the data are expressed as mean ± SE.

Fig. 3-15. Protective effect of diphlorethohydroxycarmalol isolated from *I. okamurae* on H_2O_2 induced oxidative damage of vero cells. The viability of vero cells on H_2O_2 treatment was determined by MTT assay. Experiments were performed in triplicate and the data are expressed as mean ± SE. Statistical evaluation was performed to compare the experimental groups and corresponding control groups. *, $p < 0.001$

Fig. 3-16. Inhibitory effect of different concentrations of diphlorethohydroxycarmalol isolated from *I. okamurae* on H_2O_2 induced DNA damages. The damaged cells on H_2O_2 treatment was determined by comet assay. ■, % Fluorescence in tail; ●, Inhibitory effect of cell damage. Experiments were performed in triplicate and the data are expressed as mean ± SE. Statistical evaluation was performed to compare the experimental groups and corresponding control groups. *, $p < 0.001$

Fig. 3-17. Photomicrographs of DNA damage and migration observed under diphlorethohydroxycarmalol isolated from *I. okamurae* where the tail moments were decreased. A, control; B, cells treated with 50 μM H_2O_2; C, cells treated with 50 μM compound + 50 μM H_2O_2; D, cells treated with 100 μM compound + 50 μM H_2O_2; E, cells treated with 250 μM compound + 50 μM H_2O_2.

Fig. 3-18. Protective effect of diphlorethohydroxycarmalol isolated from *I. okamurae* against H_2O_2-induced apoptosis in vero cells. Cellular morphological changes were observed under a fluorescence microscope after Hoechst 33342 staining. A, untreated; B, 500 μM H_2O_2; C, 5 μM compound + 500 μM H_2O_2; D, 50 μM compound + 500 μM H_2O_2; E, 250 μM compound + 500 μM H_2O_2. Apoptotic bodies are indicated by arrows.

Fig. 3-19. Inhibitory effect of diphlorethohydroxycarmalol isolated from *I. okamurae* against mushroom tyrosinase. L-tyrosine was used as substrate, and kojic acid and arbutin were used as positive control. Experiments were performed in triplicate and the data are expressed as mean ± SE.

Fig. 3-20. Inhibitory effect of diphlorethohydroxycarmalol isolated from *I. okamurae* on melanin synthesis. B16F10 melanoma cells were used for this experiment and PTU and retinol were used as positive control. Experiments were performed in triplicate and the data are expressed as mean ± SE.

Fig. 3-21. Effect of diphlorethohydroxycarmalol isolated from *I. okamurae* on scavenging intracellular ROS generated by UV-B radiation. The fibroblasts were treated with various concentrations of diphlorethohydroxycarmalol and after 1 h later, UV-B radiation at 50 mJ/cm^2 was applied to the cells. The intracellular ROS was detected using fluorescence spectrophotometer after DCF-DA staining. Experiments were performed in triplicate and the data are expressed as mean ± SE. Statistical evaluation was performed to compare the experimental groups and corresponding control groups. *, $p < 0.001$

Fig. 3-22. Protective effect of diphlorethohydroxycarmalol isolated from *I. okamurae* on UV-B radiation-induced cell damage of fibroblasts. The fibroblasts were treated with various concentrations of diphlorethohydroxycarmalol and after 1 h later, UV-B radiation at 50 mJ/cm^2 was applied to the cells. The viability of fibroblasts on UV-B radiation was determined by MTT assay. Experiments were performed in triplicate and the data are expressed as mean ± SE. Statistical evaluation was performed to compare the experimental groups and corresponding control groups. *, $p < 0.01$, **, $p < 0.001$

Fig. 3-23. Inhibitory effect of different concentrations of diphlorethohydroxycarmalol

a, control; b, 1 μM; c, 10 μM; d, 20 μM.

Fig. 4-7B. ESR spectrum obtained during incubation of AAPH with 4-POBN at various concentrations of eckol isolated from *E. cava*.

a, control; b, 1 μM; c, 10 μM; d, 20 μM.

Fig. 4-7C. ESR spectrum obtained during incubation of AAPH with 4-POBN at various concentrations of dieckol isolated from *E. cava*.

a, control; b, 1 μM; c, 10 μM; d, 20 μM.

Fig. 4-7D. ESR spectrum obtained during incubation of AAPH with 4-POBN at various concentrations of triphlorethol A isolated from *E. cava*.

a, control; b, 1 μM; c, 10 μM; d, 20 μM.

Fig. 4-7E. ESR spectrum obtained during incubation of AAPH with 4-POBN at various concentrations of eckstolonol isolated from *E. cava*.

a, control; b, 1 μM; c, 10 μM; d, 20 μM.

Fig. 4-8. Hydroxyl radical scavenging activity of the active compounds isolated from *E. cava*. ◆, phloroglucinol; ◇, eckol; ■, dieckol; □, triphlorethol A; ▲, eckstolonol. Experiments were performed in triplicate and the data are expressed as mean ± SE.

Fig. 4-9A. ESR spectrum obtained in Fenton reaction system at various concentrations of phloroglucinol isolated from *E. cava*.

a, control; b, 50 μM; c, 250 μM; d, 500 μM.

Fig. 4-9B. ESR spectrum obtained in Fenton reaction system at various concentrations of eckol isolated from *E. cava*.

a, control; b, 50 μM; c, 250 μM; d, 500 μM.

Fig. 4-9C. ESR spectrum obtained in Fenton reaction system at various concentrations of dieckol isolated from *E. cava*.

a, control; b, 20 μM; c, 60 μM; d, 120 μM.

Fig. 4-9D. ESR spectrum obtained in Fenton reaction system at various concentrations of triphlorethol A isolated from *E. cava*.

a, control; b, 20 μM; c, 60 μM; d, 120 μM.

Fig. 4-9E. ESR spectrum obtained in Fenton reaction system at various concentrations of eckstolonol isolated from *E. cava*.

a, control; b, 20 μM; c, 60 μM; d, 120 μM.

Fig. 4-10. Hydrogen peroxide scavenging activity of the active compounds isolated from *E. cava*. ◆, phloroglucinol; ◇, eckol; ■, dieckol; □, triphlorethol A; ▲, eckstolonol. Experiments were performed in triplicate and the data are expressed as mean ± SE.

Fig. 4-11. Effect of the active compounds isolated from *E. cava* on scavenging reactive oxygen species. The intracellular reactive oxygen species generated was detected by DCF-DA method. ◆, phloroglucinol; ◇, eckol; ■, dieckol; □, triphlorethol A; ▲, eckstolonol. Experiments were performed in triplicate and the data are expressed as mean ± SE.

Fig. 4-12. Protective effect of the active compounds isolated from *E. cava* on H_2O_2 induced oxidative damage of vero cells. The viability of vero cells on H_2O_2 treatment was determined by MTT assay. A, phloroglucinol; B, eckol; C, dieckol; D, triphlorethol A; E, eckstolonol. Experiments were performed in triplicate and the data are expressed as mean ± SE. Statistical evaluation was performed to compare the experimental groups and corresponding control groups. *, $p < 0.05$, **, $p < 0.005$, ***, $p < 0.001$

Fig. 4-13. Inhibitory effect of different concentrations of the active compounds isolated from *E. cava* on H_2O_2 induced DNA damages. The damaged cells on H_2O_2 treatment was determined by comet assay. ■, % Fluorescence in tail; ●, Inhibitory

LIST OF TABLES

INTRODUCTION

Marine algae are classified as unicellular microalgae and macroalgae, which are macroscopic plants of marine benthoses (Ricketts and Calvin, 1962). Macroalgae, also known as seaweed, are distinguished according to the nature of their pigments: brown seaweed (phaeophyta), red seaweed (rhodophyta) and green seaweed (chlorophyta). In Asian countries, several species of seaweed are used as human food, to provide nutrition and a peculiar taste. Fresh dried seaweed is extensively consumed, especially by people living in coastal areas. They are of nutritional interest as they are low calories foods but rich in vitamins, minerals and dietary fiber (Jensen, 1993; Noda, 1993; Oohusa, 1993). Currently, human consumption of brown algae (66.5%), red algae (33%) and green algae (5%) is high in Asia, mainly Korea, Japan, and China (Dawes, 1998). The marine algae have mainly been used in western countries as raw material to extract alginates (from brown algae) and agar and carragenates (from red algae) which have been used as ingredients in food, pharmaceuticals and diverse consumer products and industrial processes (Skjak-Braek and Martinsen, 1991; Lewis et al., 1998). The marine algae have recently been identified as an under-exploited plant resource and functional food (Nisizawa et al., 1987; Heo et al., 2005). They have also proven to be rich sources of structurally diverse bioactive compounds with valuable pharmaceutical and biomedical potential. In particular, brown seaweeds are plentifully present around Jeju Island, Korea, where these valuable brown algae have various biological compounds, such as xanthopophyll, pigments, fucoidans, phycocolloids, phlorotannins, and fucoxanthin (Halliwell and Gutteridge, 1999). Several researches on those kinds of compounds have pointed out a variety of biological benefits including antioxidant, anticoagulant, antihypertention, antibacterial and antitumor activities (Nagayama et al., 2002; Mayer

and Hamann, 2004; Athukorala and Jeon, 2005; Kotake-Nara et al., 2005; Heo et al., 2008).

Phycocolloids are polysaccharides of high molecular weight composed of polymers of sugars units. They are the main structural components of seaweed cell walls and may be involved in recognition mechanisms between seaweeds and pathogens (Potin et al. 1999). Although polysaccharides have been described with antioxidant, antiviral, antitumoral and anticoagulant activities (Smit, 2004; Mayer and Hamann, 2005), the most extracted polysaccharides from seaweeds are agar, carrageenan and alginate due to their extensive use in food and cosmetic industries. Agar and carrageenan are sulfated polysaccharides mainly extracted from Rhodophyceae while alginate, a binary polyuronide made up of mannuronic acid and guluronic acid, is extracted from Phaeophyceae (**Fig.** Ⅰ). The wide use of these compounds is based on their gelling, viscosifying and emulsifying properties, which have generated an increasing commercial and scientific interest.

Polyphenols are one of the most common classes of secondary metabolites in terrestrial and marine plants. Although terrestrial and marine polyphenols are similar in some respects, there are fundamental differences in their chemical structure (Shibata et al., 2002). In general, polyphenols or phenolic compounds have a similar basic structural chemistry including an “aromatic” or “phenolic” ring structure. Phenolic compounds have been associated with antioxidative action in biological systems, acting as scavengers of singlet oxygen and free radicals (Rice-Evans et al., 1995; Jorgensen et al., 1999). The protective effects of plant polyphenols in biological systems are ascribed to their capacity to transfer electrons to free radicals, chelate metal catalysts, activate antioxidant enzymes and inhibit oxidases. Polyphenols are classified broadly into two classes; condensed tannins, which are polymeric flavonoids, and hydrolysable tannins,

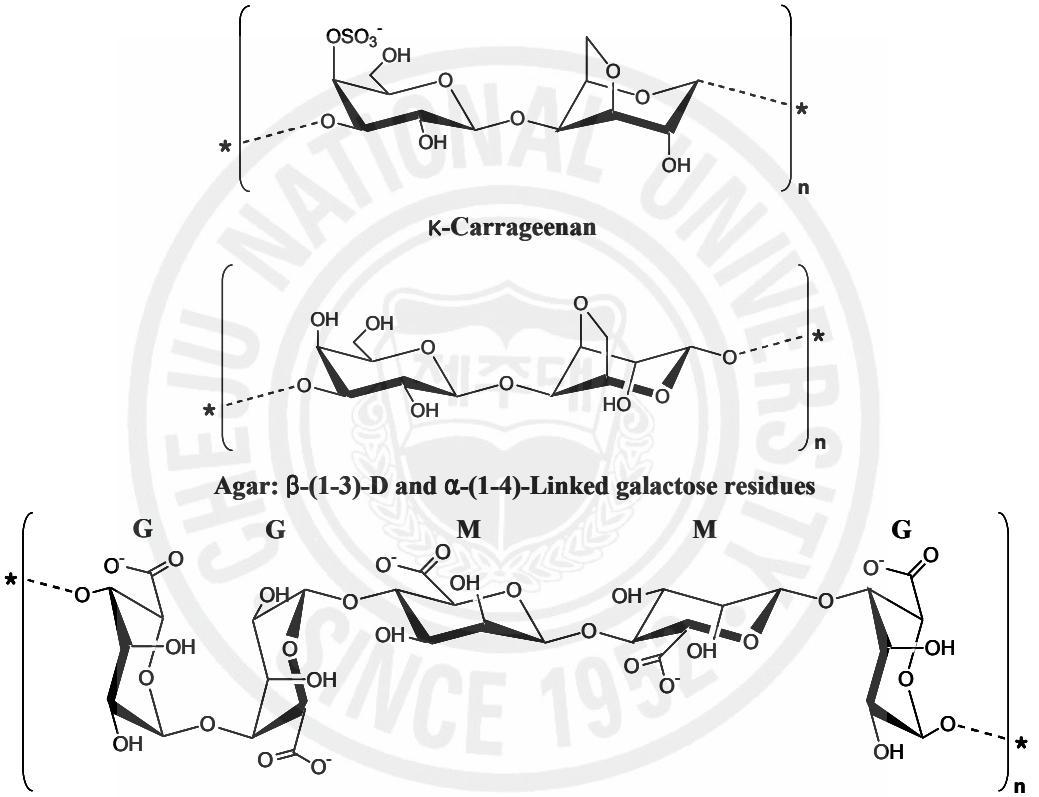

Fig. Ⅰ**.** Molecular structures of κ–carrageenan, agar, and alginate polysaccharides.

which are derivatives of gallic acid (Haslam, 1989). Marine brown algae accumulate a variety of phloroglucinol-based polyphenols of low, intermediate and high molecular weights containing both phenyl and phenoxy unit. Phlorotannins, known as marine algal polyphenols, consist of phloroglucinol (1, 3, 5 trihydroxybenzene) unit linked to each other in various ways, and are of wide occurrence amongst marine organisms, especially brown and red algae (Singh and Bharate, 2006) (**Fig.** Ⅱ). Phlorotannins reported to have several functions including antioxidant, anti-inflammatory, anti-allergic, antibacterial, antiplasmin, and antihyaluronidase activities (Fukuyama et al., 1989; Shibata et al., 2002; Nagayama et al., 2002; Kang et al., 2004; Sugiura et al. 2006).

Carotenoids are natural pigments derived from five-carbon isoprene units that are enzymatically polymerized to form regular highly conjugated 40-carbon structures (with up to 15 conjugated double bonds). One or both ends of the carbon skeleton may undergo cyclization to form ring β-ionone end groups, which additionally may be substituted by oxo, hydroxyl or epoxy groups at different positions to form the different xanthophylls (Solomons and Bulux, 1994). At least 600 different carotenoids exercising important biological functions in bacteria, algae, plants and animals have been identified to date (Polivka and Sundström, 2004) (**Fig.** Ⅲ). Fucoxanthin is a major carotenoid of edible brown algae and has a unique structure including allenic, conjugated carbonyl, epoxide, and acetyl group in its molecule. Fucoxanthin contributes >10% of the estimated total production of carotenoids in nature (Liaeen-Jensen, 1978, 1998). There have recently been several reports that fucoxanthin gave biological activities such as antioxidant, antiobesity, antitumor, and anticarcinogenic activities (Okuzumi et al., 1993; Shimidzu et al., 1996; Yan et al., 1999; Hosokawa et al., 2004; Maeda et al., 2005). Among the most relevant compounds found in the algae, antioxidants

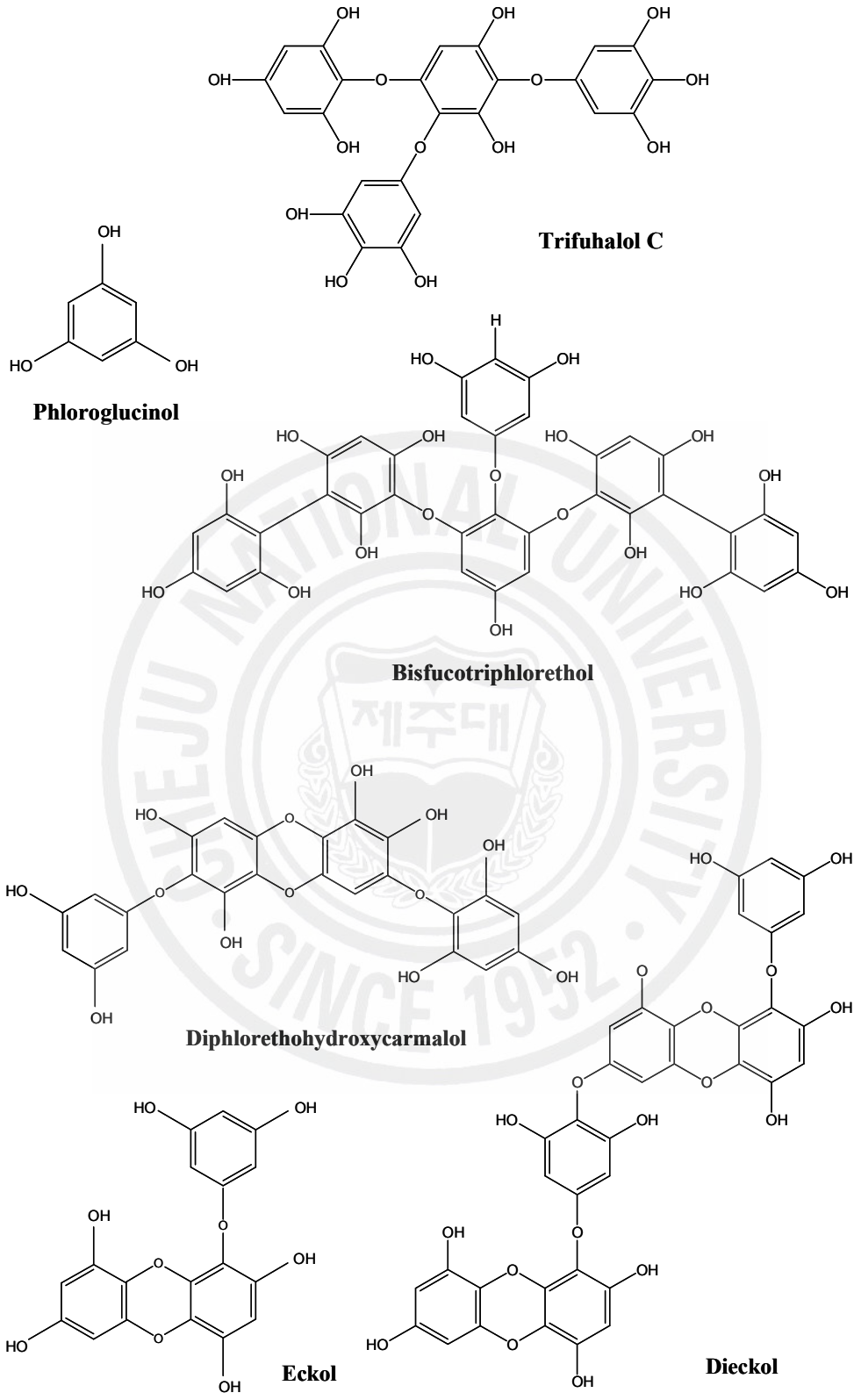

Fig. Ⅱ. Chemical structures of phlorotannins isolated from marine algae.

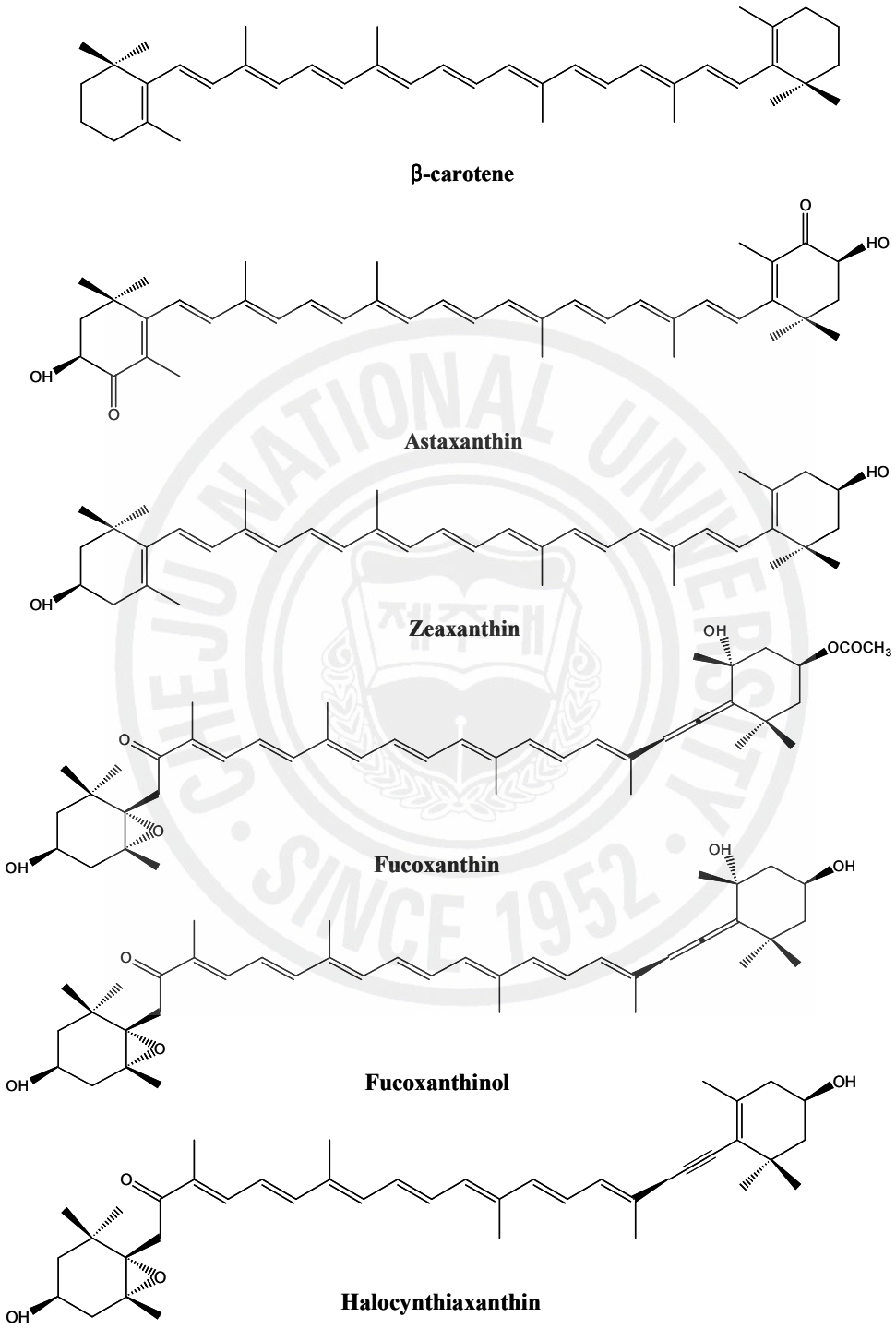

Fig. Ⅲ. Chemical structures of carotenoids isolated from nature.

are probably the substances that have attracted major interest. Oxidative stress, induced by oxygen radicals, is well known to be a primary factor in various diseases including atherosclerosis, arthritis, diabetes, cataractogenesis, muscular dystrophy, pulmonary dysfunction, inflammatory disorders, and neurological disorders such as Alzheimer's disease as well as in the normal process of aging (Aust et al., 1993; Frlich and Riederer, 1995; Stohs, 1995). The reactive oxygen species (ROS), which include free radicals such as superoxide anion radical ($O\cdot_2^-$), hydroxyl radicals (·OH) and non free-radical species such as H_2O_2 and singlet oxygen ($^1O_2$), formed during normal metabolic processes can easily initiate the peroxidation of membrane lipids, leading to the accumulation of lipid peroxides (**Fig.** Ⅳ). Free radical scavengers and antioxidants can reduce lipid peroxidation and the generation of reactive oxygen species. The importance of antioxidants in human health has become increasingly clear due to spectacular advances in understanding the mechanisms of their reaction with oxidants. Furthermore, interest in employing antioxidants from natural sources to increase the shelf life of foods is considerably enhanced by consumer preference for natural ingredients and concerns about the toxic effects of synthetic antioxidants (Schwarz et al., 2001; Tang et al., 2001; Antonella and Vincenzo, 2003; Farag et al., 2003). Algae, as photosynthetic organisms, are exposed to a combination of light and high oxygen concentrations what induces the formation of free radicals and other oxidative reagents. The absence of structural damage in the algae leads to consider that these organisms are able to generate the necessary compounds to protect themselves against oxidation. In this respect, algae can be considered as an important source of antioxidant compounds that could be suitable also for protecting our bodies against the reactive oxygen species formed e.g., by our metabolism or induced by external factors (as pollution, stress, UV radiation, etc.).

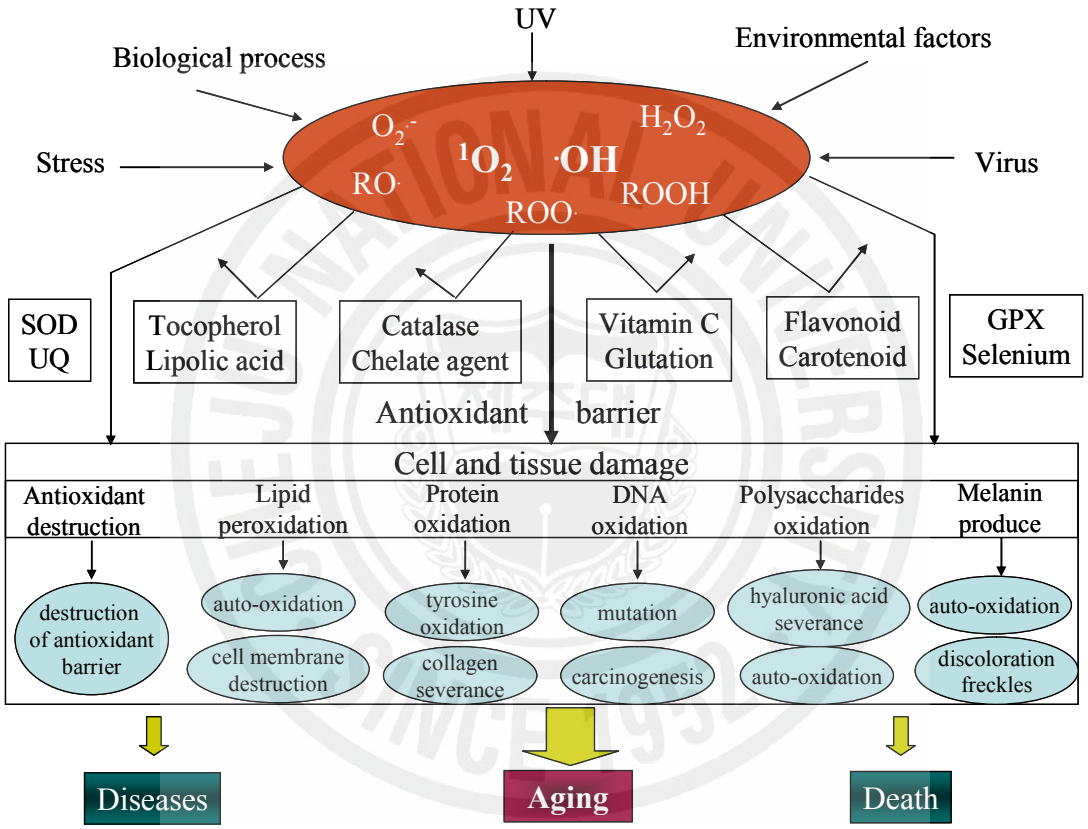

Fig. Ⅳ. Generation factors of reactive oxygen species and the biological consequences leading to a variety of physiological dysfunctions.

In algae there are antioxidant substances or very different nature, among which vitamin E (or α-tocopherol) and carotenoids can be highlighted within the fat-soluble fraction, whereas the most powerful water-soluble antioxidants found in algae are plolyphenols, vitamins (vitamin C) and phycobiliproteins (Plaza et al., 2007).

Cosmetics are commercially available products that are used to improve the appearance of the skin. Since the late 1980's, consumer demand for more effective products that more substantively beautify the appearance has resulted in increased basic science research and product development in the cosmetics industry. The result has been more ingredients that may actually improve not just the appearance of the skin, but the health of the skin as well (Lupo, 2001). Skin forms a remarkable protective barrier against the external environment, helping to regulate temperature and fluid balance, keeping out harmful microbes and chemicals and offering some protection against sunlight. Skin is a living organ that consists of epidermis, dermis and subcutaneous layers (**Fig.** Ⅴ). The dermis is a connective tissue layer that contains many elastin and collagen fibers, as well as an abundance of blood vessels and specialized nerve endings (**Fig.** Ⅵ). The epidermis consists of two main parts: the stratum germinativum and the stratum corneum, the outermost layer 'horny layer', which comes in direct contact with the environment. This horny layer is not simply a collection of dead cells, but a complex organism that is a part of a homeostatic system, and all phenomena occurring at this layer, including the use of cosmetics, are transmitted to the epidermis and the inner skin, and the disturbance of the homeostatic balance, which accompanies aging and rapid changes in the external environment, clearly affects the epidermis and dermis (Tranggono, 2000).

The skin aging is influenced by several factors, including genetics, environmental exposure (ultraviolet irradiation, xenobiotics, mechanical stress), hormonal changes, and metabolic processes (generation of reactive chemical compounds such as activated oxygen

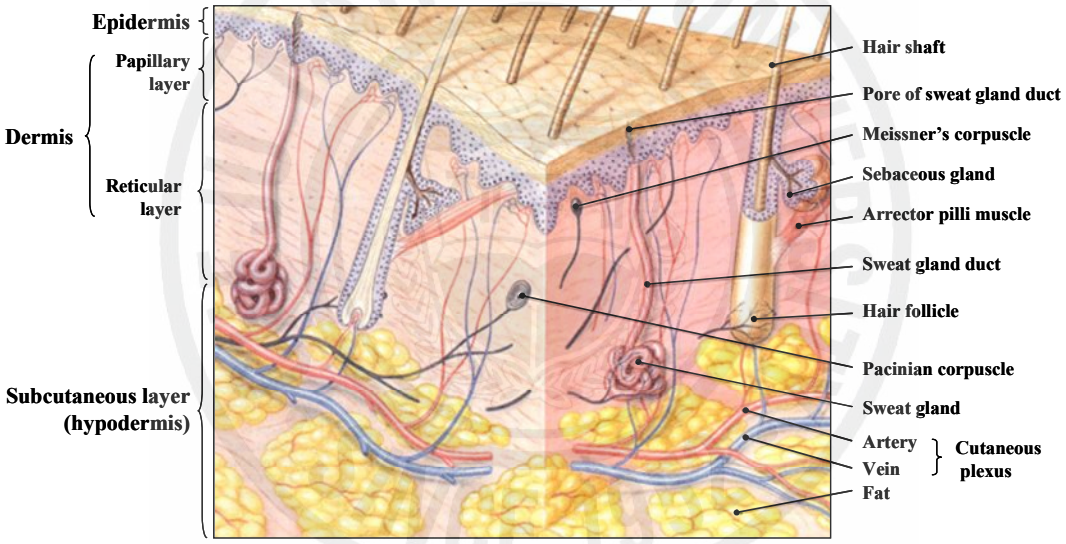

Fig. Ⅴ. The structure of human skin.

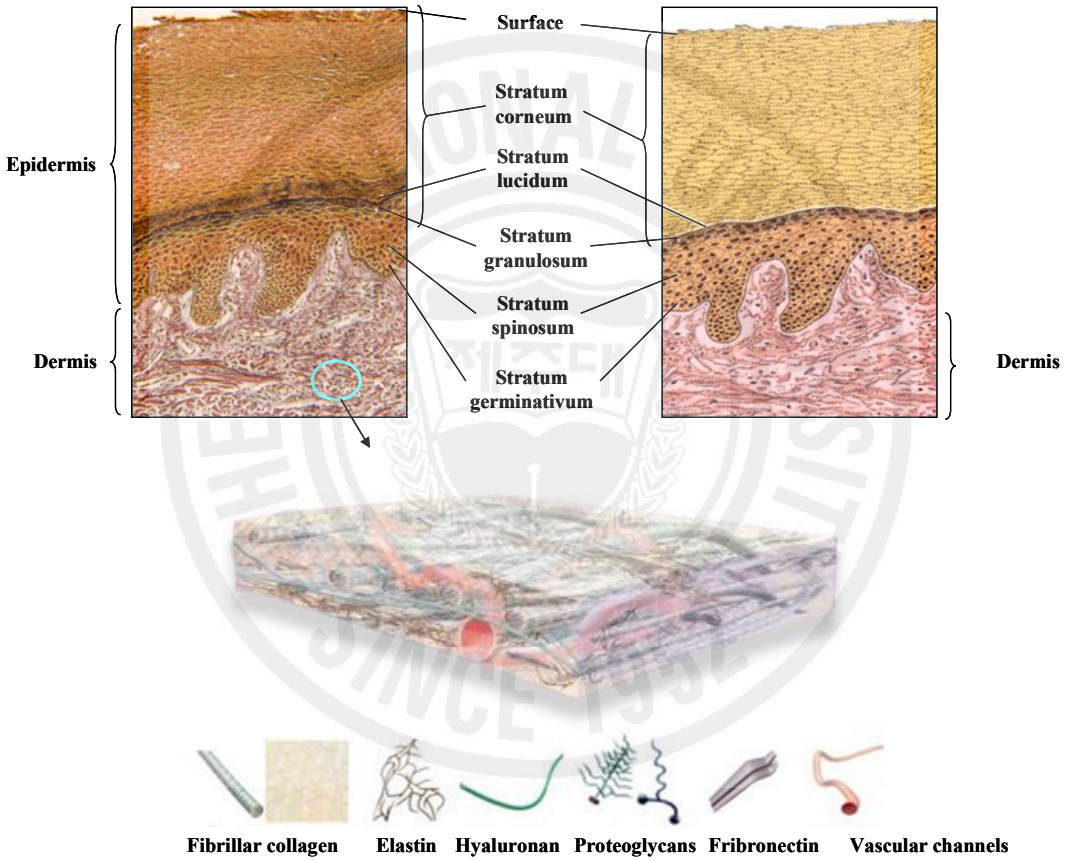

Fig. Ⅵ. The structure of skin epidermis and dermis.

species, sugars, and aldehydes). Taken together, these factors lead to cumulative alterations of skin structure, function, and appearance. The influence of the environment, especially solar UV irradiation, is of considerable importance for skin aging (Rittié and Fisher, 2002) (**Fig. Ⅶ**). Ultraviolet radiation from the sunlight can be divided into 3 components depending on their wavelength: UVC (200-280 nm), UVB (280-320 nm) and UVA (320-400 nm). All UVC and partly UVB are effectively blocked by the ozone layer, but UVA and partly UVB are reached at the Earth's surface of sufficient amount to have harmful biological effects to the skin. In particular, UVB is a major risk factor for the induction and development of nonmelanoma skin cancer and many other skin disorders including sunburn, photoaging and actinic keratoses (Black et al., 1997). Skin aging due to UV exposure (photoaging) is superimposed on chronological skin aging. Historically, photoaging and chronological skin aging have been considered to be distinct entities. Although the typical appearance of photoaged and chronologically aged human skin can be readily distinguished, recent evidence indicates that chronologically aged and UV-irradiated skin share important molecular features including altered signal transduction pathways that promote matrix-metalloproteinase (MMP) expression, decreased procollagen synthesis, and connective tissue damage. This concordance of molecular mechanisms suggests that UV irradiation accelerates many key aspects of the chronological aging process in human skin (Rittié and Fisher, 2002).

Melanins are the main pigments that impart color to our skin, hair and eyes. It is synthesized enzymatically from tyrosine within melanosomes, which are subsequently transferred to epidermal keratinocytes. Melanins play a critical role in the absorption of free radicals and melanogenesis in the skin in a kind of process that produces photoprotective agents against damaging effect of UV (Gange, 1988). However, the increase of melanin synthesis can cause local hyperpigmentation or spot. Therefore, a

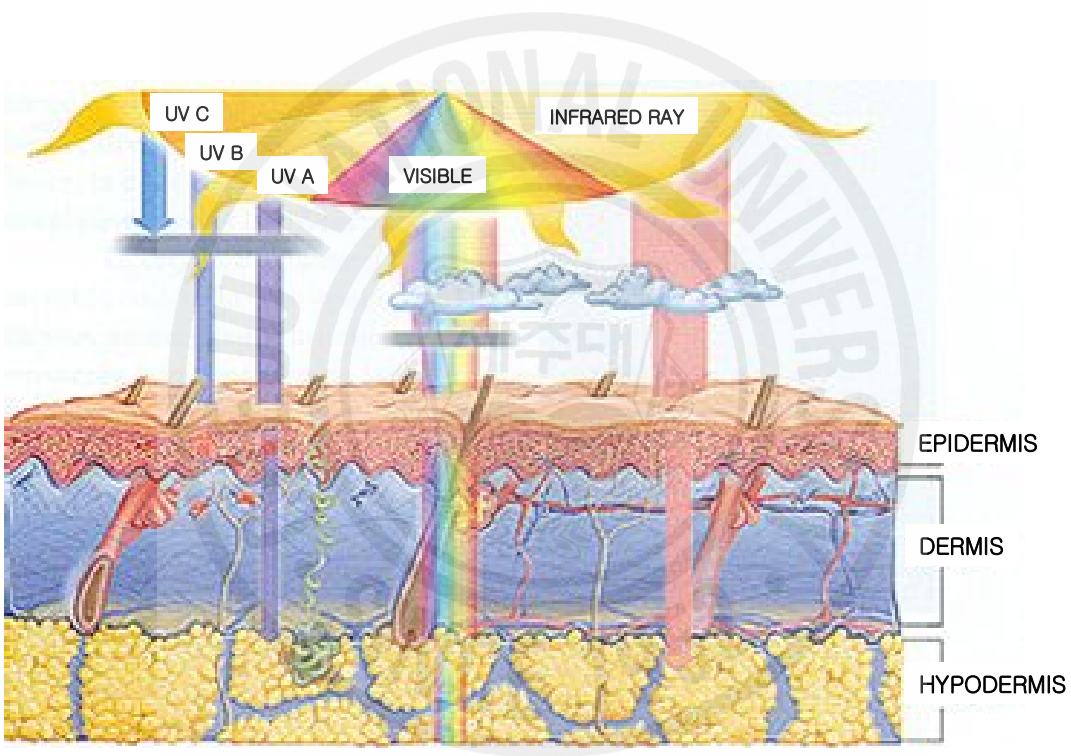

Fig. Ⅶ. The depth of penetration of the skin by UV radiation of different wavelengths.

number of depigmenting agents have been developed for cases of undesirable skin discoloration. Tyrosinase is a multifunctional copper-containing enzyme and commonly present in microorganisms, plants and animals. Tyrosinase is responsible for enzymatic browning in plants, and it may cause undesirable changes in color, flavor and nutritive values of plant-derived foods and beverages (Sánchez-Ferrer et al., 1995). This enzyme is mainly involved in the initial steps of the pathway which consist of the hydroxylation of the p-monophenolic amino acid l-tyrosine (monophenolase activity of tyrosinase) and the oxidation of the product of this reaction, the o-diphenolic amino acid L-DOPA (diphenolase activity), to give rise to o-dopaquinone (Baurin et al., 2002) (**Fig. Ⅷ**). Tyrosinase catalyzes the reaction of melanin biosynthesis in human skin and the epidermal hyperpimentation results in various dermatological disorders, such as melasma, freckles and age spots. Recently, safe and effective tyrosinase inhibitors have become important for their potential applications in improving food quality and preventing pigmentation disorders and others melanin-related health problems in human beings (Seo et al., 2003). Furthermore, tyrosinase inhibitors are also important in cosmetic applications for skin whitening effects, because many men and women prefer lighter skin color (Dooley, 1997).

Elastin is the main component of the elastic fiber of the connective tissue and tendons. In the skin, the elastic fiber, together with the collagenous fibers, form a network developing under the epidermis. Elastase is the only proteinase that is able to split elastin, and plays a critical role in inflammatory processes. The enzyme has received great attention, primarily because of its reactivity and non-specificity (Wiedow et al., 1990; Yan et al., 1994). In contrast to elastase, collagenase is a specific proteinase with a limited number of substrates. In UV-irradiated skin, mild inflammation occurs repeatedly in the dermis, and it is assumed that connective tissue proteins may be attacked

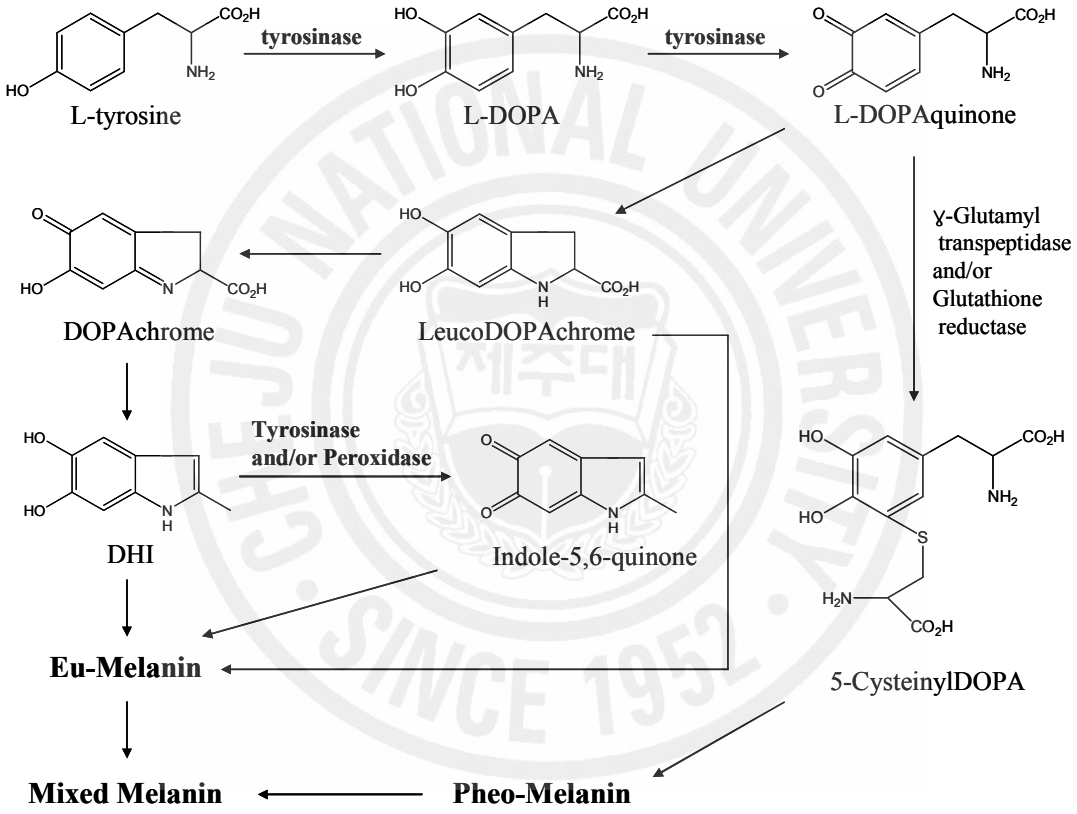

Fig. Ⅷ. The melanogenic pathway from tyrosine.

by elastase released from polymorphonuclear leukocytes, resulting in damage to elastin and collagen fibers and finally causing sagging. Moreover, inhibition of elastase and collagenase are an important therapeutic target due to the enzyme's involvement in tissue destruction of a number of inflammatory disease states. These enzymes have been shown to contribute to the pathogenesis of rheumatoid arthritis, periodontitis, pulmonary emphysema and corneal ulceration (Ekerot and Ohlsson, 1984; Nakagawa et al., 1995; Shapiro, 2002). In recent years, much attention has focused on the inhibition of elastase and collagenase by low molecular weight inhibitors that might serve as therapeutic agents. Many types of peptidic and nonpeptidic inhibitors, employing both reversible and nonreversible mechanisms of action, have been reported (Powers et al., 1993; Edwards and Bernstein, 1994).

The inflammatory mechanisms in the body are very complicated and they cannot be attributed to a single mediator or factor. Inflammation mediators, such as histamine, serotonin, arachidonic acid metabolites and quinines, are known as having a role in generation of the inflammatory reactions (Portanova et al., 1996). Inflammatory process has two phases: acute and chronic. Acute inflammation is characterized by fever, pain, and edema, while chronic inflammation is characterized by cellular proliferation. Complement system, fibrinolytic system and hyaluronidase enzyme are activated in plasma during inflammation. In normal skin, hyaluronidase is localized in the intercellular space of the epidermis, except the corneal and upper granular layers, and between collagen and elastic fibers in dermis (Juhlin, 1997; Manuskiatti and Maibach, 1996). In addition, hyaluronidase synthesis takes place in both epidermal and dermal compartments by keratinocytes and fibroblasts. Hyaluronidase has range of different physiological and biological functions in the skin. It preserves skin hydration and is involved in the structure, organization and maintenance of the extracellular matrix. This

enzyme has therapeutic applications, as for example, in the cardiovascular field, for salvaging ischaemic tissues following myocardial infarction (May et al., 1983). It also has a range of other medical applications, diagnostic applications, and a minor application in the food industry as a meat tenderizer (Wu et al., 1981).

Recently, a number of studies have been focused on marine bio-resources. Marine natural products provide a rich source of chemical diversity that can be used to design and develop new, potentially useful therapeutic agent. In this study, therefore, we tried to screen active compounds from 40 marine algae and examined cosmeceutical activities of the active compounds which can be developed as possible cosmetic agents for human skin.

Part Ⅰ.

Screening for antioxidant activities and tyrosinase inhibitory effect of marine algae

Part Ⅰ.

Screening for antioxidant activities and tyrosinase inhibitory effect of marine algae

1. ABSTRACT

Antioxidant activities of 40 species of the marine algae collected from Jeju Island area were measured by $ABTS^+$ and $DPPH^-$ free radical scavenging assays. A variety of methanol extracts of brown seaweeds showed antioxidant activity. Among them, *Ishige okamurae*, *I. sinicola*, *Ecklonia cava* and *Sargassum siliquastrum* extracts exhibited strong free radical scavenging activities both $ABTS^+$ and $DPPH^-$. In addition, $CHCl_3$ and EtOAc fractions of these extracts also showed higher radical scavenging activities than the other organic solvent fractions. For the development of whitening agents for cosmeceutical bio-materials, we investigated the inhibitory effect of seaweed extracts against tyrosinase. Among them, *I. okamurae* (78.7%), *E. cava* (75.2%) and *I. sinicola* (42.8%) showed good activity. These results indicated that some seaweed could be utilized as potential candidates for the development of antioxidants and cosmeceuticals.

2. MATERIALS AND METHODS

2.1. Materials

Fourty species of marine algae were collected along the coast of Jeju Island, Korea, between October 2005 and March 2006 (**Table 1**). The samples were washed three times with tap water to remove salt, epiphytes, and sand attached to the surface, then carefully rinsed with fresh water, and maintained in a medical refrigerator at –20℃. Therefore, the frozen samples were lyophilized and homogenized with a grinder prior to extraction. 2,2'-azino-bis-3-ethylbenzthiazoline-6-sulfonic acid (ABTS), 1,1-diphenyl-2-picrylhydrazyl (DPPH), mushroom tyrosinase, and tyrosine were purchased from Sigma Chemical Co. (St. Louis, MO, USA). And other chemicals used were 99% or greater purity.

2.2. Extraction procedure of 80% methanolic extracts from marine algae

The marine algae samples were pulverized into powder using a grinder. The algal powder (1 g) was extracted with 80% methanol (100 ml) at a room temperature for 24 h and filtrated. After filtration, the methanolic extracts were evaporated to dryness under vacuum. This extracts were used for further biological study.

2.3. ABTS radical scavenging assay

Spectrophotometric analysis of ABTS cation radical scavenging activity was conducted according to the method of Re et al. (1999). ABTS radical was produced by

Table 1. The list of marine algae

Rot. No.	Scientific name	Rot. No.	Scientific name
Chlorophyta		AP014	*Ishige okamurae*
AC001	*Ulva conglobata*	AP015	*Ecklonia cava*
AC002	*Ulva pertusa*	AP016	*Sargassum siliquastrum*
AC003	*Capsosiphon fulvescens*		
AC004	*Codium coactum*	**Rhodophyta**	
AC005	*Codium latum*	AR001	*Gelidium amansii*
AC006	*Codium contractum*	AR002	*Gloiopeltis furcata*
AC007	*Codium fragile*	AR003	*Hypnea japonica*
Phaeophyta		AR004	*Lomentaria catenata*
AP001	*Hizikia fusiformis*	AR005	*Champia parvula*
AP002	*Sargassum thunbergii*	AR006	*Grateloupia lanceolata*
AP003	*Sargassum confusum*	AR007	*Chondria crassicaulis*
AP004	*Undaria pinnatifida*	AR008	*Neorhodomela munita*
AP005	*Colpomenia sinuosa*	AR009	*Martensia* sp.
AP006	*Myelophycus simplex*	AR010	*Gloiopeltis tenax*
AP007	*Scytosiphon lomentaria*	AR011	*Galaxaura falcata*
AP008	*Ishige sinicola*	AR012	*Gracilariopsis chorda*
AP009	*Petrospongium rugosum*	AR013	*Chondrus ocellatus*
AP010	*Dictyota dichotoma*	AR014	*Laurencia okamurae*
AP011	*Leathesia difformis*	AR015	*Callophyllis japonica*
AP012	*Sargassum hemiphyllum*	AR016	*Hypnea charoides*
AP013	*Sargassum hornerii*	AR017	*Acanthopeltis longiramulosa*

the reaction between 7 mM ABTS/H_2O and 2.45 mM potassium persulfate for 12 h in the dark at room temperature. The ABTS radical solution was diluted with PBS until A_{734} = 0.7. The reaction was initiated by adding 190 μl of ABTS radical solution to 10 μl of sample solution. After 7 min, the absorbance at 734 nm was recorded and the reduction of the absorbance was plotted as a function of the samples concentration. The scavenged ABTS radical was calculated as:

$$\text{Scavenged ABTS (\%)} = (1 - A_{test} / A_{control}) \times 100$$

where A_{test} is the absorbance of a sample at a given concentration after 7 min reaction time and $A_{control}$ is the absorbance recorded for 10 μl of methanol.

2.4. DPPH radical scavenging assay

DPPH radical scavenging activity was assessed according to the method of Lee et al. (1998) with minor modifications. Ten micro liters of samples or methanol (control) was added to 190 μl of a 1.5×10^{-4} M EtOH solution of DPPH radical in a well of a 96-well plate. The absorbance of the reaction mixture at 517 nm was measured at steady state after 30 min of incubation at room temperature using a microplate reader. The scavenged DPPH radical was calculated in the same way as described in the ABTS assay.

2.5. Tyrosinase inhibition assay

Tyrosinase inhibitory activity was performed according to the method of Vanni et al. (1990) with minor modifications. The reaction mixture contains 140 μl of 0.1 M phosphate buffer (pH 6.5), 40 μl of 1.5 mM L-tyrosine and 10 μl of samples. Then, 10

μl of mushroom tyrosinase (2100 units/ml) solution was added and the reaction was incubated at 37℃ for 12 min. After incubation, the amount of dopachrome produced in the reaction mixture was determined as the optical density at 490 nm in a microplate reader. The percent inhibition of tyrosinase reaction was calculated as follows:

$$\text{Inhibition (\%)} = [1 - (B - A) / (D - C)] \times 100$$

A = Absorbance at 490 nm with test sample before incubation

B = Absorbance at 490 nm with test sample after incubation

C = Absorbance at 490 nm without test sample before incubation

D = Absorbance at 490 nm without test sample after incubation

2.6. Statistical analysis

The data are expressed as the mean ± standard error (SE). A statistical comparison was performed via the SPSS package for Windows (Version 10). P-values of less than 0.05 were considered to be significant.

3. RESULTS AND DISCUSSIONS

Antioxidants are closely related to their biofunctionalities, such as the reduction of chronic disease like DNA damage, mutagenesis, carcinogenesis and inhibition of pathogenic bacteria growth which is often associated with the termination of free radical propagation in biological systems (Zhu et al., 2002). Thus, antioxidant activity is widely used as a parameter for medicinal bioactive components. In this study, the antioxidant activity and potential cosmeceutical effect of marine algae extracts were evaluated by scavenging activities of free radicals ($ABTS^{+}$ and $DPPH^{\cdot}$) and inhibitory effect of tyrosinase.

ABTS radical cation is common organic radical that has been used to determine the antioxidant activity of hydrogen donating antioxidant and of chain breaking antioxidants (Zhou et al., 2004). The ABTS radical cation was generated by incubating ABTS with potassium persulfate or manganese oxide. The production of ABTS radical cation depends on the inhibitors during the reaction which contributors to the total ABTS radical cation scavenging capacity (Gorinstein et al., 2006). The scavenging activity of ABTS radical by marine algae extracts was presented in **Fig. 1-1**. Among the 40 kinds of marine algae extracts obtained by 80% methanol, brown algae extracts showed relatively higher ABTS radical scavenging activity than green and red algae extracts. It was observed that *Sargassum confusum* (AP003) extract showed the highest scavenging activity (90.67%) on ABTS radical and *Ishige sinicola* (AP008), *Dictyota dichotoma* (AP010), *S. hemiphyllum* (AP012), *I. okamurae* (AP014), and *Ecklonia cava* (AP015) extracts of brown algae also had 87.99, 85.31, 89.27, 88.57, and 86.47% ABTS radical scavenging activities, respectively. *Martensia* sp. (AR009) extract showed the highest scavenging activity among the red algae tested (78.93%) and the

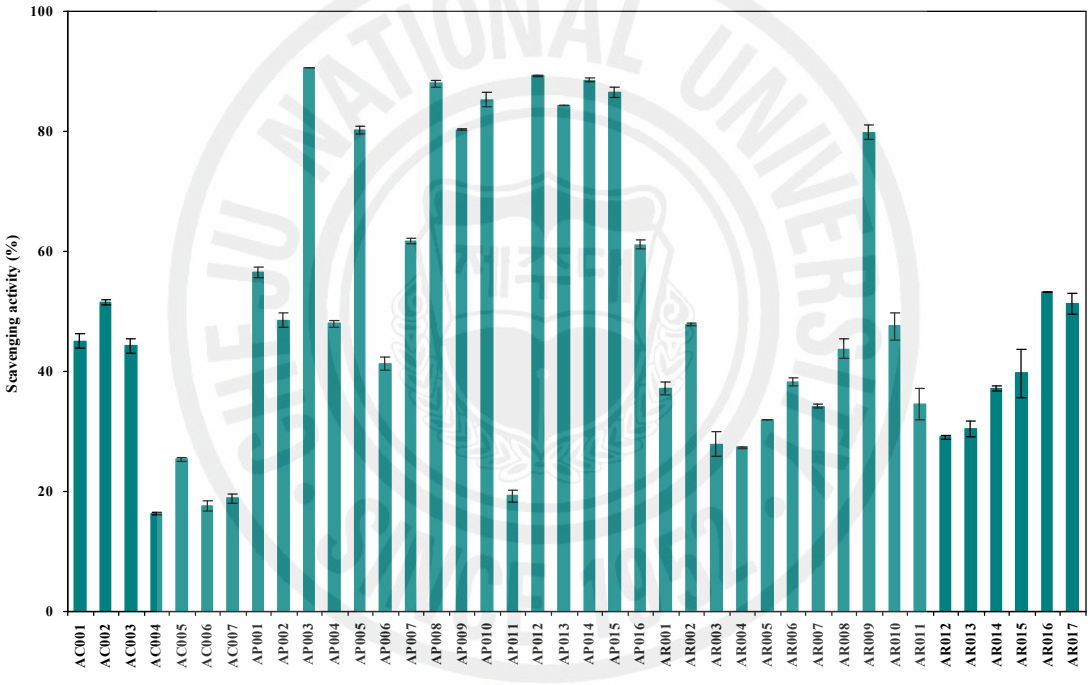

Fig. 1-1. ABTS radical scavenging activity of 80% MeOH extracts from marine algae. Experiments were performed in triplicate and the data are expressed as mean ± SE.

green algae extracts exhibited less than 50% scavenging activities. Polyphenols constitute one of the major groups of compounds acting as primary antioxidant free radical terminators. Phlorotannins, as one of the most diverse and widespread groups of natural compounds, are probably the most natural phenolics in marine algae. These compounds possess a wide spectrum of chemical and biological activities including radical scavenging properties. A strong relationship between total phenolics content and antioxidant activity in natural products has been reported (Velioglu et al., 1998; Dorman et al., 2003; Heo et al., 2005). In this study, the extracts of brown algae displayed higher ABTS radical scavenging activities. These results indicated that active compounds of different polarity could be present in brown algae such as polypenolic compounds.

DPPH is known as a stable free radical that has been widely used to evaluate the free radical scavenging ability of various antioxidative compounds. The DPPH radical is scavenged by antioxidants through the donation of hydrogen to form the stable reduced DPPH molecule. The antioxidant radicals formed are stabilized through the formation of non-radical products (Argolo et al., 2004). The scavenging activities of marine algae extracts on DPPH radical are shown in **Fig. 1-2**. Brown algae extracts obtained by 80% methanol exhibited relatively higher scavenging activity than the green and red algae extracts on DPPH radical. Among them, *I. okamurae* (AP014) showed the highest scavenging activity (93.11%) and *I. sinicola* (AP008), *E. cava* (AP015) and *S. siliquastrum* (AP016) also scavenged 77.12, 88.86 and 73.88% on DPPH radical, respectively. However, all the tested green and red algae extracts showed less than 50% DPPH radical scavenging activities. Many reports have recently described the ability to scavenge DPPH radical on marine algae (Heo et al., 2005; Karawita et al., 2005; Kuda et al., 2005; Heo et al., 2006; Nahas et al., 2007). These researches indicated that some

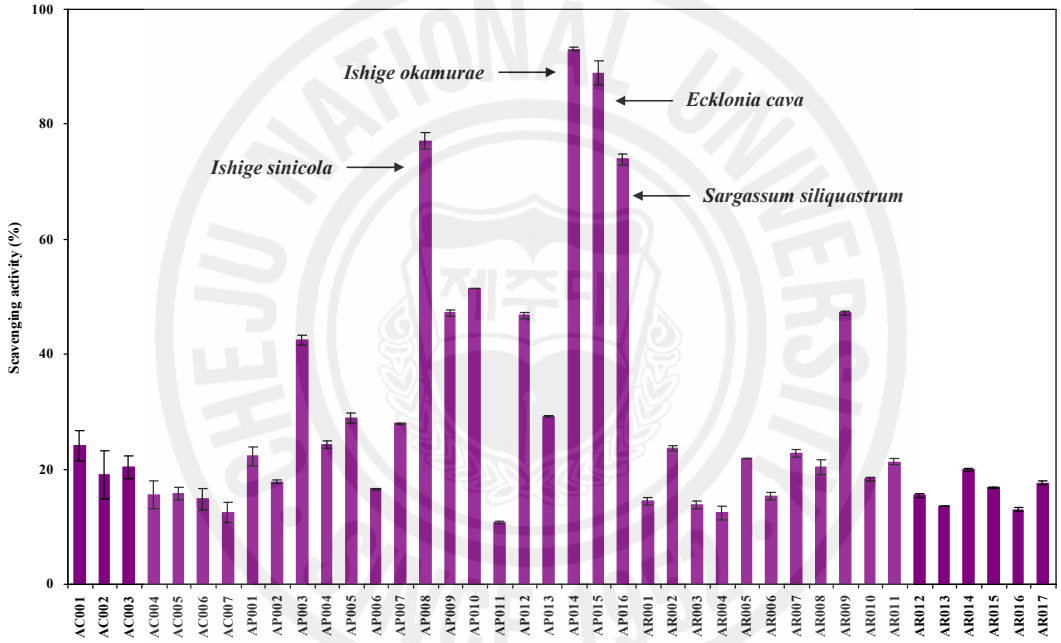

Fig. 1-2. DPPH radical scavenging activity of 80% MeOH extracts from marine algae. Experiments were performed in triplicate and the data are expressed as mean ± SE.

kinds of marine algae could be used to potential antioxidant and pharmaceutical industries.

In this study, we are screened antioxidant activities of marine algae extracted by 80% methanol to find potential antioxidative sources from marine algae. Among these results, *I. okamurae*, *E. cava* and *S. siliquastrum* showed relatively higher scavenging activity both ABTS and DPPH radicals than the other marine algae. Therefore, those samples were partitioned with hexane, $CHCl_3$, EtOAc and BuOH to find bioactive compounds and the radical scavenging activities were investigated. The scavenging activities of the organic solvent fractions on ABTS and DPPH radicals were shown in **Figs. 1-3** and **1-4**. The 80% methanol extracts were successfully partitioned according to their polarity. It was observed that the EtOAc fraction obtained by *E. cava* and *I. okamurae* exhibited the highest scavenging activities whereas $CHCl_3$ fraction obtained by *S. siliquastrum* showed the highest scavenging activities on ABTS and DPPH radicals compared to the other organic solvent fractions. Natural extracts with proven antioxidant activity usually contain compounds with a phenolic moiety, for example coumarins, flavonoids, tocopherols and catechins. Organic acids, carotenoids, protein and tannins can also be present and act as antioxidants or have a synergistic effect with phenolic compounds (Dapkevicius et al., 1998). Recent studies have demonstrated that the antioxidant activity is correlated with the number of available hydroxyl groups (Brand-Williams et al., 1995). It was well known that marine algae have variety phenolic moiety such as xanthins and tannins. This structural requirement could be linked to the presence of phlorotannins or carotenoids in EtOAc and $CHCl_3$ fractions.

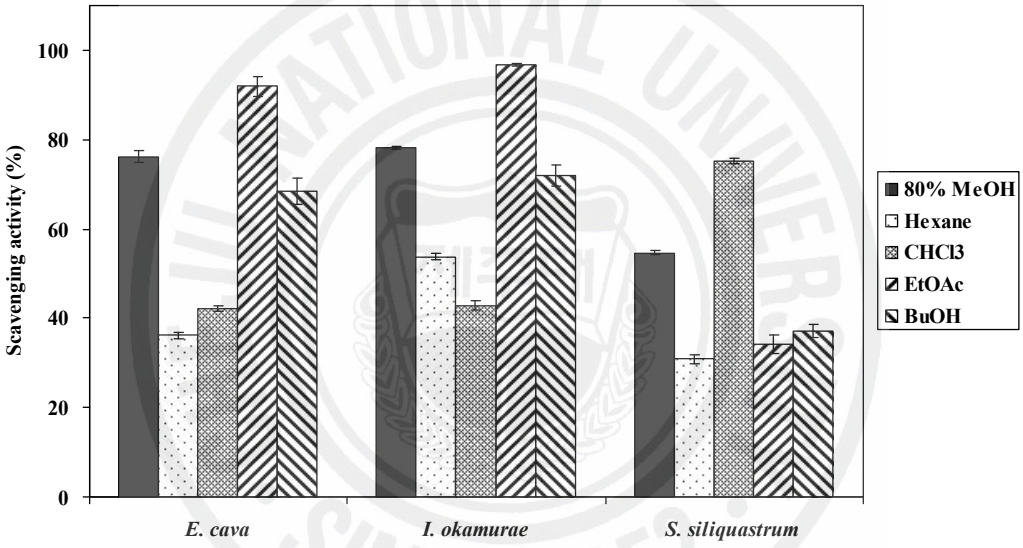

Fig. 1-3. ABTS radical scavenging activity of brown algae extracts partitioned by various organic solvents. Experiments were performed in triplicate and the data are expressed as mean ± SE.

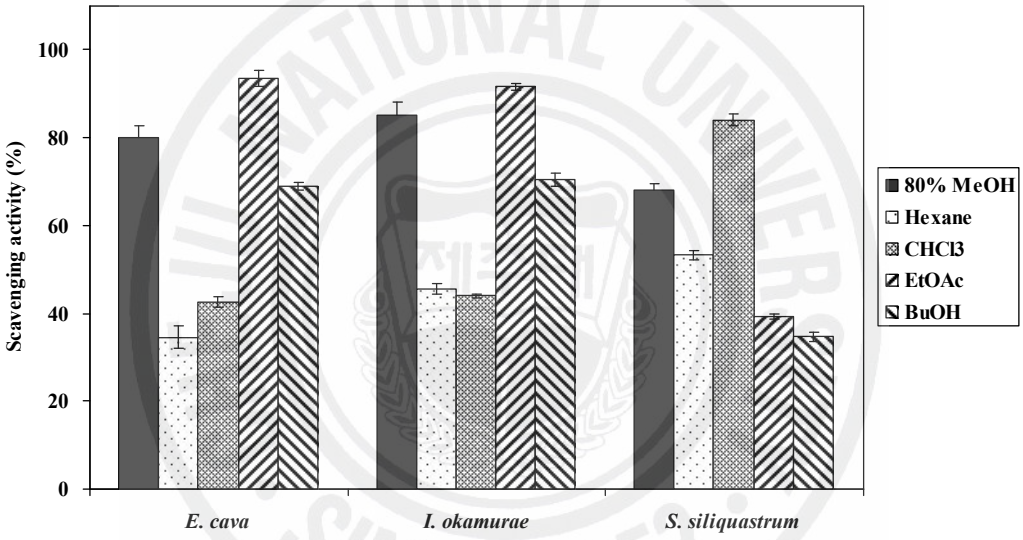

Fig. 1-4. DPPH radical scavenging activity of brown algae extracts partitioned by various organic solvents. Experiments were performed in triplicate and the data are expressed as mean ± SE.

Melanin synthesis in animals proceeds from L-tyrosine through a series of enzymatic and chemical steps initiated by tyrosine hydroxylation to yield L-DOPA, and subsequent L-DOPA oxidation to L-DOPA quinine. A single enzyme that catalyzes both reactions is tyrosinase (monophenol monooxygenase), a melanocyte-specific copper-containing glycoprotein located within specialized organelles called melanosomes (Jones et al., 2002). In this study, we investigated tyrosinase inhibitory activity of 40 kinds of methanol extracts from marine algae (**Fig. 1-5**). Out of these 40 marine algae extracts, *E. cava* (AP014) and *I. okamurae* (AP015) showed strong inhibitory effect of tyrosinase which values were 78.73 and 75.28%, respectively. *I. sinocola* (AP008) also exhibited relatively higher activity than the other algae extracts (42.8%). From these results, *E. cava* and *I. okamurae* were fractionated with different organic solvents to find where the active compounds existed (**Fig. 1-6**). The 80% methanol extracts were successfully partitioned according to their polarity. It was found that EtOAc fractions obtained by *E. cava* and *I. okamurae* had potent inhibitory effects on mushroom tyrosinase compared to the other organic solvent fractions (96.33 and 95.89%, respectively). It is well established that brown algae contain phenolic compounds with tyrosinase inhibitory effect. Marine algal polyphenols, known as phlorotannins, which have only been found to exist within brown algae, are restricted to polymers of phloroglucinol (1,3,5-trihydroxybenzene). Moreover, those kinds of compound were often detected in EtOAc fractions. Therefore we expected that the potential tyrosinase inhibitory effect might be due to phlorotannins in *E. cava* and *I. okamurae*.

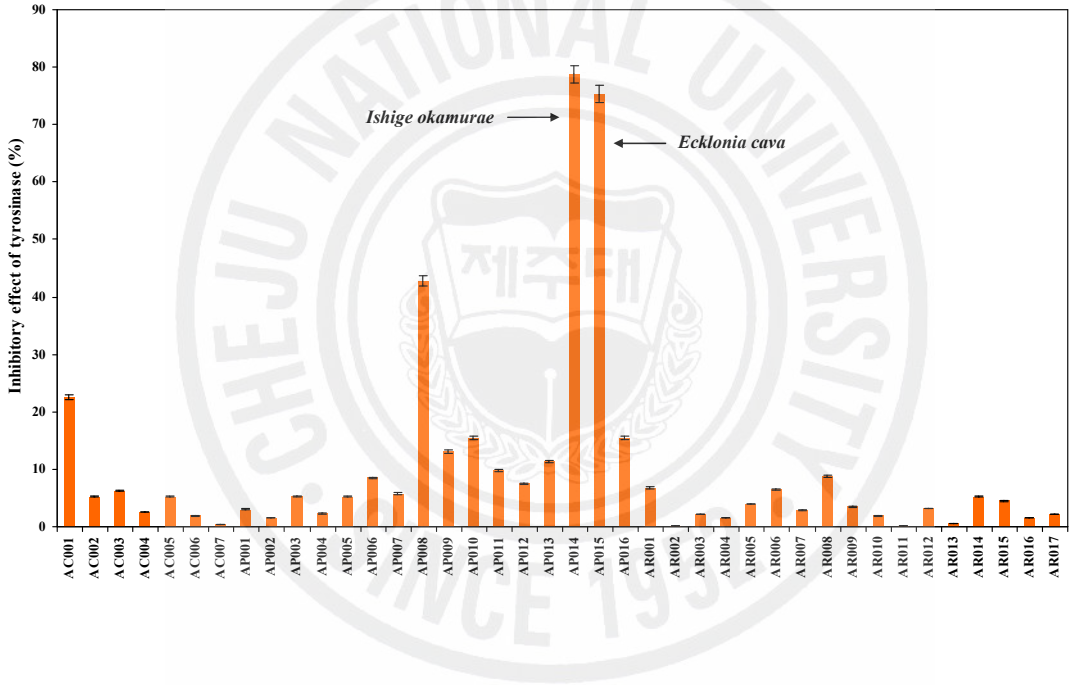

Fig. 1-5. Inhibitory effect of marine algae extracts against tyrosinase. Experiments were performed in triplicate and the data are expressed as mean ± SE.

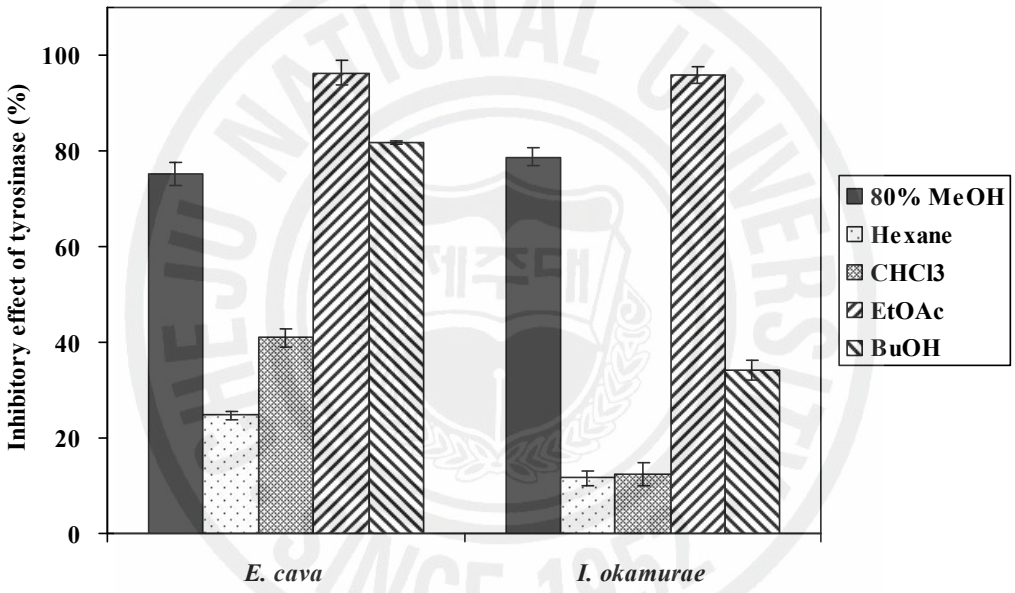

Fig. 1-6. Inhibitory effect of tyrosinase of brown algae extracts partitioned by various organic solvents. Experiments were performed in triplicate and the data are expressed as mean ± SE.

In this study, we are screened antioxidant activity and inhibitory effect of tyrosinase to find natural bioactive materials. Out of these 40 kinds of marine algae, *Ecklonia cava*, *Ishige okamurae*, and *Sargassum siliquastrum* have potential cosmeceutical values. Therefore, further experiment could be used these marine algae.

Part Ⅱ.

Isolation of cosmetic materials from *Sargassum siliquastrum*

Part Ⅱ.

Isolation of cosmetic materials from *Sargassum siliquastrum*

1. ABSTRACT

To obtain natural compounds heaving cosmeceutical activities from a marine biomass, this study investigated radical scavenging activity, protective effect against oxidative stress, and inhibitory effect of melanin synthesis. Carotenoid metabolites (**1-3**), penyl benzoquinones derivate (**4**), prenylated benzopyran derivate (**5**), and chromenes derivatives (**6-13**) have been isolated from the brown alga *Sargassum siliquastrum*. Among them, compounds **6**, **7**, **8**, **9**, **10**, and **13** showed strong DPPH radical scavenging activity while compound **1** has higher protective effect of cell damage induced by ROS and UV-B radiation, and inhibitory effect of melanin synthesis.

These results indicate that tested chromenes (**6**, **7**, **8**, **9**, **10**, and **13**) and **1** can be used to natural antioxidant, and can applied to cosmeceutial field due to their protective effect against oxidative stress and inhibitory effect of melanin synthesis.

2. MATERIALS AND METHODS

2.1. General experimental procedures

Optical rotations were measured on a JASCO P-1020 polarimeter. The UV and FT-IR spectra were recorded on a Pharmacia Biotech Ultrospec 3000 UV/Visible spectrometer and a SHIMAZU 8400s FT-IR spectrometer, respectively. NMR spectra were recorded on a Bruker 500 MHz and Varian INOVA 400 MHz NMR spectrometer. CD_3OD and $CDCl_3$ were used as a solvent for the NMR experiments, and the solvent signals were used as an internal reference. ESI and HREI mass spectra acquired using a Finnigan Navigator 30086 and JMS-700 MSTATION high resolution mass spectrometer system, respectively. The HPLC was carried out on a Waters HPLC system equipped with a Waters 996 photodiode array detector and Millenium32 software using C_{18} column (J'sphere ODS-H80, 150×20 mm, 4 μm, YMC Co.).

2.2. Materials

The marine alga *Sargassum siliquastrum* (**Fig. 2-1**) was collected along the coast of Jeju Island, Korea, between October 2005 and March 2006. The samples were washed three times with tap water to remove the salt, epiphytes, and sand attached to the surface, then carefully rinsed with fresh water, and maintained in a medical refrigerator at –20℃. Therefore, the frozen samples were lyophilized and homogenized with a grinder prior to extraction.

Fig. 2-1. The photograph of a brown alga *Sargassum siliquastrum*.

2.3. Extraction and isolation

The powdered *S. siliquastrum* (400 g) was extracted with 80% aqueous MeOH, and was evaporated under vacuo. Then, the MeOH extract was partitioned with $CHCl_3$. The chloroform extract (9 g) was fractionated by silica column chromatography with stepwise elution of $CHCl_3$-MeOH mixture (100:1-1:1) to afford separated active fractions. A combined active fraction was further subjected to a Sephadex LH-20 column saturated with 100 % MeOH, and then finally purified by reversed-phase HPLC (90% aqueous MeOH) to give compound **1** (74.9 mg). In addition, the active subfraction from the Sephadex LH-20 column was fractionated by SepPack cartridge eluted with 30, 50, and 70% aqueous MeOH, respectively. The 30% aqueous MeOH eluted fraction was finally purified with reversed-phase HPLC to yield compounds **2** (3.9 mg), and **3** (4.2 mg). The 70% aqueous MeOH eluted fraction was finally purified with reversed-phase HPLC to yield compounds **4** (4.2 mg), **6** (26.3 mg), and **7** (40.4 mg). Another active fraction from the silica gel chromatography was fractionated by a Sephadex LH-20 column with 80% aqueous MeOH, and was finally purified with reversed-phase HPLC to give compounds **5** (4.1 mg), **8** (18 mg), **9** (13.2 mg), **10** (11.4 mg), **11** (3mg), **12** (2.8 mg), and **13** (19.8 mg) (**Fig. 2-2**).

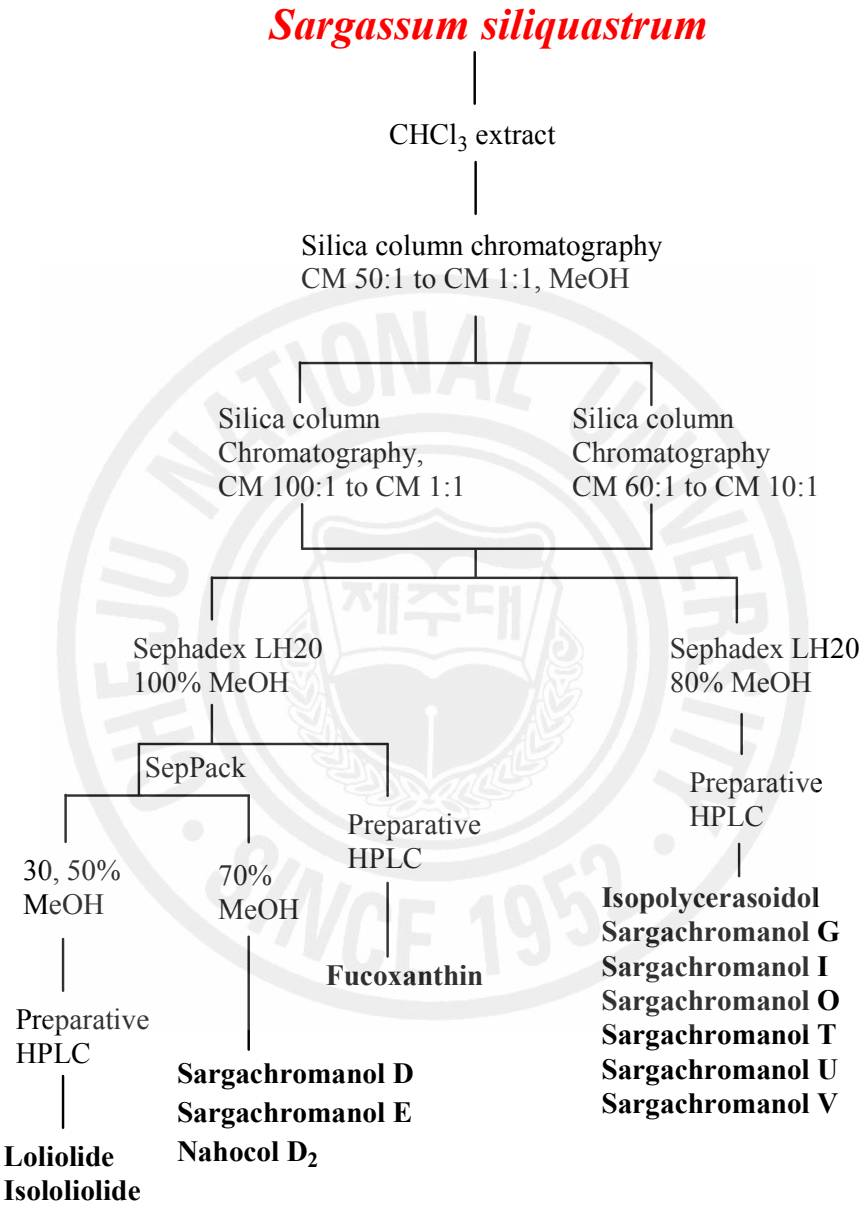

Fig. 2-2. Isolation scheme of the active compounds from *S. siliquastrum*.

Fucoxanthin (1): bright orange solid; $[\alpha]_D$ +18° (*c* 0.2, $CHCl_3$); IR (KBr) ν_{max} 3438, 2361, 2332, 1723, 1654, 1605, 1251, 1030 cm^{-1}; UV (MeOH): 468 nm (ε 51,000) (sh), 446 (56,000), 332 (17,000), 267 (24,000); ^1H and ^{13}C NMR, see **Table 2-1**; LREIMS *m*/*z* 658 $[M]^+$ (calcd for $C_{42}H_{58}O_6$, 658).

Loliolide (2): colorless gum; $[\alpha]_D$ − 100.5° (*c* 0.01, $CHCl_3$); IR (KBr) ν_{max} 3439, 1720 cm^{-1}; ^1H NMR, see **Table 2-2**; LRFABMS *m*/*z* $(C_{11}H_{16}O_3 + H)^+$ 197.

Isololiolide (3): colorless gum; $[\alpha]_D$ + 82.5° (*c* 0.01, $CHCl_3$); IR (NaCl) ν_{max} 3439, 1720 cm^{-1}; ^1H NMR, see **Table 2-2**; LRFABMS *m*/*z* $(C_{11}H_{16}O_3 + H)^+$ 197.

Nahocol D_2 (4): colorless oil; $[\alpha]_D$ + 4.5° (*c* 0.95, MeOH); IR (KBr) ν_{max} 3600, 3350, 1730, 1610, 1590, 1495, 1440, 1170, 1100, 1010 cm^{-1}; UV (MeOH): λ_{max} nm (log ε) 206 (4.4), 229 (3.9), 293 (3.4); ^1H and ^{13}C NMR, see **Table 2-3**; HREIMS *m*/*z* 468.2866 $[M-H_2O]^-$ ($C_{29}H_{42}O_6$).

Isopolycerasoidol (5): colorless oil; $[\alpha]_D$ + 6.6° (*c* 0.45, MeOH); IR (NaCl) ν_{max} 3358, 2921, 2850, 1686, 1637, 1466, 1376, 1218, 1144, 1098 cm^{-1}; UV (EtOH): λ_{max} nm (log ε) 294 (3.37), 234 (3.59); ^1H and ^{13}C NMR, see **Table 2-4**; EIMS *m*/*z* 358 $[M]^+$ ($C_{22}H_{30}O_4$).

Sargachromanol D (6): colorless gum; $[\alpha]^{20}_D$ + 19.4° (*c* 0.16, MeOH); IR (NaCl) ν_{max} 3400-3300, 2975, 2930, 1470, 1375, 1220 cm^{-1}; ^1H and ^{13}C NMR, see **Table 2-5**; HREIMS (triacetate) *m*/*z* 554.3244 $[M]^+$ (calcl for $C_{33}H_{46}O_7$, 554.3244).

Sargachromanol E (7): colorless gum; $[\alpha]^{20}_{D}$ + 14.4° (*c* 0.12, MeOH); IR (NaCl) ν_{max} 3400-3300, 2975, 2930, 1645, 1470 cm^{-1}; ^{1}H and ^{13}C NMR, see **Table 2-6**; HREIMS (triacetate) *m*/*z* 554.3239 $[M]^{+}$ (calcl for $C_{33}H_{46}O_7$, 554.3244).

Sargachromanol G (8): colorless gum; $[\alpha]^{20}_{D}$ − 79.2° (*c* 0.12, MeOH); IR (NaCl) ν_{max} 3400-3300, 2970, 2930, 1665, 1470, 1220 cm^{-1}; UV (MeOH): λ_{max} nm (log ε) 230 (3.80) nm; ^{1}H and ^{13}C NMR, see **Table 2-7**; HREIMS *m*/*z* 426.2774 $[M]^{+}$ (calcl for $C_{27}H_{38}O_4$, 426.2770).

Sargachromanol I (9): colorless gum; $[\alpha]^{20}_{D}$ − 118.2° (*c* 0.11, MeOH); IR (NaCl) ν_{max} 3400-3300, 2935, 1710, 1470, 1220 cm^{-1}; ^{1}H and ^{13}C NMR, see **Table 2-8**; HREIMS *m*/*z* 428.2924 $[M]^{+}$ (calcl for $C_{27}H_{40}O_4$, 428.2927).

Sargachromanol O (10): colorless gum; $[\alpha]^{20}_{D}$ + 12.9° (*c* 0.11, MeOH); IR (NaCl) ν_{max} 3400-3300, 2930, 1705, 1470, 1220 cm^{-1}; ^{1}H and ^{13}C NMR, see **Table 2-9**; HREIMS *m*/*z* 426.2769 $[M]^{+}$ (calcl for $C_{27}H_{38}O_4$, 426.2770).

Sargachromanol T (11): colorless oil; $[\alpha]^{20}_{D}$ + 19.3° (*c* 0.15, MeOH); IR (KBr) ν_{max} 3427, 2928, 2856, 1657, 1626 cm^{-1}; UV (MeOH) λmax (log ε) 203 (5.49), 295 (4.42) nm; ^{1}H and ^{13}C NMR, see **Table 2-10**; ESIMS (negative ion mode) *m*/*z* 429 $[M - H]^{-}$; HREIMS *m*/*z* 430.3085 $[M]^{+}$ (calcd for $C_{27}H_{42}O_4$, 430.3083).

Sargachromanol U (12): colorless oil; $[\alpha]^{20}_{D}$ − 19.3° (*c* 0.14, MeOH); IR (KBr) ν_{max} 3425, 2928, 2858, 1657, 1622 cm^{-1}; UV (MeOH) λmax (log ε) 203 (5.46), 297 (4.41) nm; ^{1}H and ^{13}C NMR, see **Table 2-11**; ESIMS (negative ion mode) *m*/*z* 429 [M −

H]$^-$; HREIMS *m*/*z* 430.3085 [M]$^+$ (calcd for $C_{27}H_{42}O_4$, 430.3083).

Sargachromanol V (13): colorless oil; $[\alpha]^{20}_D$ − 13.9° (*c* 0.94, MeOH); IR (KBr) ν_{max} 3404, 2970, 2860, 1705, 1616 cm^{-1}; UV (MeOH) λmax (log ε) 204 (5.66) and 297 (4.64) nm; ^{1}H and ^{13}C NMR, see **Table 2-12**; ESIMS (negative ion mode) *m*/*z* 359 [M − H]$^-$; HREIMS *m*/*z* 360.2303 [M]$^+$ (calcd for $C_{22}H_{32}O_4$, 360.2301).

2.4. DPPH radical scavenging assay

The DPPH radical scavenging activity was measured using an ESR spectrometer (JES-FA machine, JOEL, Tokyo, Japan) according to the technique described by Nanjo et al. (1996). 60 μl of each sample was added to 60 μl of DPPH (60 μmol/l) in ethanol. After 10 seconds of vigorous mixing, the solutions were transferred to Teflon capillary tubes and fitted into the cavity of the ESR spectrometer. The spin adduct was determined by the ESR spectrometer exactly 2 min later under the following measurement conditions: central field 3475 G, modulation frequency 100 kHz, modulation amplitude 2 G, microwave power 5 mW, gain 6.3×10^5, and temperature 298 K. All the radical scavenging activities (%) in the present study were calculated using the following equation, in which H and H_0 were the relative peak heights of the radical signals with and without a sample, respectively.

$$\text{Radical scavenging activity} = [1-(H / H_0)] \times 100$$

Table 2-1. ^{1}H and ^{13}C NMR assignments for fucoxanthin (**1**)

Position	^{13}C	^{1}H (mult. *J*=Hz)	Position	^{13}C	^{1}H (mult. *J*=Hz)
1	35.8		1'	35.2	
2	47.1	1.36 (1H, dd, *J*=8.7, 14.2) 1.49 (1H, dd, *J*=14.2)	2'	45.4	1.41 (1H, dd, *J*=10.4, 14.9) 2.00 (1H, dd, *J*=2.9, 14.9)
3	64.3	3.80 (1H, m)	3'	68.0	5.37 (1H, tt, *J*=8.8, 12.0)
4	41.6	1.77 (1H, dd, *J*=8.7, 14.2) 2.29 (1H, dd, *J*=2.9, 17.8)	4'	45.2	1.53 (1H, dd, *J*=10.4, 14.9) 2.29 (1H, dd, *J*=2.9, 17.8)
5	66.2		5'	72.7	
6	67.1		6'	117.5	
7	40.8	2.59, 3.64 (2H, d, *J*=20.4)	7'	202.4	
8	170.5		8'	103.4	6.04 (1H, s)
9	134.5		9'	132.5	
10	139.1	7.14 (1H, d, *J*=12.8)	10'	128.5	6.12 (1H, d, *J*=11.6)
11	123.4	6.58 (1H, m)	11'	125.7	6.71 (1H, t, *J*=12.0)
12	145.0	6.66 (1H, t, *J*=12.8)	12'	137.1	6.34 (1H, d, *J*=11.6)
13	135.4		13'	138.1	
14	136.6	6.40 (1H, d, *J*=11.6)	14'	132.2	6.26 (1H, d, *J*=11.6)
15	129.4	6.67 (1H, m)	15'	132.5	6.71 (1H, t, *J*=12.0, 14.2)
16	25.0	1.02 (3H, s)	16'	29.2	1.37 (3H, s)
17	28.1	0.95 (3H, s)	17'	32.1	1.06 (3H, s)
18	21.2	1.21 (3H, s)	18'	31.3	1.34 (3H, s)
19	11.8	1.93 (3H, s)	19'	14.0	1.80 (3H, s)
20	12.8	1.98 (3H, s)	20'	12.9	1.98 (3H, s)
			3'OAc, CH_3	21.4	2.03 (3H, s)
			3'OAc, C=O	197.9	

* 400 MHz for ^{1}H and 100 MHz for ^{13}C

Table 2-2. ^{1}H NMR assignments for loliolide (**2**) and isololiolide (**3**)

Position	^{1}H (mult. *J*=Hz)	
	Loliolide	**Isololiolide**
1		
2	1.53 (1H, dd, *J*=14.4, 3.6) 1.99 (1H, dt, J=14.4,2.4)	1.27 (1H, dd, *J*=12.8, 12.8) 1.99 (1H, ddd, J=12.8, 4.4, 2.4)
3	4.21 (1H, quintet, *J*=3.6)	4.08 (1H, tt, *J*=12.0, 4.4)
4	1.75 (1H, dd, *J*=14.0, 4.0) 2.42 (1H, dt, *J*=14.0, 2.4)	1.40 (1H, dd, *J*=11.6, 11.6) 2.53 (1H, ddd, *J*=11.6, 4.0, 2.0)
5		
6		
7	5.74 (1H,s)	5.76 (1H,s)
8		
9	1.46 (3H,s)	1.27 (3H,s)
10	1.27 (3H,s)	1.29 (3H,s)
11	1.76 (3H,s)	1.57 (3H,s)

* 400 MHz for ^{1}H and 100 MHz for ^{13}C

Table 2-3. ^{1}H and ^{13}C NMR assignments for nahocol D_2 (**4**)

Position	^{13}C	^{1}H (mult. *J*=Hz)
1	113.6	5.16 (1H, dd, *J*=10.4, 1.0)
		5.21 (1H, dd, *J*=17.6, 1.0)
2	144.0	6.06 (1H, dd, *J*=17.6, 10.4)
3	81.5	
4	42.0	1.72 (2H, m)
5	22.2	2.09 (2H, m)
6	124.8	
7	135.0	
8	39.1	2.03 (2H, m)
9	26.0	2.14 (2H, m)
10	127.7	5.40 (1H, t, *J*=6.8)
11	134.7	
12	80.4	3.84 (1H, d, *J*=6.0)
13	69.3	4.27 (1H, dd, *J*=8.8, 6.0)
14	124.3	5.16 (1H, t, *J*=8.8)
15	136.1	
16	25.0	1.74 (3H, s)
17	17.4	1.69 (3H, s)
18	11.2	1.64 (3H, s)
19	14.8	1.60 (3H, s)
20	22.0	1.35 (3H, s)
1'	147.4	
2'	119.7	6.89 (1H, d, *J*= 8.8)
3'	113.4	6.53 (1H, dd, *J*= 8.8, 3.2)
4'	151.4	
5'	117.6	6.63 (1H, d, *J*= 3.2)
6'	127.3	
7'	36.2	3.56 (2H, d, *J*= 3.2)
8'	173.1	
9'	51.1	3.66 (3H, s)

* 400 MHz for ^{1}H and 100 MHz for ^{13}C

Table 2-4. ^{1}H and ^{13}C NMR assignments for isopolycerasoidol (**5**)

Position	^{13}C	^{1}H (mult. *J*=Hz)
1	23.6	2.68 (2H, t, *J*=6.5)
2	32.9	1.78 (1H, m)
		1.72 (1H, m)
3	76.3	
4	40.6	1.63 (1H, m)
		1.53 (1H, m)
5	23.4	2.16 (2H, m)
6	126.7	5.20 (1H, t, *J*=7.0)
7	135.2	
8	39.5	2.12 (2H, t, *J*=7.0)
9	28.4	2.28 (2H, q, *J*=7.0)
10	143.1	6.71 (1H, t, *J*=7.0)
11	141.5	
12	12.7	1.78 (3H, s)
13	172.2	
14	15.9	1.60 (3H, s)
15	24.6	1.24 (3H, s)
1'	146.5	
2'	122.5	
3'	113.7	6.32 (1H, d, *J*=2.5)
4'	150.5	
5'	116.7	6.41 (1H, d, *J*=2.5)
6'	127.9	
7'	16.5	2.08 (3H, s)

* 500 MHz for ^{1}H and 125 MHz for ^{13}C

Table 2-5. ^{1}H and ^{13}C NMR assignments for sargachromanol D (**6**)

Position	^{13}C	^{1}H (mult. *J*=Hz)
1	23.6	2.68 (2H, t, *J*=6.5)
2	32.9	1.78 (1H, m)
		1.72 (1H, m)
3	76.3	
4	40.7	1.62 (1H, dt, *J*=15.1, 7.3)
		1.53 (1H, m)
5	23.4	2.11 (2H, dh, *J*=7.3, 7.0)
6	126.0	5.17 (1H, t, *J*=7.0)
7	136.0	
8	40.6	2.00 (2H, t, *J*=7.5)
9	27.5	2.12 (2H, m)
10	129.0	5.39 (1H, t, *J*=7.0)
11	136.0	
12	81.7	3.84 (1H, d, *J*=6.5)
13	70.7	4.27 (1H, dd, *J*=9.0, 6.5)
14	126.1	5.23 (1H, dt, *J*=9.0, 1.0)
15	137.4	
16	26.3	1.74 (3H, s)
17	18.7	1.68 (3H, s)
18	12.6	1.63 (3H, s)
19	16.1	1.59 (3H, s)
20	24.6	1.24 (3H, s)
1'	146.5	
2'	122.4	
3'	113.7	6.32 (1H, d, *J*=2.5)
4'	150.5	
5'	116.7	6.41 (1H, d, *J*=2.5)
6'	127.9	
7'	16.5	2.08 (3H, s)

* 500 MHz for ^{1}H and 125 MHz for ^{13}C

Table 2-6. ^{1}H and ^{13}C NMR assignments for sargachromanol E (**7**)

Position	^{13}C	^{1}H (mult. *J*=Hz)
1	23.6	2.68 (2H, t, *J*=6.5)
2	32.9	1.78 (1H, dt, *J*=13.2, 6.8)
		1.72 (1H, dt, *J*=13.2, 6.8)
3	76.3	
4	40.7	1.62 (1H, m)
		1.53 (1H, m)
5	23.4	2.11 (2H, dt, *J*=6.8, 7.3)
6	126.0	5.17 (1H, t, *J*=6.8)
7	136.0	
8	40.6	2.00 (2H, t, *J*=7.3)
9	27.5	2.12 (2H, dt, *J*=6.8, 7.3)
10	129.0	5.39 (1H, t, *J*=6.8)
11	136.0	
12	81.7	3.84 (1H, d, *J*=6.5)
13	70.7	4.27 (1H, dd, *J*=9.0, 6.5)
14	126.1	5.23 (1H, dt, *J*=9.0, 1.0)
15	137.4	
16	26.3	1.74 (3H, d, *J*=1.0)
17	18.7	1.68 (3H, d, *J*=1.5)
18	12.6	1.63 (3H, s)
19	16.1	1.59 (3H, s)
20	24.6	1.24 (3H, s)
1'	146.5	
2'	122.4	
3'	113.7	6.32 (1H, d, *J*=2.5)
4'	150.5	
5'	116.7	6.41 (1H, d, *J*=2.5)
6'	127.9	
7'	16.5	2.08 (3H, s)

* 500 MHz for ^{1}H and 125 MHz for ^{13}C

Table 2-7. ^{1}H and ^{13}C NMR assignments for sargachromanol G (**8**)

Position	^{13}C	^{1}H (mult. *J*=Hz)
1	22.2	2.65 (2H, *J*=7.2)
2	31.6	1.79 (1H, m)
		1.72 (1H, m)
3	75.0	
4	39.1	1.63 (1H, m)
		1.48 (1H, m)
5	22.1	2.12 (2H, m)
6	125.6	5.14 (1H, t, *J*=7.3)
7	133.7	
8	37.9	2.00 (2H, t, *J*=7.8)
9	27.1	2.34 (2H, m)
10	144.5	6.55 (1H, t, *J*=7.3)
11	134.4	
12	201.3	
13	69.8	5.36 (1H, d, *J*=9.6)
14	123.4	5.00 (1H, dh, *J*=9.6, 1.5)
15	137.9	
16	24.9	1.71 (3H, s)
17	17.3	1.82 (3H, s)
18	10.7	1.80 (3H, s)
19	14.6	1.59 (3H, s)
20	23.3	1.25 (3H, s)
1'	145.1	
2'	121.1	
3'	112.4	6.30 (1H, d, *J*=2.8)
4'	149.2	
5'	115.4	6.39 (1H, d, *J*=2.8)
6'	126.5	
7'	15.2	2.05 (3H, s)

* 400 MHz for ^{1}H and 100 MHz for ^{13}C

Table 2-8. ^{1}H and ^{13}C NMR assignments for sargachromanol I (**9**)

Position	^{13}C	^{1}H (mult. J=Hz)
1	23.6	2.68 (2H, t, J=6.5)
2	32.9	1.78 (1H, dt, J=13.7, 6.8)
		1.73 (1H, dt, J=13.7, 6.8)
3	76.3	
4	40.7	1.62 (1H, m)
		1.53 (1H, m)
5	23.3	2.10 (2H, m)
6	126.2	5.15 (1H, t, J=7.0)
7	135.7	
8	40.7	1.93 (2H, dd, J=6.8, 5.4)
9	26.6	1.32 (2H, m)
10	34.6	1.32 (2H, m)
11	42.6	2.69 (1H, m)
12	216.0	
13	75.9	4.87 (1H, d, J=9.8)
14	122.4	5.02 (1H, br d, J=9.8)
15	140.7	
16	26.2	1.78 (3H, s)
17	18.9	1.82 (3H, s)
18	17.0	1.01 (3H, d, J=6.5)
19	15.9	1.56 (3H, s)
20	24.6	1.24 (3H, s)
1'	146.5	
2'	122.7	
3'	113.7	6.32 (1H, d, J=2.5)
4'	152.7	
5'	226.7	6.41 (1H, d, J=2.5)
6'	127.9	
7'	16.0	2.07 (3H, s)

* 500 MHz for ^{1}H and 125 MHz for ^{13}C

Table 2-9. ^{1}H and ^{13}C NMR assignments for sargachromanol O (**10**)

Position	^{13}C	^{1}H (mult. *J*=Hz)
1	22.3	2.68 (2H, t, *J*=7.2)
2	31.5	1.79 (1H, m)
		1.74 (1H ,m)
3	75.0	
4	39.3	1.61 (1H, m)
		1.52 (1H, m)
5	22.0	2.10 (2H, m)
6	124.8	5.14 (1H, t, *J*=7.3)
7	132.9	
8	37.9	2.00 (2H, t, *J*=7.8)
9	26.3	2.26 (2H, m)
10	126.8	5.29 (1H, d, *J*=9.6)
11	134.2	
12	53.8	3.78 (1H, d, *J*=9.6)
13	121.1	5.37 (1H, d, *J*=9.6)
14	134.4	
15	178.5	
16	13.5	1.62 (3H, s)
17	16.9	1.60 (3H, s)
18	24.9	1.72 (3H, s)
19	14.7	1.57 (3H, s)
20	23.2	1.24 (3H, s)
1'	145.2	
2'	121.4	
3'	112.3	6.32 (1H, d, *J*=2.8)
4'	149.2	
5'	115.4	6.40 (1H, d, *J*=2.8)
6'	126.6	
7'	15.1	2.07 (3H, s)

* 400 MHz for ^{1}H and 100 MHz for ^{13}C

Table 2-10. ^{1}H and ^{13}C NMR assignments for sargachromanol T (**11**)

Position	^{13}C	^{1}H (mult. J=Hz)
1	23.6	2.68 (2H, t, J=6.5)
2	32.9	1.73 (1H, m)
		1.78 (1H, m)
3	76.4	
4	40.7	1.53 (1H, m)
		1.62 (1H, m)
5	23.4	2.13 (2H, dt, J=8.0, 8.0)
6	125.8	5.14 (1H, t, J=7.0)
7	136.3	
8	41.3	1.94 (2H, t, J=7.5)
9	27.0	1.22 (1H, m)
		1.48 (1H, m)
10	31.7	1.10 (1H, m)
		1.41 (1H, m)
11	36.4	1.56 (1H, m)
12	80.8	3.17 (1H, dd, J=9.0, 6.5)
13	70.5	4.27 (1H, dd, J=9.0, 6.5)
14	126.5	5.19 (1H, d, J=9.0)
15	136.7	
16	26.3	1.74 (3H, d, J=1.5)
17	18.7	1.69 (3H, d, J=1.5)
18	17.5	0.95 (3H, d, J=7.0)
19	16.0	1.56 (3H, s)
20	24.6	1.25 (3H, s)
1'	146.5	
2'	122.4	
3'	113.7	6.32 (1H, d, J=2.5)
4'	150.5	
5'	116.8	6.41 (1H, d, J=2.5)
6'	127.9	
7'	16.5	2.08 (3H, s)

* 500 MHz for ^{1}H and 125 MHz for ^{13}C

Table 2-11. ^{1}H and ^{13}C NMR assignments for sargachromanol U (**12**)

Position	^{13}C	^{1}H (mult. *J*=Hz)
1	23.6	2.68 (2H, t, *J*=6.5)
2	32.9	1.73 (1H, m)
		1.78 (1H, m)
3	76.4	
4	40.7	1.53 (1H, m)
		1.62 (1H, m)
5	23.4	2.13 (2H, dt, *J*=7.5, 7.5)
6	125.8	5.15 (1H, t, *J*=7.0)
7	136.3	
8	41.1	1.96 (2H, t, *J*=7.5)
9	26.6	1.35 (1H, m)
		1.44 (1H, m)
10	34.7	1.17 (1H, m)
		1.33 (1H, m)
11	35.4	1.70 (1H, m)
12	78.6	3.33 (1H, dd, *J*=6.5, 4.5)
13	69.9	4.24 (1H, dd, *J*=9.0, 6.5)
14	126.5	5.28 (1H, d, *J*=9.0)
15	137.6	
16	26.4	1.76 (3H, d, *J*=1.0)
17	18.7	1.71 (3H, d, *J*=1.0)
18	14.4	0.91 (3H, d, *J*=6.5)
19	15.9	1.57 (3H, s)
20	24.6	1.25 (3H, s)
1'	146.5	
2'	122.4	
3'	113.7	6.32 (1H, d, *J*=2.5)
4'	150.5	
5'	116.7	6.41 (1H, d, *J*=2.5)
6'	127.9	
7'	16.5	2.08 (3H ,s)

* 500 MHz for ^{1}H and 125 MHz for ^{13}C

Table 2-12. ^{1}H and ^{13}C NMR assignments for sargachromanol V (**13**)

Position	^{13}C	^{1}H (mult. *J*=Hz)
1	23.6	2.67 (2H, t, *J*=6.5)
2	32.9	1.78 (1H, m)
		1.72 (1H, m)
3	76.4	
4	40.8	1.62 (1H, m)
		1.52 (1H, m)
5	23.3	2.12 (2H, m)
6	126.0	5.15 (1H, t, *J*=7.0)
7	135.9	
8	40.7	1.97 (2H, t, *J*=7.0)
9	26.7	1.38 (2H, m)
10	34.6	1.58 (1H, m)
		1.33 (1H, m)
11	40.8	2.39 (1H, m)
12	17.8	1.11 (3H, s)
13	181.0	
14	15.9	1.56 (3H, s)
15	24.5	1.24 (3H, s)
1'	146.5	
2'	122.4	
3'	113.7	6.32 (1H, d, *J*=2.5)
4'	150.5	
5'	116.7	6.41 (1H, d, *J*=2.5)
6'	127.9	
7'	16.5	2.08 (3H, s)

* 500 MHz for ^{1}H and 125 MHz for ^{13}C

2.5. Hydroxyl radical scavenging assay

Hydroxyl radical scavenging activity was determined according to a slightly modified method of the 2-deoxyribose oxidation method (Chung et al., 1997). Hydroxyl radical was generated by Fenton reaction in the presence of $FeSO_4 \cdot 7H_2O$. A reaction mixture containing each 100 μl of 10 mM $FeSO_4 \cdot 7H_2O$, 10 mM EDTA and 10 mM 2-deoxyribose was mixed with 50 μl of the sample and 0.1 M phosphate buffer (pH 7.4) was added into the reaction mixture until the total volume reached to 800 μl. Then 100 μl of 10 mM H_2O_2 was finally added to the reaction mixture and incubated at 37℃ for 4 h. After incubation, each 100 μl of 2.8% TCA (trichloroacetic acid) and 1.0% TBA (thiobarbituric acid) were added. Then, the mixture was placed in a boiling water bath for 10 min. Absorbance was measured at 532 nm.

2.6. Hydrogen peroxide scavenging assay

Hydrogen peroxide scavenging activity was determined according to the method of Müller (1985). A hundred μl of 0.1 M phosphate buffer (pH 5.0) and the sample solution were mixed in a 96-well plate. A 20 μl of hydrogen peroxide was added to the mixture, and then incubated at 37℃ for 5 min. After the incubation, 30 μl of 1.25 mM ABTS and 30 μl of peroxidase (1 unit/ml) were added to the mixture, and then incubated at 37℃ for 10 min. The absorbance was read with an ELISA reader at 405 nm.

2.7. Antioxidant activities by cell lines

2.7.1. Cell culture

Cells of a monkey kidney fibroblast line (Vero) were maintained at 37℃ in an incubator with humidified atmosphere of 5% CO_2. Cells were cultured in Dulbecco's modified Eagle's medium containing 10% heat-inactivated fetal calf serum, streptomycin (100 μg/ml), and penicillin (100 unit/ml).

2.7.2. Hydrogen peroxide scavenging assay

For detection of intracellular H_2O_2, Vero cells were seeded in 96-well plates at a concentration of 1×10^5 cells/ml. After 16 h, the cells were treated with various concentrations of the compounds, and incubated at 37℃ under a humidified atmosphere. After 30 min, H_2O_2 was added at a concentration of 1 mM, and then cells were incubated for an additional 30 min at 37℃. Finally, 2',7'-dichlorodihydrofluorescein diacetate (DCFH-DA; 5 μg/ml) was introduced to the cells, and 2',7'-dichlorodihydrofluorescein fluorescence was detected at an excitation wavelength of 485 nm and an emission wavelength of 535 nm, using a Perkin-Elmer LS-5B spectrofluorometer. The percentage of H_2O_2 scavenging activity was calculated in accordance with the following equation:

$$H_2O_2 \text{ scavenging activity } (\%) = (1 - (C_1 / C_0)) \times 100$$

where C_1 is the fluorescence intensity of cells treated with H_2O_2 and compounds, and C_0 is the fluorescence intensity of cells treated with H_2O_2 and distilled water instead of compounds.

2.7.3. Assessment of cell viability

Cell viability was then estimated via an MTT assay, which is a test of metabolic competence predicated upon the assessment of mitochondrial performance. It is colorimetric assay, which is dependent on the conversion of yellow tetrazolium bromide to its purple formazan derivative by mitochondrial succinate dehydrogenase in viable cells (Mosmann, 1983). The cells were seeded in 96-well plate at a concentration of 1×10^5 cells/ml. After 16 h, the cells were treated with compounds at difference concentrations. Then, 10 μl of H_2O_2 (1 mM) was added to the cell culture medium, and incubated for 24 h at 37 ℃. MTT stock solution (50 μl; 2 mg/ml) was then applied to the wells, to a total reaction volume of 200 μl. After 4 h of incubation, the plates were centrifuged for 5 min at 800 ×g, and the supernatants were aspirated. The formazan crystals in each well were dissolved in 150 μl of dimethylsulfoxide (DMSO), and the absorbance was measured via ELISA at a wavelength of 540 nm. Relative cell viability was evaluated in accordance with the quantity of MTT converted to the insoluble formazan salt. The optical density of the formazan generated in the control cells was considered to represent 100% viability. The data are expressed as mean percentages of the viable cells versus the respective control.

2.7.4. Determination of DNA damage by comet assay

Comet assay was performed to determine the oxidative DNA damage (Singh, 2000). The cell suspension was mixed with 75 μl of 0.5% low melting agarose (LMA), and added to the slides precoated with 1.0% normal melting agarose (NMA). After solidification of the agarose, slides were covered with another 75 μl of 0.5% LMA and

then immersed in lysis solution (2.5 M NaCl, 100 mM EDTA, 10 mM Tris, and 1% sodium laurylasarcosine; 1% Triton X-100 and 10% DMSO) for 1 h at 4℃. The slides were next placed into an electrophoresis tank containing 300 mM NaOH and 10 mM Na_2EDTA (pH 13.0) for 40 min for DNA unwinding. For electrophoresis of the DNA, an electric current of 25 V/300 mA was applied for 20 min at 4℃. The slides were washed three times with a neutralizing buffer (0.4 M Tris, pH 7.5) for 5 min at 4℃, and then treated with ethanol for another 5 min before staining with 50 μl of ethidium bromide (20 μg/ml). Measurements were made by image analysis (Kinetic Imaging, Komet 5.0, U.K) and fluorescence microscope (LEICA DMLB, Germany), determining the percentage of fluorescence in the tail (tail intensity, TI; 50 cells from each of two replicate slides).

2.7.5. Nuclear staining with Hoechst 33342

The nuclear morphology of the cells was evaluated using the cell-permeable DNA dye, Hoechst 33342. Cell with homogeneously stained nuclei were considered viable, whereas the presence of chromatin condensation and/or fragmentation was indicative of apoptosis (Gschwind and Huber, 1995; Lizard et al., 1995). The cells were placed in 24-well plates at a concentration of 1×10^5 cells/ml. Sixteen hours after plating, the cells were treated with various concentration of the compounds, and further incubated for 1 h prior to expose to H_2O_2 (1 mM). After 24 h, 1.5 μl of Hoechst 33342 (stock 10 mg/ml), a DNA-specific fluorescent dye, were added to each well, followed by 10 min of incubation at 37℃. The stained cells were then observed under a fluorescence microscope equipped with a CoolSNAP-Pro color digital camera, in order to examine the degree of nuclear condensation.

2.8. Protective effect by ultra violet irradiation

2.8.1. Cell culture

Human fibroblast were kindly supplied by Surface Science Laboratory of Center for Anti-aging Molecular Science (CAMS) of Department of Chemistry and School of Molecular Science of Korea Advanced Institute of Science and Technology (KAIST), maintained at 37℃ in an incubator with humidified atmosphere of 5% CO_2. Cells were cultured in Dulbecco's modified Eagle's medium containing 10% heat-inactivated fetal calf serum, streptomycin (100 μg/ml), and penicillin (100 unit/ml).

2.8.2. UV-B irradiation

Cells were exposed to UV-B range at a dose rate of 10 to 100 mJ/cm^2 (UV Lamp, VL-6LM, Vilber Lourmat, France). Optimum irradiation dose were evaluated at 50 mJ/cm^2, therefore the 50 mJ/cm^2 of UV-B were used further experiments.

2.8.3. Intracellular reactive oxygen species measurement

For detection of intracellular ROS, fibroblast were seeded in 96-well plates at a concentration of 1×10^5 cells/ml. After 16 h, the cells were exposed to UV-B (50 mJ/cm^2) and the compounds were treated with various concentrations, and then cells were incubated for 24 h at 37℃ under a humidified atmosphere with 5% CO_2. Finally, 2',7'-dichlorodihydrofluorescein diacetate (DCFH-DA; 5 μg/ml) was introduced to the

cells, and 2',7'-dichlorodihydrofluorescein fluorescence was detected at an excitation wavelength of 485 nm and an emission wavelength of 535 nm, using a Perkin-Elmer LS-5B spectrofluorometer.

2.8.4. Assessment of cell viability

Cell viability was then estimated via an MTT assay, which is a test of metabolic competence predicated upon the assessment of mitochondrial performance. It is colorimetric assay, which is dependent on the conversion of yellow tetrazolium bromide to its purple formazan derivative by mitochondrial succinate dehydrogenase in viable cells (Mosmann, 1983). The fibroblast was seeded in 96-well plate at a concentration of 1×10^5 cells/ml. After 16 h, the cells were exposed to UV-B (50 mJ/cm^2) with compounds at difference concentrations, and then the cells were incubated for 24 h at 37℃. MTT stock solution (50 μl; 2 mg/ml) was then applied to the wells, to a total reaction volume of 200 μl. After 4 h of incubation, the plates were centrifuged for 5 min at 800 ×g, and the supernatants were aspirated. The formazan crystals in each well were dissolved in 150 μl of dimethylsulfoxide (DMSO), and the absorbance was measured via ELISA at a wavelength of 540 nm. Relative cell viability was evaluated in accordance with the quantity of MTT converted to the insoluble formazan salt. The optical density of the formazan generated in the control cells was considered to represent 100% viability. The data are expressed as mean percentages of the viable cells versus the respective control.

2.8.5. Determination of UV-B induced DNA damage by comet assay

Comet assay was performed to determine the irradiative DNA damage (Singh, 2000). The cell suspension was mixed with 75 μl of 0.5% low melting agarose (LMA), and added to the slides precoated with 1.0% normal melting agarose (NMA). After solidification of the agarose, slides were covered with another 75 μl of 0.5% LMA and then immersed in lysis solution (2.5 M NaCl, 100 mM EDTA, 10 mM Tris, and 1% sodium laurylasarcosine; 1% Triton X-100 and 10% DMSO) for 1 h at 4℃. The slides were next placed into an electrophoresis tank containing 300 mM NaOH and 10 mM Na_2EDTA (pH 13.0) for 40 min for DNA unwinding. For electrophoresis of the DNA, an electric current of 25 V/300 mA was applied for 20 min at 4℃. The slides were washed three times with a neutralizing buffer (0.4 M Tris, pH 7.5) for 5 min at 4℃, and then treated with ethanol for another 5 min before staining with 50 μl of ethidium bromide (20 μg/ml). Measurements were made by image analysis (Kinetic Imaging, Komet 5.0, U.K) and fluorescence microscope (LEICA DMLB, Germany), determining the percentage of fluorescence in the tail (tail intensity, TI; 50 cells from each of two replicate slides).

2.8.6. Microscopic analysis for dead cells

The type of cell death (apoptosis or necrosis) induced by UV-B was determined by fluorescent microscopy after staining with Hoechst 33342 and propidium iodide (PI), as described by Naito (2002). The fibroblasts were placed in 24-well plates at a concentration of 1×10^5 cells/ml. Sixteen hours after plating, the cells were exposed to UV-B (50 mJ/cm^2) with compounds at difference concentrations, and then the cells were

incubated for 24 h at 37℃. After 24 h, 1.5 μl of Hoechst 33342 (stock 10 mg/ml) and PI were added to each well, step by step, followed by 10 min of incubation at 37℃. The stained cells were then observed under a fluorescence microscope equipped with a CoolSNAP-Pro color digital camera, in order to examine the degree of nuclear condensation.

2.9. Inhibitory effect of melanin synthesis

2.9.1. Cell cultures

Mouse melanoma cell lines (B-16 F10) were maintained at 37℃ in an incubator, under a humidified atmosphere containing 5% CO_2. The cells were cultured in Dulbecco's modified Eagle's medium containing 10% heat-inactivated fetal calf serum, streptomycin (100 mg/ml), and penicillin (100 unit/ml).

2.9.2. Inhibitory effect of melanin synthesis

Melanin contents were measured according to the method of Tsuboi et al. (1998) with a slightly modification. The B-16 F10 cells were placed in 6-well plates at a concentration of 3×10^5 cells/ml, and 24 h after plating the cells were treated with various concentrations of the compounds. After 24 h, the medium was removed and cells were washed twice with PBS. And cell pellets containing a known number of cells (usually around 1×10^6) were dissolved in 1 ml of 1 N NaOH at 60℃ for 30 min and centrifuged for 10 min at 10,000 rpm. The optical densities (OD) of the supernatants were measured at 490 nm using an ELISA reader.

2.10. Statistical analysis

The data are expressed as the mean ± standard error (SE). A statistical comparison was performed via the SPSS package for Windows (Version 10). P-values of less than 0.05 were considered to be significant.

3. RESULTS AND DISCUSSIONS

We have previously screened the radical scavenging activity of methanolic extracts of 40 kinds of marine algae. The extract of *Sargassum siliquastrum*, a brown alga, showed higher scavenging effects on ABTS and DPPH radicals, especially in $CHCl_3$ extract. Therefore, the present study clearly demonstrated that the $CHCl_3$ extract was fractionated by silica gel and Sephadex LH-20 open column chromatography and the active compounds were purified by reversed-phase HPLC.

Fucoxanthin (**1**) was isolated as a bright orange solid and the IR spectrum of **1** showed the presence of the hydroxyl (3438 cm^{-1}), sp-hybrid carbon (allenic) (2361, 2332 cm^{-1}), ester (1723, 1251 cm^{-1}), and polyene (1654, 1605 cm^{-1}). The ^{1}H and ^{13}C NMR spectra of **1** revealed signals assignable to polyene having acetyl, conjugated ketone, two quaternary geminal dimethyls, two quaternary geminal methyls of oxygen, four olefinic methyls, and allene functionalities. The physicochemical features outlined above suggested that **1** was a carotenoid in which one of the hydroxyl groups was acetylated. From detailed comparison of the data for **1** with those of fucoxanthin, **1** was in agreement with an authentic fucoxanthin in all aspects (Palermo et al., 1991; Choi et al., 2000). Based on the above evidence, **1** was determined as fucoxanthin.

Loliolide (**2**) was isolated as colorless gum and the IR spectrum of **2** showed the presence of the hydroxyl (3439 cm^{-1}), and ester (1720 cm^{-1}) groups. The ^{1}H NMR spectrum exhibits characteristic peak at δ_H 1.27, 1.46, and 1.76 attributable to three methyl protons, at δ_H 1.53, 1.75, 1.99, 2.42, and 4.21 attributable to one carbinal proton, and at δ_H 5.74 attribute to double bond on aromatic ring. In addition, the ^{13}C NMR spectrum of **2** revealed signals assignable to α, β-unsaturated-γ-lactone group and oxygenated carbon. Isololiolide (**3**) also isolated as colorless gum and the IR and NMR

spectrum showed very similar peak pattern compared to **2**. As mention of characteristics on the **2** and **3**, that was identified by comparing their ^{1}H and ^{13}C NMR data to the literature report (Pettit et al., 1980; Park et al., 2004).

Nahocol D_2 (**4**), a colorless oil, and the IR indicated the presence of hydroxyl (3600, 3500 cm^{-1}) and ester (1730 cm^{-1}). The ^{1}H NMR was consistent with the presence of four olefinic methyls, and four double bonds and the structure of the **4** identified by comparing the NMR spectral data with those in existing literature (Tsuchiya et al., 1998).

Isopolycerasoidol (**5**) was obtained as colorless oil, and the EIMS revealed a fragment ion as *m/z* 358 $[M]^{+}$, corresponding to a molecular formula of $C_{22}H_{30}O_4$. The ^{1}H NMR was consistent with four methyl protons and four olefinic protons and the structure of the **5** identified by comparing the NMR spectral data with those in existing literature (Gonzalez et al., 1995).

Sargachromanols D (**6**) and E (**7**), isomeric metabolites, were analyzed for $C_{27}H_{40}O_4$ by HREIMS and ^{13}C NMR spectrometry. The ^{1}H NMR indicated the presence of three olefinic protons at δ_H 5.39, 5.23, and 5.17, and six methyl protons at δ_H 2.08, 1.74, 1.68, 1.63, 1.59, and 1.24. A combination of 2D NMR experiments defined the structures of both compounds as tetraprenyl chromanols containing hydroxyl groups at C-12 and C-13. Significant differences between these compounds on the chemical shifts of protons and carbon at asymmetric centers and nearby positions (C-10−C-15, C-18) in the NMR data as well as coupling constants of oxymethine protons suggested that **6** and **7** were diastereomers of each other.

Sargachromanols G (**8**) showed an HREIMS $[M]^{+}$ ion peak at m/z 426.2774 for a molecular formula of $C_{27}H_{38}O_4$ (calcd 426.2770). The ^{13}C NMR data for this compound were very similar to those of **6** and **7**, with the replacement of an oxymethine with a

carbonyl carbon at δ_C 201.3 as the most significant difference. Combined analyses of 2D NMR data located the carbonyl and remaining hydroxyl group at C-12 and C-13, respectively.

Sargachromanol I (**9**) showed a molecular ion peak in the HREIMS at *m*/*z* 428.2924 for the molecular formula of $C_{27}H_{40}O_4$ (calcd 428.2927). The NMR data for the compound was very similar those of compound **8**. A combination of 2D NMR experiments readily defined the structure of **9** as the 10, 11-dihydro derivative of **8**.

Sargachromanol O (**10**) was assigned as $C_{27}H_{38}O_4$ by combined HREIMS and ^{13}C NMR spectrometry. The spectral data for this compound were very similar to those of Sargachromanol L (Jang et al., 2005). The replacement of the C-12 oxymethylene with a carboxyl group at δ_C 178.5 in the ^{13}C NMR data was deduced by detailed 2D NMR analyses and IR measurement (1705 cm^{-1}).

Sargachromanol T (**11**), a novel compound, showed a molecular ion peak in the HREIMS at *m*/*z* 430.3085 for the molecular formula of $C_{27}H_{42}O_4$ (calcd 430.3085) and, therefore, had the fourteen degrees of unsaturation number. The ^1H NMR data acquired in MeOH-d_4 (**Table 2-11**) indicated the presence of two meta-coupled aromatic protons at δ_H 6.41 and 6.32, two olefinic protons at δ_H 5.19 and 5.14, and six methyl protons at δ_H 2.08, 1.74, 1.69, 1.56, 1.25 and 0.95. The ^{13}C NMR analysis in combination with the HMQC analysis revealed the presence of six aromatic (δ_C 150.5, 146.5, 127.9, 122.4, 116.8 and 113.7), four olefinic (δ_C 136.7, 136.3, 126.5, 125.8), two hydroxyl-substituted methine (δ_C 80.8, 70.5), one methyl-substituted methine (δ_C 36.4), seven methylene (δ_C 41.3, 40.7, 32.9, 31.7, 27.0, 23.6, 23.4) and six methyl (δ_C 26.3, 24.6, 18.7, 17.5, 16.5 and 16.0) carbons. The HMQC analysis allowed the assignment of proton resonances directly bonded to carbon atoms, and three partial structures were established by the ^1H-^1H COSY analysis (**Fig. 2-18**). Partial structure was accomplished by the sequential

proton couplings between H_3-7'/H-5'/H-3'/H-1/H-2. The ^{1}H-^{1}H couplings between H-4/H-5/H-6 gave the partial structure b. Also, the proton coupling networks of H-8/H-9/H-10/H-11/H-12/H-13/H-14 and H-11/H-18 allowed the construction of partial structure c. The HMBC correlations of H_2-1 with C-1' and C-3, and H_2-2 with C-3, C-4 and C-20 connected the partial structure a with b. Also, the heteronuclear long range correlations of H-6 with C-7, C-8 and C-19, H_2-8 with C-6, C-7 and C-19, and H_2-9 with C-7 gave the connection of the partial structure c with a-b. Finally, the additional HMBC cross-peak between H-14 and C-16 and C-17 completed the planar structure of compound **11**. From the above spectroscopic analysis, the accomplished structure of **11** was found to be similar with sargachromanol D (**6**) which has the chromanol moiety attached to the sesquiterpenoid linear chain, but the subtle difference is the reduction of the double bond between C-10 and C-11 in compound **11** (Jang et al., 2005).

The HREIMS analysis for Sargachromanol U (**12**), a novel compound, suggested the same molecular formula ($C_{27}H_{42}O_4$) with 1. Also, the ^{1}H and ^{13}C NMR data for compound **12** were very similar to those obtained for **11** and the intensive 2D NMR analysis for **12** indicated the same planar structure with **11**. However, significant chemical shift differences and variations in the splitting pattern of similarly assigned protons in the ^{1}H NMR spectra of **11** and **12** were showed. Proton resonances of H-11, H-12, and H-14 were shifted to the downfield region, whereas H-13 was shifted to upfield region in ^{1}H NMR spectrum. Also, ^{13}C NMR spectrum showed the upfield shifts of C-11, C-12 and C-13. From the chemical shift differences in ^{1}H and ^{13}C NMR data, the relative stereochemistry at hydroxylated C-12 and C-13 positions was inferred for compounds **11** and **12**.

The relative configurations of compounds **11** and **12** were determined by a combination of coupling constants, ^{1}H and ^{13}C NMR chemical shifts and 2D NOE

experiments. From the published data, 12'-hydroxylated meroterpenoids isolated from S. species showed the 12'S* configuration in all cases. Therefore, the relative configurations of compounds 1 and 2 were assigned by observing the spatial proximity of H-12 with H-11, H-13, H-18 and H-14 by 2D NOE experiments without cyclic ketal formation. The NOE cross-peaks of H-12 with H-11 and H-13, and H-13 with H-11 allowed the assignment of 11'S*, 12'S* and 13'S* configurations (syn orientation between 12'-H and 13'-H) for compound **11**, whereas the NOE correlations of H-12 with H-11 and H-13 with H_3-18 indicated the 11'S*, 12'S* and 13'R* configurations (anti orientation) for compound **12** (**Fig. 2-28**).

Sargachromanol V (**13**), a novel compound, showed an HREIMS $[M]^+$ ion peak at *m*/*z* 360.2303 for a molecular formula of $C_{22}H_{32}O_4$ (calcd 360.2301). The IR spectrum exhibited the absorption bands at 3404, 1705 cm^{-1}, indicating the presence of hydroxyl and carbonyl groups. The ^1H NMR chemical shifts at δ_H 6.41, 6.32, which showed meta-coupling, 2.67, 2.07, 1.78 and 1.72, and ^{13}C NMR chemical shifts at δ_C 150.5, 146.5, 127.9, 122.4, 116.7, 113.7, 76.4, 32.9, 23.6 and 16.5 in combination with the ^1H-^1H COSY and HMBC spectra indicated the presence of 4'-hydroxylated chromene moiety as the substructure a of compound **13**. Another ^1H NMR chemical shifts at δ_H 5.15 (H-6), 2.12 (H-5), 1.62 (H-4a) and 1.52 (H-4b), and ^1H-^1H COSY correlations between H_2-4/H_2-5/H-6 revealed the substructure b of -CH_2-CH_2-CH=C-. In addition, the substructure c of –CH_2-CH_2-CH_2-CH-CH_3 was deduced by the ^1H NMR chemical shifts at δ_H 2.39 (H-11), 1.97 (H-8), 1.58 (H-10a), 1.38 (H-9), 1.33 (H-10b) and 1.11 (H-12), and the sequential proton couplings between H_2-8/H_2-9/H_2-10/H-11/H-12. The connection among the substructures a, b and c were determined by HMBC analysis. The HMBC cross peaks of H-1 with C-3, H_2-2 with C-4 and C-15, H_2-4 with C-2 and C-15, and H_2-5 with C-3 connected substructure a with b. Also, the heteronuclear long range

correlations of H-8 with C-6 and C-14, H-9 and H-5 with C7, and H6 with C-14 and C-8 indicated the connection of substructure c with a-b. Finally, the HMBC correlations of H-12 and H-10 with C-13 revealed the carboxyl substitution at C-11 position. From the above spectroscopic analysis, the compound **13** was determined as the structure which has the chromanol moiety attached to the 11-carboxylated monoterpenoid. The structure of compound **13** is similar with polycerasoidol (**3**), but small difference is the reduction of the double bond between C-10 and C-11 (Tsuchiya et al., 1998).

In the present study, we isolated 13 kinds of compounds from *S. siliquastrum* and characteristics of those compounds were described above. Out of these compounds, compounds **2** and **3** exhibited poor activities on cosmeceutical experiments, and compounds **4**, **5**, **11**, and **12** obtained a few amount compared to other compounds. Therefore, we presented compounds **1**, **6**, **7**, **8**, **9**, **10**, and **13** results regarding on cosmeceutical experiments.

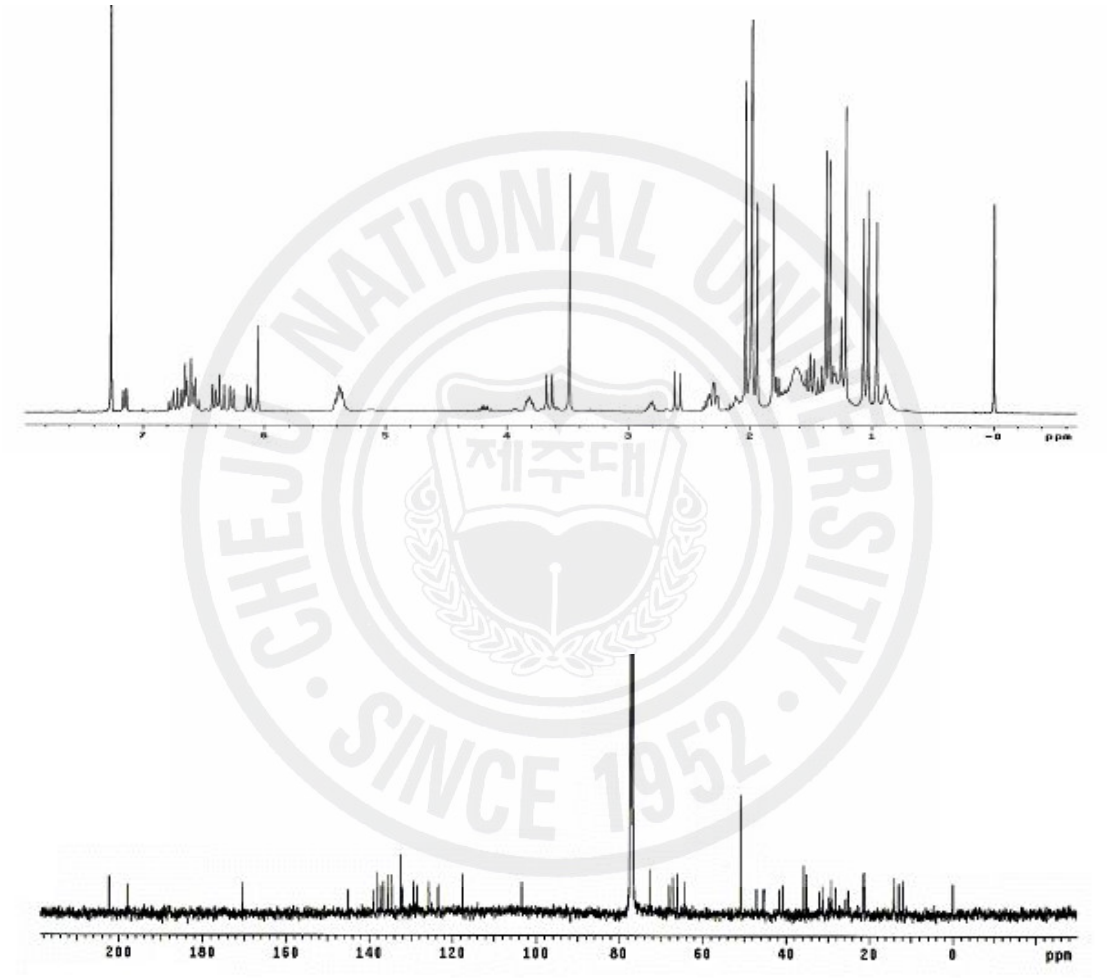

Fig. 2-3. Proton and Carbon NMR spectrum of fucoxanthin (**1**).

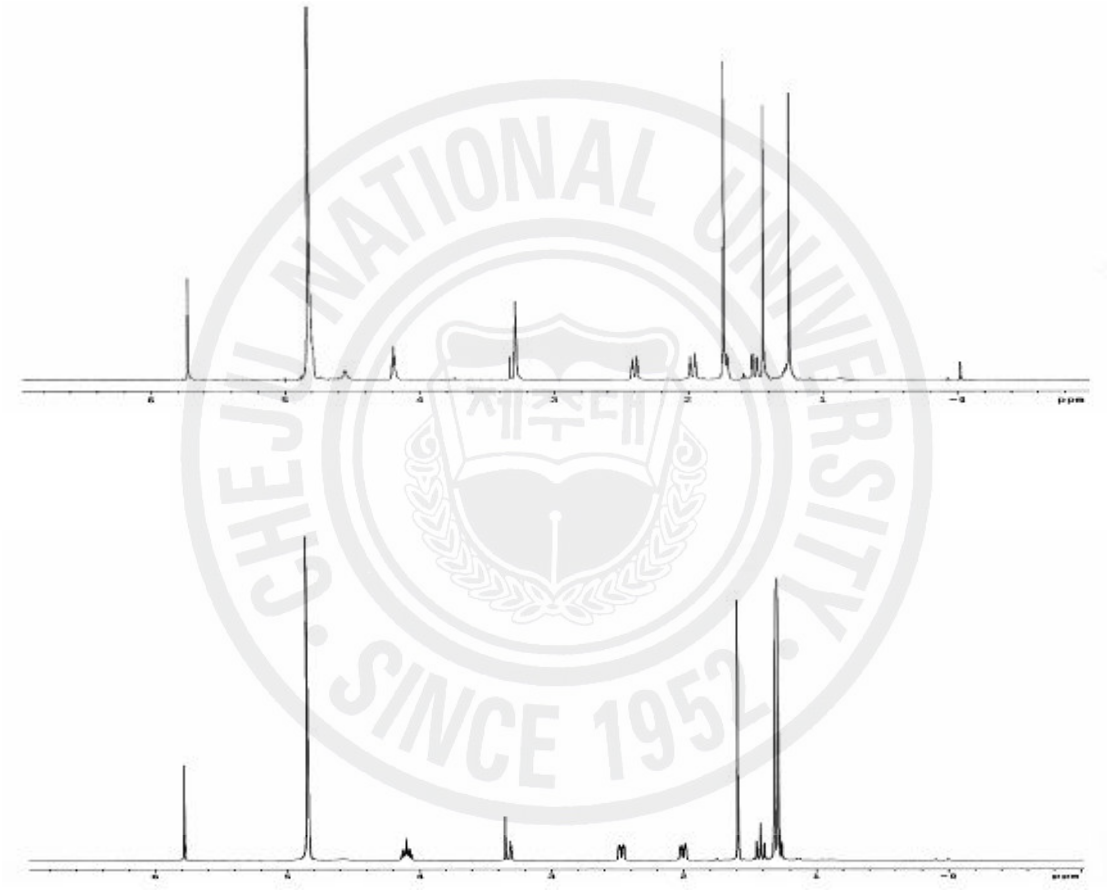

Fig. 2-4. Proton NMR spectrum of loliolide (**2**) and isololiolide (**3**).

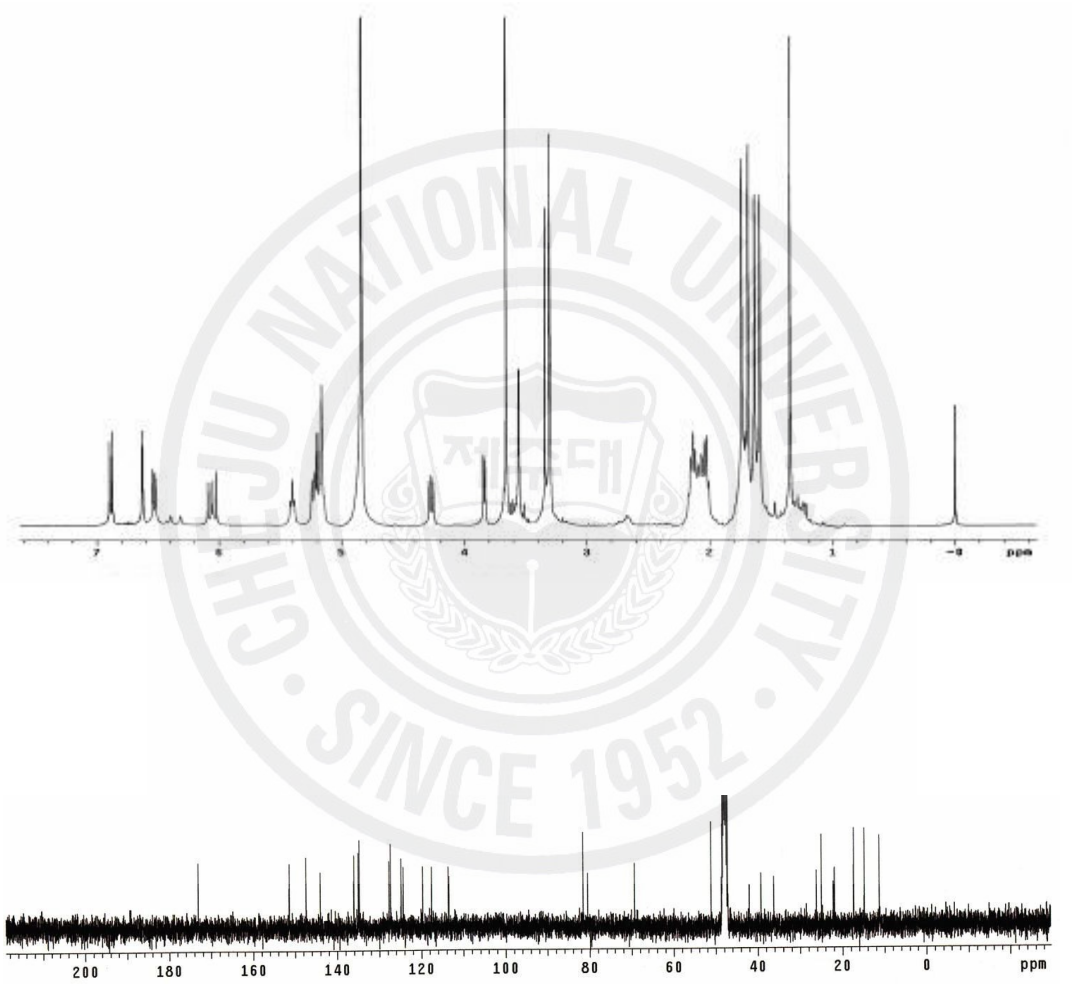

Fig. 2-5. Proton and Carbon NMR spectrum of nahocol D_2 (**4**).

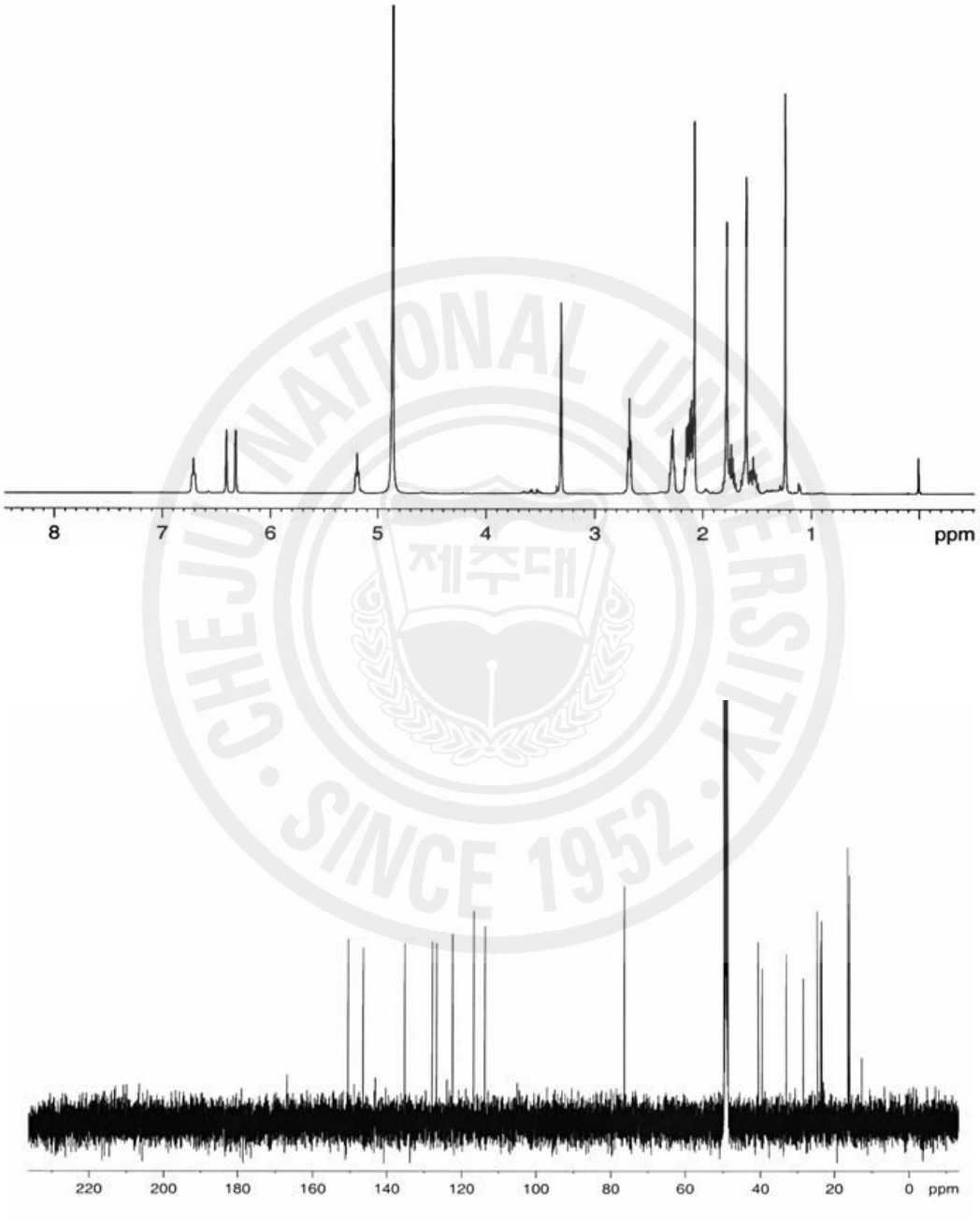

Fig. 2-6. Proton and Carbon NMR spectrum of isopolycerasoidol (**5**).

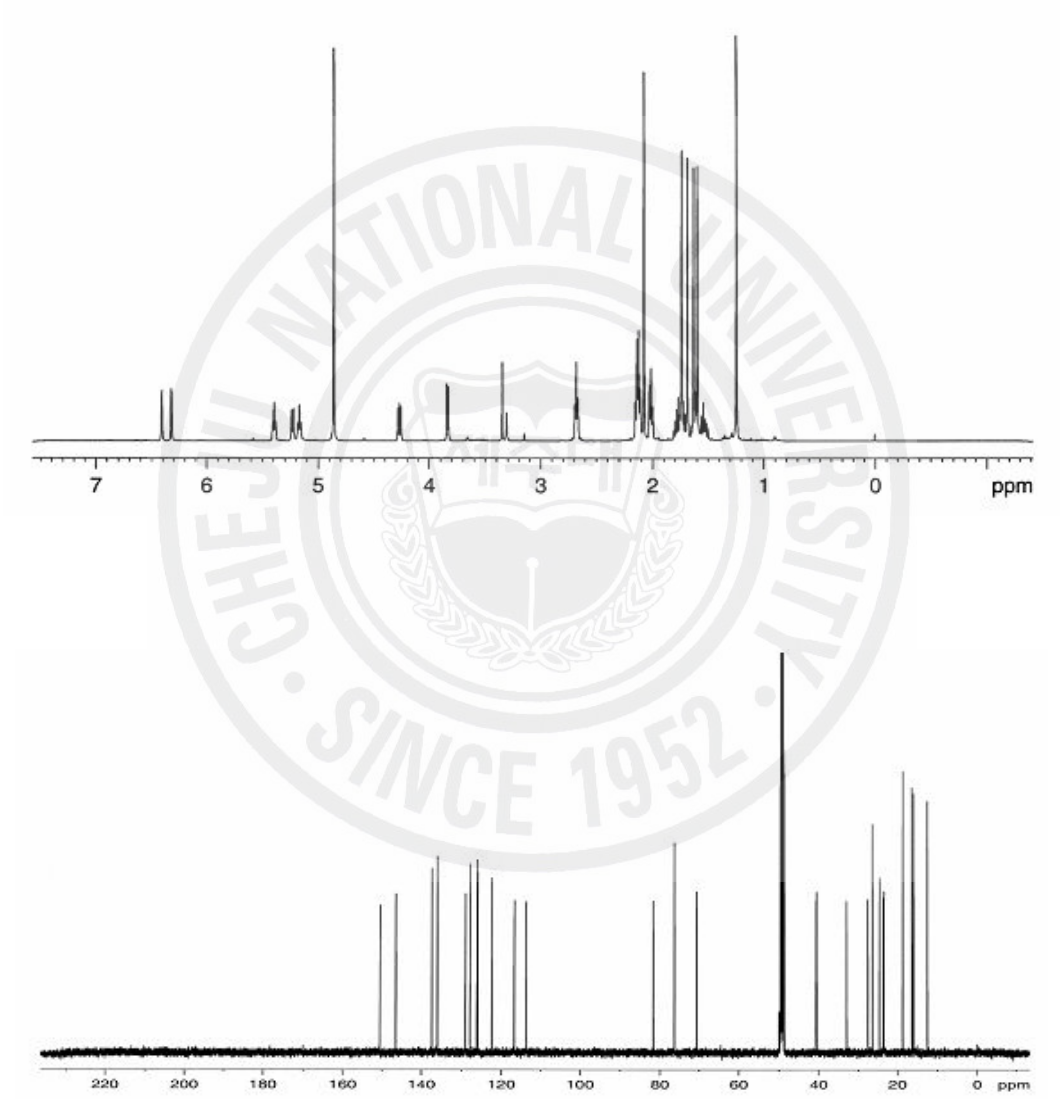

Fig. 2-7. Proton and Carbon NMR spectrum of sargachromanol D (**6**).

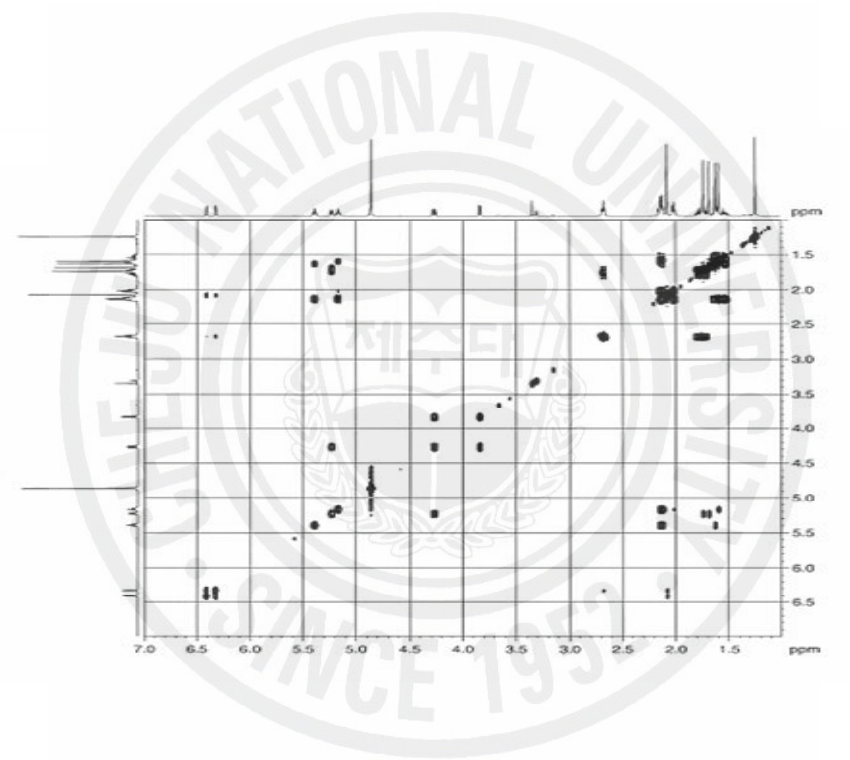

Fig. 2-8. Gradient COSY NMR spectrum of sargachromanol D (**6**).

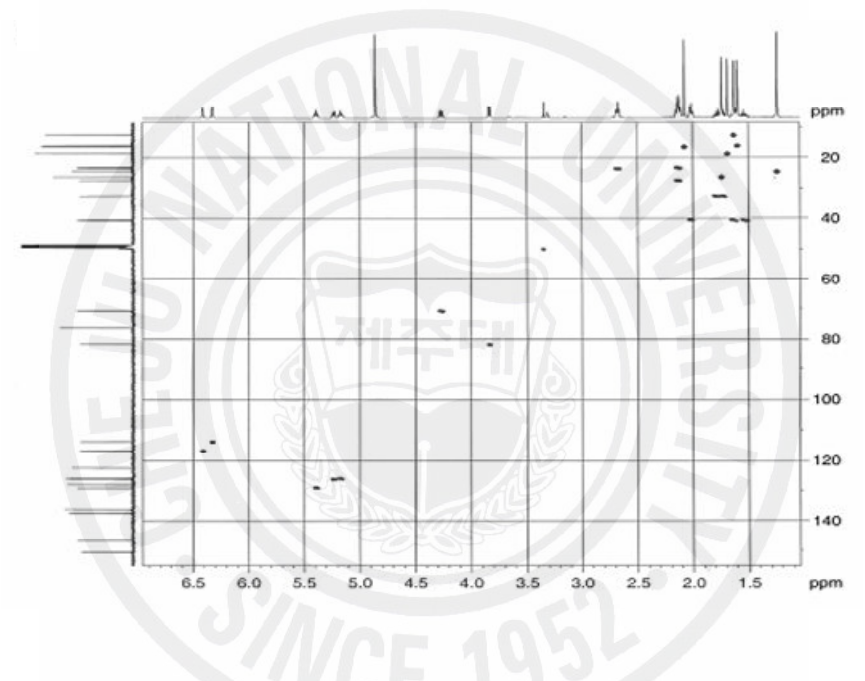

Fig. 2-9. Gradient HMQC NMR spectrum of sargachromanol D (**6**).

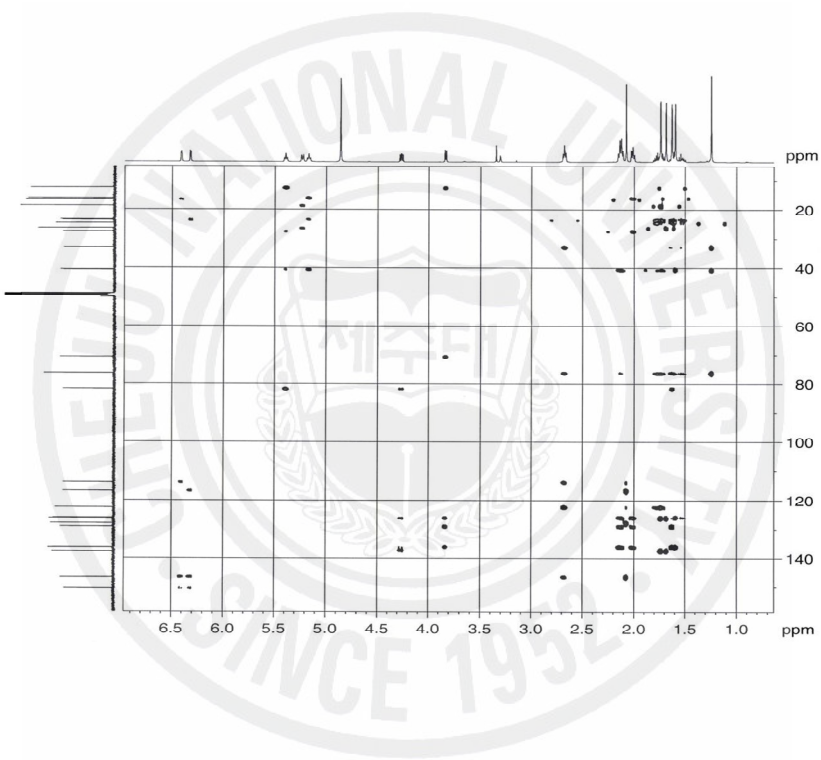

Fig. 2-10. Gradient HMBC NMR spectrum of sargachromanol D (**6**).

Fig. 2-11. Selective long range correlations for sargachromanol D (**6**).

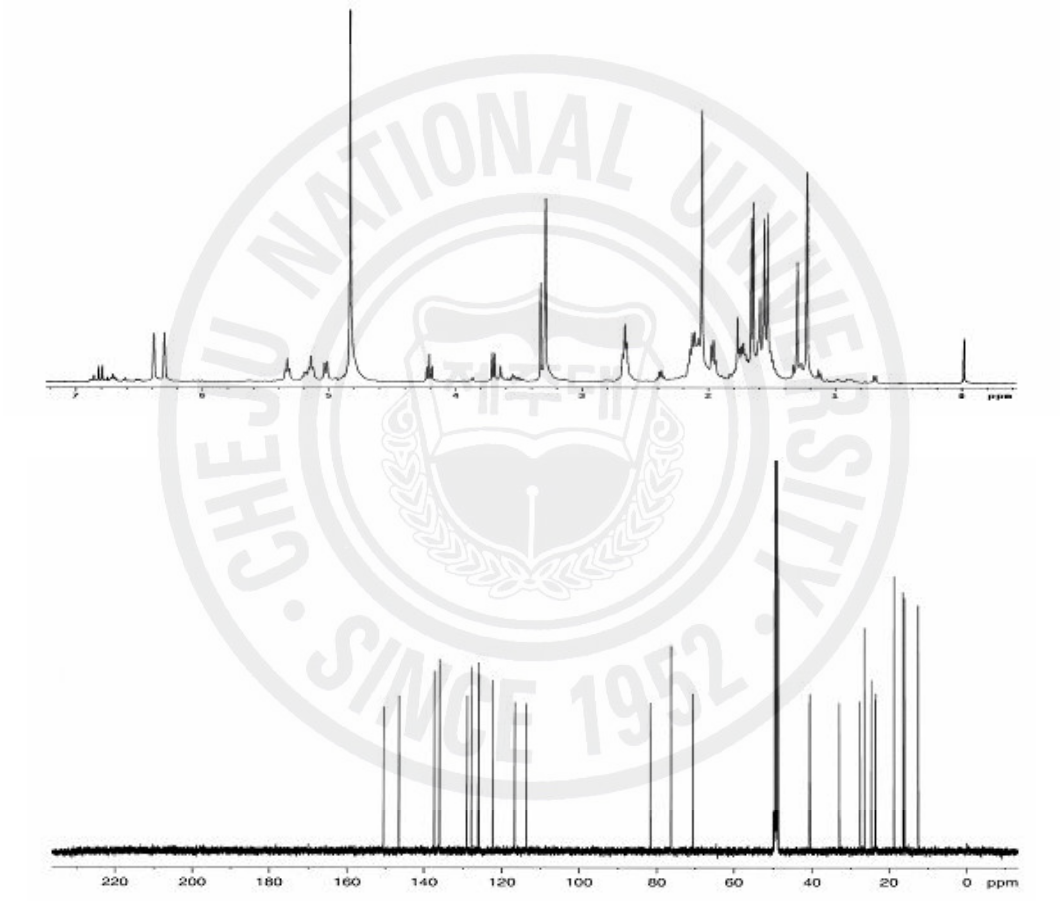

Fig. 2-12. Proton and Carbon NMR spectrum of sargachromanol E (**7**).

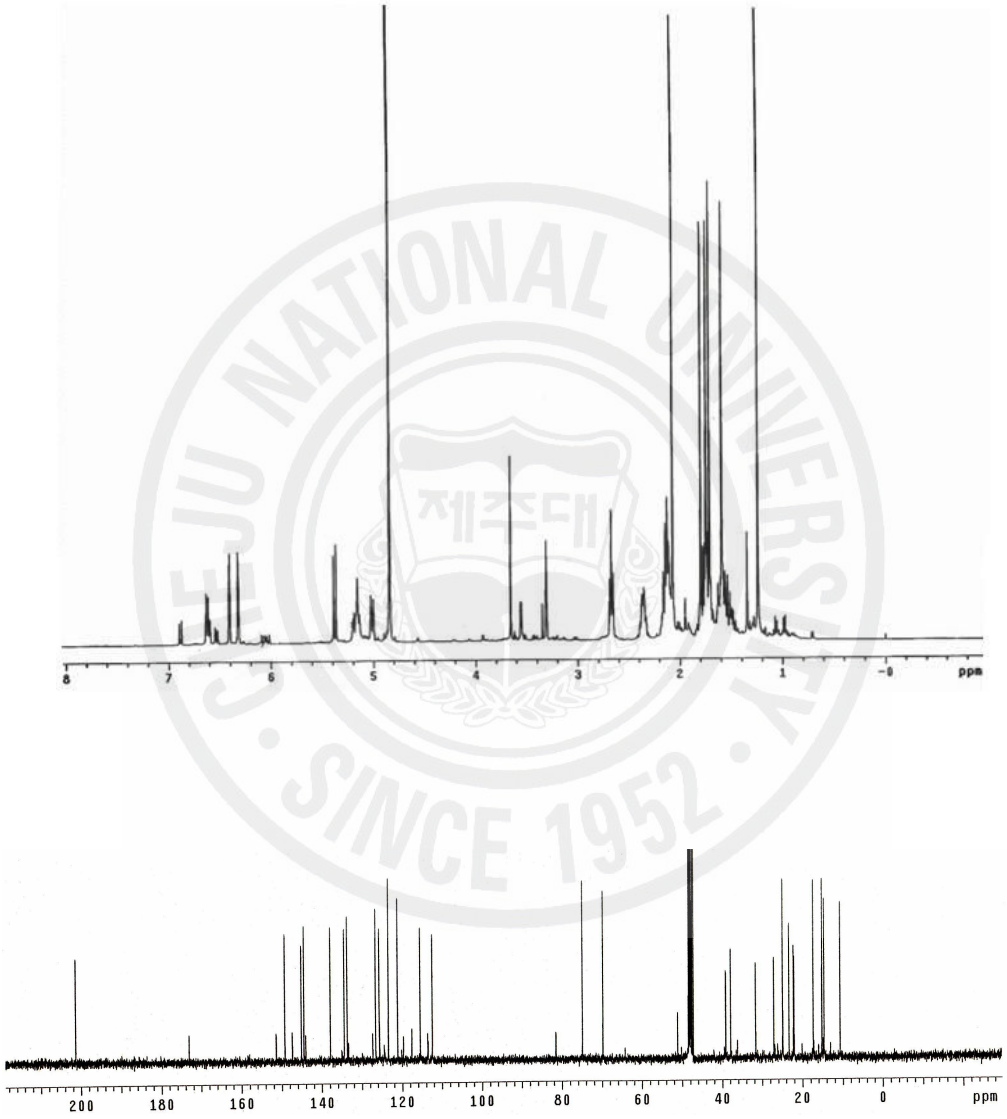

Fig. 2-13. Proton and Carbon NMR spectrum of sargachromanol G (**8**).

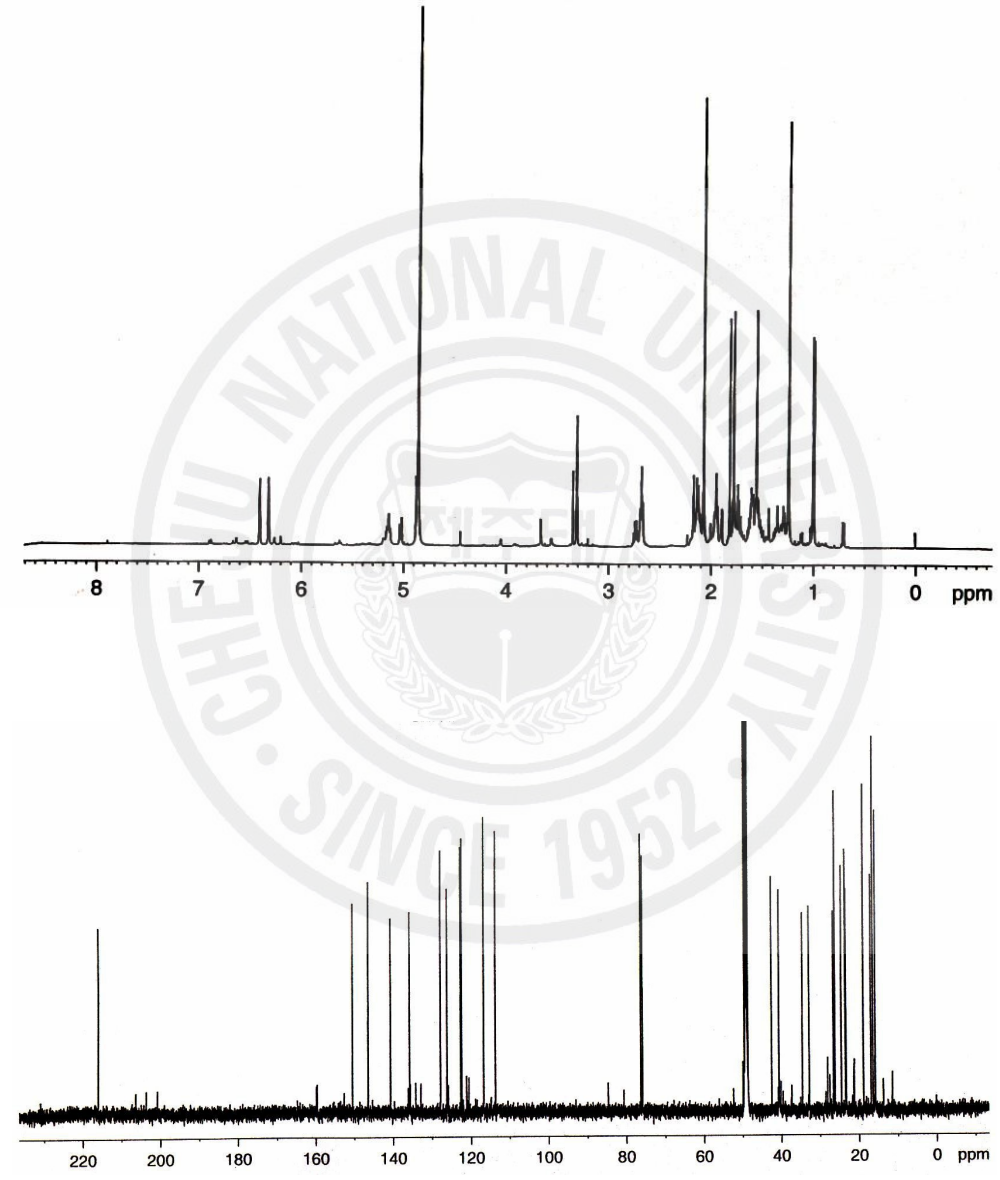

Fig. 2-14. Proton and Carbon NMR spectrum of sargachromanol I (**9**).

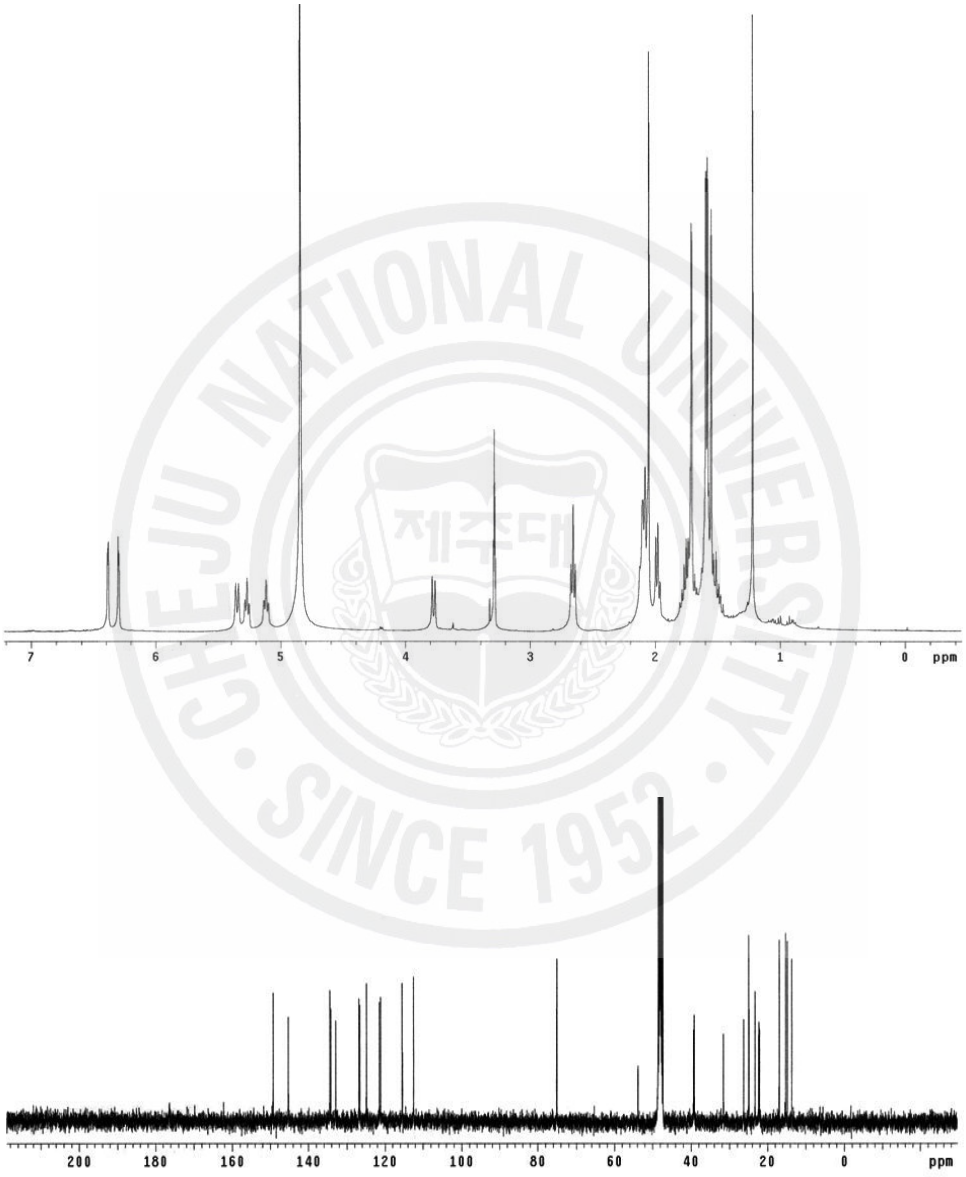

Fig. 2-15. Proton and Carbon NMR spectrum of sargachromanol O (**10**).

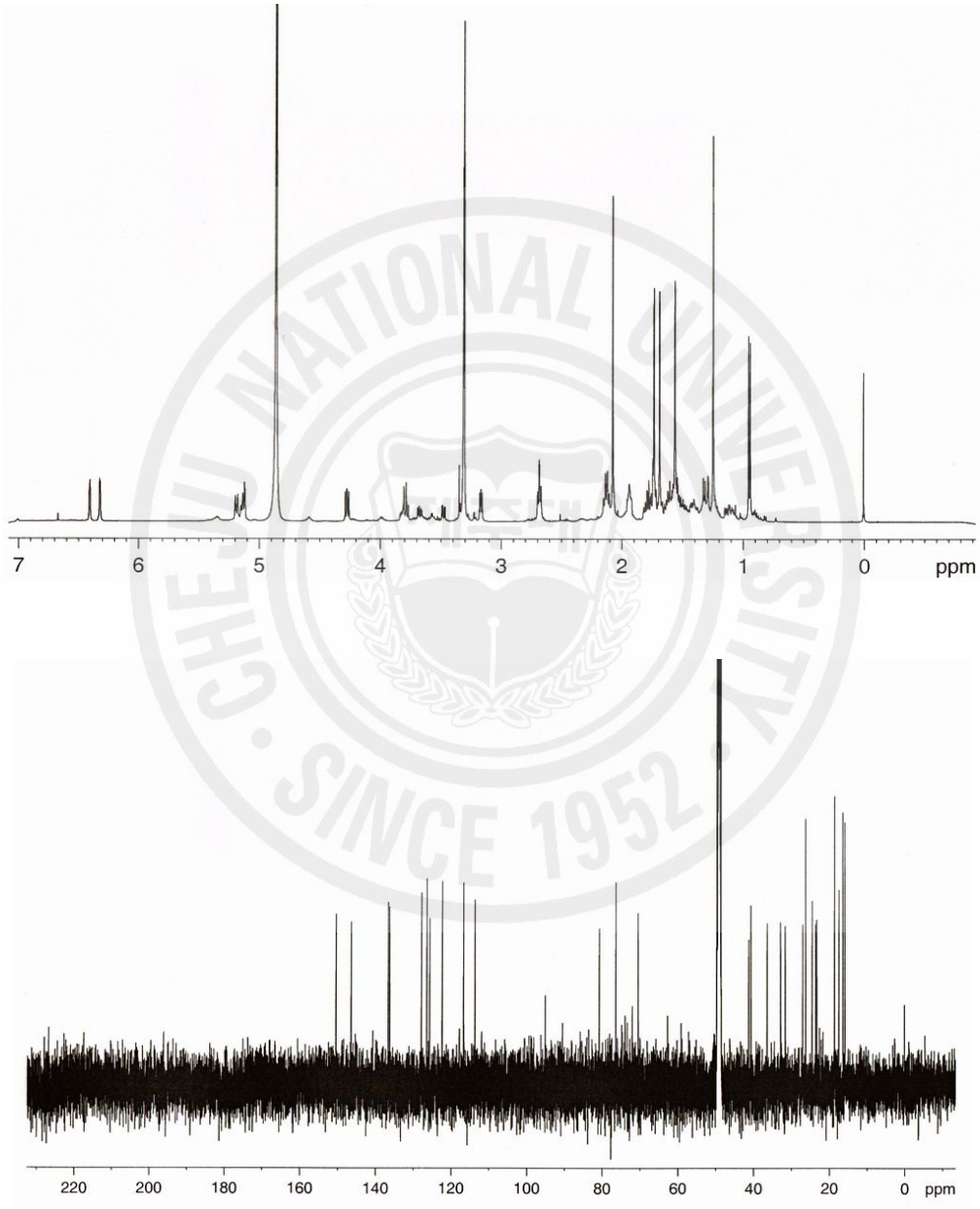

Fig. 2-16. Proton and Carbon NMR spectrum of sargachromanol T (**11**).

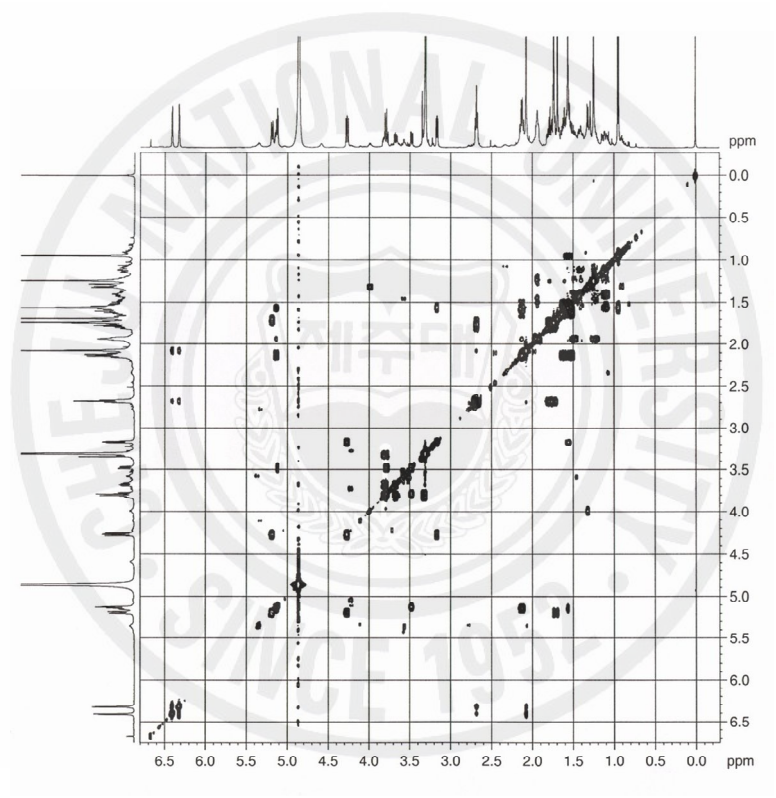

Fig. 2-17. Gradient COSY NMR spectrum of sargachromanol T (**11**).

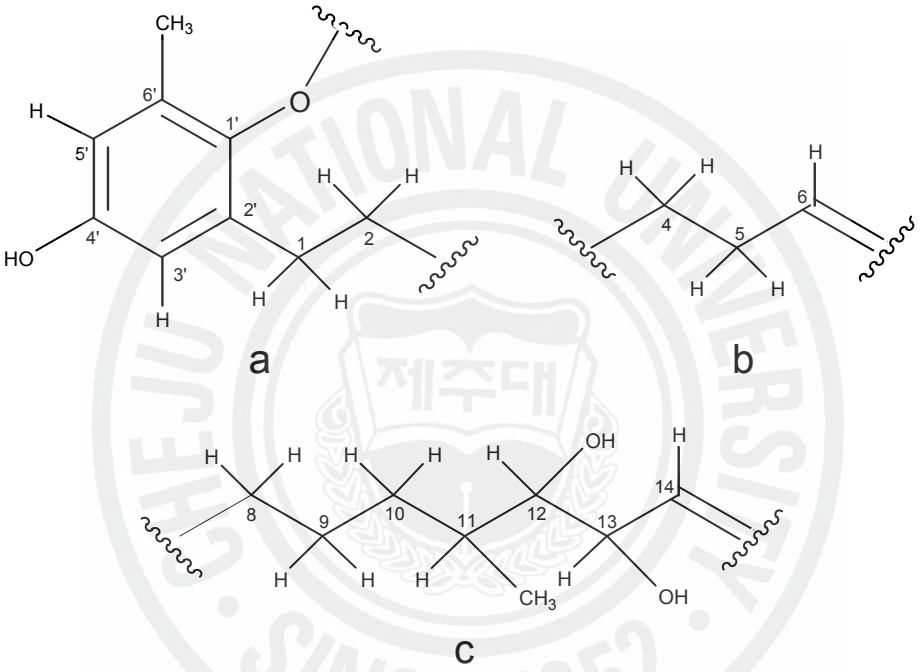

Fig. 2-18. Partial structures a, b, and c for sargachromanol T (**11**) deduced from COSY spectrum.

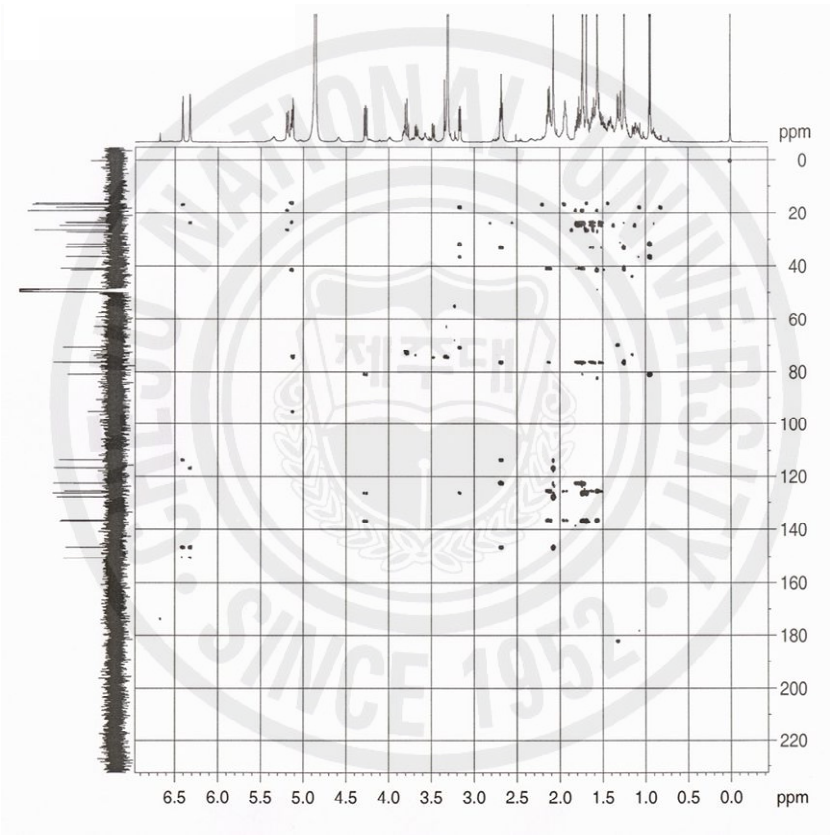

Fig. 2-19. Gradient HMBC NMR spectrum of sargachromanol T (**11**).

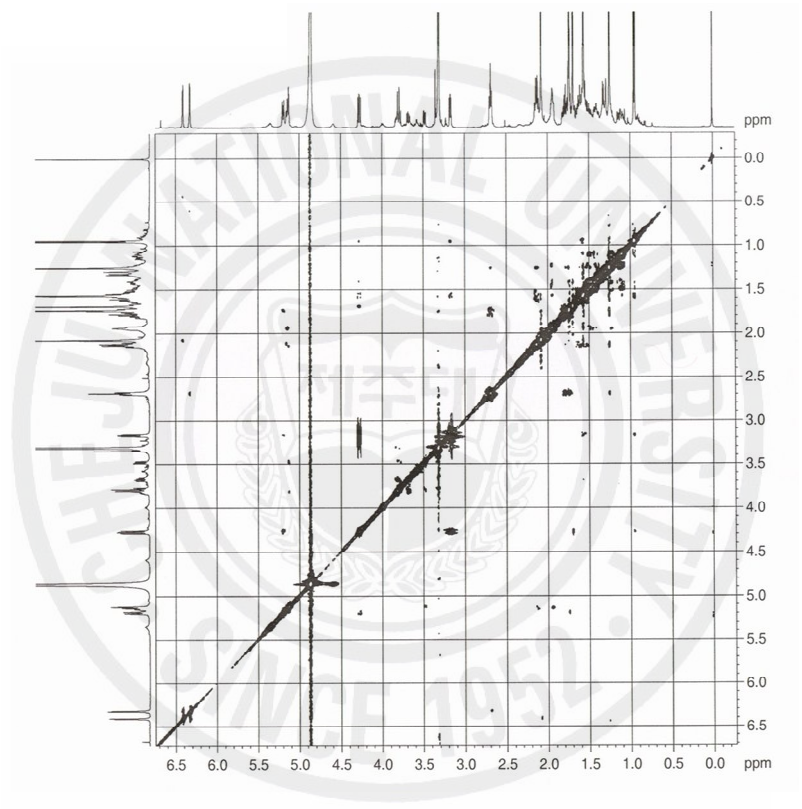

Fig. 2-20. Gradient ROESY NMR spectrum of sargachromanol T (**11**).

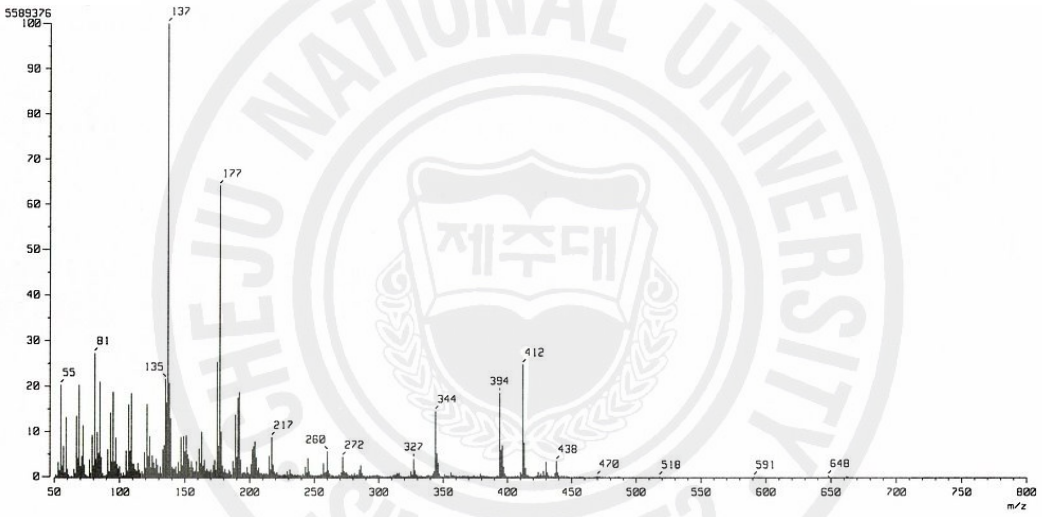

Fig. 2-21. MS spectrum of sargachromanol T (**11**).

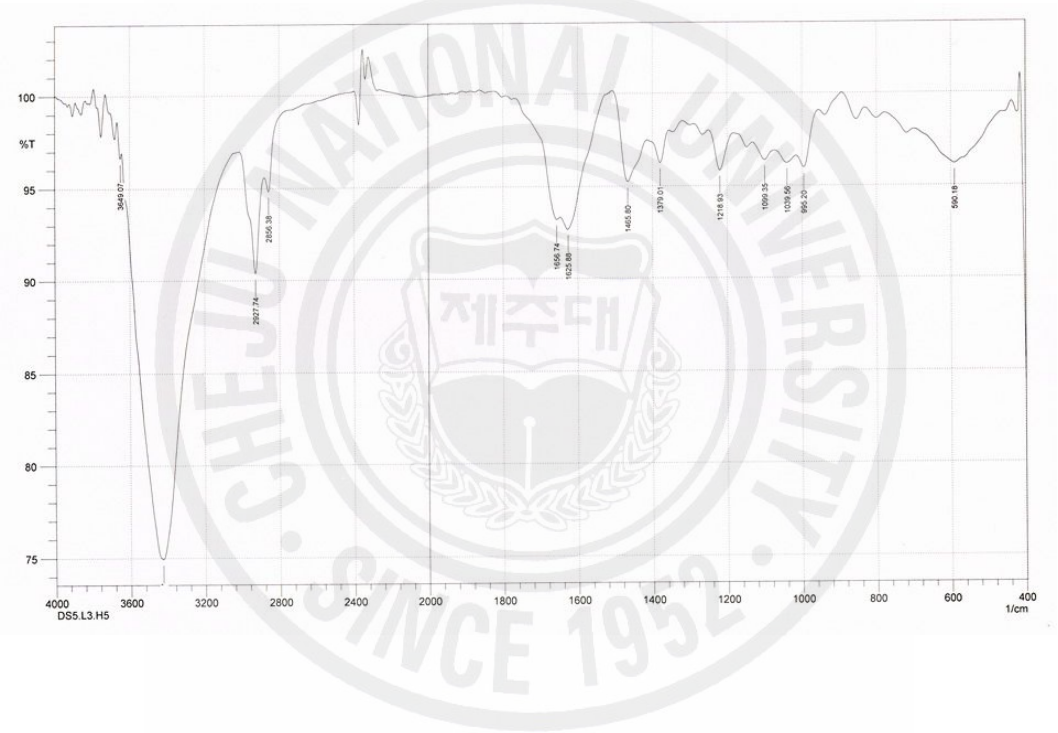

Fig. 2-22. IR spectrum of sargachromanol T (**11**).

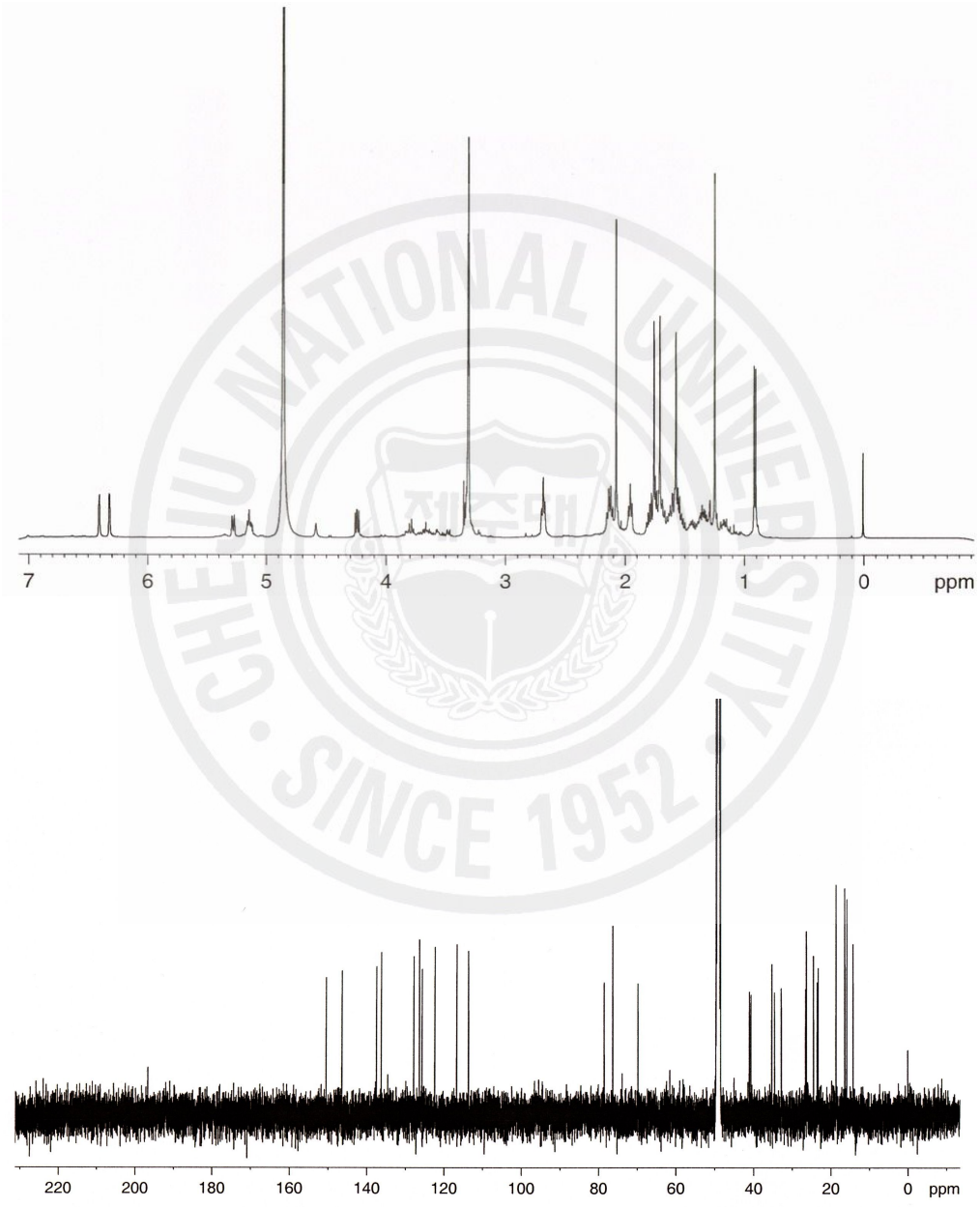

Fig. 2-23. Proton and Carbon NMR spectrum of sargachromanol U (**12**).

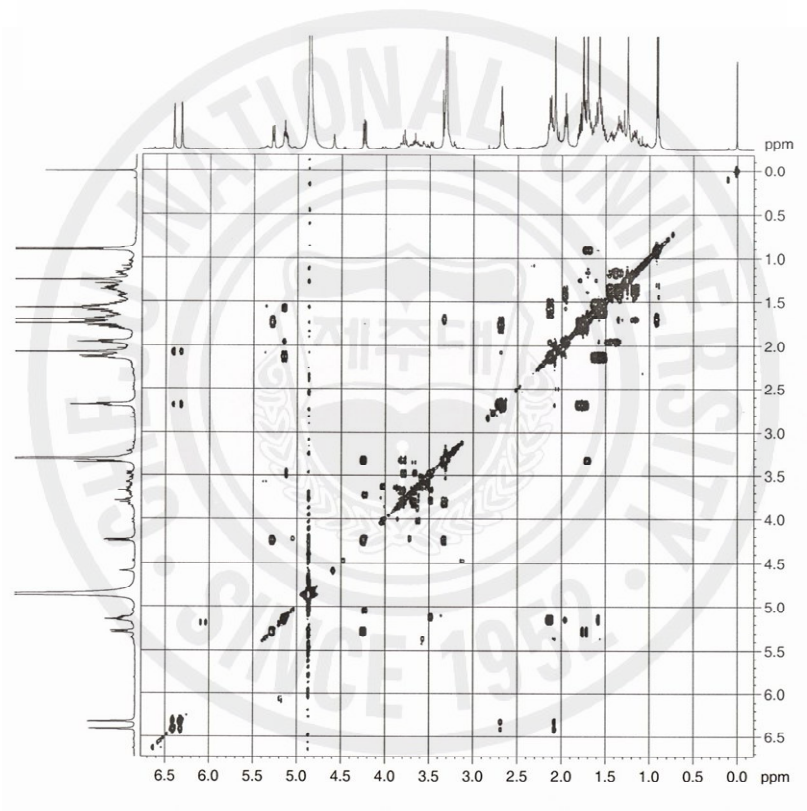

Fig. 2-24. Gradient COSY NMR spectrum of sargachromanol U (**12**).

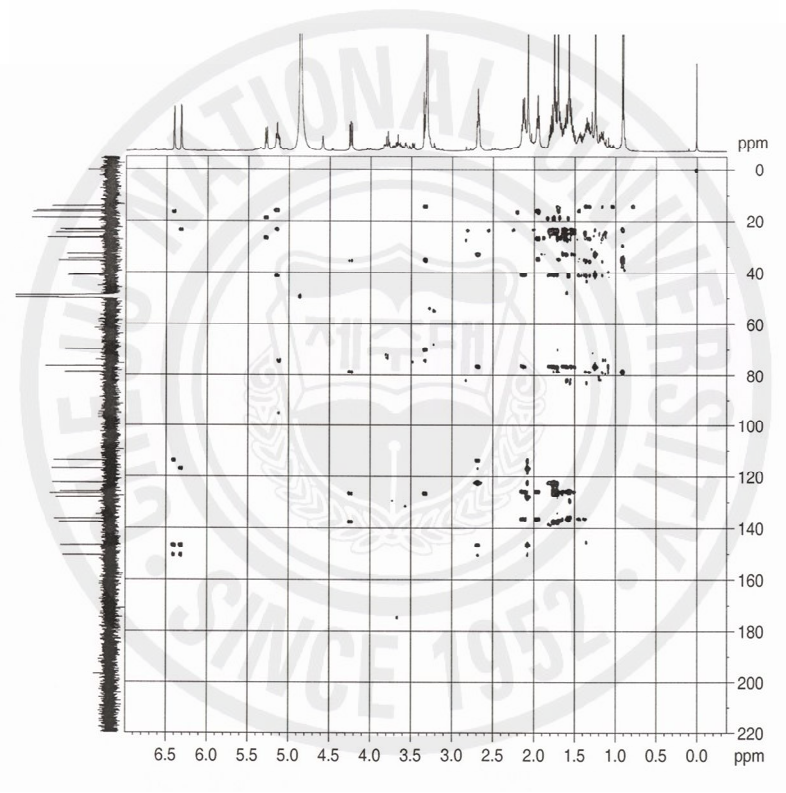

Fig. 2-25. Gradient HMBC NMR spectrum of sargachromanol U (**12**).

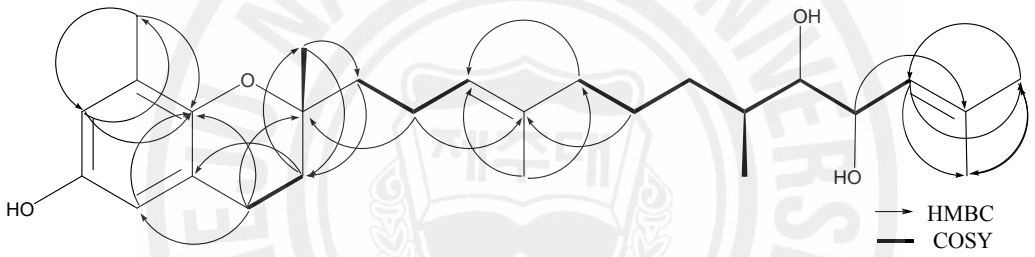

Fig. 2-26. Selective long range correlations for sargachromanol T (**11**) and sargachromanol U (**12**).

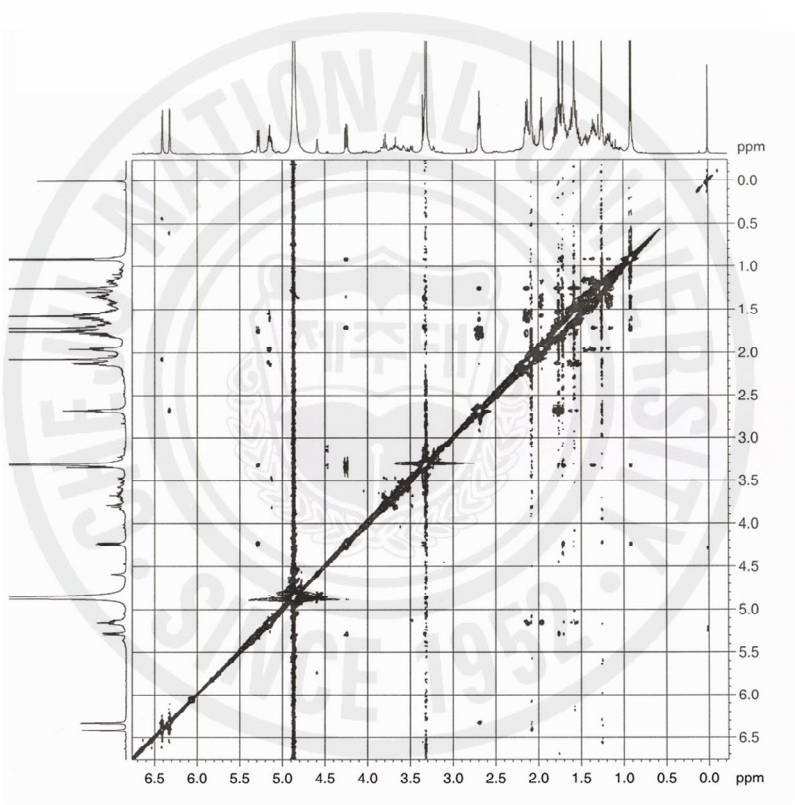

Fig. 2-27. Gradient ROESY NMR spectrum of sargachromanol U (**12**).

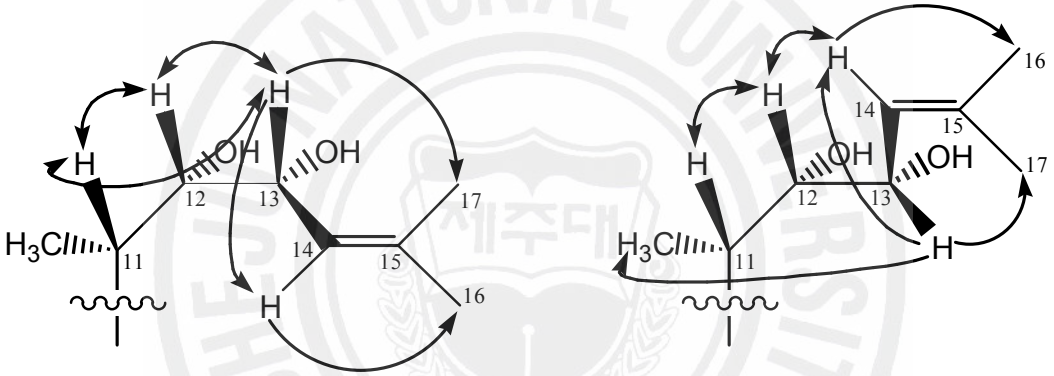

1 (11 *S**, 12 *S**, 13 *R**) **2** (11 *S**, 12 *S**, 13 *S**)

Fig. 2-28. Key NOE correlations of sargachromanol T (**11**) and sargachromanol U (**12**) to allow the assignment of relative configuration.

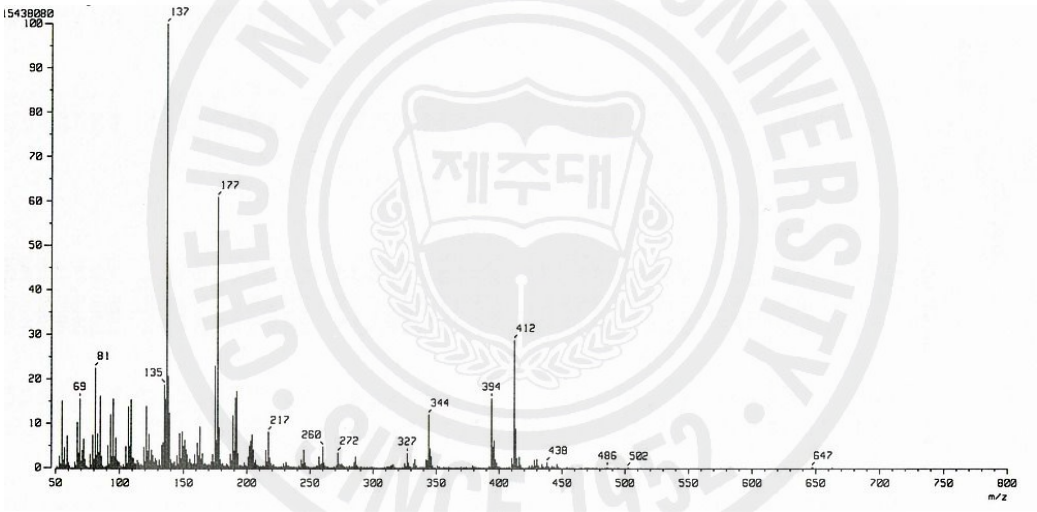

Fig. 2-29. MS spectrum of sargachromanol U (**12**).

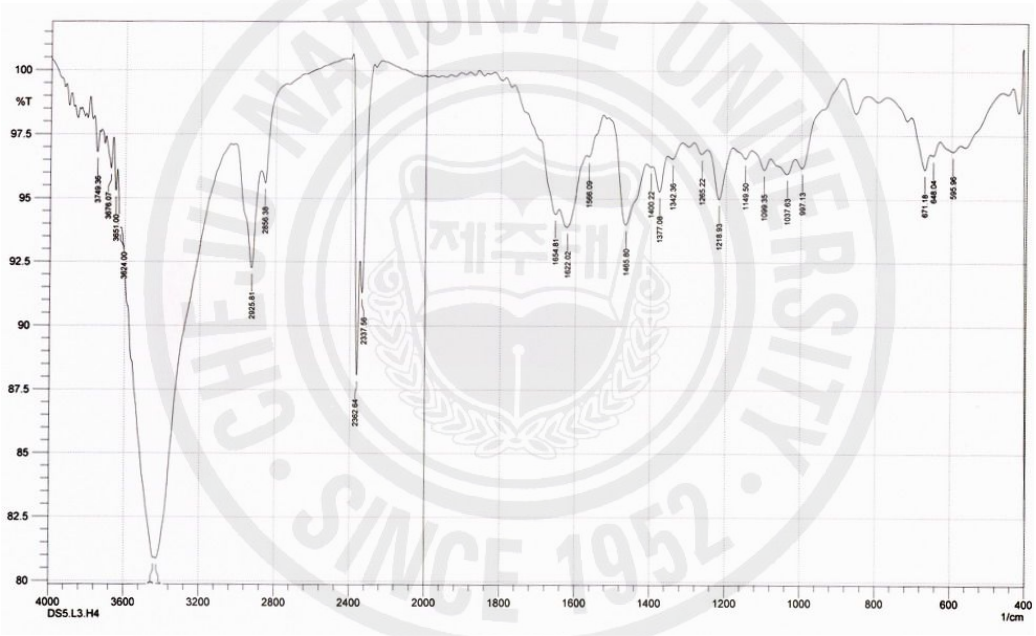

Fig. 2-30. IR spectrum of sargachromanol U (**12**).

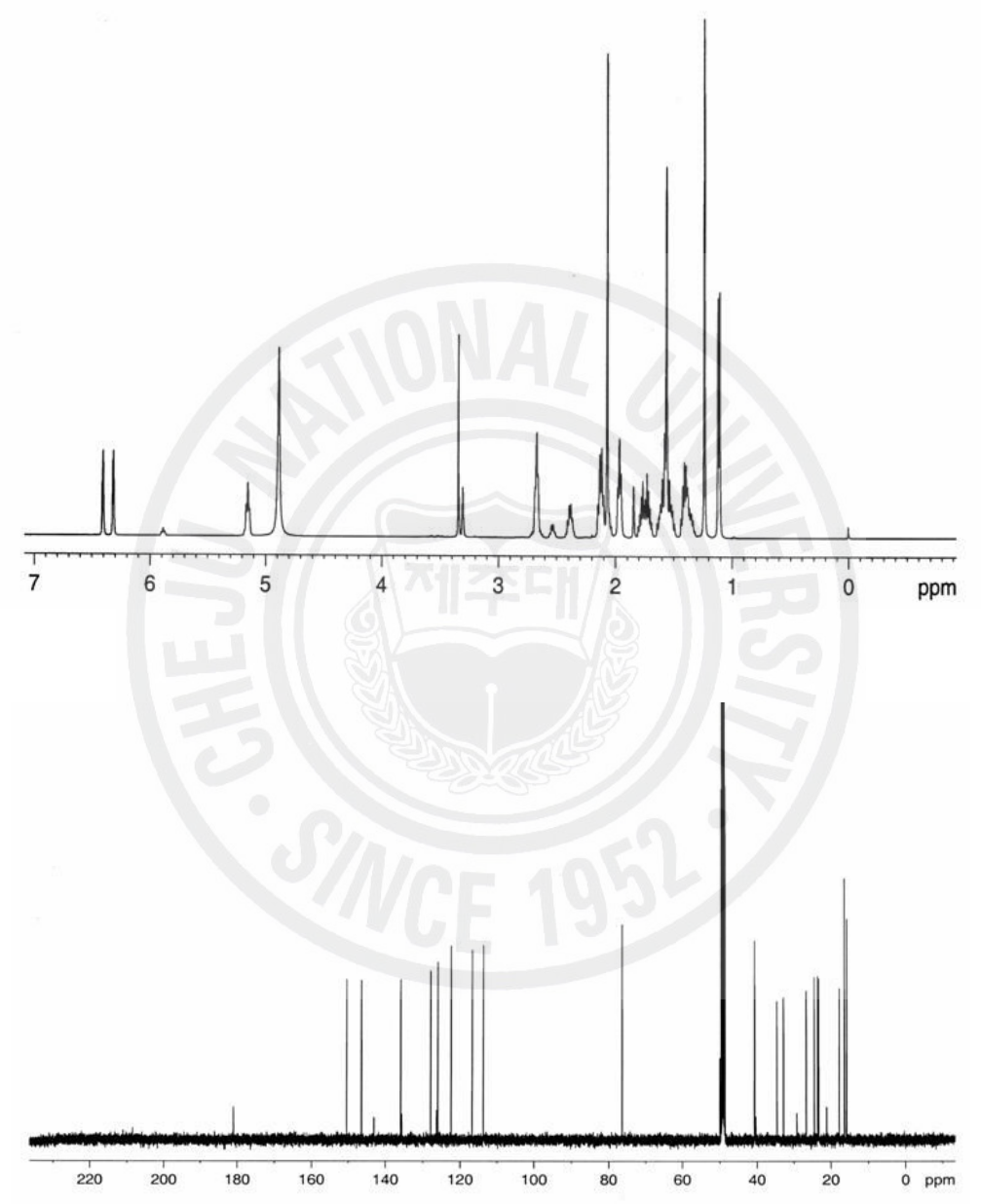

Fig. 2-31. Proton and Carbon NMR spectrum of sargachromanol V (**13**).

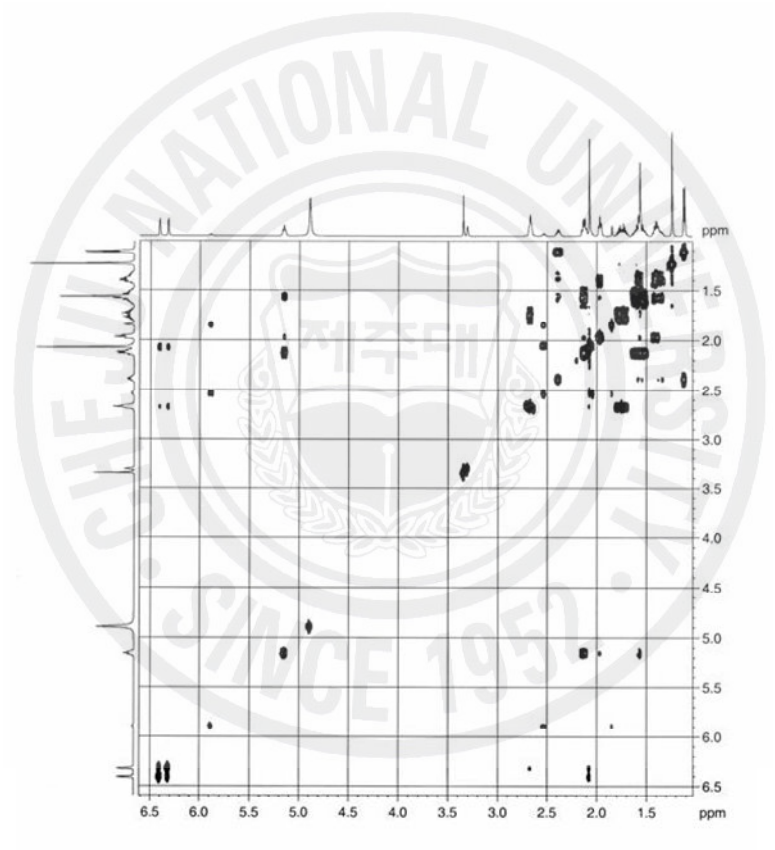

Fig. 2-32. Gradient COSY NMR spectrum of sargachromanol V (**13**).

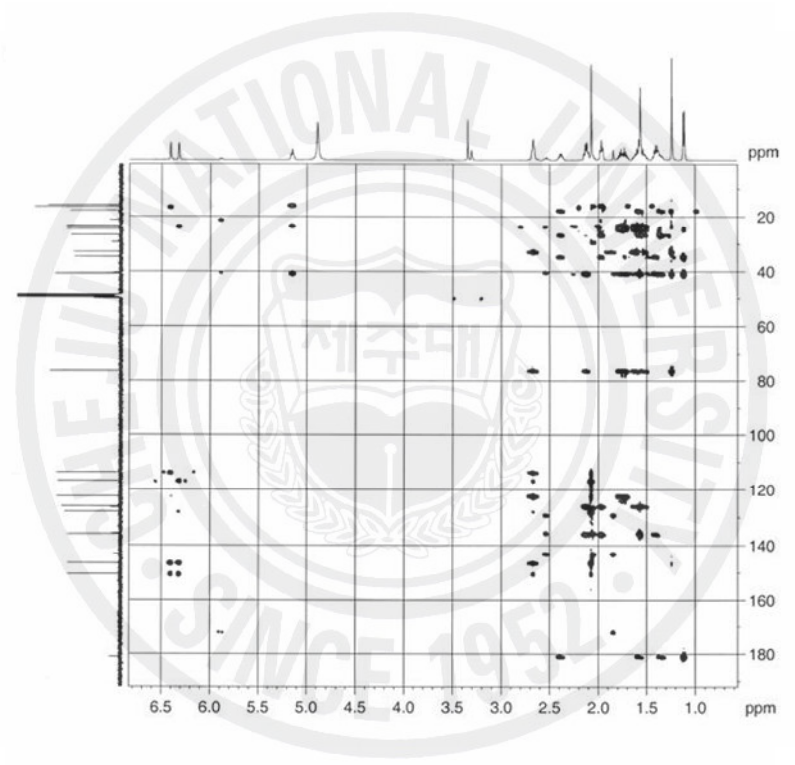

Fig. 2-33. Gradient HMBC NMR spectrum of sargachromanol V (**13**).

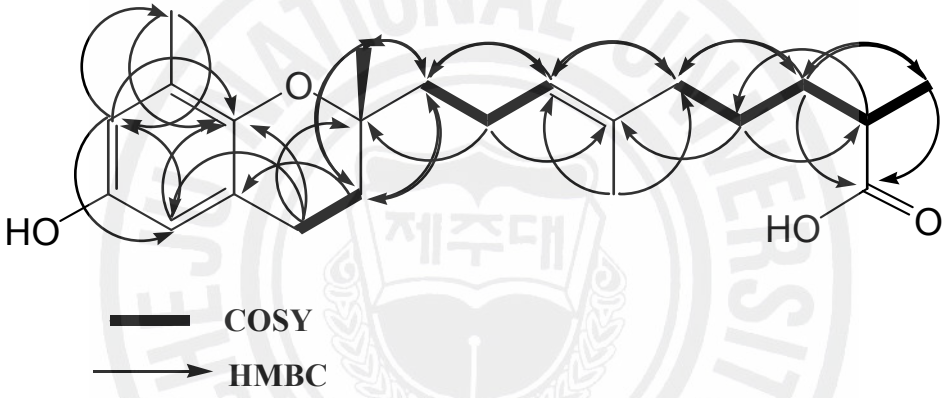

Fig. 2-34. Selective long range correlations for sargachromanol V (**13**).

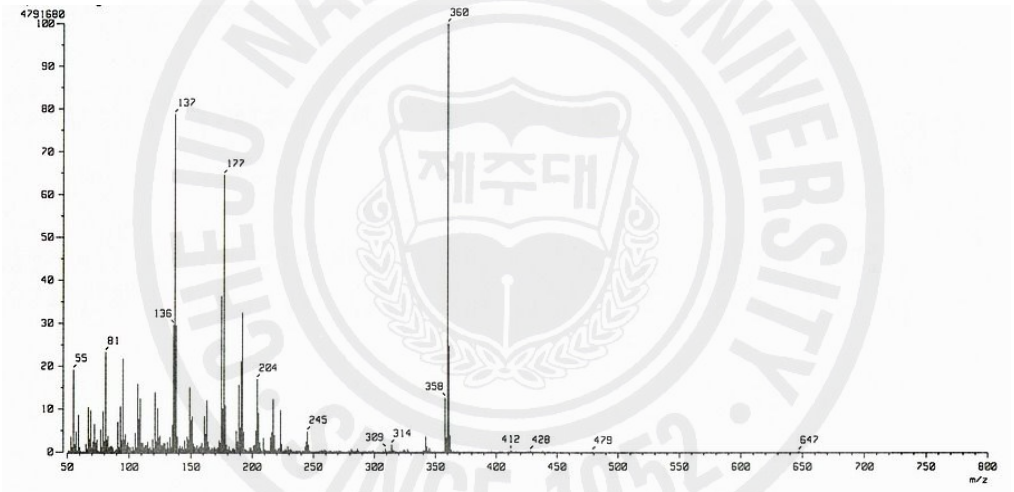

Fig. 2-35. MS spectrum of sargachromanol V (**13**).

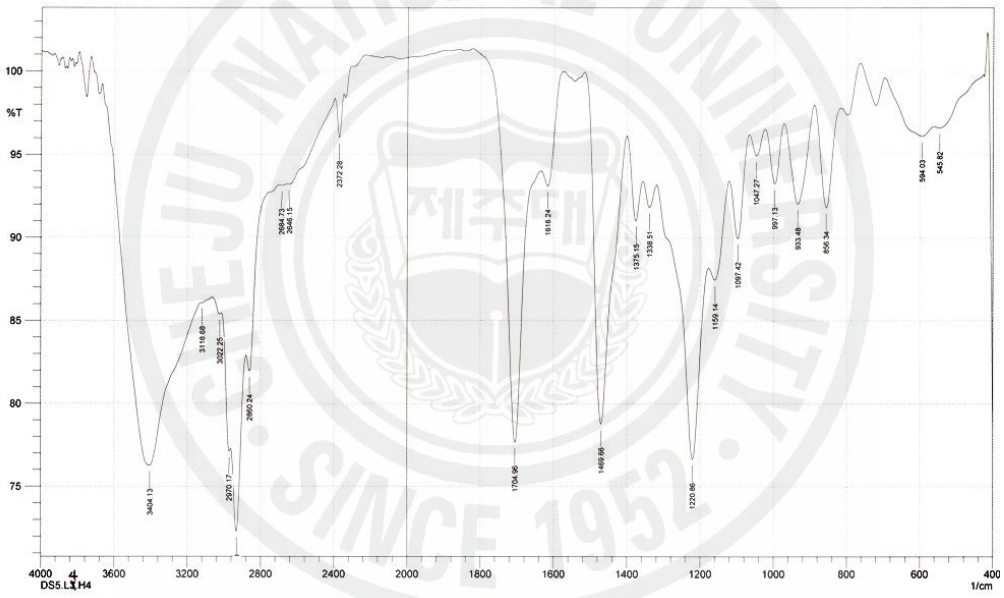

Fig. 2-36. IR spectrum of sargachromanol V (**13**).

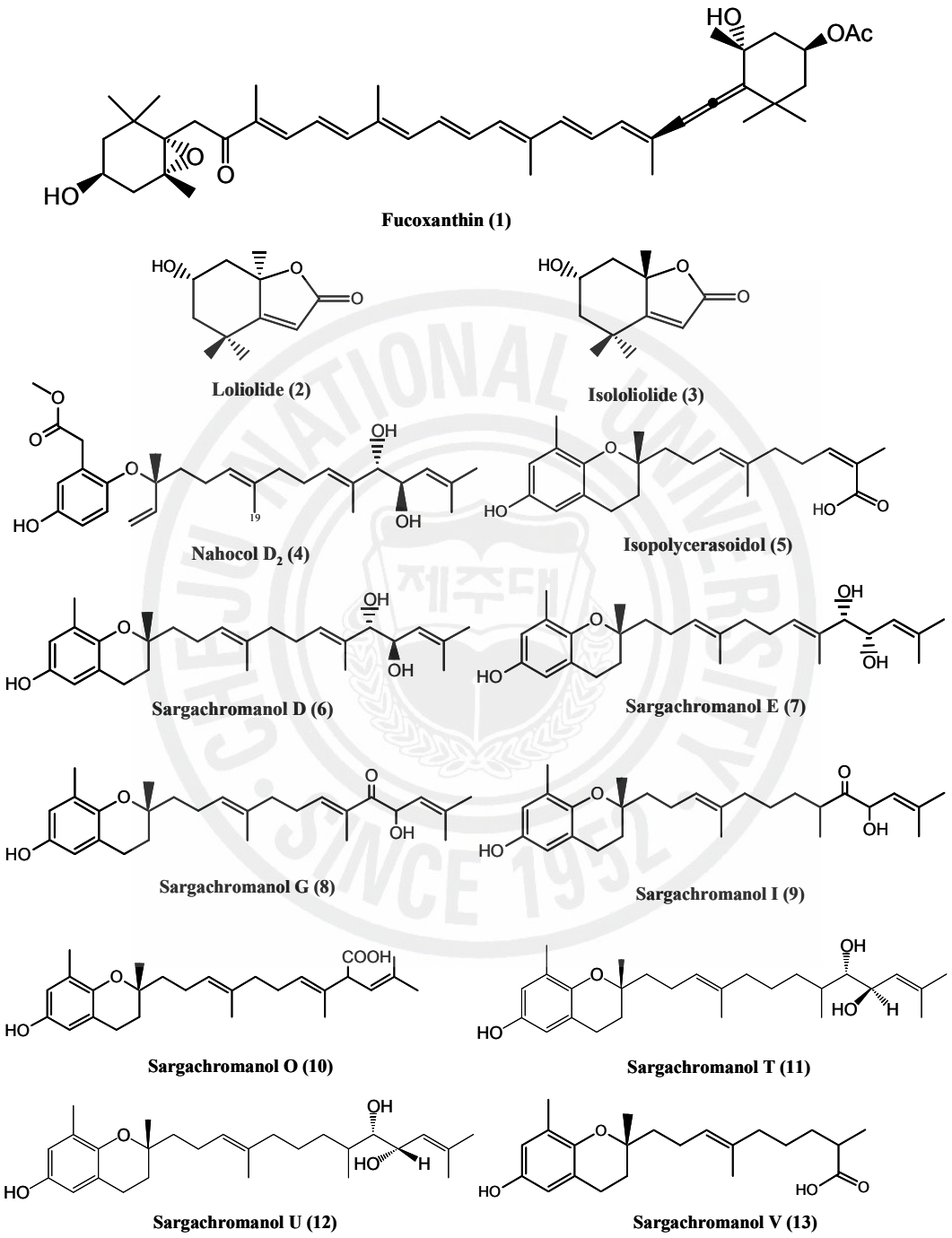

Fig. 2-37. Chemical structures of isolated compounds from *S. siliquastrum*.

Free radical scavenging activity of those active compounds (**1**, **6**, **7**, **8**, **9**, **10**, and **13**) isolated from *S. siliquastrum* was evaluated with the change of absorbance caused by the reduction of DPPH radical. The scavenging activity of each compound against DPPH was presented in **Fig. 2-38**. It was observed that the DPPH radical scavenging activity of **6**, **7**, and **8** were better than those of the other compounds, which values recorded 95.42, 97.57, and 68.41% at 40 μM, respectively. Moreover, **9**, **10**, and **13** also showed prominent scavenging activity on DPPH radical, which values were reached around 80% at 90 μM, whereas **1** showed relatively lower scavenging activity. The scavenging activity on DPPH radical was increased when increasing the compound concentrations (**Fig. 2-39**). In addition, the **6**, **7**, and **8** exhibited a higher DPPH radical scavenging activity (IC_{50}=13.51, 13.20, and 17.81 μM, respectively) than the commercial antioxidant ascorbic acid (IC_{50}=19.94 μM). Scavenging activity of those compounds against hydroxyl radical (**Fig. 2-40**) was measured as the percentage of inhibition of hydroxyl radicals generated in the Fenton reaction ($Fe^{2+} + H_2O_2 \rightarrow Fe^{3+} + OH^- + {}^{\cdot}OH$). Hydrogen peroxide scavenging activity also expressed as an inhibition rate by colorimetric assay (**Fig. 2-41**). The scavenging activities against both hydroxyl radical and hydrogen peroxide were observed dose-dependent manner but those compounds showed relatively lower than that of the commercial antioxidant such as ascorbic acid and BHA (**Tables 2-14** and **2-15**). Brown algae are well-known to be the producer of great variety of secondary metabolites with different carbon skeletons (Blunt et al., 2006). Major metabolite classes found in brown algae are carotenoids, terpenes and polyphenolic compounds. The genus *Sargassum* widely distributed in tropical areas of the world have been known to posses the diverse compounds containing fucoxanthin as a carotenoid, meroterpenoids, and phloroglucinol derivatives with many biological activities (Yan et al., 1996; Jang et al., 2005). Among the classes,

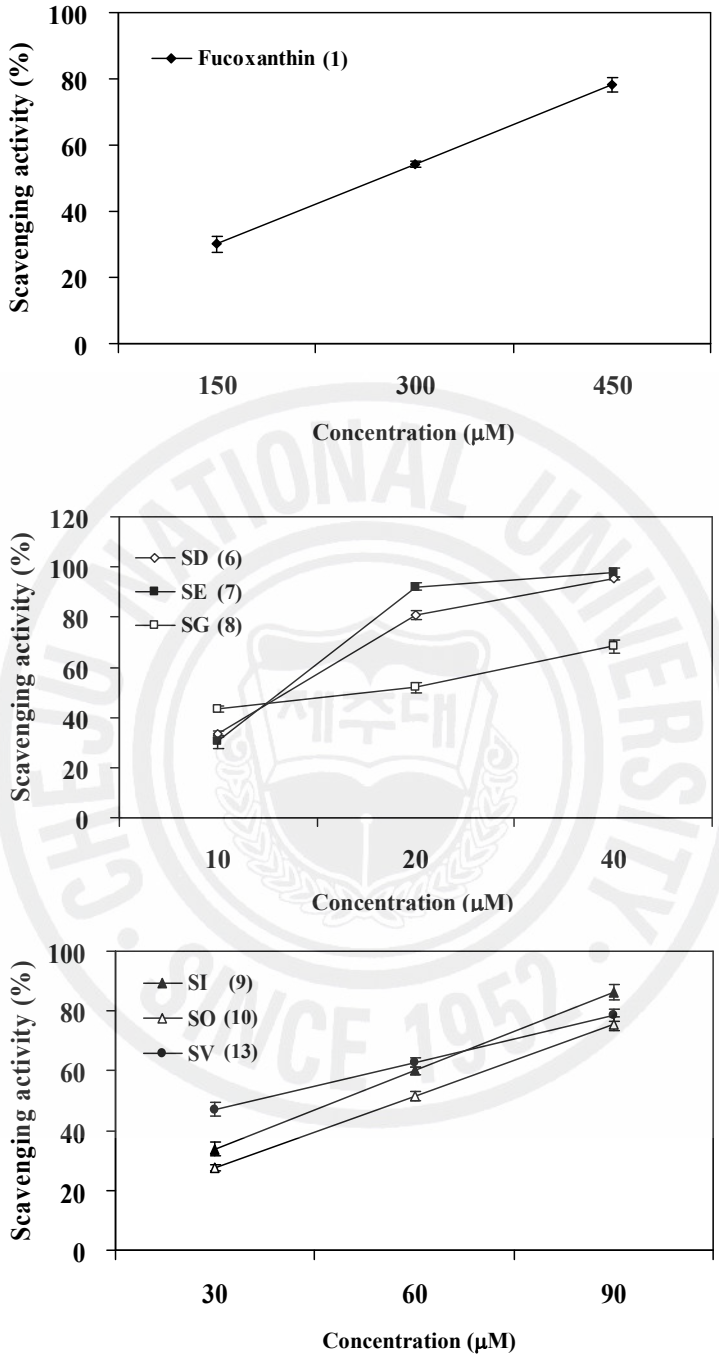

Fig. 2-38. DPPH radical scavenging activity of the active compounds isolated from *S. siliquastrum*. ◆, fucoxanthin; ◇, sargachromanol D; ■, sargachromanol E; □, sargachromanol G; ▲, sargachromanol I; △, sargachromanol O; ●, sargachromanol V. Experiments were performed in triplicate and the data are expressed as mean ± SE.

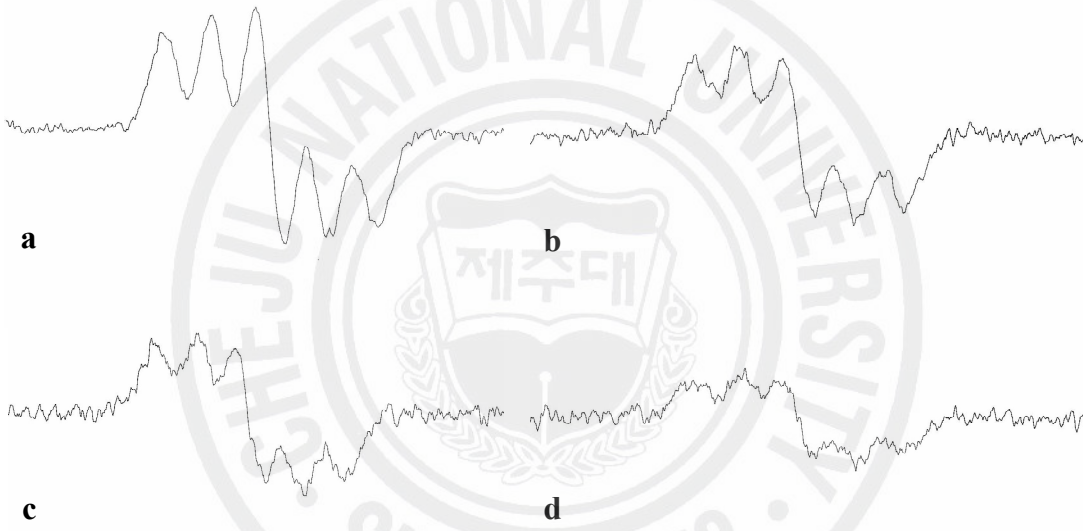

Fig. 2-39A. ESR spectrum obtained in an ethanol solution of 30 μmol/l DPPH at various concentrations of fucoxanthin isolated from *S. siliquastrum*. a, control; b, 150 μM; c, 300 μM; d, 450 μM.

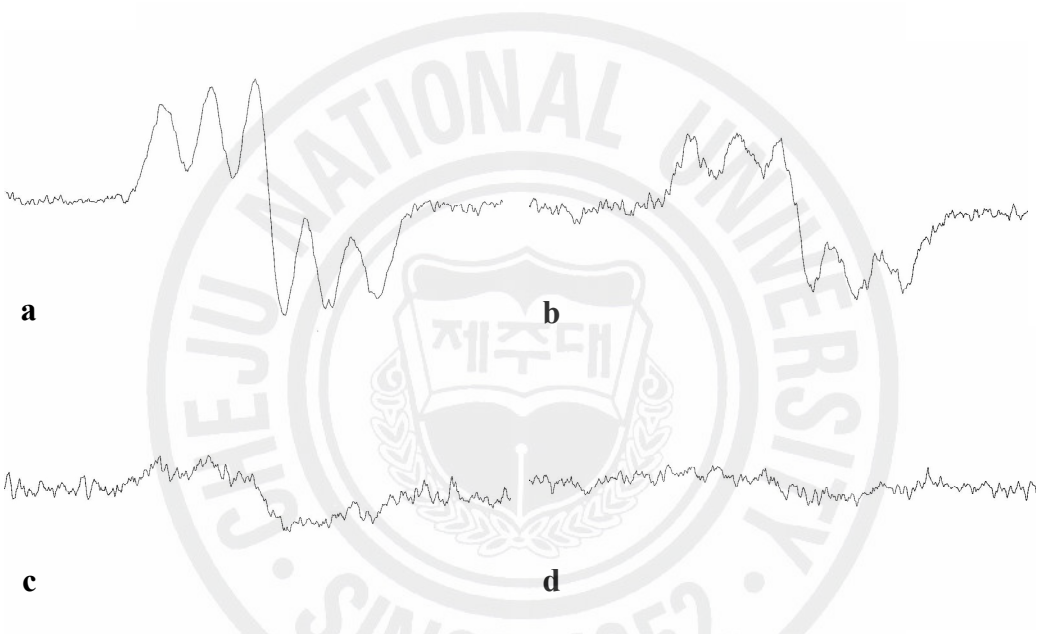

Fig. 2-39B. ESR spectrum obtained in an ethanol solution of 30 μmol/l DPPH at various concentrations of sargachromanol D isolated from *S. siliquastrum*. a, control; b, 10 μM; c, 20 μM; d, 40 μM.

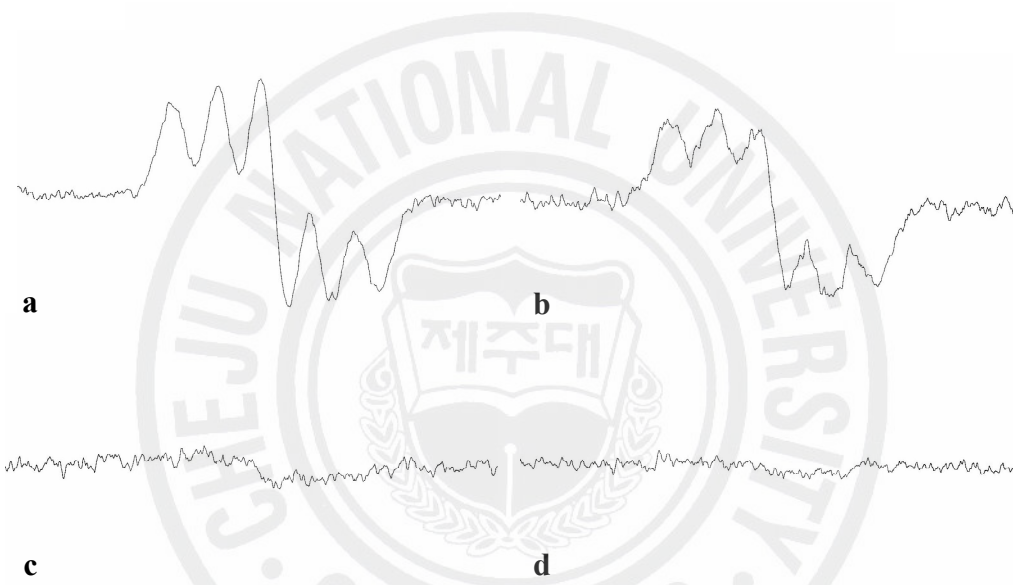

Fig. 2-39C. ESR spectrum obtained in an ethanol solution of 30 μmol/l DPPH at various concentrations of sargachromanol E isolated from *S. siliquastrum*. a, control; b, 10 μM; c, 20 μM; d, 40 μM.

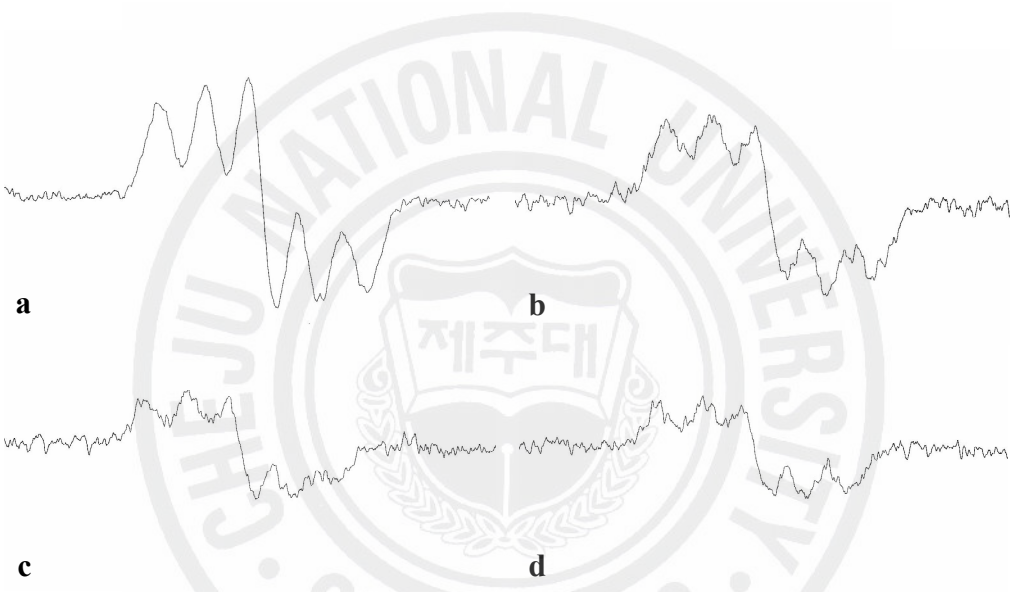

Fig. 2-39D. ESR spectrum obtained in an ethanol solution of 30 μmol/l DPPH at various concentrations of sargachromanol G isolated from *S. siliquastrum*. a, control; b, 10 μM; c, 20 μM; d, 40 μM.

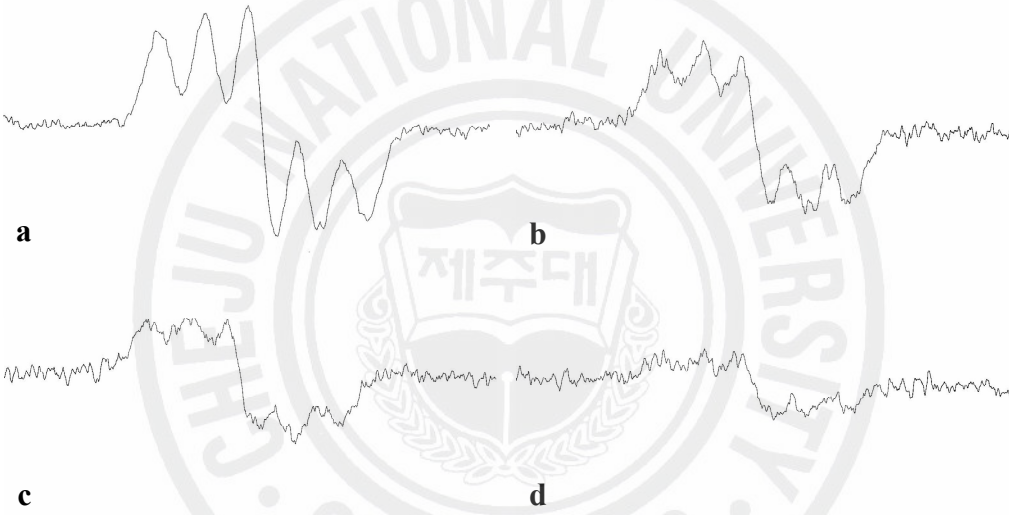

Fig. 2-39E. ESR spectrum obtained in an ethanol solution of 30 μmol/l DPPH at various concentrations of sargachromanol I isolated from *S. siliquastrum*. a, control; b, 30 μM; c, 60 μM; d, 90 μM.

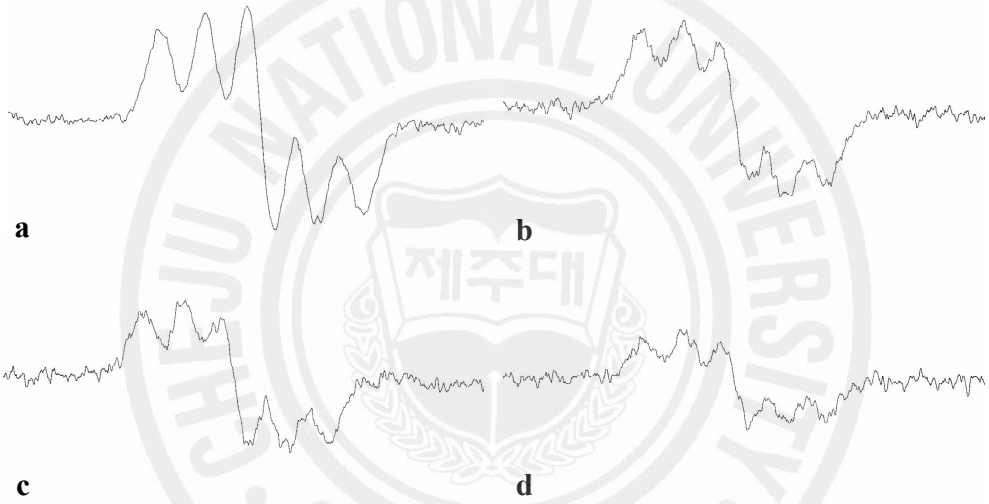

Fig. 2-39F. ESR spectrum obtained in an ethanol solution of 30 μmol/l DPPH at various concentrations of sargachromanol O isolated from *S. siliquastrum*. a, control; b, 30 μM; c, 60 μM; d, 90 μM.

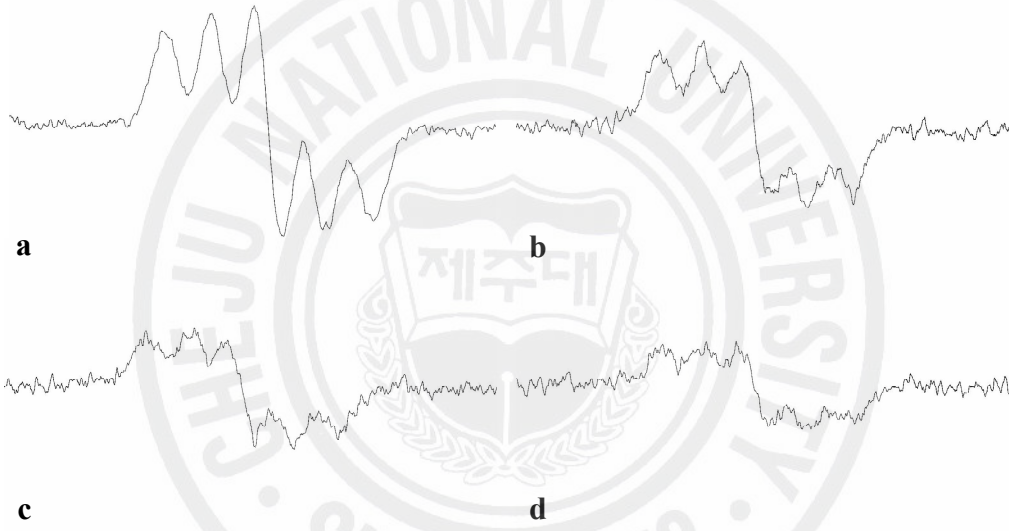

Fig. 2-39G. ESR spectrum obtained in an ethanol solution of 30 μmol/l DPPH at various concentrations of sargachromanol V isolated from *S. siliquastrum*. a, control; b, 30 μM; c, 60 μM; d, 90 μM.

Table 2-13. Scavenging activity of the active compounds isolated from *S. siliquastrum* against DPPH radical

	IC_{50} (μM)
Sargachromanol D	**13.51**
Sargachromanol E	**13.20**
Sargachromanol G	**17.81**
Sargachromanol I	**48.53**
Sargachromanol O	**58.10**
Sargachromanol V	**35.37**
Fucoxanthin	**273.62**
Ascorbic acid	**19.94**

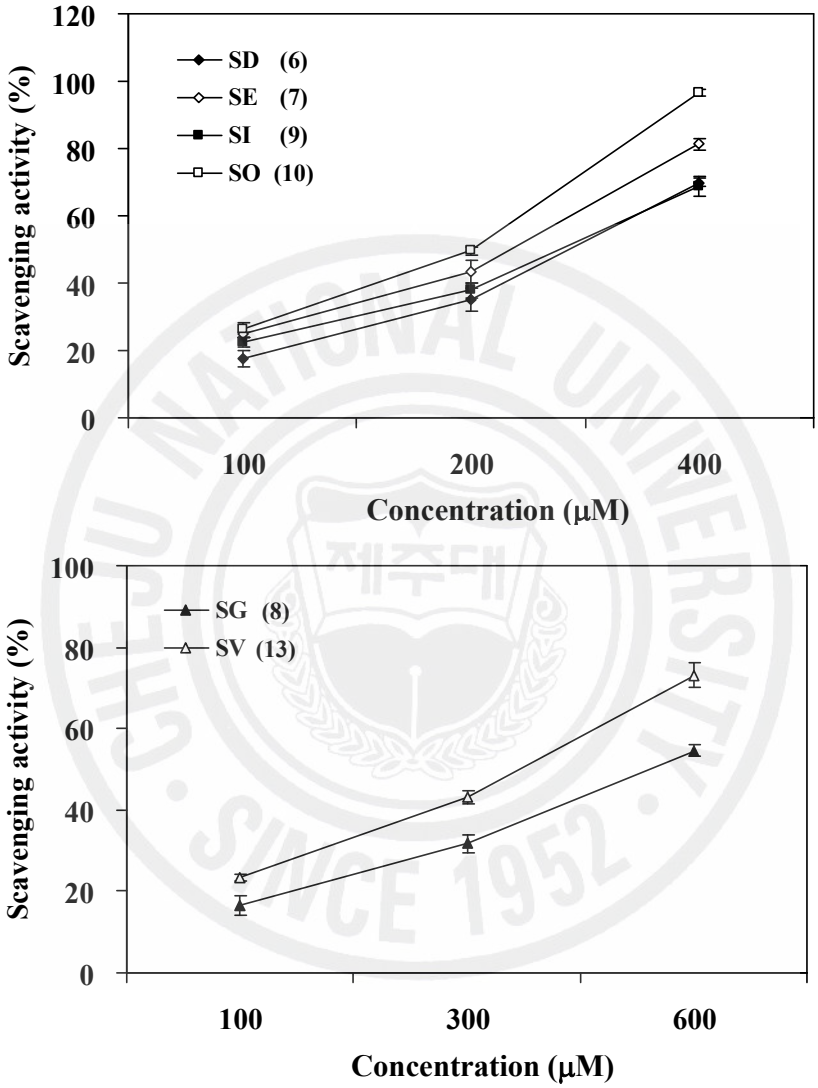

Fig. 2-40. Hydroxyl radical scavenging activity of the active compounds isolated from *S. siliquastrum*. ◆, sargachromanol D; ◇, sargachromanol E; ■, sargachromanol I; □, sargachromanol O; ▲, sargachromanol G; △, sargachromanol V. Experiments were performed in triplicate and the data are expressed as mean ± SE.

Table 2-14. Scavenging activity of the active compounds isolated from *S. siliquastrum* against hydroxyl radical

	IC_{50} (μM)
Sargachromanol D	**285.56**
Sargachromanol E	**234.36**
Sargachromanol G	**540.30**
Sargachromanol I	**277.79**
Sargachromanol O	**201.58**
Sargachromanol V	**368.73**
Ascorbic acid	**69.75**

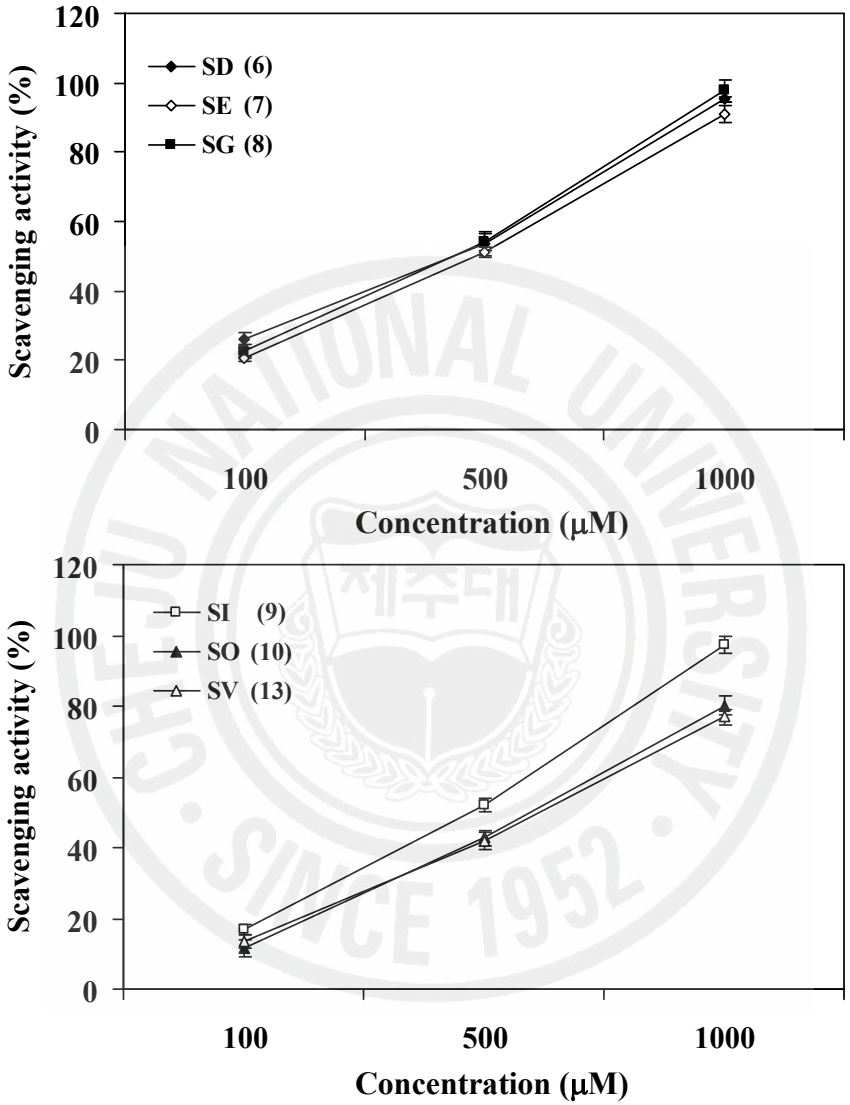

Fig. 2-41. Hydrogen peroxide scavenging activity of the active compounds isolated from *S. siliquastrum*. ◆, sargachromanol D; ◇, sargachromanol E; ■, sargachromanol G; □, sargachromanol I; ▲, sargachromanol O; △, sargachromanol V. Experiments were performed in triplicate and the data are expressed as mean ± SE.

Table 2-15. Scavenging activity of the active compounds isolated from *S. siliquastrum* against hydrogen peroxide

	IC_{50} (μM)
Sargachromanol D	**459.99**
Sargachromanol E	**483.89**
Sargachromanol G	**450.95**
Sargachromanol I	**478.61**
Sargachromanol O	**598.01**
Sargachromanol V	**615.52**
BHA	**73.92**

the term ‘meroterpenoid’ refers to the compounds which consist of a propenyl chain attached to a hydroquinone or similar aromatic rings (Blunt et al., 2006). Plastoquinones and chromene derivatives are major meroterpenoids found in *Sargassum* species and these compounds exhibited various biological activities such as cytotoxicity, antioxidant activity, antiviral activity, and bone resorption inhibitory activity (Kusumi et al., 1979; Kikuchi et al., 1983; Sato et al., 1989; Iwashima et al., 2005; Mori et al., 2005). In our measurement by DPPH, hydroxyl radical and hydrogen peroxide scavenging assays, all of the tested sargachromanols (a kinds of chromene derivative) D, E, G, I, O, and V (**6**, **7**, **8**, **9**, **10**, and **13**) showed significant DPPH radical scavenging activity while the hydroxyl radical and hydrogen peroxide scavenging activity exhibited relatively lower activity. Therefore, the sargachromanols (**6**, **7**, **8**, **9**, **10**, and **13**) isolated from *S. siliquastrum* would appear to be a good potential DPPH free radical scavenger.

Cells are protected from ROS-induced damage by a variety of endogenous ROS-scavenging enzymes, chemical compounds, and natural products. Recently, interest has been increasing in the therapeutic potential of natural plants as antioxidants in the reduction of such free radical-induced tissue injuries, thereby suggesting that many plants may prove to possess therapeutically useful antioxidant activities. In this study, we investigated the antioxidant effects of the isolated compounds after the administration of H_2O_2 treatment in cell lines. The intracellular ROS scavenging activity of the compounds was shown in **Fig. 2-42**. Fucoxanthin (**1**) exhibited the highest intracellular ROS scavenging activity (57.74%) while **6**, **7**, **8**, **9**, **10**, and **13** showed less than 35% scavenging activities at the concentration of 100 μM, and was dose-dependent manners. The intracellular ROS scavenging assay was basic experiment for screen to antioxidant activity in cell lines. As the **1** generated in this study evidenced such as ROS scavenging activity, **1** was evaluated further with regard to its protective effects against

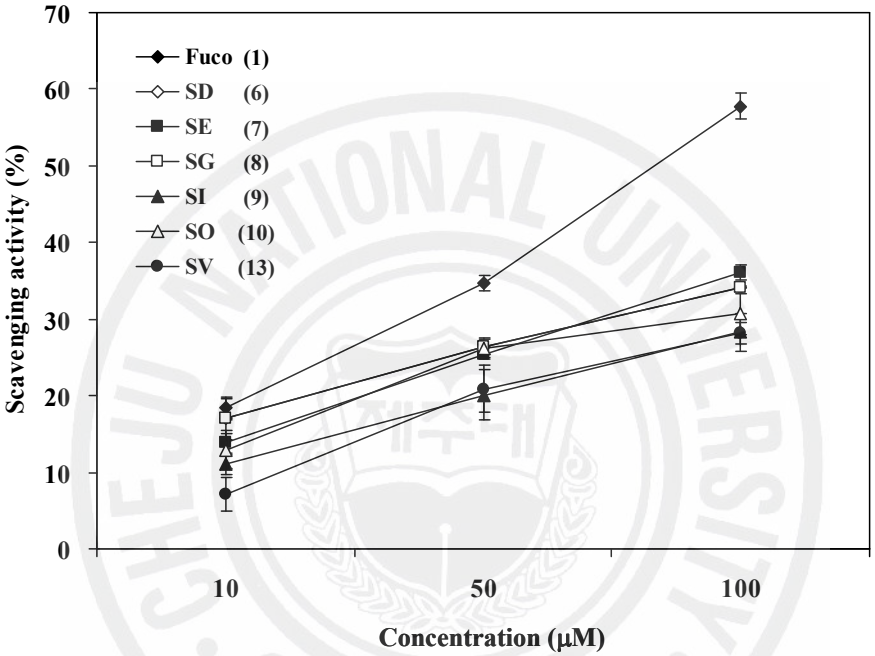

Fig. 2-42. Effect of the active compounds isolated from *S. siliquastrum* on scavenging reactive oxygen species. The intracellular reactive oxygen species generated was detected by DCF-DA method. ◆, fucoxanthin; ◇, sargachromanol D; ■, sargachromanol E; □, sargachromanol G; ▲, sargachromanol I; △, sargachromanol O; ●, sargachromanol V. Experiments were performed in triplicate and the data are expressed as mean ± SE.

the cellular damage induced by H_2O_2. The protective effect of **1** on cell survival in H_2O_2 treated Vero cells were measured via MTT assay. As shown in **Fig. 2-43**, H_2O_2 treatment decreased cell viability to 43.71%, while **1** (5, 50, 100, 200 μM) prevented cells from H_2O_2-induced damage, restoring cell survival to 63.59, 69.36, 78.47, and 89.18%, respectively. The protective effect of **1** on cell damages were also confirmed by comet assay (**Fig. 2-44**), which showed photomicrographs of different DNA migration profiles, when treated with different concentrations of the **1**. The inhibition activities of **1** on DNA damage were 38.79, 52.48, and 63.37% at the concentration of 5, 50, and 250 μM, respectively. In the group treated with only H_2O_2, the DNA was completely damaged but the addition of **1** with H_2O_2 reduced the damage caused by H_2O_2 (**Fig. 2-45**). In the application of **1** at different concentrations the DNA migration changed according to the concentrations. In order to study the cytoprotective effect of **1** on apoptosis induced by H_2O_2, nuclei of Vero cells were stained with Hoechst 33342 for microscopic analysis. The microscopic photograph in **Fig. 2-46**, the control cells (**Fig. 2-46A**) generated clear images, which suggests that no DNA damage took place in the absence of H_2O_2, and the H_2O_2 treated cells showed significant nuclear fragmentation, characteristic of apoptosis (**Fig. 2-46B**). However, when the cells were treated with **1** for 1 h prior to H_2O_2 treatment, a dramatic reduction in the amount of apoptotic bodies was observed. Therefore, the obtained photograph clearly (**Figs. 2-46C, D and E**) suggest the ability of the **1** to protect against cell damage in the event of challenge with H_2O_2. These results suggested that **1** protected the cell induced by oxidative stress-related cellular injuries.

Photosynthesis is one of the most important metabolic activities of algae because it is the main source of biomass and energy for the support ecosystem. So the effect of solar

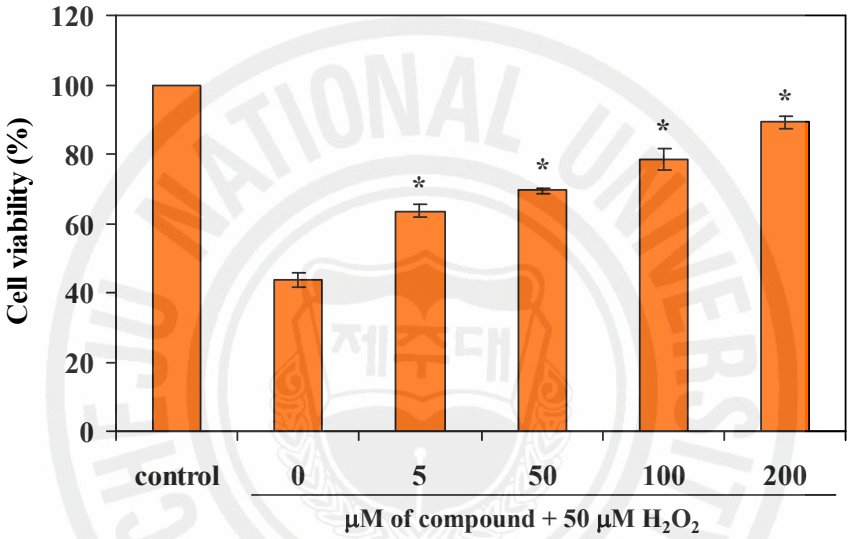

Fig. 2-43. Protective effect of the fucoxanthin isolated from *S. siliquastrum* on H_2O_2 induced oxidative damage of vero cells. The viability of vero cells on H_2O_2 treatment was determined by MTT assay. Experiments were performed in triplicate and the data are expressed as mean ± SE. Statistical evaluation was performed to compare the experimental groups and corresponding control groups. *, $p < 0.001$

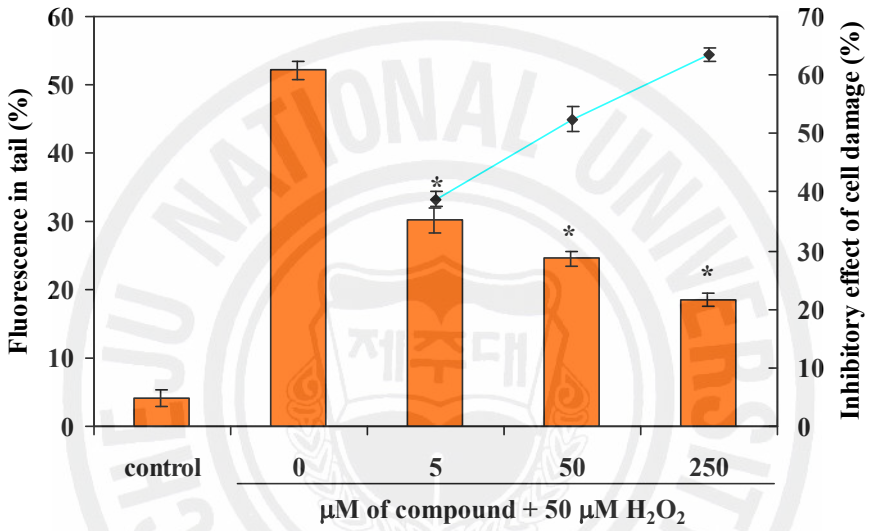

Fig. 2-44. Inhibitory effect of different concentrations of fucoxanthin isolated from *S. siliquastrum* on H_2O_2 induced DNA damages. The damaged cells on H_2O_2 treatment was determined by comet assay. ■, % Fluorescence in tail; ●, Inhibitory effect of cell damage. Experiments were performed in triplicate and the data are expressed as mean ± SE. Statistical evaluation was performed to compare the experimental groups and corresponding control groups. *, $p < 0.001$

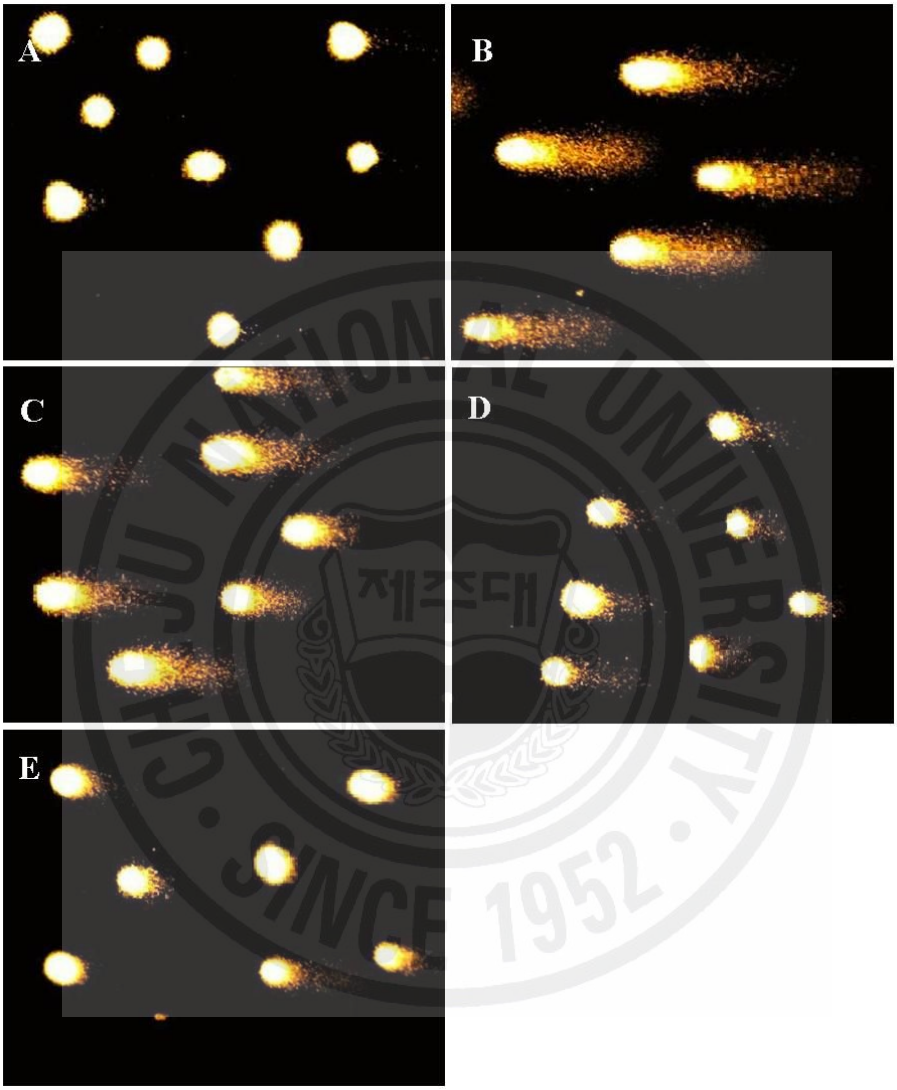

Fig. 2-45. Photomicrographs of DNA damage and migration observed under fucoxanthin isolated from *S. siliquastrum* where the tail moments were decreased. A, control; B, cells treated with 50 μM H_2O_2; C, cells treated with 5 μM compound + 50 μM H_2O_2; D, cells treated with 50 μM compound + 50 μM H_2O_2; E, cells treated with 250 μM compound + 50 μM H_2O_2.

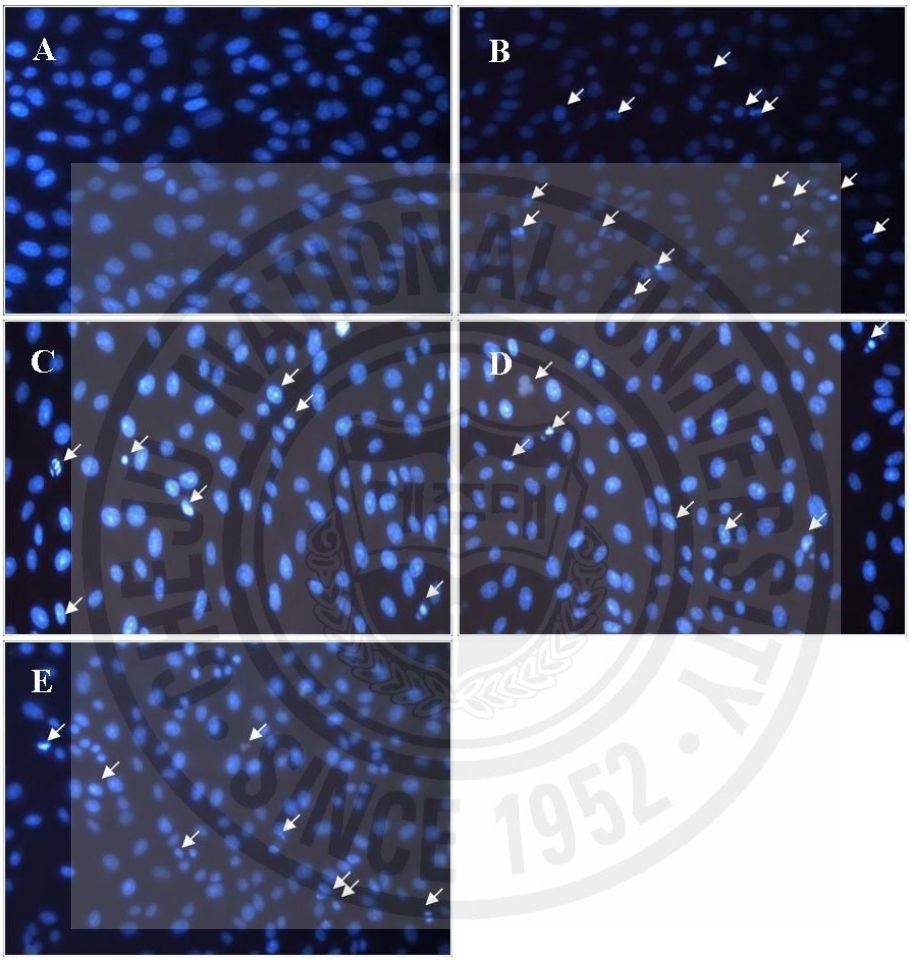

Fig. 2-46. Protective effect of fucoxanthin isolated from *S. siliquastrum* against H_2O_2-induced apoptosis in vero cells. Cellular morphological changes were observed under a fluorescence microscope after Hoechst 33342 staining. A, untreated; B, 500 μM H_2O_2; C, 5 μM compound + 500 μM H_2O_2; D, 50 μM compound + 500 μM H_2O_2; E, 250 μM compound + 500 μM H_2O_2. Apoptotic bodies are indicated by arrows.

light on photosynthesis is one of critical conditions for the survival of algae (Wang et al., 2007). However, overexposure to the UV radiation causes cell damage through the production of ROS which induce oxidative stress. UV-B (280-320 nm) irradiation can induce the formation of bulky DNA adducts such as pyrimidine dimmers and 6-4 photoproducts (Cadet et al., 1997). Although human skin has an extensive antioxidant defense mechanism to protect cellular DNA from oxidative damage this protection can be overwhelmed by UV-B exposure (Podda et al., 1992). In this present study, we report the protective effect of **1** caused by UV-B radiation. The scavenging effect of **1** on the intracellular ROS generated by UV-B radiation was shown in **Fig. 2-47**. The level of ROS detected using spectrofluorometer were dose-dependent decreased (except to the concentration of 50 μM), and showed 78.31% of ROS level in 250 μM of **1** treated irradiated cells compared to 169.31% of ROS level in irradiated cells. The protective effect of **1** on cell survival in fibroblast exposed to UV-B radiation was also measured (**Fig. 2-48**). The irradiated cells without **1** showed 43.48% cell survival rate, whereas treatment with **1** at 50 μM increased 76.66% of cell survival rate compared to non irradiated cells. To evaluate whether **1** protects from UV-B radiation, cells were pretreated with **1** in the absence or presence of UV-B radiation. After then, DNA damage was measured by comet assay. **1** significantly increased inhibitory effect of cell damage, which values recorded 61.24% at 250 μM (**Fig. 2-49**). UV-B radiation decreased the damaged tail length markedly, while **1** protected cell from UV-B induced damage in a concentration-dependent manner (**Fig. 2-50**). Exposure of fibroblast to UV-B radiation causes strand breaks and other type of damage in the cellular DNA. To analyses the protective effect of the **1** on UV-B radiation-induced cell damage, nuclei of fibroblast was double stained with Hoechst 33342 and propidium iodide for detect both apoptosis and necrosis configurations.

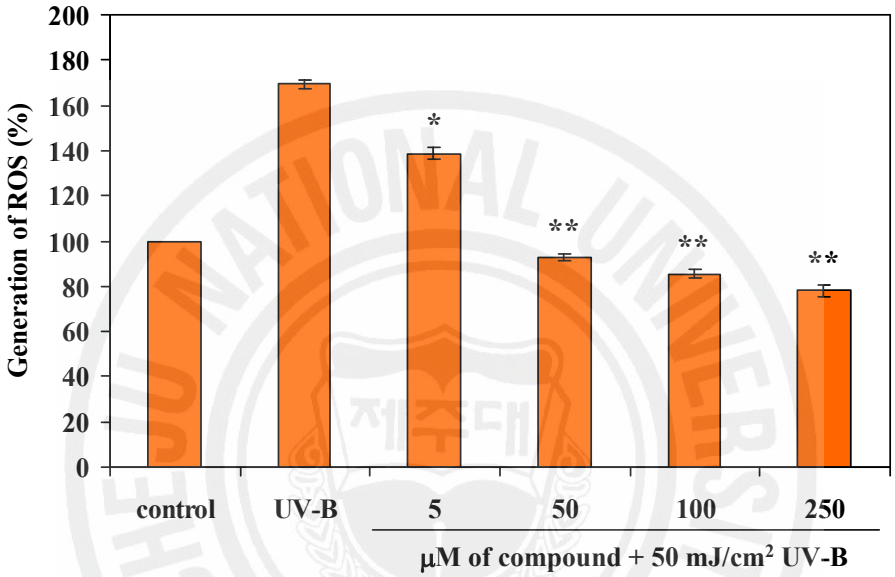

Fig. 2-47. Effect of fucoxanthin isolated from *S. siliquastrum* on scavenging intracellular ROS generated by UV-B radiation. The fibroblasts were treated with various concentrations of fucoxanthin and after 1h later, UV-B radiation at 50 mJ/cm^2 was applied to the cells. The intracellular ROS was detected using fluorescence spectrophotometer after DCF-DA staining. Experiments were performed in triplicate and the data are expressed as mean ± SE. Statistical evaluation was performed to compare the experimental groups and corresponding control groups. *, $p < 0.005$, **, $p < 0.001$

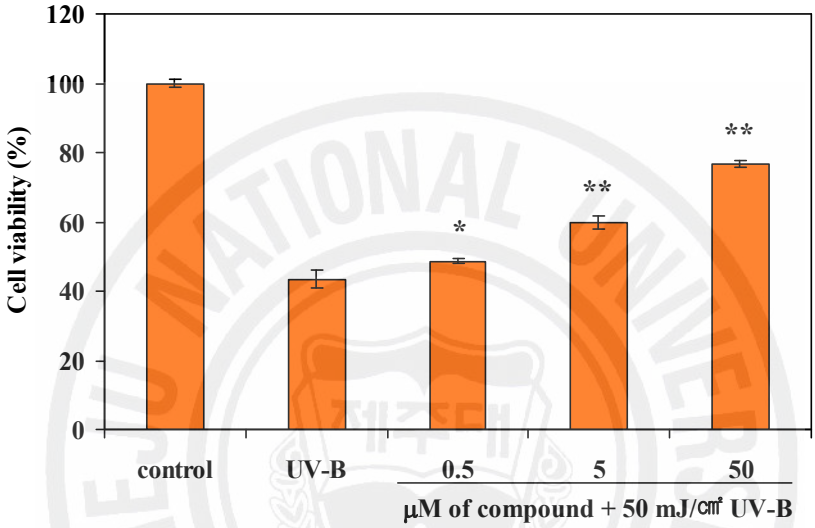

Fig. 2-48. Protective effect of fucoxanthin isolated from *S. siliquastrum* on UV-B radiation-induced cell damage of fibroblasts. The fibroblasts were treated with various concentrations of fucoxanthin and after 1h later, UV-B radiation at 50 mJ/cm^2 was applied to the cells. The viability of fibroblasts on UV-B radiation was determined by MTT assay. Experiments were performed in triplicate and the data are expressed as mean ± SE. Statistical evaluation was performed to compare the experimental groups and corresponding control groups. *, $p < 0.005$, **, $p < 0.001$

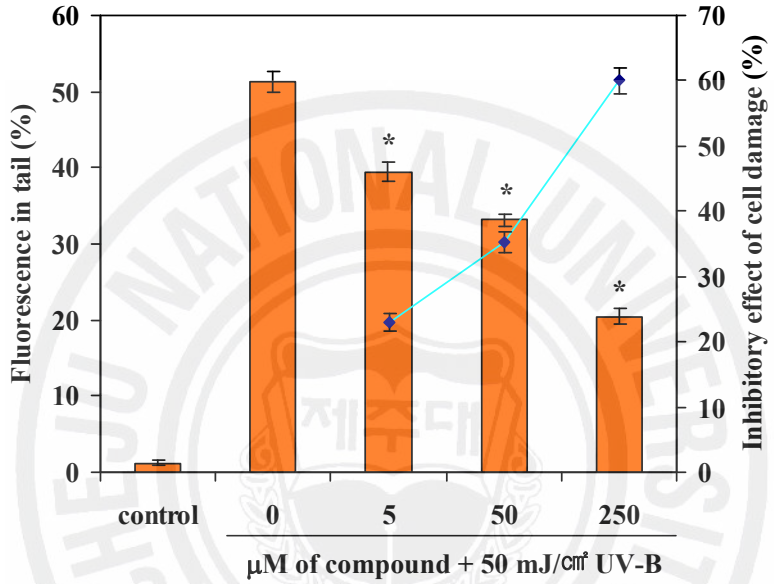

Fig. 2-49. Inhibitory effect of different concentrations of fucoxanthin isolated from *S. siliquastrum* on UV-B radiation induced DNA damages. The damaged cells on UV-B radiation was determined by comet assay. ■, % Fluorescence in tail; ●, Inhibitory effect of cell damage. Experiments were performed in triplicate and the data are expressed as mean ± SE. Statistical evaluation was performed to compare the experimental groups and corresponding control groups. *, $p < 0.001$

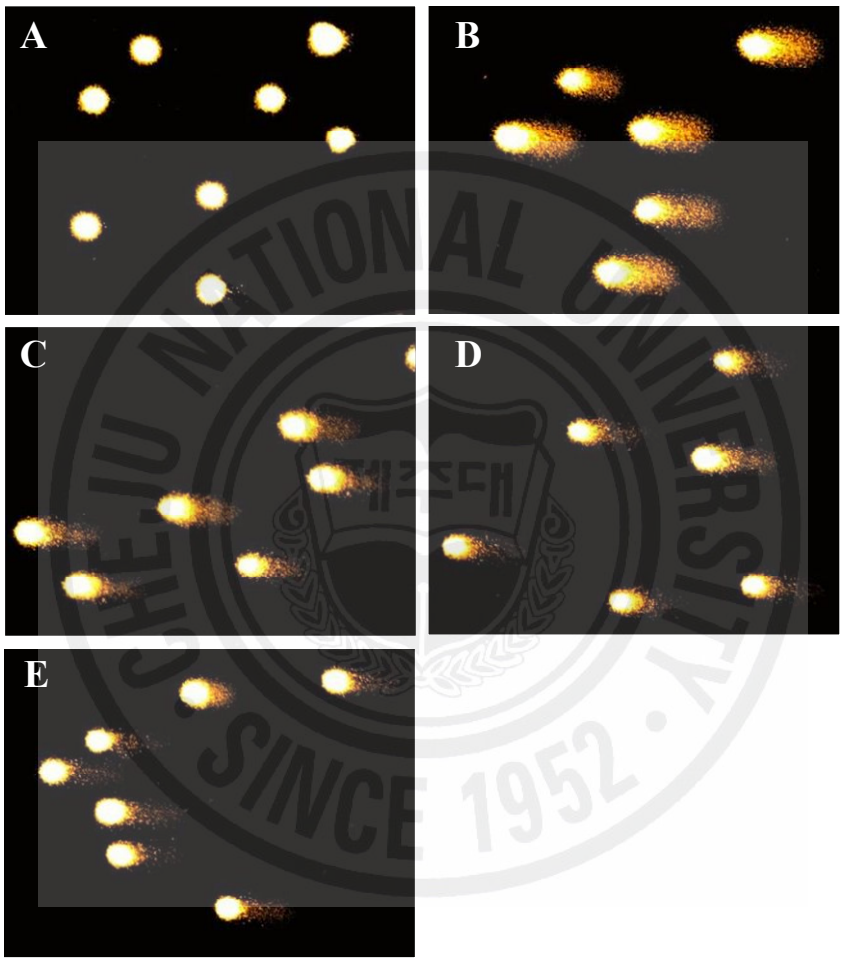

Fig. 2-50. Photomicrographs of DNA damage and migration observed under fucoxanthin isolated from *S. siliquastrum* where the tail moments were decreased. A, control; B, UV-B radiation at 50 mJ/cm^2; C, cells treated with 5 μM compound + UV-B radiation at 50 mJ/cm^2; D, cells treated with 50 μM compound + UV-B radiation at 50 mJ/cm^2; E, cells treated with 250 μM compound + UV-B radiation at 50 mJ/cm^2.

The microscopic photograph in **Fig. 2-51** showed that the control cells had intact nuclei, and the radiation-exposed cells exhibited significant nuclear fragmentation and destruction which is characteristic of apoptosis (bright blue color) and necrosis (red color), respectively. However, the amount of fragmentation and destruction of irradiated cells were dramatically reduce when the cell treat with **1**. DNA damage can be enhanced by exposure to various chemicals, environmental pollutants, steroid hormones, and radiation which led to the diseases such as cancer and heart disease (Singh et al., 1995; Betii et al., 1995; Senthilmohan et al., 2003). The cells of human body are continuously attacked by physical agent (like solar radiation), a variety of chemical compounds and reactive oxygen species, which arise as natural by-products of metabolic process. These substances can induce the DNA damage. If the DNA lesions are not repaired, these can initiate cascade of biological consequences at the population and can also promote cancer development via several mechanism (Bagchi et al., 2000). Hence, many natural and synthetic compounds have been investigated in the recent past for their efficacy to protect against oxidative stress in biological systems (Wei et al., 1999; Sørensen et al., 2001; Kang et al., 2005; Maurya et al., 2006). Fucoxanthin is one of the most abundant carotenoids in nature, especially in brown algae and diatoms, and it exhibited diverse biological activities such as antioxidant, anticarcinogenesis, and antimutagenesis (Nishino, 1995, 1998; Yan et al., 1999). In this study demonstrated that **1** had not only antioxidant effect against oxidative stress but also protective effect against UV-B irradiation. These results indicate that the **1** can be used to natural antioxidant, and can applied to cosmeceutial field due to their protective effect against UV radiation.

Melanin formation is the most important determinant of mammalian skin color (Hearing, 2005). Melanin is synthesized in al multi-step biochemical pathway that

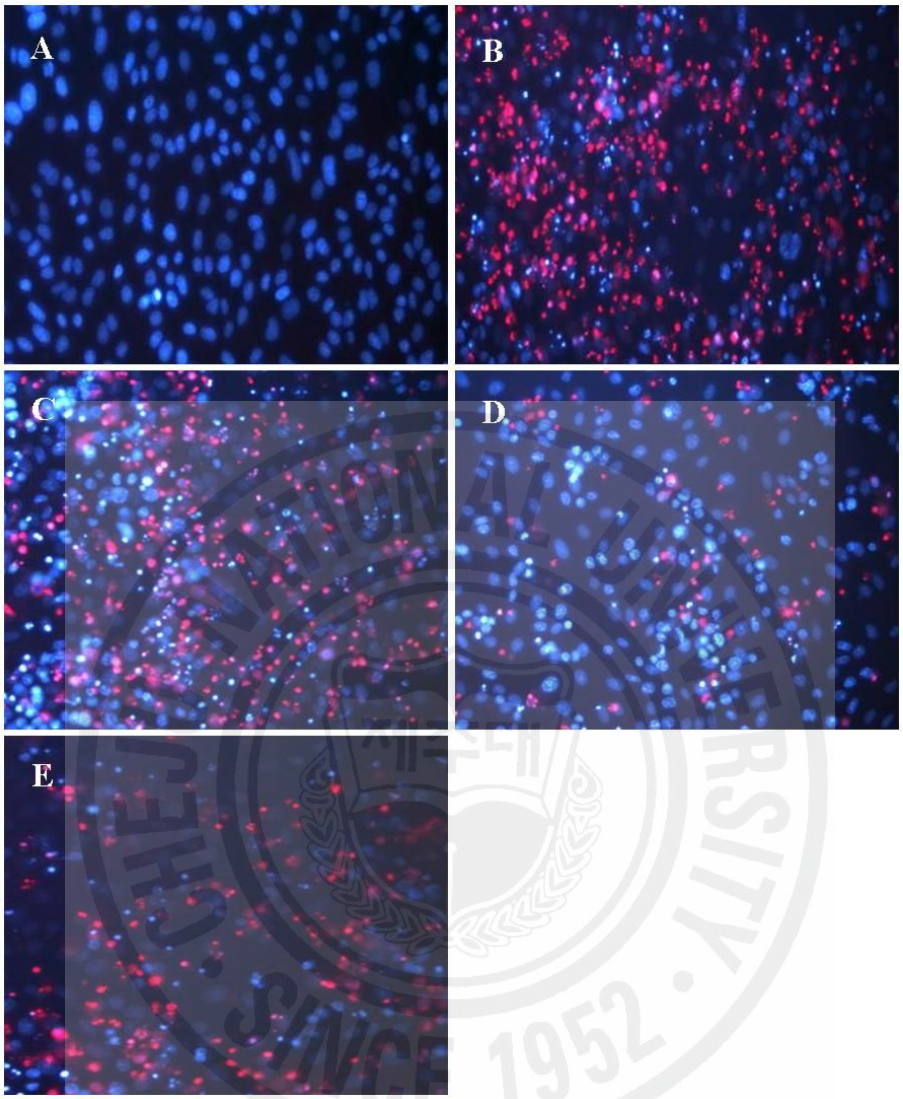

Fig. 2-51. Protective effect of fucoxanthin isolated from *S. siliquastrum* on UV-B radiation-induced cell damage of fibroblasts. The fibroblasts were treated with various concentrations of fucoxanthin and after 1h later, UV-B radiation at 50 mJ/cm^2 was applied to the cells. Cellular morphological changes were observed under a fluorescence microscope after Hoechst 33342 and PI double staining. A, untreated; B, UV-B radiation at 50 mJ/cm^2; C, 5 μM compound + UV-B radiation at 50 mJ/cm^2; D, 50 μM compound + UV-B radiation at 50 mJ/cm^2; E, 250 μM compound + UV-B radiation at 50 mJ/cm^2.

operates within a specialized intracellular organelle, the molanosome. In melanogenesis, the proximal pathway consists of the enzymatic oxidation of tyrosine or $_{L}$-DOPA to its corresponding *o*-dopaquinone catalyzed by tyrosine. After multi-biosynthesis steps, further polymerization yield melanin (Kim and Uyama, 2005). In the present study, B16 mouse melanoma cell were used for determination of inhibitory effect of melanin content (**Fig. 2-52**). Phenylthiourea (PTU) and retinol, well known inhibitors of melanin synthesis, are together used as positive controls. The inhibitory effect of melanin synthesis of **1** showed 54.35% at 100 μM, and the IC_{50} values were recorded as 89.33 μM, while the positive controls (PTU and retinol) have 32.72 and 50.25 μM, respectively (**Table 2-16**). Several studies reported melanin inhibition effect of various natural organisms. However, the minimum number of natural product (Broussonetia extract, oil soluble Licorice extract etc.) can be used for whitening materials. Although **1** possess relatively lower than that of PTU and retinol, it can be applied to whitening materials as natural compounds.

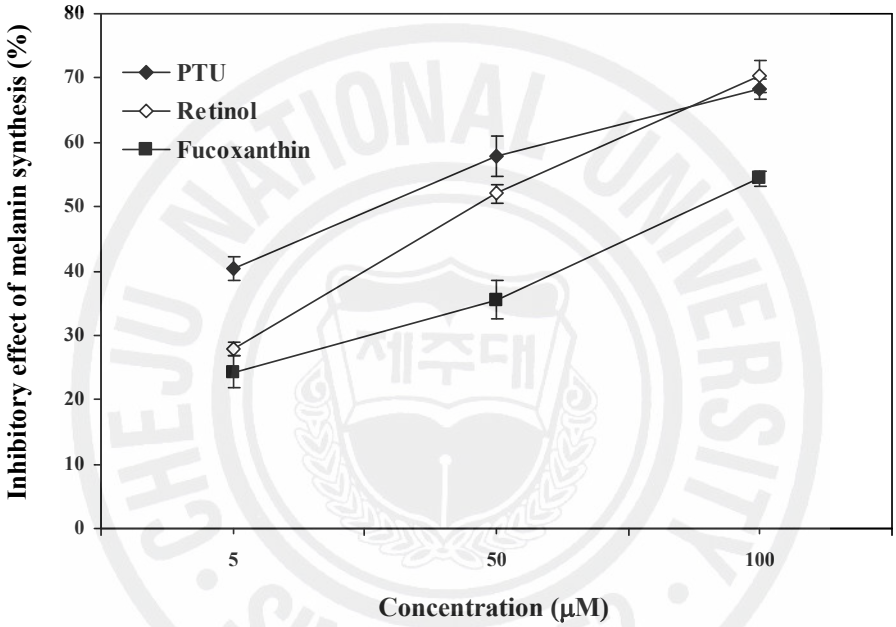

Fig. 2-52. Inhibitory effect of fucoxanthin isolated from *S. siliquastrum* on melanin synthesis. B16F10 melanoma cells were used for this experiment and PTU and retinol were used as positive control. Experiments were performed in triplicate and the data are expressed as mean ± SE.

Table 2-16. Inhibitory effect of fucoxanthin isolated from *S. siliquastrum* on melanin synthesis

	$IC_{50}(\mu M)$
PTU	**32.72**
Retinol	**50.25**
Fucoxanthin	**89.33**

Part Ⅲ.

Isolation of cosmetic materials from *Ishige okamurae*

Part Ⅲ.

Isolation of cosmetic materials from *Ishige okamurae*

1. ABSTRACT

To obtain a natural antioxidant and potential cosmetic materials from a marine biomass, this study investigated by colorimetric and cell lines from the brown alga, *Ishige okamurae* collected off Jeju Island. A potent biological activity was detected in the ethyl acetate fraction containing polyphenolic components, and the potent compound elucidated as a kind of phlorotannin, diphlorethohydroxycarmalol (**14**), by NMR and mass spectroscopic data. The antioxidant activities of the diphlorethohydroxycarmalol were investigated to scavenging 1,1-diphenyl-2-picrylhydrazyl (DPPH), alkyl, hydroxyl radicals and hydrogen peroxide. The diphlorethohydroxycarmalol exhibited powerful antioxidant effect than those of commercial antioxidants. Moreover, the diphlorethohydroxycarmalol showed potential cosmeceutical activities by inhibitory effects of tyrosinase and melanin synthesis and protective effect against oxidative stress induced UV radiation. Therefore, these results present diphlorethohydroxycarmalol as a new phlorotannin with a potent antioxidant and cosmeceutical activities that could be useful in cosmetics, foods, and pharmaceuticals.

2. MATERIALS AND METHODS

2.1. General experimental procedures

The UV spectra were recorded on a Pharmacia Biotech Ultrospec 3000 UV/visible spectrometer, the NMR spectra recorded on a Varian INOVA 500 MHz NMR spectrometer, and the ESI and HREI mass spectra acquired using a Finnigan Navigator 30086 and JMS-700 Mstation high-resolution mass spectrometer system, respectively. The HPLC was carried out using a Waters HPLC system equipped with a Waters 996 photodiode array detector and C18 column (J'sphere ODS-H80, 150×20 mm, 4 μm, YMC Co.).

2.2. Materials

The marine alga *Ishige okamuare* (**Fig. 3-1**) was collected along the coast of Jeju Island, Korea, between October 2005 and March 2006. The samples were washed three times with tap water to remove the salt, epiphytes, and sand attached to the surface, then carefully rinsed with fresh water, and maintained in a medical refrigerator at –20℃. Therefore, the frozen samples were lyophilized and homogenized with a grinder prior to extraction.

Fig. 3-1. The photograph of a brown alga *Ishige okamurae*.

2.3. Extraction and isolation

The powdered *I. okamurae* (500 g) was extracted with 80% aqueous MeOH, and filtered. The filtrate was the evaporated at 40℃ to obtain the methanol extract, which was dissolved in water, then partitioned with EtOAc. The EtOAc extract (18.7 g) was fractionated by silica column chromatography with stepwise elution of $CHCl_3$-MeOH mixture (20:1-0:1) to afford separated active fractions. A combined active fraction was further subjected to a Sephadex LH-20 column saturated with 70 % aqueous Acetone, and then finally purified by reversed-phase HPLC to give compound diphlorethohydroxycarmalol (780 mg) (**Fig. 3-2**).

Diphlorethohydroxycarmalol (14): brownish yellow amorphous powder; IR (KBr) ν_{max} 3391, 1615, 1498, 1279, 1188, 965, 818 cm^{-1}; UV (MeOH): λ_{max} nm (log ε) 232 (3.7); ^{1}H and ^{13}C NMR, see **Table 3-1**; ESIMS *m/z* 512 $[M]^+$; HREIMS *m/z* 512.0589 $[M]^+$ (calcd for $C_{24}H_{16}O_{13}$, 512.0591).

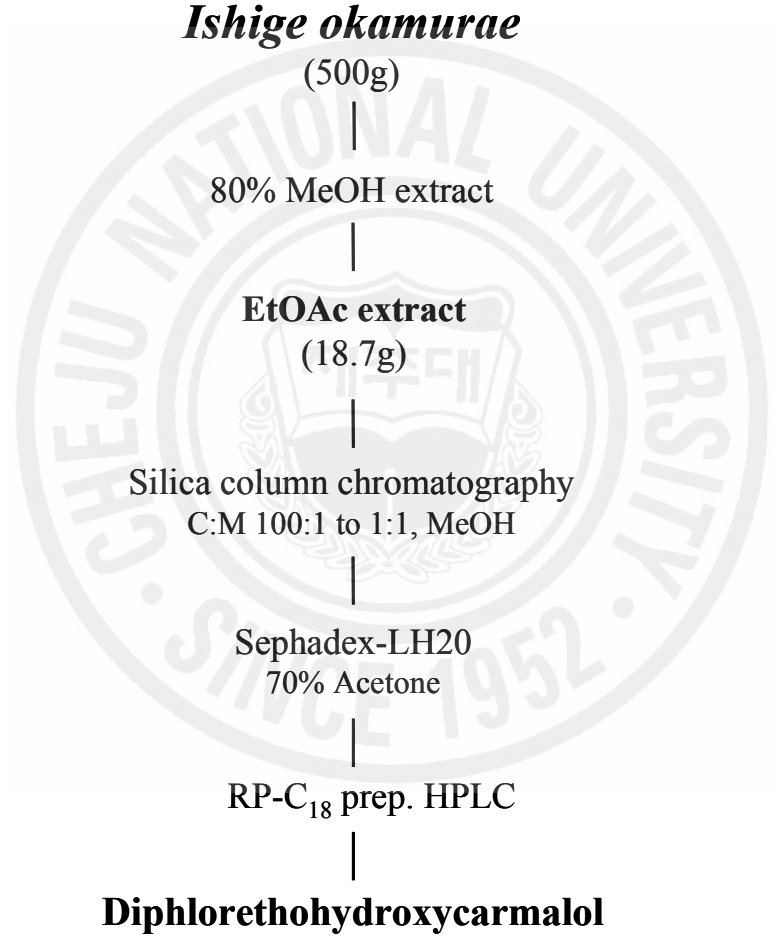

Fig. 3-2. Isolation scheme of diphlorethohydroxycarmalol (**14**) from *I. okamurae*.

Table 3-1. ^{1}H and ^{13}C NMR assignments for diphlorethohydroxycarmalol (**14**)

Position	^{13}C	^{1}H (mult. J=Hz)
1	135.1	
2	125.5	
3	133.8	
4	92.4	5.69 (1H, s)
4a	143	
5a	146	
6	139.6	
7	138.8	
8	124.1	
9	94.3	6.06 (1H, s)
9a	126.4	
10a	130.7	
1'	122.9	
2'	151.3	
3'	95	5.87 (2H, s)
4'	154.9	
5'	95	5.87 (2H, s)
6'	151.3	
1"	160.1	
2"	93.7	5.67 (2H, d, J=2)
3"	158.9	
4"	96.1	5.78 (1H, t, J=2)
5"	158.9	
6"	93.7	5.67 (2H, d, J=2)

* 500 MHz for ^{1}H and 125 MHz for ^{13}C

2.4. DPPH radical scavenging assay

The DPPH radical scavenging activity was measured using an ESR spectrometer (JES-FA machine, JOEL, Tokyo, Japan) according to the technique described by Nanjo et al. (1996). 60 μl of each sample was added to 60 μl of DPPH (60 μmol/l) in ethanol. After 10 seconds of vigorous mixing, the solutions were transferred to Teflon capillary tubes and fitted into the cavity of the ESR spectrometer. The spin adduct was determined by the ESR spectrometer exactly 2 min later under the following measurement conditions: central field 3475 G, modulation frequency 100 kHz, modulation amplitude 2 G, microwave power 5 mW, gain 6.3×10^5, and temperature 298 K. All the radical scavenging activities (%) in the present study were calculated using the following equation, in which H and H_0 were the relative peak heights of the radical signals with and without a sample, respectively.

$$\text{Radical scavenging activity} = [1-(H / H_0)] \times 100$$

2.5. Alkyl radical scavenging assay

Alkyl radicals were generated via AAPH. Thus, reaction mixtures containing 10 mmol/l AAPH and 10 mmol/l 4-POBN were mixed with the tested samples. The solutions were incubated for 30 min at 37℃ in a water bath, then transferred to Teflon capillary tubes (Hiramoto et al., 1993). The spin adduct was recorded using a JES-FA ESR spectrometer under the following measurement conditions: central field 3475 G, modulation frequency 100 kHz, modulation amplitude 2 G, microwave power 10 mW, gain 6.3×10^5, and temperature 298 K. The alkyl radical scavenging activity (%) was

presented as described above.

2.6. Hydroxyl radical scavenging assay

Hydroxyl radicals were generated via a Fenton reaction, and reacted rapidly with nitrone spin trap DMPO. The resultant DMPO-OH adducts were detected using an ESR spectrometer (Rosen and Rauckman, 1984). Reaction mixtures containing 100 μl of 0.3 M DMPO, 100 μl of 10 mM $FeSO_4$, and 100 μl of 10 mM H_2O_2 were mixed with the test samples, then transferred to Teflon capillary tube. The spin adduct was measured on an ESR spectrometer exactly 2.5 min later under the following measurement conditions: central field 3475 G, modulation frequency 100 kHz, modulation amplitude 2 G, microwave power 1 mW, gain 6.3×10^5, and temperature 298 K. The hydroxyl radical scavenging activity (%) was presented as described above.

2.7. Hydrogen peroxide scavenging assay

Hydrogen peroxide scavenging activity was determined according to the method of Müller (1985). A hundred μl of 0.1 M phosphate buffer (pH 5.0) and the sample solution were mixed in a 96-well plate. A 20 μl of hydrogen peroxide was added to the mixture, and then incubated at 37℃ for 5 min. After the incubation, 30 μl of 1.25 mM ABTS and 30 μl of peroxidase (1 unit/ml) were added to the mixture, and then incubated at 37℃ for 10 min. The absorbance was read with an ELISA reader at 405 nm.

2.8. Antioxidant activities by cell lines

2.8.1. Cell culture

Cells of a monkey kidney fibroblast line (Vero) were maintained at 37℃ in an incubator with humidified atmosphere of 5% CO_2. Cells were cultured in Dulbecco's modified Eagle's medium containing 10% heat-inactivated fetal calf serum, streptomycin (100 μg/ml), and penicillin (100 unit/ml).

2.8.2. Hydrogen peroxide scavenging assay

For detection of intracellular H_2O_2, Vero cells were seeded in 96-well plates at a concentration of 1×10^5 cells/ml. After 16 h, the cells were treated with various concentrations of the compounds, and incubated at 37℃ under a humidified atmosphere. After 30 min, H_2O_2 was added at a concentration of 1 mM, and then cells were incubated for an additional 30 min at 37℃. Finally, 2',7'-dichlorodihydrofluorescein diacetate (DCFH-DA; 5 μg/ml) was introduced to the cells, and 2',7'-dichlorodihydrofluorescein fluorescence was detected at an excitation wavelength of 485 nm and an emission wavelength of 535 nm, using a Perkin-Elmer LS-5B spectrofluorometer. The percentage of H_2O_2 scavenging activity was calculated in accordance with the following equation:

$$H_2O_2 \text{ scavenging activity (\%)} = (1 - (C_1 / C_0)) \times 100$$

where C_1 is the fluorescence intensity of cells treated with H_2O_2 and compounds, and C_0 is the fluorescence intensity of cells treated with H_2O_2 and distilled water instead of compounds.

2.8.3. Determination of DNA damage by comet assay

Comet assay was performed to determine the oxidative DNA damage (Singh, 2000). The cell suspension was mixed with 75 μl of 0.5% low melting agarose (LMA), and added to the slides precoated with 1.0% normal melting agarose (NMA). After solidification of the agarose, slides were covered with another 75 μl of 0.5% LMA and then immersed in lysis solution (2.5 M NaCl, 100 mM EDTA, 10 mM Tris, and 1% sodium laurylasarcosine; 1% Triton X-100 and 10% DMSO) for 1 h at 4℃. The slides were next placed into an electrophoresis tank containing 300 mM NaOH and 10 mM Na_2EDTA (pH 13.0) for 40 min for DNA unwinding. For electrophoresis of the DNA, an electric current of 25 V/300 mA was applied for 20 min at 4℃. The slides were washed three times with a neutralizing buffer (0.4 M Tris, pH 7.5) for 5 min at 4℃, and then treated with ethanol for another 5 min before staining with 50 μl of ethidium bromide (20 μg/ml). Measurements were made by image analysis (Kinetic Imaging, Komet 5.0, U.K) and fluorescence microscope (LEICA DMLB, Germany), determining the percentage of fluorescence in the tail (tail intensity, TI; 50 cells from each of two replicate slides).

2.8.4. Assessment of cell viability

Cell viability was then estimated via an MTT assay, which is a test of metabolic competence predicated upon the assessment of mitochondrial performance. It is colorimetric assay, which is dependent on the conversion of yellow tetrazolium bromide to its purple formazan derivative by mitochondrial succinate dehydrogenase in viable cells (Mosmann, 1983). The cells were seeded in 96-well plate at a concentration of

1×10^5 cells/ml. After 16 h, the cells were treated with compounds at difference concentrations. Then, 10 μl of H_2O_2 (1 mM) was added to the cell culture medium, and incubated for 24 h at 37 ℃. MTT stock solution (50 μl; 2 mg/ml) was then applied to the wells, to a total reaction volume of 200 μl. After 4 h of incubation, the plates were centrifuged for 5 min at 800 ×g, and the supernatants were aspirated. The formazan crystals in each well were dissolved in 150 μl of dimethylsulfoxide (DMSO), and the absorbance was measured via ELISA at a wavelength of 540 nm. Relative cell viability was evaluated in accordance with the quantity of MTT converted to the insoluble formazan salt. The optical density of the formazan generated in the control cells was considered to represent 100% viability. The data are expressed as mean percentages of the viable cells versus the respective control.

2.8.5. Nuclear staining with Hoechst 33342

The nuclear morphology of the cells was evaluated using the cell-permeable DNA dye, Hoechst 33342. Cell with homogeneously stained nuclei were considered viable, whereas the presence of chromatin condensation and/or fragmentation was indicative of apoptosis (Gschwind and Huber, 1995; Lizard et al., 1995). The cells were placed in 24-well plates at a concentration of 1×10^5 cells/ml. Sixteen hours after plating, the cells were treated with various concentration of the compounds, and further incubated for 1 h prior to expose to H_2O_2 (1 mM). After 24 h, 1.5 μl of Hoechst 33342 (stock 10 mg/ml), a DNA-specific fluorescent dye, were added to each well, followed by 10 min of incubation at 37℃. The stained cells were then observed under a fluorescence microscope equipped with a CoolSNAP-Pro color digital camera, in order to examine the degree of nuclear condensation.

2.9. Tyrosinase inhibition assay

Tyrosinase inhibitory activity was performed according to the method of Vanni et al. (1990) with minor modifications. The reaction mixture contains 140 µl of 0.1 M phosphate buffer (pH 6.5), 40 µl of 1.5 mM L-tyrosine and 10 µl of samples. Then, 10 µl of mushroom tyrosinase (2100 units/ml) solution was added and the reaction was incubated at 37℃ for 12 min. After incubation, the amount of dopachrome produced in the reaction mixture was determined as the optical density at 490 nm in a microplate reader. The percent inhibition of tyrosinase reaction was calculated as follows:

$$\text{Inhibition (\%)} = [1 - (B - A) / (D - C)] \times 100$$

A = Absorbance at 490 nm with test sample before incubation

B = Absorbance at 490 nm with test sample after incubation

C = Absorbance at 490 nm without test sample before incubation

D = Absorbance at 490 nm without test sample after incubation

2.10. Inhibitory effect of melanin synthesis

2.10.1. Cell cultures

Mouse melanoma cell lines (B-16 F10) were maintained at 37℃ in an incubator, under a humidified atmosphere containing 5% CO_2. The cells were cultured in Dulbecco's modified Eagle's medium containing 10% heat-inactivated fetal calf serum,

streptomycin (100 mg/ml), and penicillin (100 unit/ml).

2.10.2. Inhibitory effect of melanin synthesis

Melanin contents were measured according to the method of Tsuboi et al. (1998) with a slightly modification. The B-16 F10 cells were placed in 6-well plates at a concentration of 3×10^5 cells/ml, and 24 h after plating the cells were treated with various concentrations of the compounds. After 24 h, the medium was removed and cells were washed twice with PBS. And cell pellets containing a known number of cells (usually around 1×10^6) were dissolved in 1 ml of 1 N NaOH at 60 ℃ for 30 min and centrifuged for 10 min at 10,000 rpm. The optical densities (OD) of the supernatants were measured at 490 nm using an ELISA reader.

2.11. Protective effect by ultra violet irradiation

2.11.1. Cell culture

Human fibroblast were kindly supplied by Surface Science Laboratory of Center for Anti-aging Molecular Science (CAMS) of Department of Chemistry and School of Molecular Science of Korea Advanced Institute of Science and Technology (KAIST), maintained at 37℃ in an incubator with humidified atmosphere of 5% CO_2. Cells were cultured in Dulbecco's modified Eagle's medium containing 10% heat-inactivated fetal calf serum, streptomycin (100 μg/ml), and penicillin (100 unit/ml).

2.11.2. UV-B irradiation

Cells were exposed to UV-B range at a dose rate of 10 to 100 mJ/cm^2 (UV Lamp, VL-6LM, Vilber Lourmat, France). Optimum irradiation dose were evaluated at 50 mJ/cm^2, therefore the 50 mJ/cm^2 of UV-B were used further experiments.

2.11.3. Intracellular reactive oxygen species measurement

For detection of intracellular ROS, fibroblast were seeded in 96-well plates at a concentration of 1×10^5 cells/ml. After 16 h, the cells were exposed to UV-B (50 mJ/cm^2) and the compounds were treated with various concentrations, and then cells were incubated for 24 h at 37℃ under a humidified atmosphere with 5% CO_2. Finally, 2',7'-dichlorodihydrofluorescein diacetate (DCFH-DA; 5 μg/ml) was introduced to the cells, and 2',7'-dichlorodihydrofluorescein fluorescence was detected at an excitation wavelength of 485 nm and an emission wavelength of 535 nm, using a Perkin-Elmer LS-5B spectrofluorometer.

2.11.4. Assessment of cell viability

Cell viability was then estimated via an MTT assay, which is a test of metabolic competence predicated upon the assessment of mitochondrial performance. It is colorimetric assay, which is dependent on the conversion of yellow tetrazolium bromide to its purple formazan derivative by mitochondrial succinate dehydrogenase in viable cells (Mosmann, 1983). The fibroblast was seeded in 96-well plate at a concentration of 1×10^5 cells/ml. After 16 h, the cells were exposed to UV-B (50 mJ/cm^2) with

compounds at difference concentrations, and then the cells were incubated for 24 h at 37℃. MTT stock solution (50 μl; 2 mg/ml) was then applied to the wells, to a total reaction volume of 200 μl. After 4 h of incubation, the plates were centrifuged for 5 min at 800 ×g, and the supernatants were aspirated. The formazan crystals in each well were dissolved in 150 μl of dimethylsulfoxide (DMSO), and the absorbance was measured via ELISA at a wavelength of 540 nm. Relative cell viability was evaluated in accordance with the quantity of MTT converted to the insoluble formazan salt. The optical density of the formazan generated in the control cells was considered to represent 100% viability. The data are expressed as mean percentages of the viable cells versus the respective control.

2.11.5. Determination of UV-B induced DNA damage by comet assay

Comet assay was performed to determine the irradiative DNA damage (Singh, 2000). The cell suspension was mixed with 75 μl of 0.5% low melting agarose (LMA), and added to the slides precoated with 1.0% normal melting agarose (NMA). After solidification of the agarose, slides were covered with another 75 μl of 0.5% LMA and then immersed in lysis solution (2.5 M NaCl, 100 mM EDTA, 10 mM Tris, and 1% sodium laurylasarcosine; 1% Triton X-100 and 10% DMSO) for 1 h at 4℃. The slides were next placed into an electrophoresis tank containing 300 mM NaOH and 10 mM Na_2EDTA (pH 13.0) for 40 min for DNA unwinding. For electrophoresis of the DNA, an electric current of 25 V/300 mA was applied for 20 min at 4℃. The slides were washed three times with a neutralizing buffer (0.4 M Tris, pH 7.5) for 5 min at 4℃, and then treated with ethanol for another 5 min before staining with 50 μl of ethidium bromide (20 μg/ml). Measurements were made by image analysis (Kinetic Imaging,

Komet 5.0, U.K) and fluorescence microscope (LEICA DMLB, Germany), determining the percentage of fluorescence in the tail (tail intensity, TI; 50 cells from each of two replicate slides).

2.11.6. Microscopic analysis for dead cells

The type of cell death (apoptosis or necrosis) induced by UV-B was determined by fluorescent microscopy after staining with Hoechst 33342 and propidium iodide (PI), as described by Naito (2002). The fibroblasts were placed in 24-well plates at a concentration of 1×10^5 cells/ml. Sixteen hours after plating, the cells were exposed to UV-B (50 mJ/cm^2) with compounds at difference concentrations, and then the cells were incubated for 24 h at 37℃. After 24 h, 1.5 μl of Hoechst 33342 (stock 10 mg/ml) and PI were added to each well, step by step, followed by 10 min of incubation at 37℃. The stained cells were then observed under a fluorescence microscope equipped with a CoolSNAP-Pro color digital camera, in order to examine the degree of nuclear condensation.

2.12. Animal test

2.12.1. UV absorption assay

Test material was dissolved in methanol at the concentration of 100 μg/ml and put in a quartz cuvette. The absorption spectrum of compound from *I. okamurae* was measured between 280 and 420 nm using a double beam spectrophotometer (U-2800, Hitachi).

2.12.2. UV-B protection test for erythema and edema

UV radiation experiments were carried out on male hairless (Hr-1) mice at 8 weeks of age obtained from Japan SLC, Inc. (Shizuoka, Japan). The colony was maintained under controlled conditions of temperature (19-25℃), humidity (40-60%) and a 12 h light-dark cycle with the light intensity of 150-300 Lux. The animals were housed in sanitized polycarbonate cages (260W × 420L × 180H). They had free access to standard mouse food and water. All animals were raised in SPF condition of the Clinical Research Center of Dong-A University Hospital according to Good Laboratory Practices (GLP) OECD guidelines.

Test material (0.5~1 ㎎/㎠) was applied to the left side of dorsal skin and vehicle was applied to the right side for 30 min. Animals were wrapped with tapes containing two exposure windows of 1 ㎠ at each side of back and placed under a bank of 5 UV-B lamps positioned 15 ㎝ above their backs. The irradiation at this distance was of 100 ㎼/s when measured with a research radiometer. The radiation dosage was set 60 mJ/㎠ for upper window and 80 mJ/㎠ for lower window. At the completion of irradiation, tapes were removed and skin lesions (erythema and edema) were observed at 24 h.

2.13. Statistical analysis

The data are expressed as the mean ± standard error (SE). A statistical comparison was performed via the SPSS package for Windows (Version 10). P-values of less than 0.05 were considered to be significant.

3. RESULT AND DISCUSION

Ishige okamurae is abundant along the coast of Jeju Island and regarded as an edible alga. However, since biological studies of this alga are relatively rare, this study screened its radical scavenging activity and inhibitory effect of tyrosinase using various solvent fractions. As the EtOAc extract showed prominent effect both radical scavenging and tyrosinase inhibition, the active compound of this extract was fractionated by silica gel and Sephadex LH-20 open column chromatography and the active compounds were purified by reversed-phase HPLC.

Diphlorethohydroxycarmalol (**14**) was isolated as a brownish yellow amorphous powder, and its molecular formula deduced as $C_{24}H_{16}O_{13}$ based on NMR (**Table 3-1**) and HRESI-MS analyses (M^+, *m/z*: 512.0589 calcd for $C_{24}H_{16}O_{13}$ *m/z*: 512.0591). The IR spectrum of diphlorethohydroxycarmalol showed the presence of 3391 (OH) and 1645 (C-O) cm^{-1}, and the ^1H NMR spectrum exhibits characteristic peak at δ_H 5.67 (H-2", 6"), 5.69 (H-4), 5.78 (H-4"), 5.87 (H-3', 5'), and 6.06 (H-9) attributable to seven methyl protons. The diphlorethohydroxycarmalol was then used in further experiments regarding on antioxidant and cosmeceuticals.

ESR spin trapping provides a sensitive, direct, and accurate means of monitoring reactive species (Guo et al., 1999). Therefore, this study used ESR technique to compare the DPPH, alkyl, and hydroxyl radical scavenging abilities of the diphlorethohydroxycarmalol isolated from *I. okamurae* with those of a commercial antioxidant, such as ascorbic acid. DPPH is a stable free radical donor that is widely used to test the free radical scavenging effect of natural antioxidants. The scavenging activity of the diphlorethohydroxycarmalol towards DPPH free radicals is shown in **Fig. 3-7**, where 74.68% of the DPPH free radicals were scavenged even at 10 μM, and the

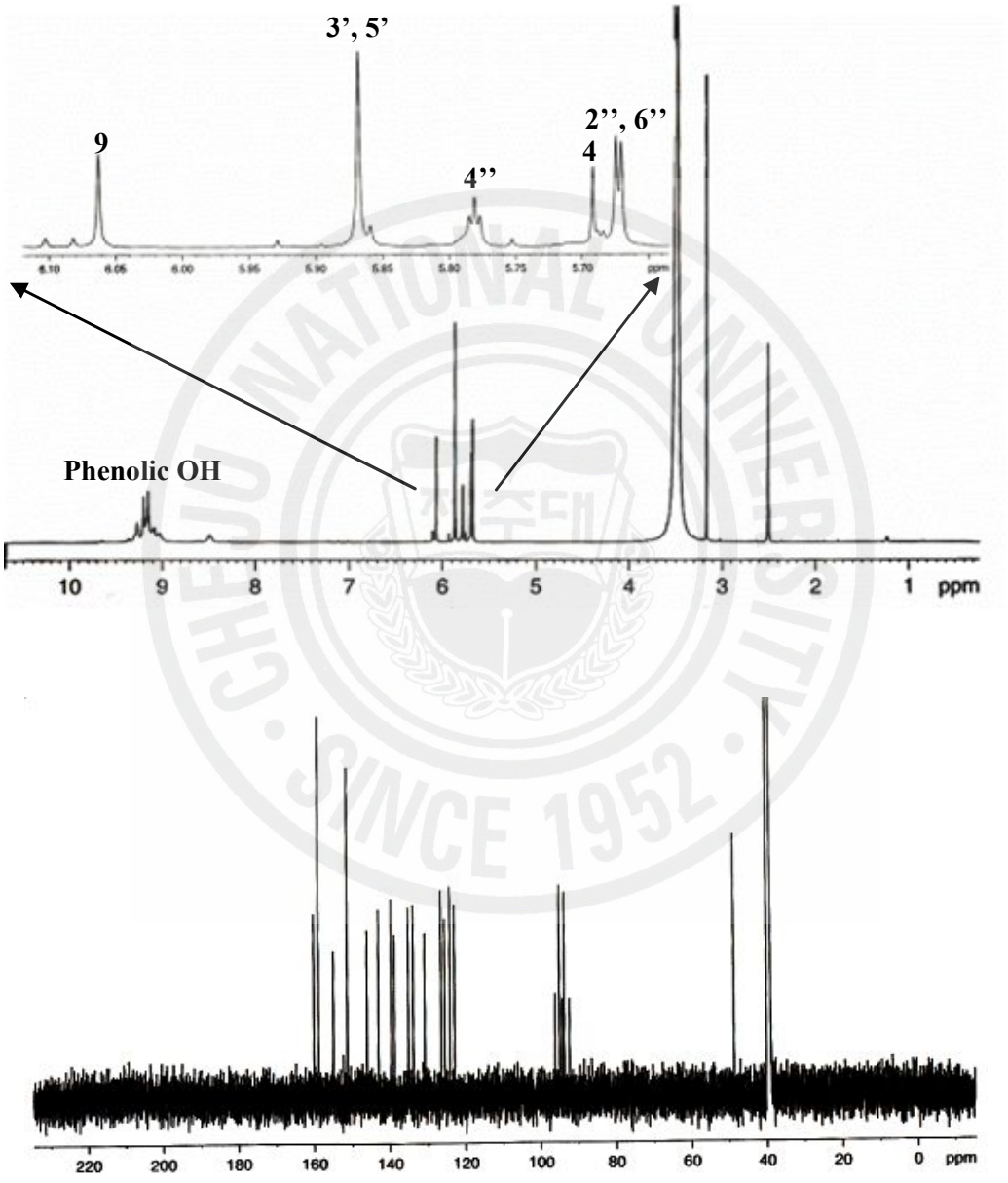

Fig. 3-3. Proton and Carbon NMR spectrum of diphlorethohydroxycarmalol (**14**).

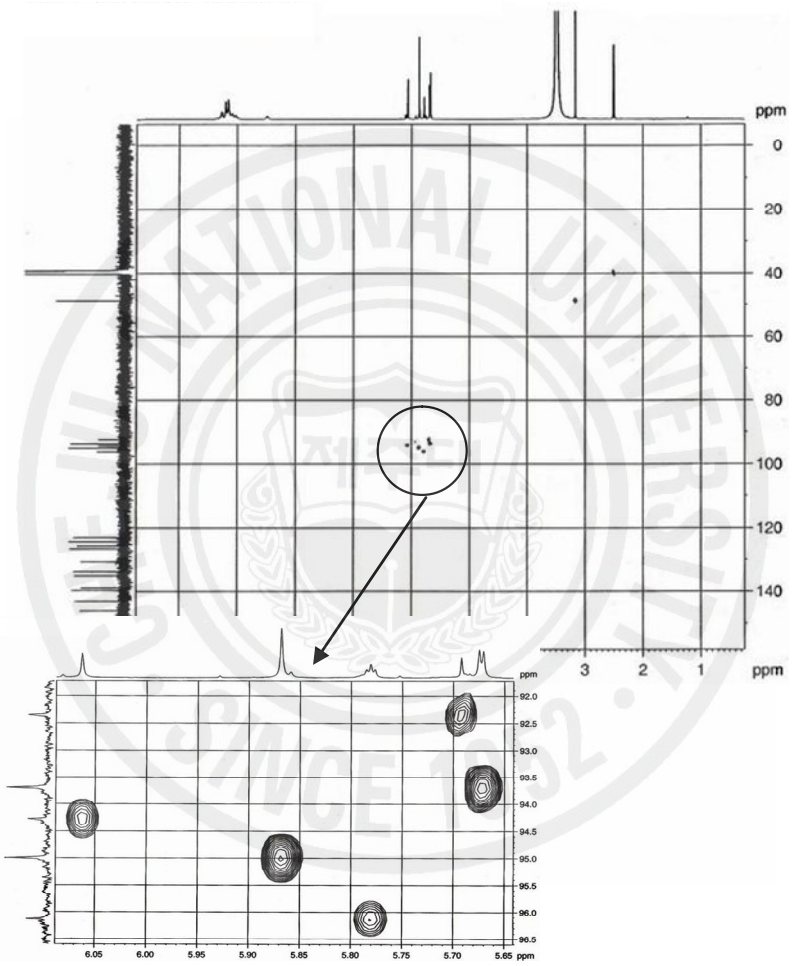

Fig. 3-4. Gradient HMQC NMR spectrum of diphlorethohydroxycarmalol (**14**).

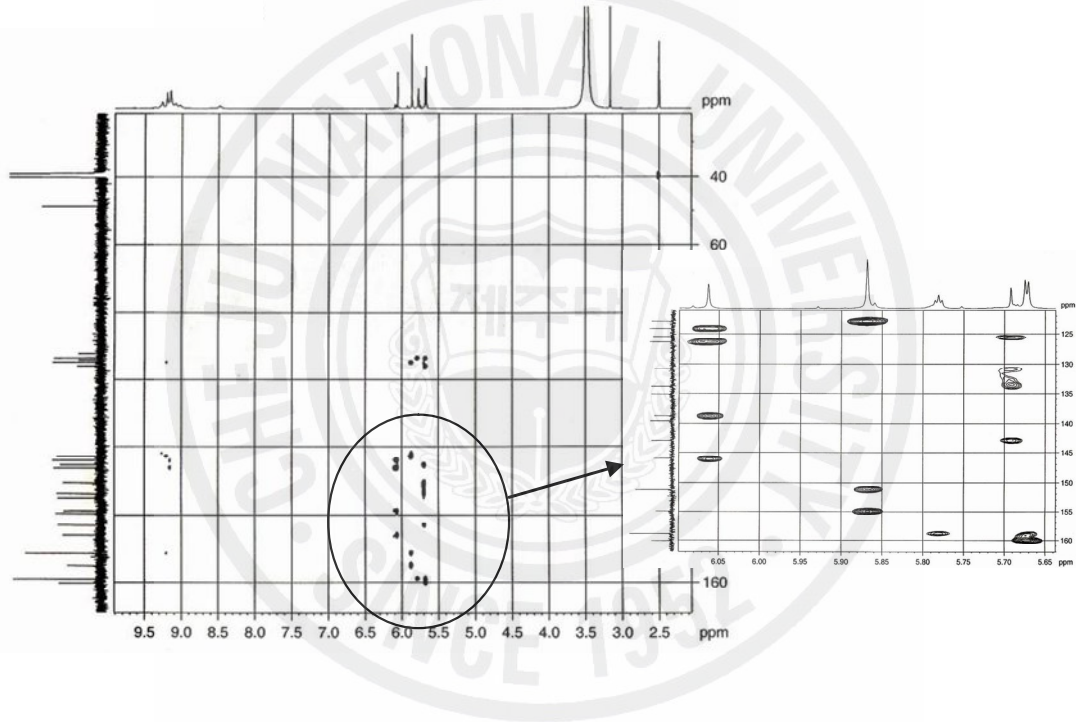

Fig. 3-5. Gradient HMBC NMR spectrum of diphlorethohydroxycarmalol (**14**).

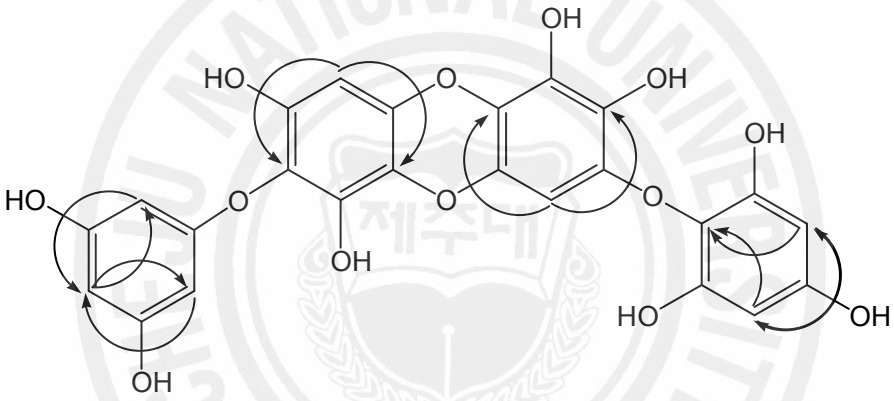

Fig. 3-6. Selective long range correlations for diphlorethohydroxycarmalol (**14**).

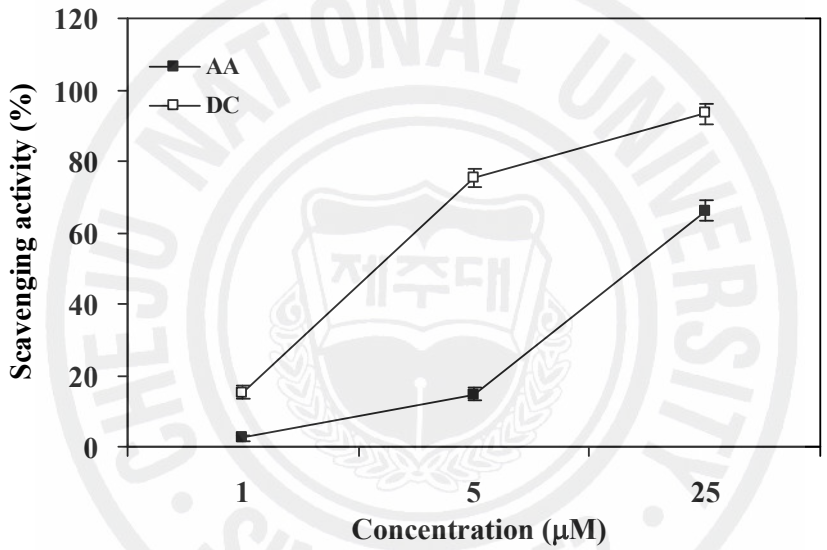

Fig. 3-7. DPPH radical scavenging activity of diphlorethohydroxycarmalol isolated from *I. okamurae*. ■, AA (ascorbic acid); □, DC (diphlorethohydroxycarmalol). Experiments were performed in triplicate and the data are expressed as mean ± SE

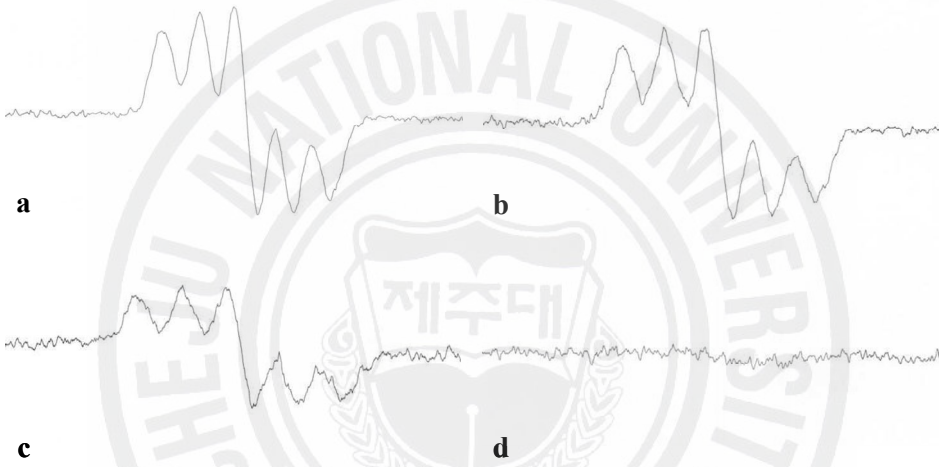

Fig. 3-8. ESR spectrum obtained in an ethanol solution of 30 μmol/l DPPH at various concentrations of diphlorethohydroxycarmalol isolated from *I. okamurae*.
a, control; b, 1 μM; c, 5 μM; d, 25 μM.

radical scavenging occurred in a dose-dependent manner (**Fig. 3-8**). In addition, the diphlorethohydroxycarmalol (IC_{50}=3.41 μM) exhibited stronger DPPH free radical scavenging than the commercial antioxidant, ascorbic acid (**Table 3-2**). Several previous reports have emphasized an association between DPPH radical scavenging and phenolic compounds. For example, Tepe and Sokmen (2007) reported that a high total phenolic content was correlated with high antioxidant activity in a DPPH assay, while Yuan et al. (2005) noted a positive relationship between phenolic functional groups and DPPH free radical scavenging activity. Phenols are particularly effective antioxidants for polyunsaturated fatty acids, and can easily transfer a hydrogen atom into lipid peroxyl radicals to form aryloxyl, which being incapable of acting as a chain carrier, then couples with other radicals, thereby quenching the radical propagation process (Ruberto et al., 2001). Phlorotannins are also known to exist in marine alga polyphenols, as evidenced by the positive effect on DPPH free radicals in this study.

Alkyl radicals are a primary intermediate in many hydrocarbon reactions, and can be easily detected with ESR, a technique that has been found to be very useful in the characterization of solid surfaces and in the elucidation of active surface sites, as well as surface reactions (Adebajo and Gesser, 2001). The ability of the diphlorethohydroxy-carmalol to scavenge alkyl radicals is presented in **Fig. 3-9**, where 83.24% of the alkyl radicals were scavenged at 20 μM, and the scavenging activities increased when increasing the compound concentrations (**Fig. 3-10**). Moreover, the diphlorethohydroxy-carmalol exhibited a higher alkyl radical scavenging activity (IC_{50}=4.92 μM) than the commercial antioxidant ascorbic acid (IC_{50}=19.26 μM). In the previous studies, Park et al. (2005) observed that *Sargassum thunbergii* had a strong radical scavenging effect on alkyl radicals, while Ahn et al. (2007) reported that the dieckol isolated from *Ecklonia cava* scavenged 90% of alkyl radicals at 50 μg/ml. Although phenolic antioxidants are

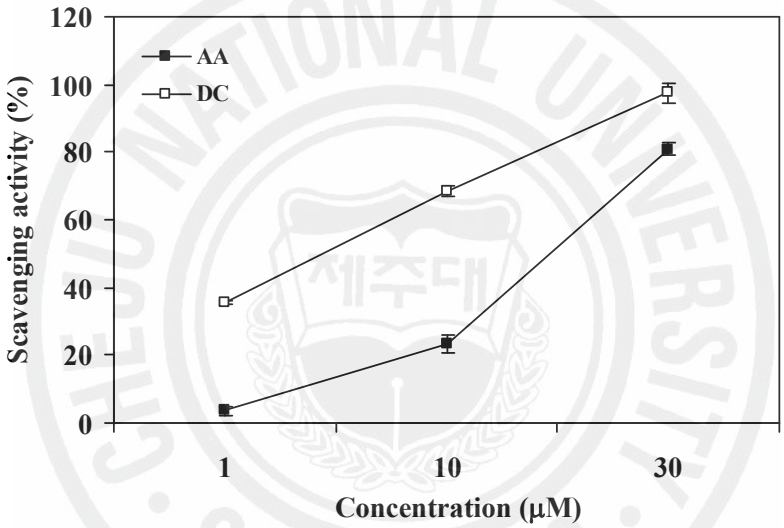

Fig. 3-9. Alkyl radical scavenging activity of diphlorethohydroxycarmalol isolated from *I. okamurae*. ■, AA (ascorbic acid); □, DC (diphlorethohydroxycarmalol). Experiments were performed in triplicate and the data are expressed as mean ± SE.

Fig. 3-10. ESR spectrum obtained during incubation of AAPH with 4-POBN at various concentrations of diphlorethohydroxycarmalol isolated from *I. okamurae*. a, control; b, 1 μM; c, 10 μM; d, 30 μM.

well known for trapping peroxy radicals to prevent organic materials from oxidative degradation, trapping alkyl radicals is also important to prevent such degradation, as autoxidation includes both peroxy and alkyl radicals as chain carriers (Nisizawa et al., 1987). Therefore, the scavenging abilities of the phlorotannins towards alkyl radicals confirm their potential as a source of alkyl radical scavengers.

In cells, hydroxyl radicals are generated from hydrogen peroxide via the so-called Fenton reaction (Huang et al., 2002). Therefore, to investigate the ability of the phlorotannins to scavenge hydroxyl radicals, the following *in vitro* reaction was generated: $Fe^{2+} + H_2O_2 \rightarrow Fe^{3+} + {}^{-}OH + {}^{\cdot}OH$. The hydroxyl radical scavenging activities of the diphlorethohydroxycarmalol are then shown in **Fig. 3-11**, where a decrease in the amount of DMPO-OH adducts was exhibited by the ESR signals after the addition of the diphlorethohydroxycarmalol from *I. okamurae*, and the values were dose-dependent. However, the diphlorethohydroxycarmalol exhibited relatively lower levels of activity (IC_{50}=114.80 μM) than the commercial antioxidant ascorbic acid (IC_{50}=69.75 μM). Hydroxyl radicals are an extremely reactive oxygen species, capable of modifying almost every molecule in living cells and causing strand damage in DNA, leading to carcinogenesis, mutagenesis, and cytotoxicity. Moreover, hydroxyl radicals can rapidly initiate the lipid peroxidation process by abstracting hydrogen atoms from unsaturated fatty acids (Kappus, 1991; Aruoma, 1998). Thus, due to this high reactivity of hydroxyl radicals, measurements based on scavenging hydroxyl radicals, such as nonsite-specific methods, are not accurate reflections of the oxidative protection of an antioxidant molecule *in vivo* (Halliwell and Gutteridge, 1999), as the radicals are more likely to be scavenged by direct reactions with other surrounding molecules before attacking the target molecule. Therefore, the present study used the ESR system, where the hydroxyl radicals were trapped by DMPO, forming a spin adducts that could be

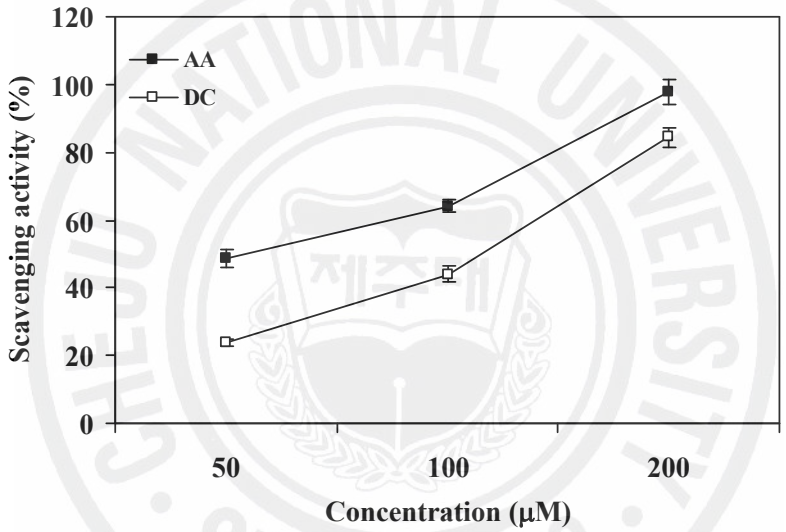

Fig. 3-11. Hydroxyl radical scavenging activity of diphlorethohydroxycarmalol isolated from *I. okamurae*. ■, AA (ascorbic acid); □, DC (diphlorethohydroxycarmalol). Experiments were performed in triplicate and the data are expressed as mean ± SE.

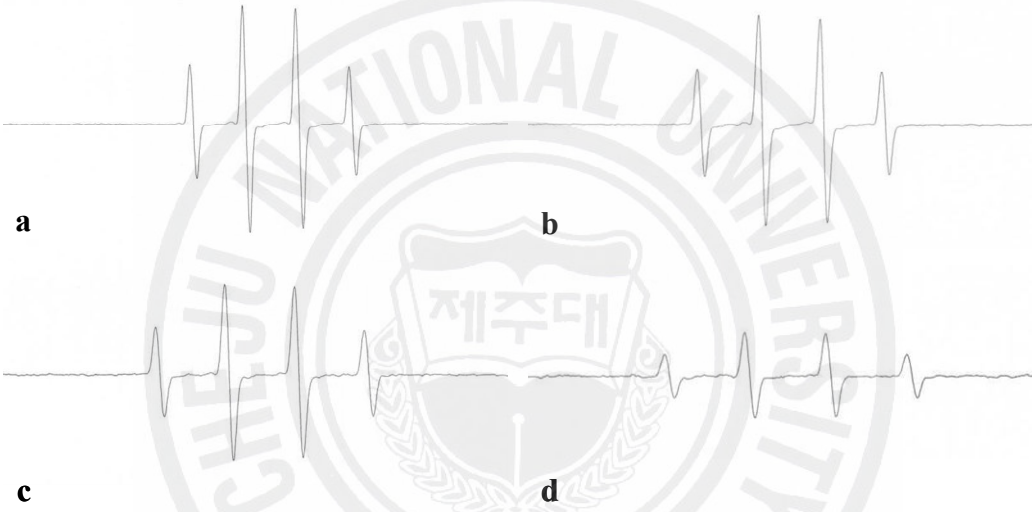

Fig. 3-12. ESR spectrum obtained in Fenton reaction system at various concentrations of diphlorethohydroxycarmalol isolated from *I. okamurae*.

a, control; b, 50 μM; c, 100 μM; d, 200 μM.

Table 3-2. Scavenging activity of diphlorethohydroxycarmalol isolated from *I. okamurae* against DPPH, alkyl, and hydroxyl radicals

	IC_{50} (μM)		
	DPPH	**Alkyl**	**OH**
AA	**19.94**	**19.26**	**69.75**
DC	**3.41**	**4.92**	**114.80**

*AA, ascorbic acid; DC, diphlorethohydroxycarmalol

detected. The findings indicated that the diphlorethohydroxycarmalol exerted a protective effect against reactive radical species, such as hydroxyl radicals. Brown algae are rich in polyphenolic compounds, called phlorotannins, and many researchers have already reported that the phlorotannins from brown algae exhibit antioxidative capacities. For example, Kang et al. (2003) isolated the phlorotannins dieckol, eckol, eckstolonol, and phlorofucofuroeckol from *Ecklonia stolonifera*, all of which showed potent radical scavenging activity with IC_{50} values of 8.8, 11.5, 4.6, and 6.2 μM, respectively. Nakai et al. (2006) also isolated a bifuhalol oligomer, a kind of phlorotannin from *Sargassum ringgoldianum*, that exhibited strong superoxide anion radical scavenging activity (IC_{50}=1 μg/ml), while Kim et al. (2004) and Kang et al. (2006) reported that several phlorotannins demonstrated a lipid peroxidation inhibitory effect and cytoporotective effect on oxidative stress induced cell damage. However, the diphlorethohydroxycarmalol isolated from *Ishige okamurae* showed a powerful radical scavenging activity compared to other phlorotannins in existing literature.

Hydrogen peroxide is an important reactive non-radical compound since it can penetrate biological membranes. As a molecule, hydrogen peroxide is not very reactive, but the single bond between its two oxygen atoms is easily broken, so that it readily fragments into hydrogen and a reactive hydroperoxyl radical, or into two hydroxyl radicals. Hence, measuring H_2O_2 scavenging activity is a useful method for determining the ability of antioxidants to decrease levels of prooxidants such as H_2O_2 (Pazdzioch-Czochra and Widenska, 2002). The hydrogen peroxide scavenging activity by diphlorethohydroxycarmalol is expressed in **Fig. 3-13**. As shown in the results, remarkable scavenging effects were observed for diphlorethohydroxycarmalol where 78.45% of the hydrogen peroxide was scavenged, even at the 25 μM concentration. In addition, diphlorethohydroxycarmalol showed more effective scavenging for hydrogen

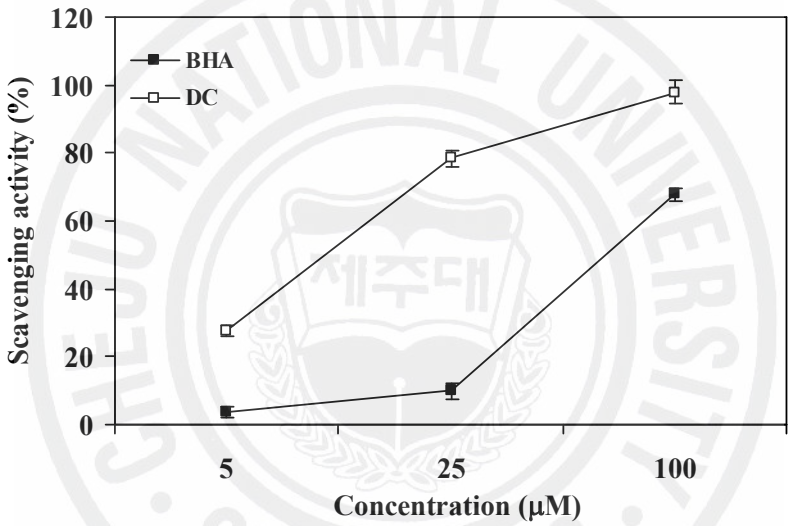

Fig. 3-13. Hydrogen peroxide scavenging activity of diphlorethohydroxycarmalol isolated from *I. okamurae*. ■, BHA (butylatedhydroxyanisol); □, DC (diphlorethohydroxycarmalol). Experiments were performed in triplicate and the data are expressed as mean ± SE.

Table 3-3. Scavenging activity of diphlorethohydroxycarmalol isolated from *I. okamurae* against hydrogen peroxide

	IC_{50} (μM)
	H_2O_2
BHA	**73.92**
DC	**12.32**

*BHA, butylatedhydroxyanisol,
DC, diphlorethohydroxycarmalol

peroxide (IC_{50}=12.32 μM) than a commercial antioxidant, BHA (IC_{50}=73.92 μM). In general, H_2O_2 levels over 50 mM are considered cytotoxic. H_2O_2 can produce other ROS such as hypochlorous acid (HOCl), by the enzymatic (myeleperoxidase) oxidation of chloride ions. HOCl can lead to the production of highly reactive singlet oxygen $^1O_2$, or even hydroxyl radicals. Furthermore, in the presence of abundant hydrogen carbonate (HCO_3^-), H_2O_2 reacts to produce hydrogen peroxycarbonate, which reacts with bimolecular substances *in vitro* (Watts et al., 1999). Therefore, elevated H_2O_2 levels must be minimized by the action of antioxidants. The activity of diphlorethohydroxycarmalol observed in this study implies diphlorethohydroxycarmalol may be used as a natural antioxidant to potentially decrease pro-oxidants such H_2O_2.

Recently, many researchers have focused on natural marine compounds with various biological activities, due to the limited sources of land biomass. Phlorotannins, well known marine algal polyphenols, are recognized to have defensive or protective functions against oxidative stress. Although some reports suggest that the phlorotannins from algae exhibit antioxidant effects on free radicals, there are no reports on their cytoprotective effects against oxidative stress or the underlying mechanism of diphlorethohydroxycarmalol. Therefore, we demonstrated the cytoprotective effects of diphlorethohydroxycarmalol after exposure to H_2O_2. The intracellular ROS scavenging activity of diphlorethohydroxycarmalol was expressed as 62.43% at 200 μM, and the 50% inhibitory concentration was 128.86 μM (**Fig. 3-14**). Since diphlorethohydroxy-carmalol produced evidence of ROS scavenging activity, it was further evaluated with regard to its protective effects against the cellular damage induced by H_2O_2. The protective effects of diphlorethohydroxycarmalol on cell survival in H_2O_2-induced vero cells were measured via the MTT assay. As shown in **Fig. 3-15**, treating with H_2O_2 induced a reduction in the cell survival rate, to 41.31%, while diphlorethohydroxycarmalol

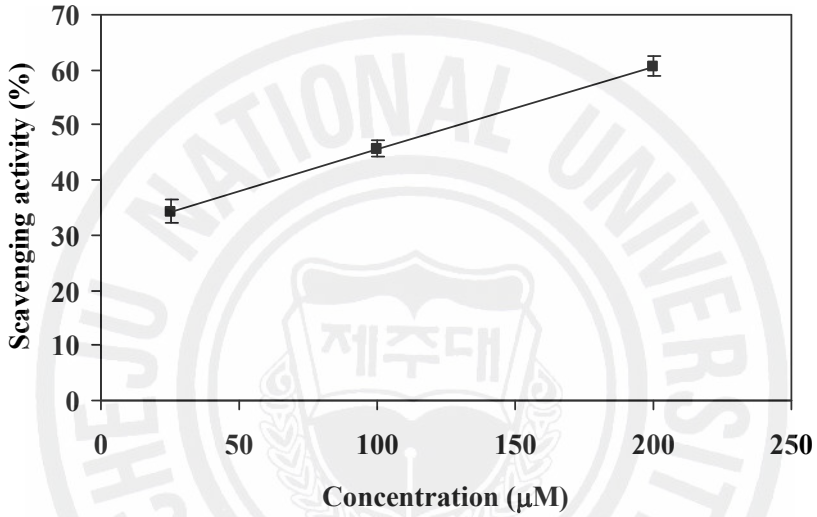

Fig. 3-14. Effect of diphlorethohydroxycarmalol isolated from *I. okamurae* on scavenging reactive oxygen species. The intracellular reactive oxygen species generated was detected by DCF-DA method. Experiments were performed in triplicate and the data are expressed as mean ± SE.

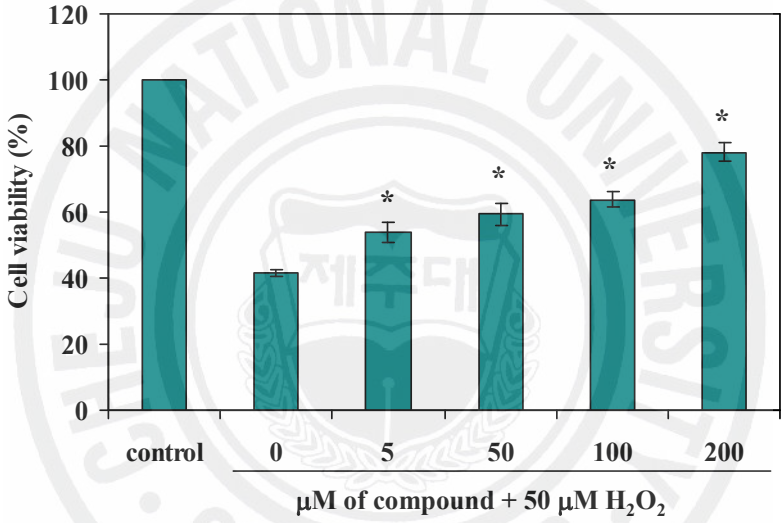

Fig. 3-15. Protective effect of diphlorethohydroxycarmalol isolated from *I. okamurae* on H_2O_2 induced oxidative damage of vero cells. The viability of vero cells on H_2O_2 treatment was determined by MTT assay. Experiments were performed in triplicate and the data are expressed as mean ± SE. Statistical evaluation was performed to compare the experimental groups and corresponding control groups. *, $p < 0.001$

(5, 50, 100, and 200 μM) prevented the H_2O_2-induced damage, restoring cell survival to 51.89, 59.42, 63.74, and 78.17%, respectively. The protective effects of diphlorethohydroxycarmalol on cell damages were also confirmed by a comet assay, which is a rapid and sensitive fluorescence microscopic method for detecting primary DNA damage at the individual cell level, and is extensively used to evaluate the genotoxicity of test substances (Olive et al., 1990). The percent fluorescence tail DNA intensity of Vero cells treated for 30 min with the negative control was significantly different from the positive control (H_2O_2 preincubated in PBS, 50 μM). This increase in DNA damage induced by H_2O_2 was significantly inhibited in a dose-dependent manner by preincubating the H_2O_2 and diphlorethohydroxycarmalol together with the negative cells (**Fig. 3-16**). The inhibitory activities of diphlorethohydroxycarmalol on DNA damage were 27.89, 42.35, and 60.12% at the concentrations of 50, 100, and 250 μM, respectively, and the IC_{50} values was 176.66 μM. In addition, we examined the photomicrographs of different DNA migration profiles, when treated with the different concentrations of diphlorethohydroxycarmalol (**Fig. 3-17**). In the group treated with only H_2O_2, the DNA was completely damaged, and the amounts of tail DNA were significantly increased as compared to those of the negative control. However, when we treated diphlorethohydroxycarmalol to the cells, we found that the amounts of tail DNA were increasingly reduced with increasing concentrations of diphlorethohydroxycarmalol. The cytoprotective effects of diphlorethohydroxycarmalol on apoptosis induced by H_2O_2 were investigated via nuclear staining with Hoechst 33342. Hoechst 33342 dye specifically stains DNA, and is widely used to detect nuclear shrinkage such as chromatin condensation, nuclear fragmentation, and the appearance of apoptotic bodies, which are all indicative of apoptosis. As shown in **Fig. 3-18**, the negative control, which contained no compound or H_2O_2, possessed intact nuclei (**Fig. 3-18A**),

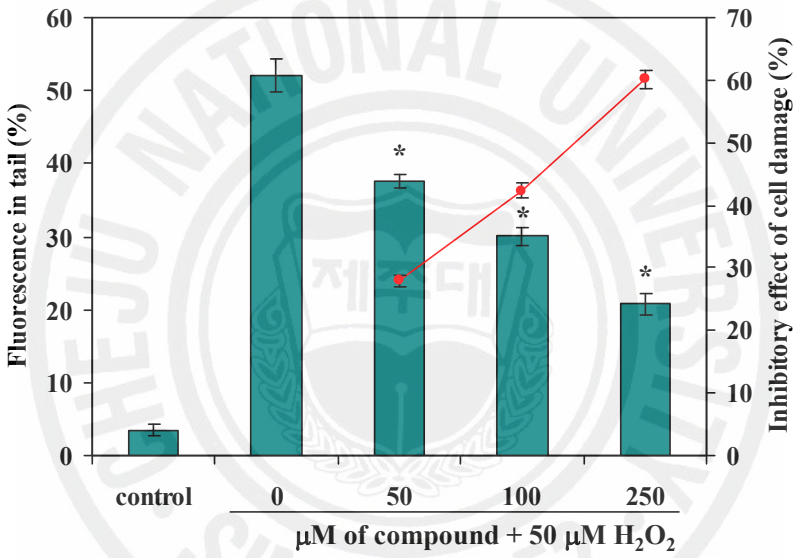

Fig. 3-16. Inhibitory effect of different concentrations of diphlorethohydroxycarmalol isolated from *I. okamurae* on H_2O_2 induced DNA damages. The damaged cells on H_2O_2 treatment was determined by comet assay. ■, % Fluorescence in tail; ●, Inhibitory effect of cell damage. Experiments were performed in triplicate and the data are expressed as mean ± SE. Statistical evaluation was performed to compare the experimental groups and corresponding control groups. *, $p < 0.001$

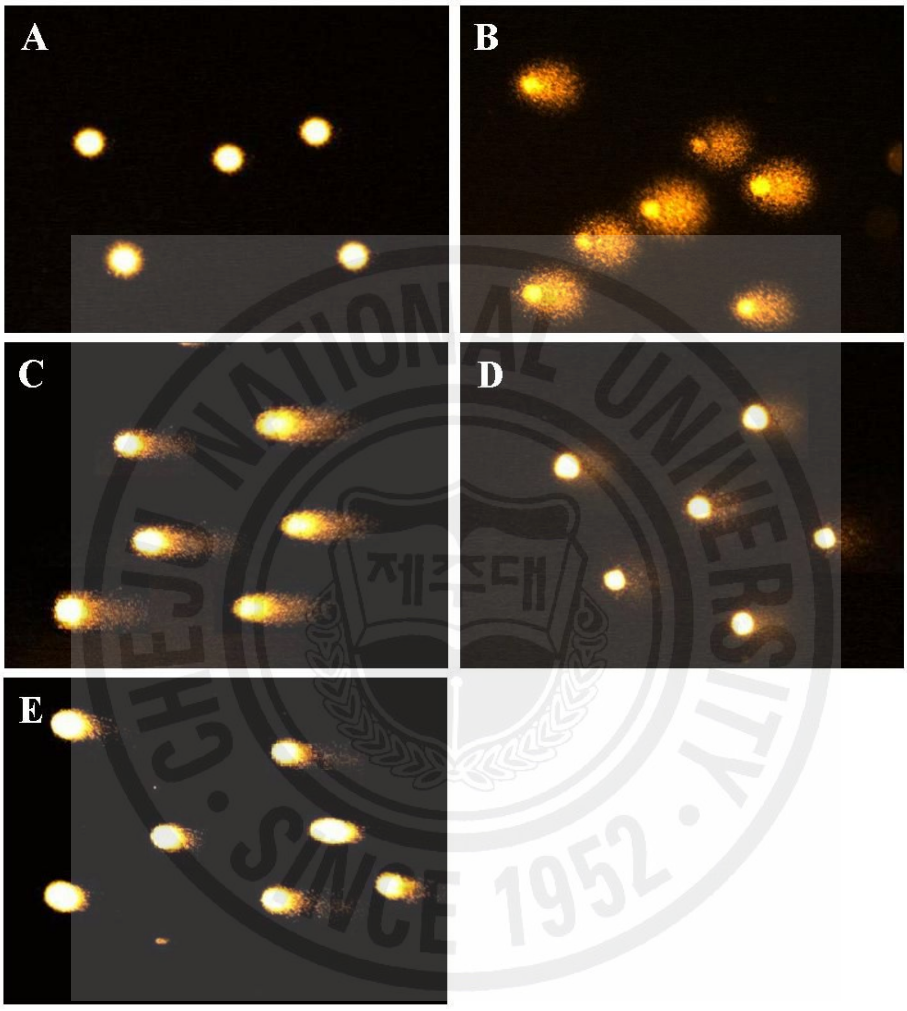

Fig. 3-17. Photomicrographs of DNA damage and migration observed under diphlorethohydroxycarmalol isolated from *I. okamurae* where the tail moments were decreased. A, control; B, cells treated with 50 μM H_2O_2; C, cells treated with 50 μM compound + 50 μM H_2O_2; D, cells treated with 100 μM compound + 50 μM H_2O_2; E, cells treated with 250 μM compound + 50 μM H_2O_2.

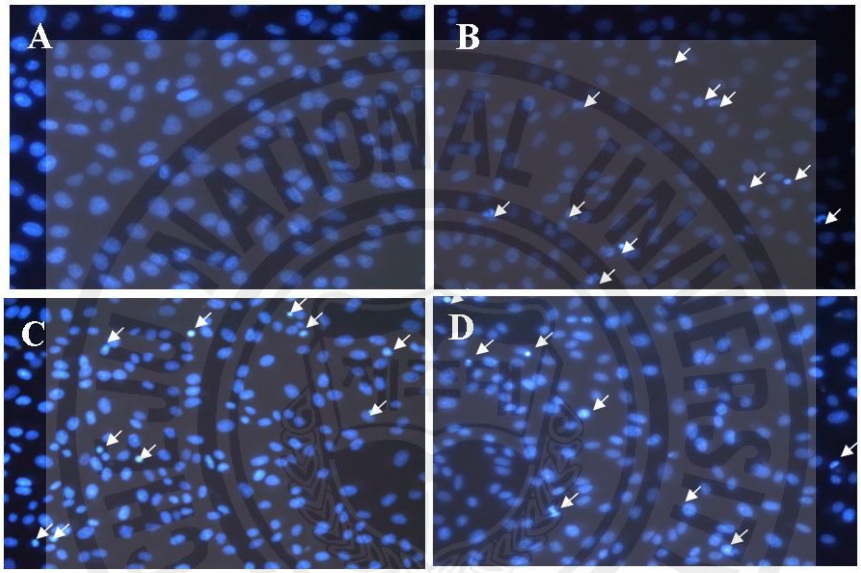

Fig. 3-18. Protective effect of diphlorethohydroxycarmalol isolated from *I. okamurae* against H_2O_2-induced apoptosis in vero cells. Cellular morphological changes were observed under a fluorescence microscope after Hoechst 33342 staining. A, untreated; B, 500 μM H_2O_2; C, 50 μM compound + 500 μM H_2O_2; D, 250 μM compound + 500 μM H_2O_2. Apoptotic bodies are indicated by arrows.

and the positive control (H_2O_2 treated cells) exhibited significant nuclear fragmentation, indicating apoptosis (**Fig. 3-18B**). However, the addition of diphlorethohydroxy-carmalol with H_2O_2 reduced the apoptotic bodies (**Figs. 3-18C and D**), which suggested diphlorethohydroxycarmalol's ability to protect against nuclear fragmentation in the event of an H_2O_2 challenge, and that the cells were protected from oxidative stress-related cellular injuries.

Melanogenesis is a physiological process resulting in the synthesis of melanin pigments, which play a crucial protective role against skin photocarcinogenesis. In humans and other mammals, the biosynthesis of melanins takes place in a lineage of cells known as the melanocytes, which contain the enzyme tyrosinase (Baurin et al., 2002). Tyrosinase plays an important role in melanogenesis. Dopaquinone, an intermediate of melanogenesis, is unstable and converted to dopachrome by tyrosinase or autoxidation, and melanin can be formed through a subsequent polymerization reaction. Thus, the inhibition of melanogenesis can be achieved by antioxidation and the inhibition of tyrosinase. In this study, the effect of diphlorethohydroxycarmalol on melanogenesis was examined using an *in vitro* enzyme assay (tyrosinase inhibition assay) and cell culture method. First, the inhibition of tyrosinase-catalyzed dopachrome formation was evaluated, as shown in **Fig. 3-19**. Diphlorethohydroxycarmalol showed tyrosinase inhibitory effects of 32.99, 76.84, and 86.31%, at the concentrations of 100, 250, and 500 μM, respectively. Moreover, diphlorethohydroxycarmalol exhibited stronger inhibition (IC_{50}=142.20 μM) than the commercial tyrosinase inhibitor arbutin (IC_{50}=384.82 μM), but weaker inhibition than kojic acid (IC_{50}=34.88 μM) (**Table 3-4**). The inhibitory effects of melanin synthesis were also examined for inhibiting melanogenesis in B-16 melanoma cells. The results for the various concentrations of diphlorethohydroxycarmalol are illustrated in **Fig. 3-20**, and the inhibitory effects were

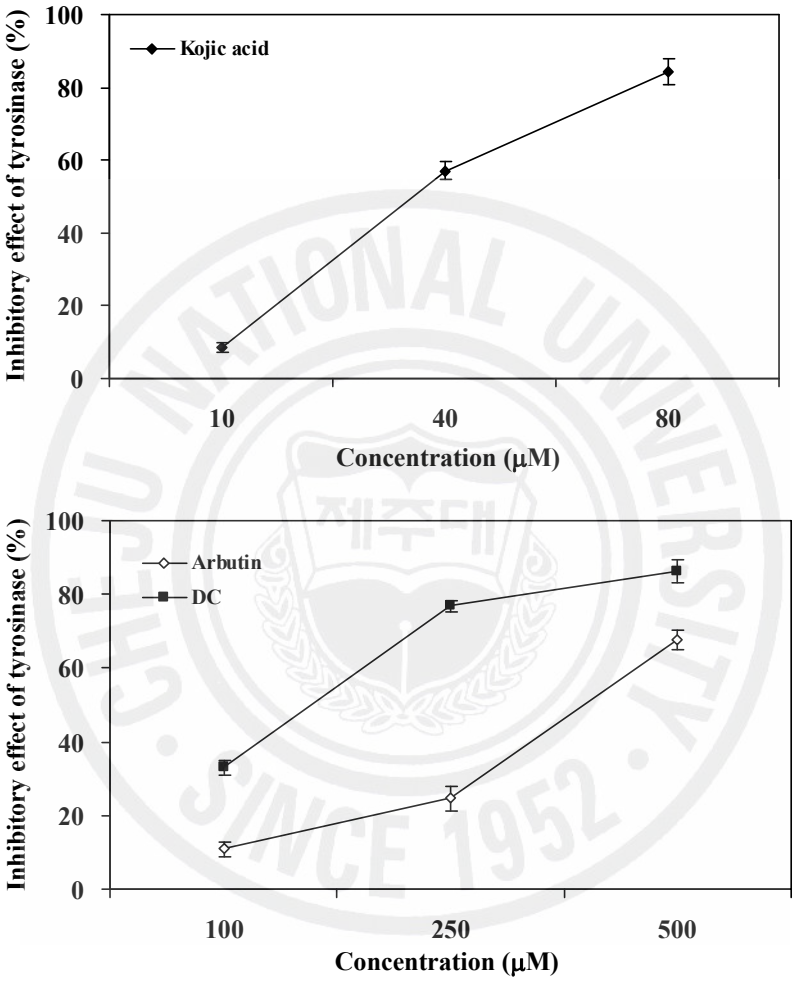

Fig. 3-19. Inhibitory effect of diphlorethohydroxycarmalol isolated from *I. okamurae* against mushroom tyrosinase. L-tyrosine was used as substrate, and kojic acid and arbutin were used as positive control. Experiments were performed in triplicate and the data are expressed as mean ± SE.

Table 3-4. Inhibitory effect of diphlorethohydroxycarmalol isolated from *I. okamurae* against mushroom tyrosinase

	IC_{50} (μM)
Kojic acid	**34.88**
Arbutin	**384.82**
DC	**142.20**

*DC, diphlorethohydroxycarmalol

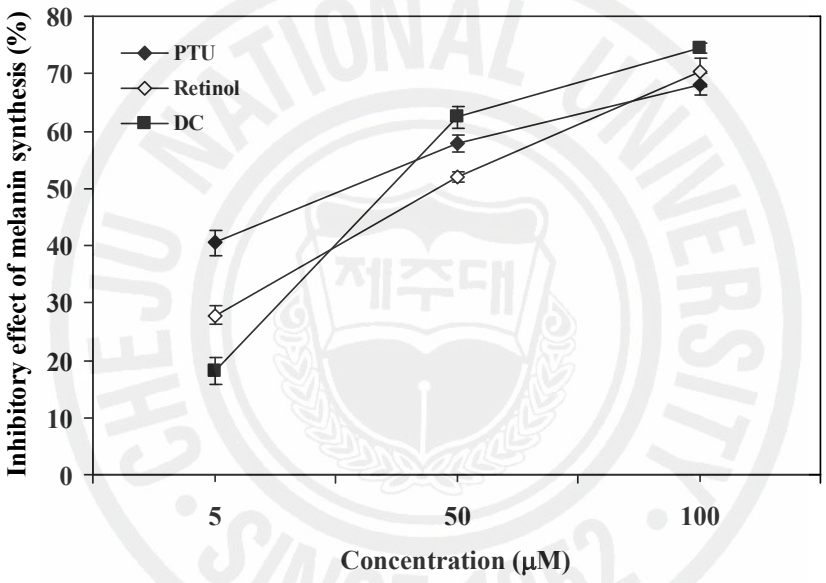

Fig. 3-20. Inhibitory effect of diphlorethohydroxycarmalol isolated from *I. okamurae* on melanin synthesis. B16F10 melanoma cells were used for this experiment and PTU and retinol were used as positive control. Experiments were performed in triplicate and the data are expressed as mean ± SE.

Table 3-5. Inhibitory effect of diphlorethohydroxycarmalol isolated from *I. okamurae* on melanin synthesis

	IC_{50}(μM)
PTU	**32.72**
Retinol	**50.25**
DC	**37.73**

*DC, diphlorethohydroxycarmalol

recorded as 18.12, 62.46, and 74.56%, at the concentrations of 5, 50, and 100 μM, respectively. In addition, diphlorethohydroxycarmalol possessed stronger inhibition (IC_{50}=37.73 μM) than retinol (IC_{50}=50.25 μM), and was similar to PTU (IC_{50}=32.72 μM), as the positive controls (**Table 3-5**). From these results, it was deduced that diphlorethohydroxycarmalol inhibited cellular pigmentation more effectively than arbutin and retinol by its melanin synthesis inhibitory effects, as well as by the direct inhibition of tyrosinase. Therefore, diphlorethohydroxycarmalol could be used as a natural marine compound in cosmetic materials. The skin, which is continuously exposed to sunlight and environmental oxidizing pollutants, is a preferred target of oxidative stress. Evidence suggests that the signs of skin ageing, such as wrinkling, sagging, and actinic lentigo, may be connected to the cumulative oxidative damage incurred throughout a life time (Thiele et al., 1997; Guarneri et al., 2000). It is well known that UV-A and UV-B irradiations induce the formation of reactive oxygen species (ROS) in cutaneous tissues provoking toxic changes such as lipid peroxidation, protein cross-linking, and enzyme inactivation (Emerit, 1992). To counteract this oxidative injury, skin is equipped with a network of enzymatic and non-enzymatic antioxidant systems. The most biologically active antioxidants revealed so far are the tocopherols, ascorbate, polyphenols, and carotenoids. All these compounds, administered topically by cosmetics or orally by dietary supplements, are shown to exert antioxidant/protective effects in the skin or skin cells (Lopez-Torres et al., 1998; Santos et al., 1998; Rao and Agarwal, 1998). Therefore, in this study, we report the protective effects of diphlorethohydroxycarmalol against UV-B radiation for antioxidant and whitening purposes. To confirm that the diphlorethohydroxycarmalol dose for reducing UV-B induced oxidative stress in cells, intracellular ROS production was assessed by monitoring DCFH-DA fluorescence (**Fig. 3-21**). The levels of produced ROS reached

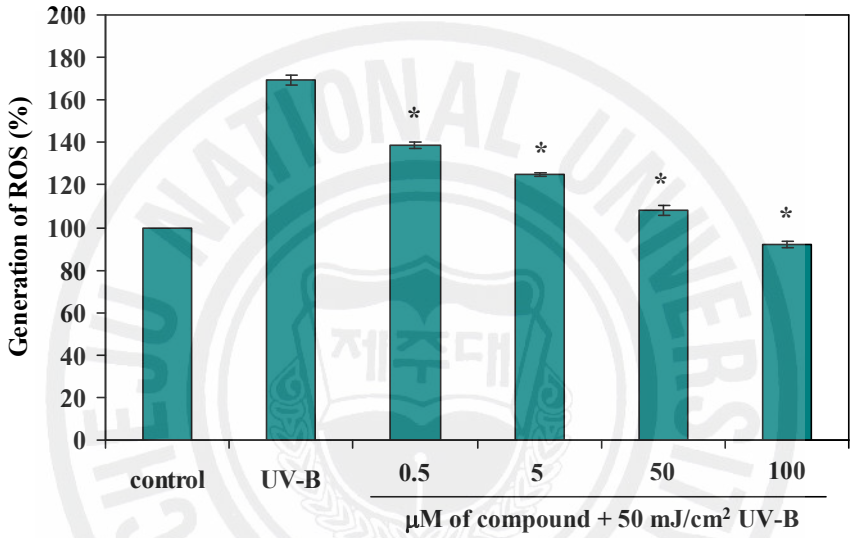

Fig. 3-21. Effect of diphlorethohydroxycarmalol isolated from *I. okamurae* on scavenging intracellular ROS generated by UV-B radiation. The fibroblasts were treated with various concentrations of diphlorethohydroxycarmalol and after 1h later, UV-B radiation at 50 mJ/cm^2 was applied to the cells. The intracellular ROS was detected using fluorescence spectrophotometer after DCF-DA staining. Experiments were performed in triplicate and the data are expressed as mean ± SE. Statistical evaluation was performed to compare the experimental groups and corresponding control groups. *, $p < 0.001$

169.31% in the irradiated cells, whereas treating with diphlorethohydroxycarmalol at 250 μM decreased the level of ROS to 92.15%, and the ROS level was reduced dose-dependently. In order to determine the protection afforded to cells by diphlorethohydroxycarmalol**,** against UV-B induced oxidative cytotoxicity and DNA damage, cell viability and DNA damage inhibitory effects were measured via the MTT and comet assays, respectively. The protective effects of diphlorethohydroxycarmalol on cell survival in fibroblasts exposed to UV-B radiation, is expressed in **Fig. 3-22**. At 50 mJ/cm^2 of UV-B radiation, there were only 43.48% viable cells as compared to the control cells, while diphlorethohydroxycarmalol (0.5, 5, and 50 μM) protected the cells from the UV-B induced damage, restoring cell survival to 49.29, 56.16, and 65.85%, respectively. The cellular DNA damage that was induced by UV-B radiation was detected via the comet assay. By exposing the cells to radiation the comet parameters increased, including tail length and the percentage of DNA in the comet tails of the cells. When the cells were expose to UV-B at 50 mJ/cm^2, the percentage of DNA in the tail increased to 52.37 (**Fig. 3-23**). However, treating with diphlorethohydroxycarmalol resulted in a decrease to 26.14, which indicated a protective effect of diphlorethohydroxycarmalol on UV-B induced DNA damage, and these protective effects presented in dose-dependent manners (**Fig. 3-24**). A nuclear staining assay was used to evaluate the morphological changes of the irradiated cells, which were absorbed by Hoechst 33342/PI staining. As shown in **Fig. 3-25**, the control cells without exposure to UV-B radiation exhibited intact nuclei, while the cells exposed to 50 mJ/cm^2 of UV-B radiation showed typical characteristics of apoptosis (bright blue color) and necrosis (red color). However, the addition of diphlorethohydroxycarmalol with UV-B radiation markedly decreased the apoptotic bodies and necrotic cells. These results indicated that diphlorethohydroxycarmalol offered cytoprotective effects against the oxidative

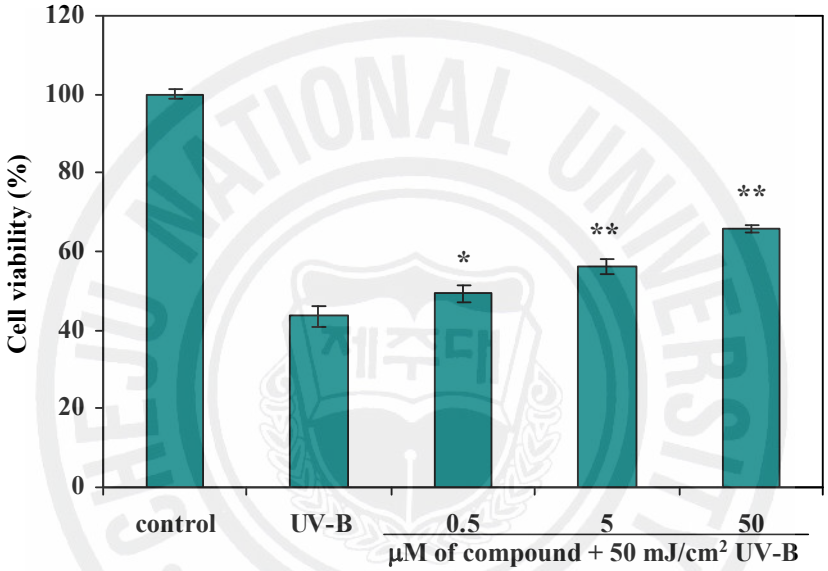

Fig. 3-22. Protective effect of diphlorethohydroxycarmalol isolated from *I. okamurae* on UV-B radiation-induced cell damage of fibroblasts. The fibroblasts were treated with various concentrations of diphlorethohydroxycarmalol and after 1h later, UV-B radiation at 50 mJ/cm^2 was applied to the cells. The viability of fibroblasts on UV-B radiation was determined by MTT assay. Experiments were performed in triplicate and the data are expressed as mean ± SE. Statistical evaluation was performed to compare the experimental groups and corresponding control groups. *, $p < 0.01$, **, $p < 0.001$

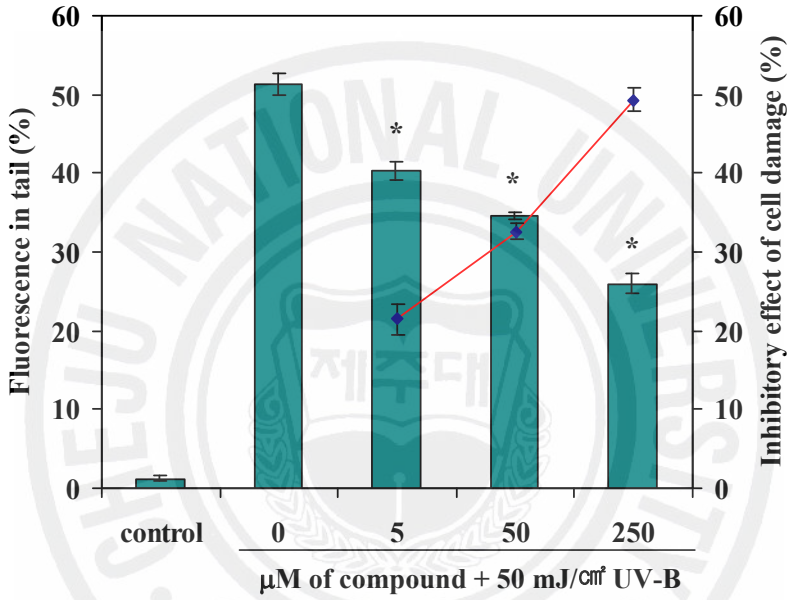

Fig. 3-23. Inhibitory effect of different concentrations of diphlorethohydroxycarmalol isolated from *I. okamurae* on UV-B radiation induced DNA damages. The damaged cells on UV-B radiation was determined by comet assay. ■, % Fluorescence in tail; ●, Inhibitory effect of cell damage. Experiments were performed in triplicate and the data are expressed as mean ± SE. Statistical evaluation was performed to compare the experimental groups and corresponding control groups. *, $p < 0.001$

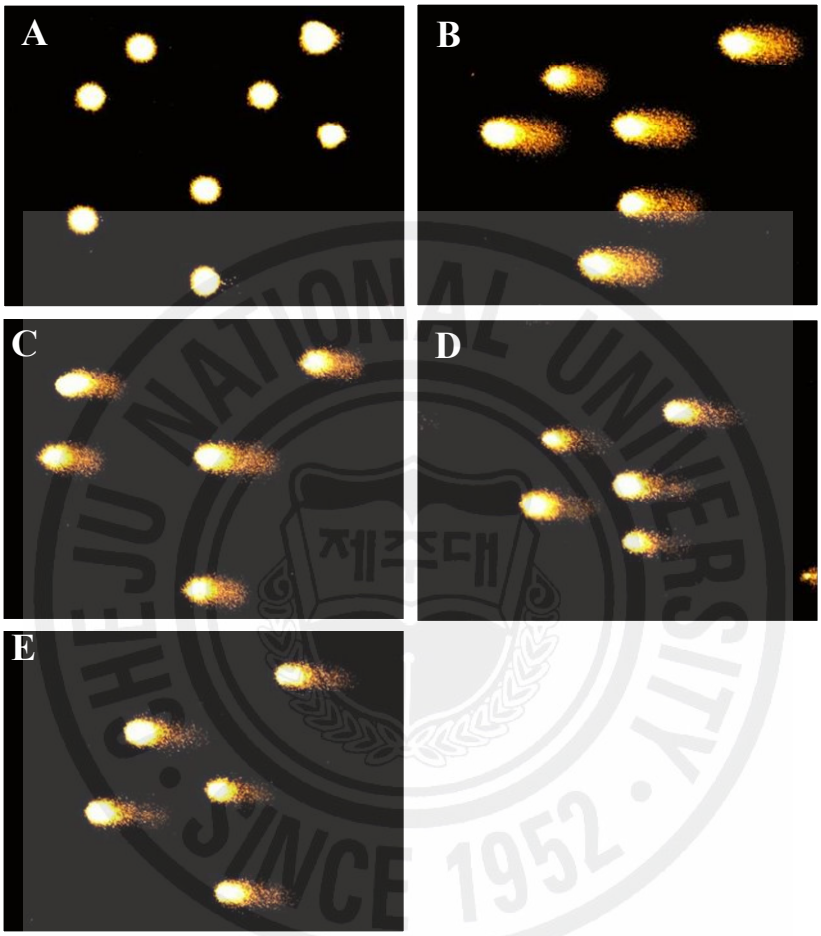

Fig. 3-24. Photomicrographs of DNA damage and migration observed under diphlorethohydroxycarmalol isolated from *I. okamurae* where the tail moments were decreased. A, control; B, UV-B radiation at 50 mJ/cm^2; C, cells treated with 5 μM compound + UV-B radiation at 50 mJ/cm^2; D, cells treated with 50 μM compound + UV-B radiation at 50 mJ/cm^2; E, cells treated with 250 μM compound + UV-B radiation at 50 mJ/cm^2.

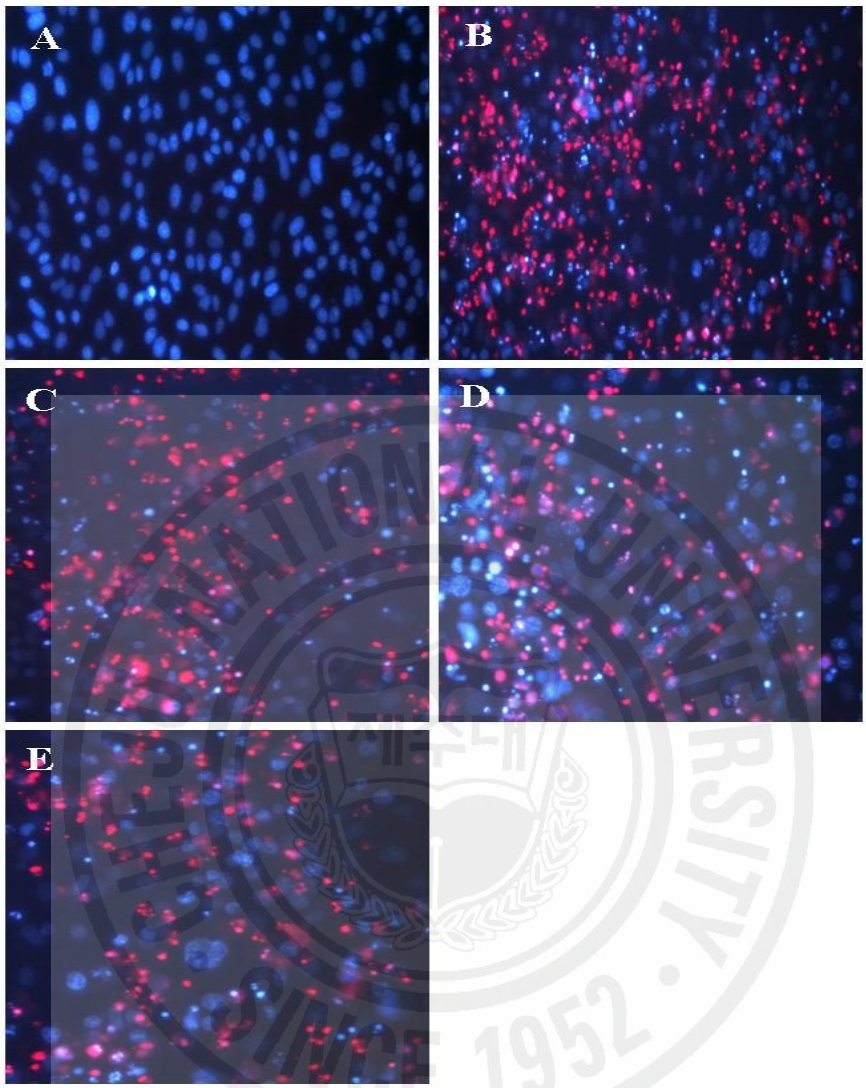

Fig. 3-25. Protective effect of diphlorethohydroxycarmalol isolated from *I. okamurae* on UV-B radiation-induced cell damage of fibroblasts. The fibroblasts were treated with various concentrations of diphlorethohydroxycarmalol and after 1h later, UV-B radiation at 50 mJ/cm^2 was applied to the cells. Cellular morphological changes were observed under a fluorescence microscope after Hoechst 33342 and PI double staining. A, untreated; B, UV-B radiation at 50 mJ/cm^2; C, 5 μM compound + UV-B radiation at 50 mJ/cm^2; D, 50 μM compound + UV-B radiation at 50 mJ/cm^2; E, 250 μM compound + UV-B radiation at 50 mJ/cm^2.

stress induced by UV-B radiation. To clarify the protective effects of diphlorethohydroxycarmalol against UV-B radiation, we used a UV-vis absorption assay and UV-B protection test in a mouse model. As shown in **Fig. 3-26**, diphloretho-hydroxycarmalol absorbed a wide range of the UV region, specifically highlighting the absorption spectrum from 280 to 320 nm, the UV-B region. This result indicates that diphlorethohydroxycarmalol possessed potential protective effects against UV-B radiation. Thus, we applied *in vivo* tests to demonstrate the inhibitory effects for erythema and edema. The erythema production rate increased under the tested UV-B radiation intensity, and there was a 12.13% erythema inhibitory effect expressed at 5 J of radiations (**Fig. 3-27A**). Edema was also examined in hairless mice (**Fig. 3-27B**). The skin expanded as a result of UV-B radiation exposure, but the expansion rate decreased slightly with the treatment of diphlorethohydroxycarmalol.

Natural products with proven biological activities usually contain compounds with a phenolic moiety; for example, coumarins, flavonoids, tocopherols, and catechins. Organic acids, carotenoids, protein, and tannins can also be present and act as antioxidants, or may have synergistic effects with phenolic compounds (Dapkevicius et al., 1998). Diphlorethohydroxycarmalol, a carmalol derivative, is a phlorotannins that consists of four phloroglucinol units and functional hydroxyl groups. Several studies report that phloroglucinols, and their metabolites, have radical scavenging activity and cytoprotective effects against oxidative stress induced cell damage (Lee et al., 1998; Kang et al., 2005; Hwang et al., 2006; Nakai et al., 2006). However, there are no reports regarding diphlorethohydroxycarmalol in terms of its antioxidant and cosmeceutical activities. In this study, we demonstrated that diphlorethohydroxycarmalol has not only antioxidant activity against oxidative stress, but also cosmeceutical activities, including inhibitory effects for tyrosinase and melanin synthesis, and cytoprotective effects for

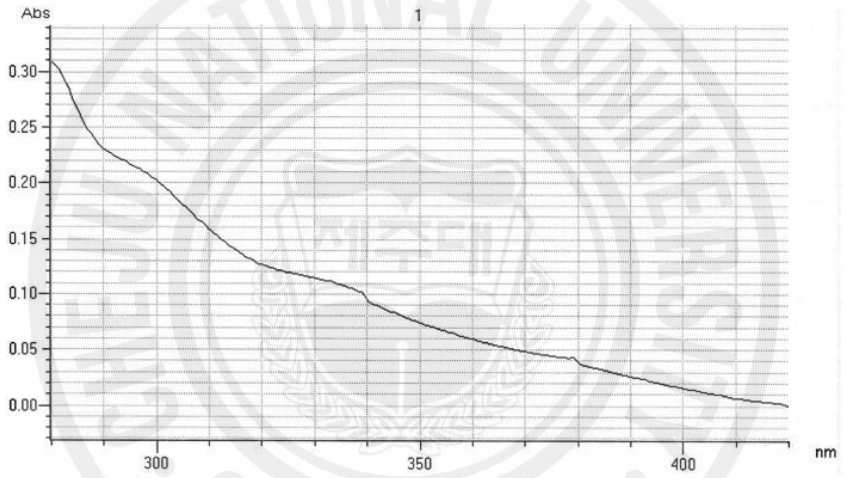

Fig. 3-26. UV absorption spectrum of diphlorethohydroxycarmalol isolated from *I. okamurae*.

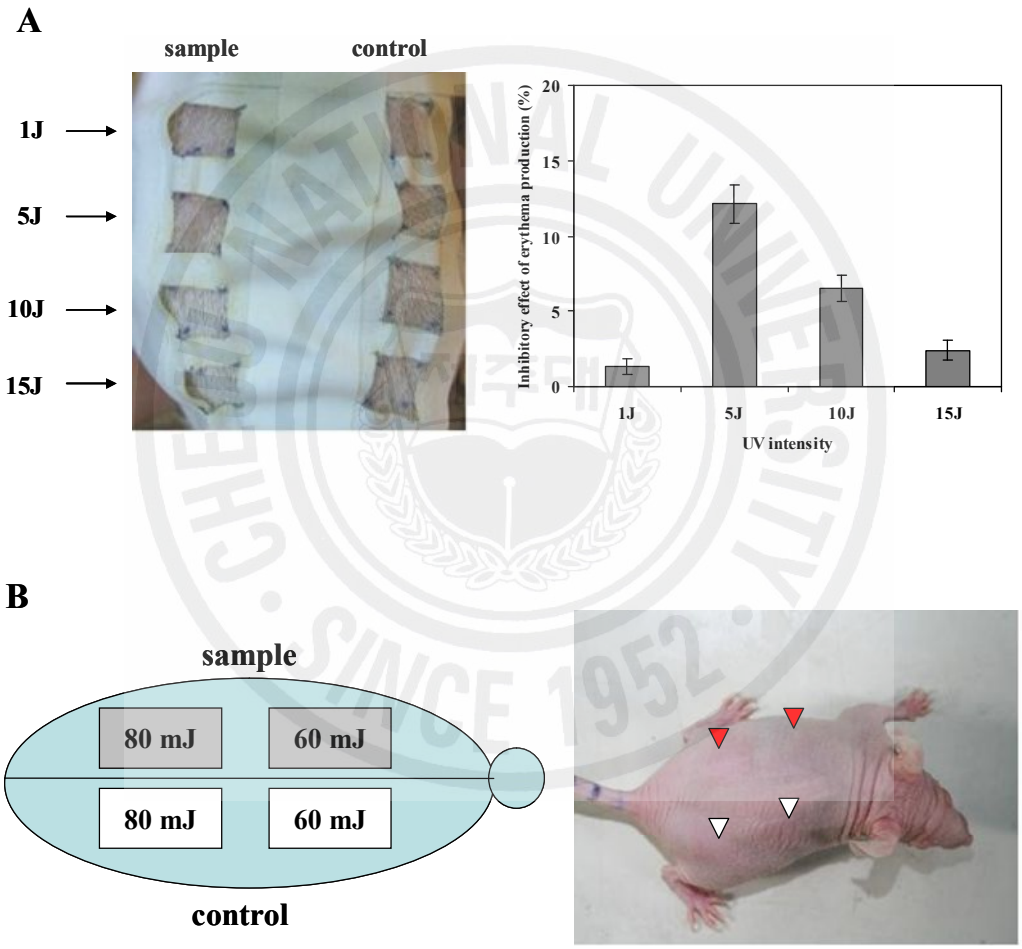

Fig. 3-27. Protective effect of diphlorethohydroxycarmalol isolated from *I. okamurae* on UV-B radiation-induced erythema (A) and edema (B).

UV-B radiation. Therefore, diphlorethohydroxycarmalol could be used as a natural antioxidant, and applied in the cosmetic industry.

Part Ⅳ.

Isolation of cosmetic materials from *Ecklonia cava*

Part Ⅳ.

Isolation of cosmetic materials from *Ecklonia cava*

1. ABSTRACT

In order to obtain natural antioxidant and potential cosmetic materials from marine biomass, the potent antioxidative and cosmeceutial activities of five phlorotannins (phloroglucinol, eckol, dieckol, triphlorethol-A, and eckstolonol) purified from *Ecklonia cava* collected in Jeju Island were investigated. Antioxidant activities were measured by electron spin resonance (ESR) system for scavenging effects of free radicals (alkyl, DPPH, and hydroxyl radicals) and protective effect via H_2O_2 induced oxidative stress in cell lines. All of the tested phlorotannins could scavenge more profound than a commercial antioxidant on free radicals, and more effective than those of commercial whitening agent on cosmeceutial activities. Among them, dieckol possess higher protective effect induced by ROS and UV radiation, and inhibitory effect of melanin synthesis. These results showed that dieckol could be used as natural antioxidants in food, cosmetic, and pharmaceutical industries.

2. MATERIALS AND METHODS

2.1. General experimental procedures

The UV and FT-IR spectra were recorded on a Pharmacia Biotech Ultrospec 3000 UV/Visible spectrometer and a SHIMAZU 8400s FT-IR spectrometer, respectively. NMR spectra were recorded on a Varian INOVA 400 MHz NMR spectrometer. CD_3OD were used as a solvent for the NMR experiments, and the solvent signals were used as an internal reference. The HPLC was carried out on a YoungLin Instrument HPLC system equipped with a YoungLin acme 9000 UV/VIS detector and Autochrome software using C_{18} column (Waters Spherisorb® DOS-2 RP-18, 4.6×250 mm, 5 μm, Waters Co.).

2.2. Materials

The marine alga *Ecklonia cava* (**Fig. 4-1**) was collected along the coast of Jeju Island, Korea, between October 2005 and March 2006. The samples were washed three times with tap water to remove the salt, epiphytes, and sand attached to the surface, then carefully rinsed with fresh water, and maintained in a medical refrigerator at –20°C. Therefore, the frozen samples were lyophilized and homogenized with a grinder prior to extraction.

Fig. 4-1. The photograph of a brown alga *Ecklonia cava*.

2.3. Extraction and isolation

The dried *E. cava* powder (500 g) was extracted with 80% aqueous MeOH, and filtered. The filtrate was evaporated at 40℃ to obtain the methanol extract, which was dissolved in water, then partitioned with EtOAc. The EtOAc extract (45.65 g) was mixed with celite. The mixed celite was dried and packed into a glass column, and eluted in the order of hexane, methylene chloride, diethyl ether, and methanol. The diethyl ether fraction (26.69 g) was subjected to Sephadex LH-20 column chromatography using stepwise gradient chloroform/methanol (2/1→0/1) solvents system, and then finally purified by reversed-phase HPLC to give compound **15** (13.5 mg), **16** (198.7 mg), **17** (275.8 mg), **18** (67.4 mg), and **19** (38.1 mg) (**Fig. 4-2**).

Phloroglucinol (15): white powder; IR (KBr) ν_{max} 3481, 1617 cm^{-1}; ^{1}H-NMR (400 MHz, CD_3OD): δ 5.78 (3H, s, H-2, 4, 6); ^{13}C-NMR (100 MHz, CD_3OD): δ 160.9 (C-1, 3, 5), 96.3 (C-2, 4, 6); EIMS *m/z* 126 $[M]^+$ ($C_6H_6O_3$).

Eckol (16): amorphous powder; IR (KBr) ν_{max} 3250, 1605 cm^{-1}; UV (MeOH): λ_{max} nm (log ε) 230 (4.4), 290 (3.4); ^{1}H and ^{13}C NMR, see **Table 4-1**; HREIMS *m/z* 372.0460 $[M]^+$ (calcd for $C_{18}H_{12}H_9$, 372.0481).

Dieckol (17): amorphous powder; IR (KBr) ν_{max} 3250, 1605 cm^{-1}; UV (EtOH): λ_{max} nm 225; ^{1}H and ^{13}C NMR, see **Table 4-2**; FABMS *m/z* 742 $[M]^+$ ($C_{36}H_{22}H_{18}$).

Triphlorethol A (18): amorphous powder; IR (KBr) ν_{max} 3245, 1615 cm^{-1}; ^{1}H and ^{13}C NMR, see **Table 4-3**; FABMS *m/z* 374 $[M]^+$ ($C_{18}H_{14}H_9$).

Eckstolonol (19): off-white powder; $[\alpha]^{20}_{D}$ 0° (*c* 0.008, MeOH); IR (KBr) ν_{max} 3243, 1635, 1518, 1494, 1396, 1281, 1243, 1207, 1154, 1118, 1089, 1012, 810 cm^{-1}; ^{1}H and ^{13}C NMR, see **Table 4-4**; negative FABMS *m*/*z* 369.0; HRFABMS *m*/*z* 370.0324 $[M]^{+}$ (calcd for $C_{18}H_{10}H_{9}$, 370.0325).

2.4. DPPH radical scavenging assay

The DPPH radical scavenging activity was measured using an ESR spectrometer (JES-FA machine, JOEL, Tokyo, Japan) according to the technique described by Nanjo et al. (1996). 60 μl of each sample was added to 60 μl of DPPH (60 μmol/l) in ethanol. After 10 seconds of vigorous mixing, the solutions were transferred to Teflon capillary tubes and fitted into the cavity of the ESR spectrometer. The spin adduct was determined by the ESR spectrometer exactly 2 min later under the following measurement conditions: central field 3475 G, modulation frequency 100 kHz, modulation amplitude 2 G, microwave power 5 mW, gain 6.3×10^{5}, and temperature 298 K. All the radical scavenging activities (%) in the present study were calculated using the following equation, in which H and H_0 were the relative peak heights of the radical signals with and without a sample, respectively.

$$\text{Radical scavenging activity} = [1-(H / H_0)] \times 100$$

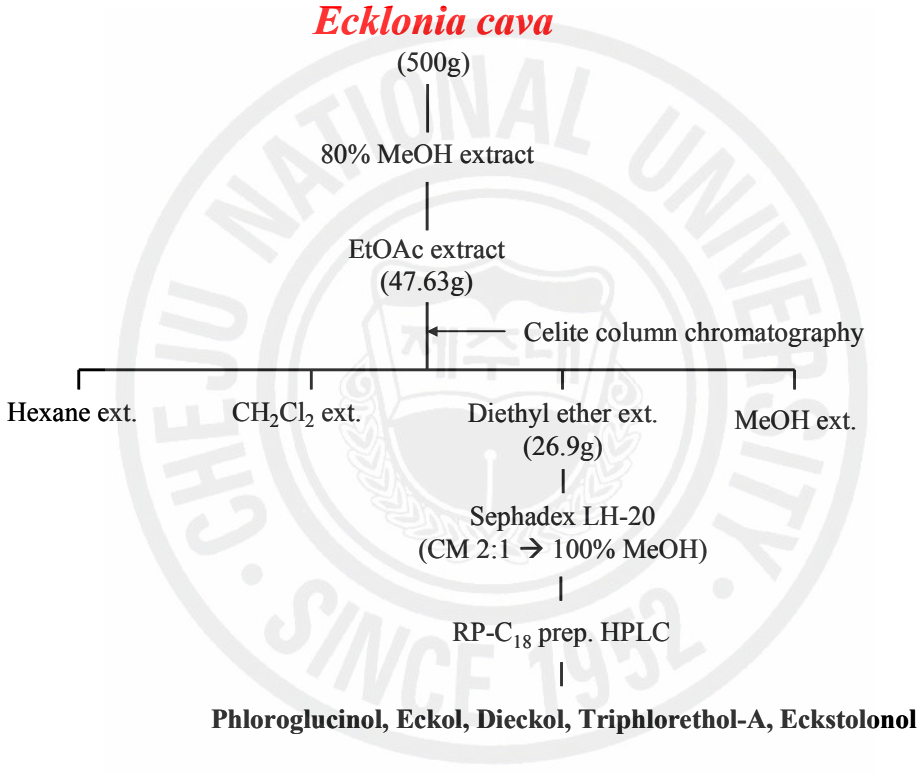

Fig. 4-2. Isolation scheme of the active compounds from *E. cava*.

Table 4-1. ^{1}H and ^{13}C NMR assignments for eckol (**16**)

Position	^{13}C	^{1}H (mult. *J*=Hz)
1	143.8	
2	99.9	
3	147.7	6.13 (1H, s)
4	126.1	
4a	139.0	
5a	125.3	
6	147.6	5.94 (2H, s)
7	100.3	
8	150.0	5.94 (2H, s)
9	96.3	
9a	144.7	
10a	125.1	
1'	162.4	
2'	95.9	5.93 (3H, s)
3'	160.7	
4'	98.2	5.93 (3H, s)
5'	160.7	
6'	95.9	5.93 (3H, s)

* 400 MHz for ^{1}H and 100 MHz for ^{13}C

Table 4-2. ^{1}H and ^{13}C NMR assignments for dieckol (**17**)

Position	^{13}C	^{1}H (mult. *J*=Hz)	Position	^{13}C	^{1}H (mult. *J*=Hz)
1	126.46		1	158.61	
2	148.09		2	148.14	
3	100.30	6.13 (1H, s)	3	153.19	6.15 (1H, s)
4	144.10		4	144.20	
4a	125.38		4a	125.45	
5a	144.95		5a	145.10	
6	96.57	5.95 (1H, d, *J*=2.76)	6	97.02	6.05 (1H, d, *J*=2.85)
7	156.81		7	155.33	
8	100.56	6.06 (1H, d, *J*=2.85)	8	100.67	5.98 (1H, d, *J*=2.76)
9	147.92		9	147.71	
9a	127.00		9a	125.67	
10a	139.44		10a	139.27	
1'	162.67		1'	126.41	
2'	96.17	5.92 (3H, s)	2'	97.02	6.09 (2H, s)
3'	160.95		3'	100.19	
4'	98.47	5.92 (3H, s)	4'	127.28	
5'	160.95		5'	153.19	
6'	96.17	5.92 (3H, s)	6'	96.65	6.09 (2H, s)

* 400 MHz for ^{1}H and 100 MHz for ^{13}C

Table 4-3. ^{1}H and ^{13}C NMR assignments for triphlorethol A (**18**)

Position	^{13}C	^{1}H (mult. *J*=Hz)
1	125.7	
2	152.7	
3	98.4	5.7 (d, *J*=2.7)
4	156.1	
5	94.9	6.0 (d, *J*=2.9)
6	153.7	
1'	124.6	
2'	152.1	
3'	96.2	5.8 (s)
4'	156.4	
5'	96.2	5.8 (s)
6'	152.1	
1"	162.4	
2"	95.4	6.0 (d, *J*=2.2)
3"	160.3	
4"	97.5	5.9 (t, *J*=2.2)
5"	160.3	
6"	95.4	6.0 (d, *J*=2.2)

* 400 MHz for ^{1}H and 100 MHz for ^{13}C

Table 4-4. ^{1}H and ^{13}C NMR assignments for eckstolonol (**19**)

Position	^{13}C	^{1}H (mult. *J*=Hz)
1	146.1	
2	98.8	6.04 (d, *J*=2.7)
3	153.3	
4	93.9	5.84 (d, *J*=2.7)
4a	142.1	
5a	125.9	
6	140.1	
7	97.6	6.10 (s)
7a	137.2	
8a	122.7	
9	146	
10	98.8	6.01 (d, *J*=2.7)
11	153	
12	93.9	5.82 (d, *J*=2.7)
12a	141.7	
13a	122.5	
13b	131.6	
14a	122.3	
1-OH		9.77 (s)
9-OH		9.64 (s)
6-OH		9.60 (s)
3-OH		9.27 (s)
11-OH		9.26 (s)

* 400 MHz for ^{1}H and 100 MHz for ^{13}C

2.5. Alkyl radical scavenging assay

Alkyl radicals were generated via AAPH. Thus, reaction mixtures containing 10 mmol/l AAPH and 10 mmol/l 4-POBN were mixed with the tested samples. The solutions were incubated for 30 min at 37℃ in a water bath, then transferred to Teflon capillary tubes (Hiramoto et al., 1993). The spin adduct was recorded using a JES-FA ESR spectrometer under the following measurement conditions: central field 3475 G, modulation frequency 100 kHz, modulation amplitude 2 G, microwave power 10 mW, gain 6.3×10^5, and temperature 298 K. The alkyl radical scavenging activity (%) was presented as described above.

2.6. Hydroxyl radical scavenging assay

Hydroxyl radicals were generated via a Fenton reaction, and reacted rapidly with nitrone spin trap DMPO. The resultant DMPO-OH adducts were detected using an ESR spectrometer (Rosen and Rauckman, 1984). Reaction mixtures containing 100 μl of 0.3 M DMPO, 100 μl of 10 mM $FeSO_4$, and 100 μl of 10 mM H_2O_2 were mixed with the test samples, then transferred to Teflon capillary tube. The spin adduct was measured on an ESR spectrometer exactly 2.5 min later under the following measurement conditions: central field 3475 G, modulation frequency 100 kHz, modulation amplitude 2 G, microwave power 1 mW, gain 6.3×10^5, and temperature 298 K. The hydroxyl radical scavenging activity (%) was presented as described above.

2.7. Hydrogen peroxide scavenging assay

Hydrogen peroxide scavenging activity was determined according to the method of Müller (1985). A hundred μl of 0.1 M phosphate buffer (pH 5.0) and the sample solution were mixed in a 96-well plate. A 20 μl of hydrogen peroxide was added to the mixture, and then incubated at 37℃ for 5 min. After the incubation, 30 μl of 1.25 mM ABTS and 30 μl of peroxidase (1 unit/ml) were added to the mixture, and then incubated at 37℃ for 10 min. The absorbance was read with an ELISA reader at 405 nm.

2.8. Antioxidant activities by cell lines

2.8.1. Cell culture

Cells of a monkey kidney fibroblast line (Vero) were maintained at 37℃ in an incubator with humidified atmosphere of 5% CO_2. Cells were cultured in Dulbecco's modified Eagle's medium containing 10% heat-inactivated fetal calf serum, streptomycin (100 μg/ml), and penicillin (100 unit/ml).

2.8.2. Hydrogen peroxide scavenging assay

For detection of intracellular H_2O_2, Vero cells were seeded in 96-well plates at a concentration of 1×10^5 cells/ml. After 16 h, the cells were treated with various concentrations of the compounds, and incubated at 37℃ under a humidified atmosphere. After 30 min, H_2O_2 was added at a concentration of 1 mM, and then cells were incubated for an additional 30 min at 37℃. Finally, 2',7'-dichlorodihydrofluorescein diacetate (DCFH-DA; 5 μg/ml) was introduced to the cells,

and 2',7'-dichlorodihydrofluorescein fluorescence was detected at an excitation wavelength of 485 nm and an emission wavelength of 535 nm, using a Perkin-Elmer LS-5B spectrofluorometer. The percentage of H_2O_2 scavenging activity was calculated in accordance with the following equation:

$$H_2O_2 \text{ scavenging activity } (\%) = (1 - (C_1 / C_0)) \times 100$$

where C_1 is the fluorescence intensity of cells treated with H_2O_2 and compounds, and C_0 is the fluorescence intensity of cells treated with H_2O_2 and distilled water instead of compounds.

2.8.3. Assessment of cell viability

Cell viability was then estimated via an MTT assay, which is a test of metabolic competence predicated upon the assessment of mitochondrial performance. It is colorimetric assay, which is dependent on the conversion of yellow tetrazolium bromide to its purple formazan derivative by mitochondrial succinate dehydrogenase in viable cells (Mosmann, 1983). The cells were seeded in 96-well plate at a concentration of 1×10^5 cells/ml. After 16 h, the cells were treated with compounds at difference concentrations. Then, 10 μl of H_2O_2 (1 mM) was added to the cell culture medium, and incubated for 24 h at 37 ℃. MTT stock solution (50 μl; 2 mg/ml) was then applied to the wells, to a total reaction volume of 200 μl. After 4 h of incubation, the plates were centrifuged for 5 min at 800 ×g, and the supernatants were aspirated. The formazan crystals in each well were dissolved in 150 μl of dimethylsulfoxide (DMSO), and the absorbance was measured via ELISA at a wavelength of 540 nm. Relative cell viability was evaluated in accordance with the quantity of MTT converted to the insoluble formazan salt. The optical density of the formazan generated in the control cells was

considered to represent 100% viability. The data are expressed as mean percentages of the viable cells versus the respective control.

2.8.4. Determination of DNA damage by comet assay

Comet assay was performed to determine the oxidative DNA damage (Singh, 2000). The cell suspension was mixed with 75 μl of 0.5% low melting agarose (LMA), and added to the slides precoated with 1.0% normal melting agarose (NMA). After solidification of the agarose, slides were covered with another 75 μl of 0.5% LMA and then immersed in lysis solution (2.5 M NaCl, 100 mM EDTA, 10 mM Tris, and 1% sodium laurylasarcosine; 1% Triton X-100 and 10% DMSO) for 1 h at 4℃. The slides were next placed into an electrophoresis tank containing 300 mM NaOH and 10 mM Na_2EDTA (pH 13.0) for 40 min for DNA unwinding. For electrophoresis of the DNA, an electric current of 25 V/300 mA was applied for 20 min at 4℃. The slides were washed three times with a neutralizing buffer (0.4 M Tris, pH 7.5) for 5 min at 4℃, and then treated with ethanol for another 5 min before staining with 50 μl of ethidium bromide (20 μg/ml). Measurements were made by image analysis (Kinetic Imaging, Komet 5.0, U.K) and fluorescence microscope (LEICA DMLB, Germany), determining the percentage of fluorescence in the tail (tail intensity, TI; 50 cells from each of two replicate slides).

2.9. Tyrosinase inhibition assay

Tyrosinase inhibitory activity was performed according to the method of Vanni et al. (1990) with minor modifications. The reaction mixture contains 140 μl of 0.1 M

phosphate buffer (pH 6.5), 40 μl of 1.5 mM L-tyrosine and 10 μl of samples. Then, 10 μl of mushroom tyrosinase (2100 units/ml) solution was added and the reaction was incubated at 37℃ for 12 min. After incubation, the amount of dopachrome produced in the reaction mixture was determined as the optical density at 490 nm in a microplate reader. The percent inhibition of tyrosinase reaction was calculated as follows:

$$\text{Inhibition (\%)} = [1 - (B - A) / (D - C)] \times 100$$

A = Absorbance at 490 nm with test sample before incubation

B = Absorbance at 490 nm with test sample after incubation

C = Absorbance at 490 nm without test sample before incubation

D = Absorbance at 490 nm without test sample after incubation

2.10. Inhibitory effect of melanin synthesis

2.10.1. Cell cultures

Mouse melanoma cell lines (B-16 F10) were maintained at 37℃ in an incubator, under a humidified atmosphere containing 5% CO_2. The cells were cultured in Dulbecco's modified Eagle's medium containing 10% heat-inactivated fetal calf serum, streptomycin (100 mg/ml), and penicillin (100 unit/ml).

2.10.2. Inhibitory effect of melanin synthesis

Melanin contents were measured according to the method of Tsuboi et al. (1998) with a slightly modification. The B-16 F10 cells were placed in 6-well plates at a concentration of 3×10^5 cells/ml, and 24 h after plating the cells were treated with

various concentrations of the compounds. After 24 h, the medium was removed and cells were washed twice with PBS. And cell pellets containing a known number of cells (usually around 1×10^6) were dissolved in 1 ml of 1 N NaOH at 60 ℃ for 30 min and centrifuged for 10 min at 10,000 rpm. The optical densities (OD) of the supernatants were measured at 490 nm using an ELISA reader.

2.11. Protective effect by ultra violet irradiation

2.11.1. Cell culture

Human fibroblast were kindly supplied by Surface Science Laboratory of Center for Anti-aging Molecular Science (CAMS) of Department of Chemistry and School of Molecular Science of Korea Advanced Institute of Science and Technology (KAIST), maintained at 37℃ in an incubator with humidified atmosphere of 5% CO_2. Cells were cultured in Dulbecco's modified Eagle's medium containing 10% heat-inactivated fetal calf serum, streptomycin (100 μg/ml), and penicillin (100 unit/ml).

2.11.2. UV-B irradiation

Cells were exposed to UV-B range at a dose rate of 10 to 100 mJ/cm^2 (UV Lamp, VL-6LM, Vilber Lourmat, France). Optimum irradiation dose were evaluated at 50 mJ/cm^2, therefore the 50 mJ/cm^2 of UV-B were used further experiments.

2.11.3. Assessment of cell viability

Cell viability was then estimated via an MTT assay, which is a test of metabolic competence predicated upon the assessment of mitochondrial performance. It is colorimetric assay, which is dependent on the conversion of yellow tetrazolium bromide to its purple formazan derivative by mitochondrial succinate dehydrogenase in viable cells (Mosmann, 1983). The fibroblast was seeded in 96-well plate at a concentration of 1×10^5 cells/ml. After 16 h, the cells were exposed to UV-B (50 mJ/cm^2) with compounds at difference concentrations, and then the cells were incubated for 24 h at 37℃. MTT stock solution (50 μl; 2 mg/ml) was then applied to the wells, to a total reaction volume of 200 μl. After 4 h of incubation, the plates were centrifuged for 5 min at 800 × g, and the supernatants were aspirated. The formazan crystals in each well were dissolved in 150 μl of dimethylsulfoxide (DMSO), and the absorbance was measured via ELISA at a wavelength of 540 nm. Relative cell viability was evaluated in accordance with the quantity of MTT converted to the insoluble formazan salt. The optical density of the formazan generated in the control cells was considered to represent 100% viability. The data are expressed as mean percentages of the viable cells versus the respective control.

2.12. Animal test

2.12.1. UV absorption assay

Test material was dissolved in methanol at the concentration of 100 μg/ml and put in a quartz cuvette. The absorption spectrum of compound from *Ecklonia cava* was measured between 280 and 420 nm using a double beam spectrophotometer (U-2800, Hitachi).

2.12.2. UV-B protection test for erythema and edema

UV radiation experiments were carried out on male hairless (Hr-1) mice at 8 weeks of age obtained from Japan SLC, Inc. (Shizuoka, Japan). The colony was maintained under controlled conditions of temperature (19-25℃), humidity (40-60%) and a 12 h light-dark cycle with the light intensity of 150-300 Lux. The animals were housed in sanitized polycarbonate cages (260W × 420L × 180H). They had free access to standard mouse food and water. All animals were raised in SPF condition of the Clinical Research Center of Dong-A University Hospital according to Good Laboratory Practices (GLP) OECD guidelines.

Test material (0.5~1 ㎎/㎠) was applied to the left side of dorsal skin and vehicle was applied to the right side for 30 min. Animals were wrapped with tapes containing two exposure windows of 1 ㎠ at each side of back and placed under a bank of 5 UV-B lamps positioned 15 ㎝ above their backs. The irradiation at this distance was of 100 ㎼/s when measured with a research radiometer. The radiation dosage was set 60 mJ/㎠ for upper window and 80 mJ/㎠ for lower window. At the completion of irradiation, tapes were removed and skin lesions (erythema and edema) were observed at 24 h.

2. 13. Statistical analysis

The data are expressed as the mean ± standard error (SE). A statistical comparison was performed via the SPSS package for Windows (Version 10). P-values of less than 0.05 were considered to be significant.

3. RESULT AND DISCUSION

In the previous part Ⅰ, we have found that the brown alga *Ecklonia cava* exhibited prominent radical scavenging activity and inhibitory effect of tyrosinase, especially in EtOAc extract. Therefore, the present study clearly demonstrated that the EtOAc extract was fractionated by celite and Sephadex LH-20 open column chromatography and the active compounds were purified by reversed-phase HPLC.

Phloroglucinol (**15**) was assigned as $C_6H_6O_3$ by combined EIMS and ^{13}C NMR spectrometry. The ^1H NMR spectrum exhibits characteristic peak at δ_H 5.78 (H-2, 4, 6) attributable to three phenolic hydroxy protons, and the IR spectrum of **15** showed the presence of hydroxyl group (3481 cm^{-1}).

Eckol (**16**) was isolated as amorphous powder, and its molecular formula deduced as $C_{18}H_{12}O_9$ based on NMR (**Table 4-1**) and HREI-MS analyses (M^+, *m/z*: 372.0460 calcd for $C_{18}H_{12}O_9$ *m/z*: 372.0481), and the IR spectrum of **16** showed the presence of 3250 (OH) and 1605 (aromatic) cm^{-1}. The ^{13}C NMR spectrum indicated the presence of six non-substituted and twelve O-bearing aromatic carbons, whereas the ^1H NMR spectrum contained signals characteristic of six aromatic protons as well as six phenolic hydroxyl protons.

Dieckol (**17**) was obtained as amorphous powder, and the FABMS revealed a fragment ion as *m/z* 742 $[M]^+$, corresponding to a molecular formula of $C_{36}H_{22}H_{18}$. A combination of 2D NMR experiments readily defined the structure of **17** as a dimmer of **16**.

Triphlorethol A (**18**) was isolated as amorphous powder, and the FABMS revealed a fragment ion as *m/z* 374 $[M]^+$, corresponding to a molecular formula of $C_{18}H_{14}O_9$. The NMR data for the compound was very similar to those of compound **16** indicating that

18 is a composed of three phloroglucinol units. The only difference between the ^{1}H NMR spectrum of **16** and **18** is that the former lacks the signals for one phenolic OH and one aromatic proton.

Eckstolonol (**19**) was obtained as off-white amorphous powder, and the molecular formula of 19 was determined as $C_{18}H_{10}H_9$ based on the NMR and HRFABMS data (M^+, *m/z*: 370.0324 calcd for $C_{18}H_{10}H_9$ *m/z*: 370.0325). The IR of **19** showed the absorption bands at 3243 (OH), and 1635 (aromatic) cm^{-1}. The ^{13}C NMR spectrum of **19** indicated the presence of five non-substituted and thirteen O-bearing aromatic carbons, whereas the ^{1}H NMR spectrum contained signals characteristic of five aromatic protens, as well as five singlet indicating phenolic hydroxyl protons. These NMR spectral features are very similar to those of **16** indicating that **19** is a composed of three phloroglucinol units. The only difference between the ^{1}H NMR spectrum of **16** and **19** is that the former lacks the signals for one phenolic OH and one aromatic proton. The chemical structures of the five phlorotannins isolated from *E. cava* were indicated in **Fig. 4-3**.

DPPH radical is scavenged by antioxidants through the donation of hydrogen to form the stable reduced DPPH molecule. The antioxidant radicals formed are stabilized through the formation of non radical products (Argolo et al., 2004). The scavenging activities of isolated compounds from *E. cava* **15**, **16**, **17**, **18**, and **19** on DPPH free radicals are provided in **Fig. 4-4**. It was observed that **16**, **17**, **18**, and **19** scavenged 85.15, 97.68, 75.44, and 89.45% of DPPH radical at 30 μM, respectively, while 15 showed 69.42% DPPH radical scavenging activity at 150 μM. Those radical scavenging levels illustrated in **Fig. 4-5**, which values were dose-dependent manners. In addition, the **16**, **17**, **18**, and **19** possess higher DPPH radical scavenging activity (IC_{50}=9.13, 3.03, 15.29, and 5.73 μM, respectively) than the commercial antioxidant ascorbic acid (IC_{50}=19.94 μM) (**Table 4-5**). It has been well-established that free radical

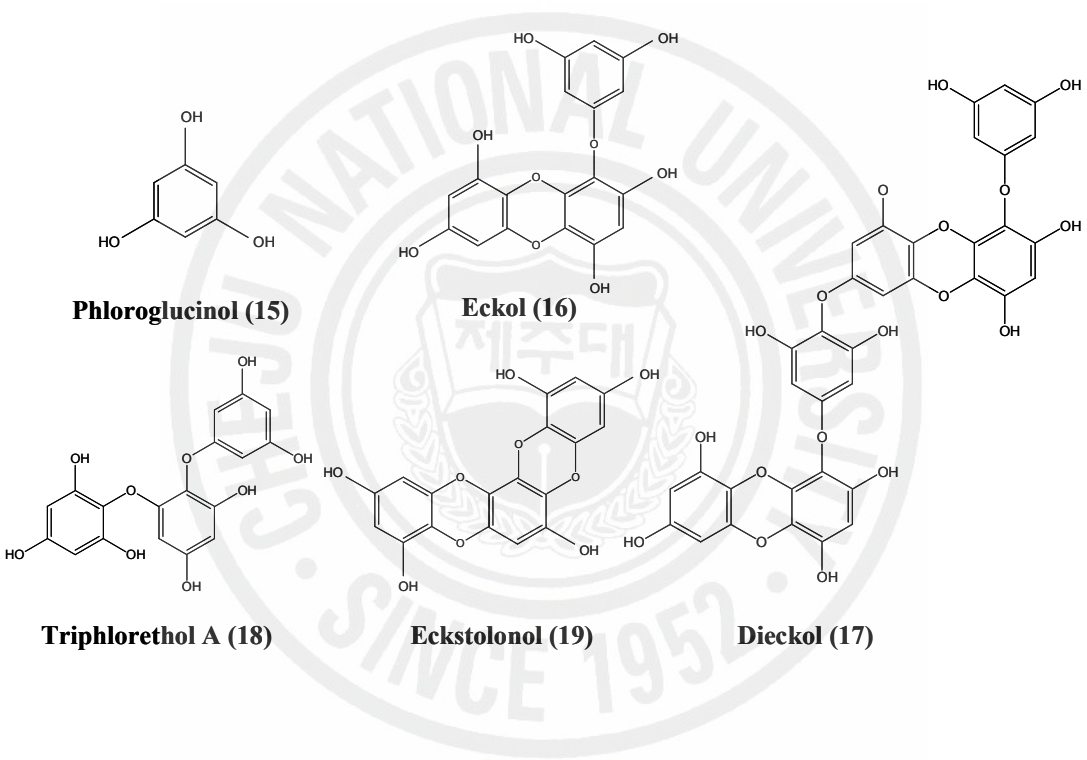

Fig. 4-3. Chemical structures of the five phloratannins isolated from *E. cava*.

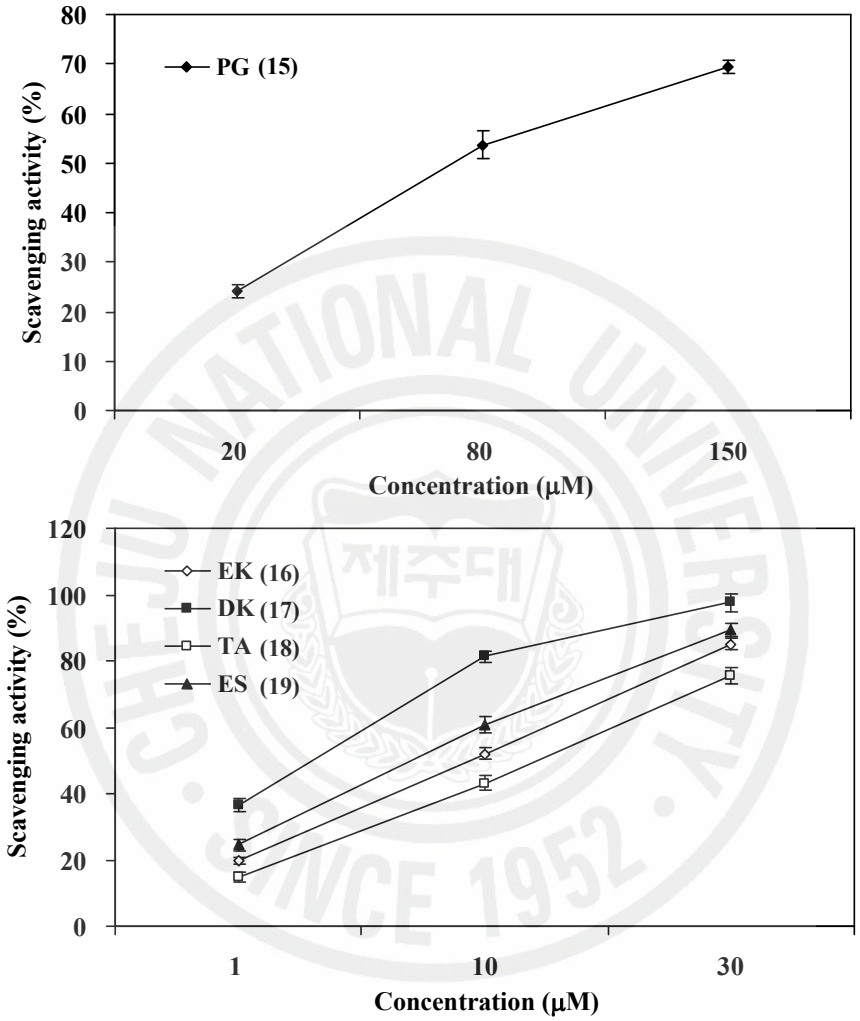

Fig. 4-4. DPPH radical scavenging activity of the active compounds isolated from *E. cava*. ◆, phloroglucinol; ◇, eckol; ■, dieckol; □, triphlorethol A; ▲, eckstolonol. Experiments were performed in triplicate and the data are expressed as mean ± SE.

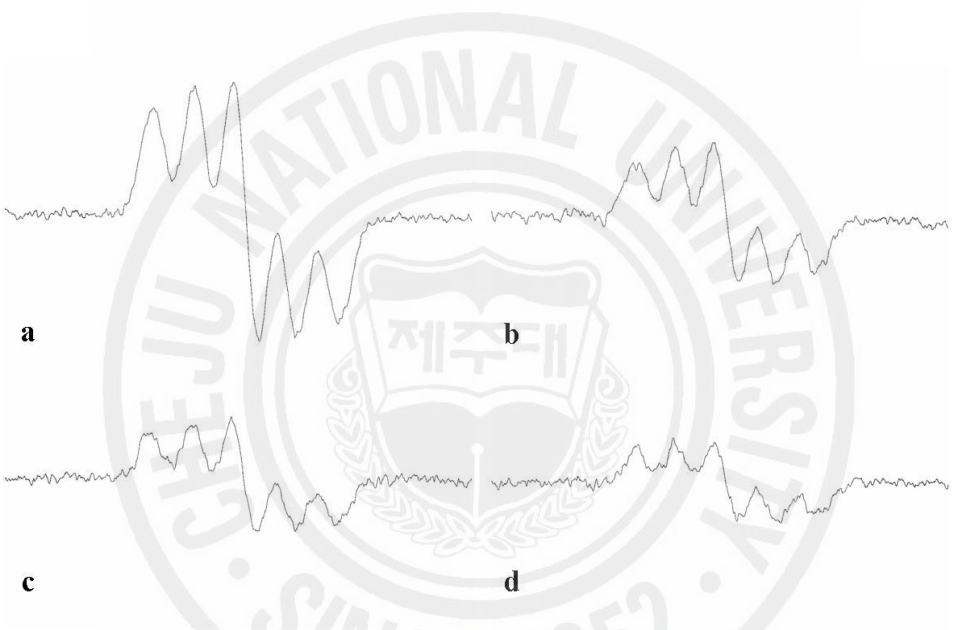

Fig. 4-5A. ESR spectrum obtained in an ethanol solution of 30 μmol/l DPPH at various concentrations of phloroglucinol isolated from *E. cava*.

a, control; b, 20 μM; c, 80 μM; d, 150 μM.

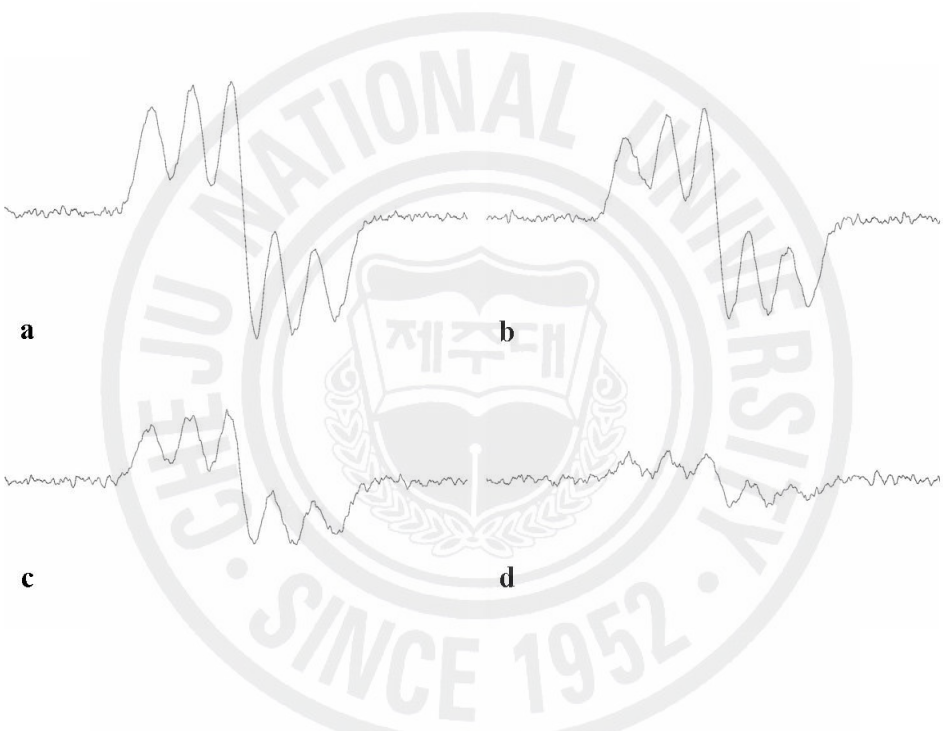

Fig. 4-5B. ESR spectrum obtained in an ethanol solution of 30 μmol/l DPPH at various concentrations of eckol isolated from *E. cava*.

a, control; b, 1 μM; c, 10 μM; d, 30 μM.

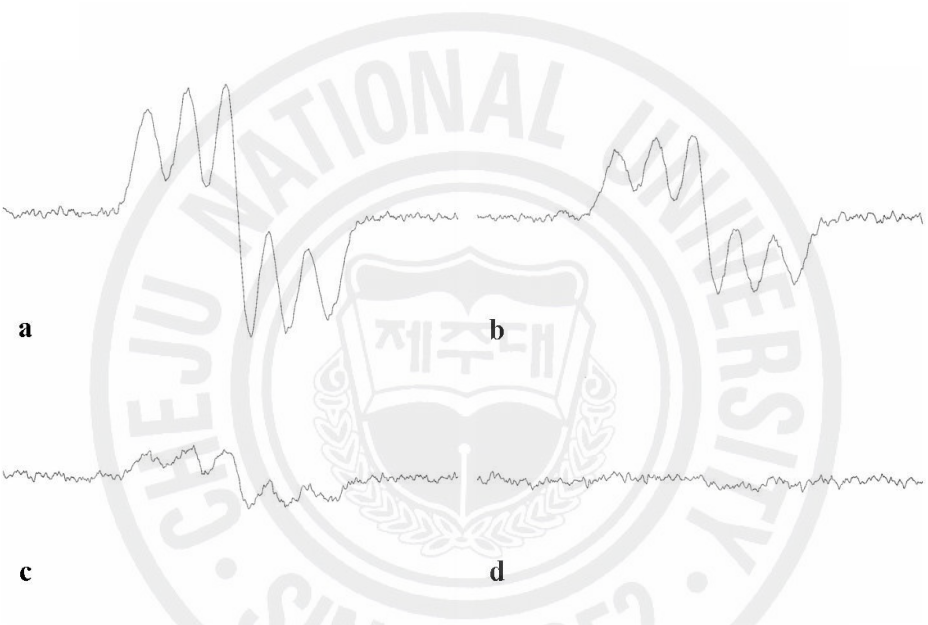

Fig. 4-5C. ESR spectrum obtained in an ethanol solution of 30 μmol/l DPPH at various concentrations of dieckol isolated from *E. cava*.

a, control; b, 1 μM; c, 10 μM; d, 30 μM.

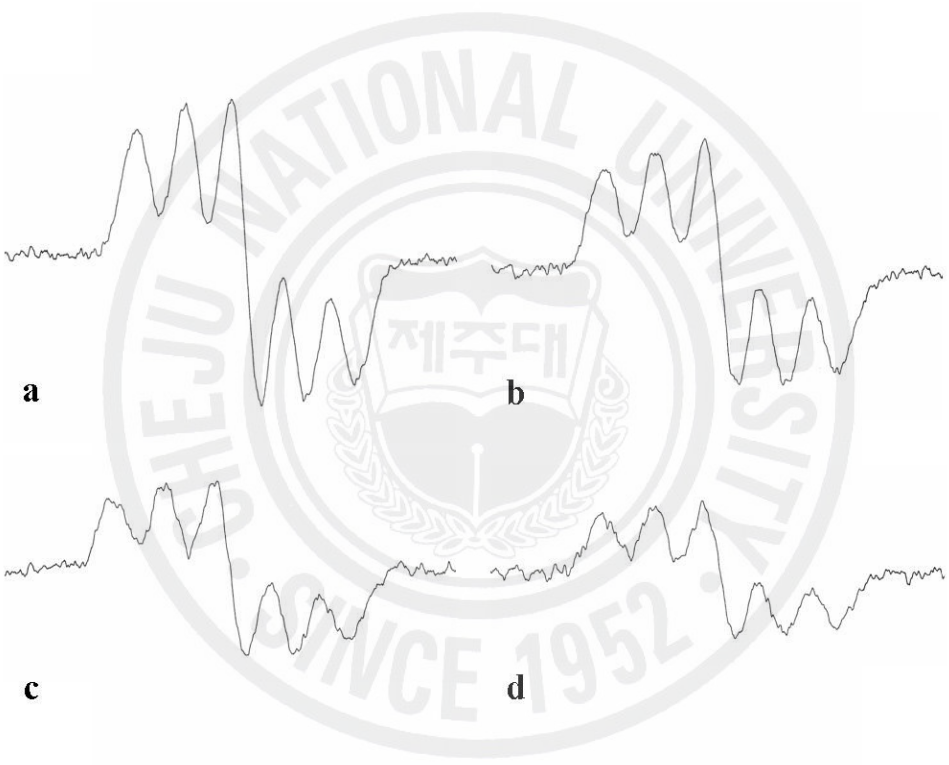

Fig. 4-5D. ESR spectrum obtained in an ethanol solution of 30 μmol/l DPPH at various concentrations of triphlorethol A isolated from *E. cava*.

a, control; b, 1 μM; c, 10 μM; d, 30 μM.

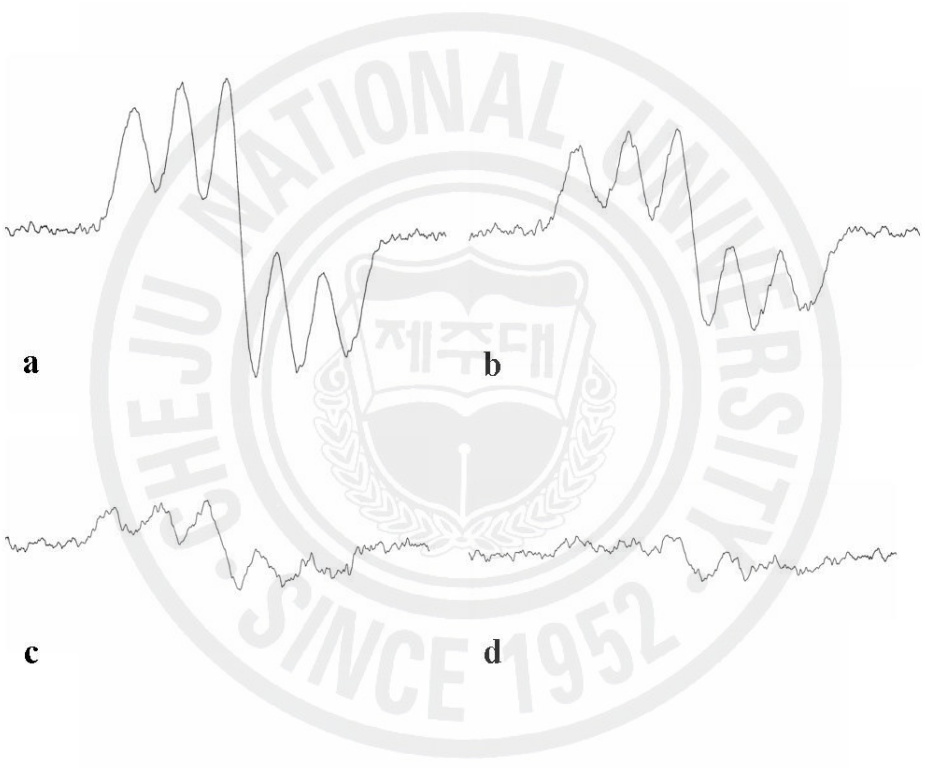

Fig. 4-5E. ESR spectrum obtained in an ethanol solution of 30 μmol/l DPPH at various concentrations of eckstolonol isolated from *E. cava*.

a, control; b, 1 μM; c, 10 μM; d, 30 μM.

Table 4-5. Scavenging activity of the active compounds isolated from *E. cava* against DPPH radical

	IC_{50} (μM)
Phloroglucinol	**99.14**
Eckol	**9.13**
Dieckol	**3.03**
Triphlorethol A	**15.29**
Eckstolonol	**5.73**
Ascorbic acid	**19.94**

scavenging activity is correlated with higher phenolic compound content. Nagai and Yukimoto (2003) reported that high polyphenol content could be correlated with high antioxidant ability in a linoleic acid model system, as well as with high levels of DPPH radical scavenging ability. Tepe and Sokmen (2007) also reported that the phenolic contents have a positive relationship with DPPH free radical scavenging activity. Phlorotannins are also known to marine alga polyphenols, which evidenced positive effect on DPPH free radical in this study. These results indicated that **16**, **17**, **18**, and **19**, kinds of phlorotannins, isolated from *E. cava* appear to be good potential candidates for DPPH free radical scavenger.

The alkyl radicals are a primary intermediate in many hydrocarbon reactions, and can be easily detected with ESR, a technique that has been found to be very useful in the characterization of solid surfaces and in the elucidation of active surface sites, as well as surface reactions (Adebajo and Gesser, 2001). As shown in **Fig. 4-6**, it was observed that the alkyl radical scavenging activities of **15**, **16**, **17**, **18**, and **19** were 70.37, 83.31, 94.67, 84.68, and 82.46% at 20 μM, and **17** showed 85.49% of scavenging activity at even 10 μM. The decrease of ESR signals was observed with the dose increment of phlorotannins (**Fig. 4-7**). Moreover, all of those tested phlorotannins have strong scavenging activity on alkyl radical than the commercial antioxidant (**Table 4-6**). Some researchers showed that seaweed extracts have strong antioxidative activities on alkyl radical. Ahn et al. (2004) reported that *Scytosiphon lomentaria* exerts positive effects against alkyl radical. Park et al. (2004) also studied reactive radical scavenging effect, and observed that *Sargassum honeri* have profound capacity against alkyl radical. Phenolic antioxidants are well known for trapping alkyl radicals to prevent organic materials from oxidative degradation (Ohkatsu et al., 2003). These facts suggest that the **15**, **16**, **17**, **18**, and **19** might be potential source of alkyl radical scavenger.

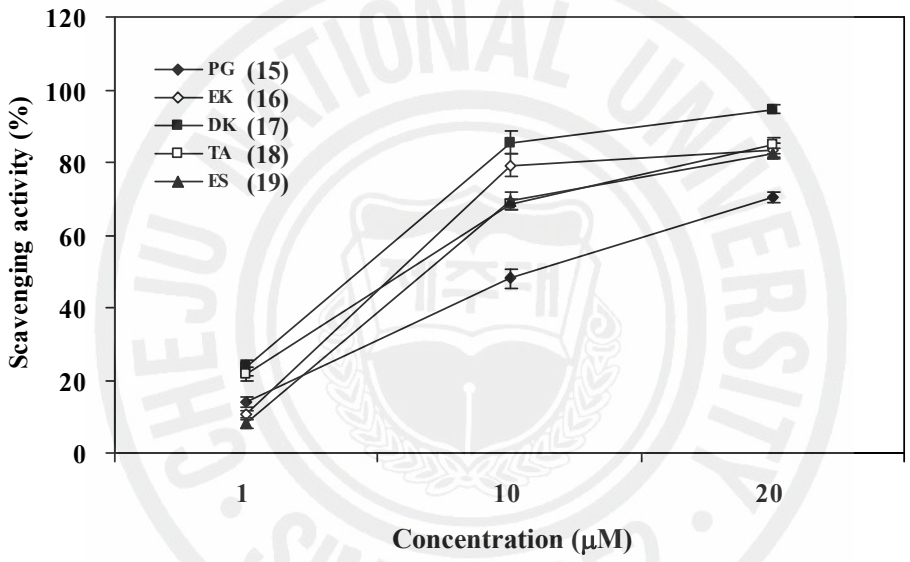

Fig. 4-6. Alkyl radical scavenging activity of the active compounds isolated from *E. cava*. ◆, phloroglucinol; ◇, eckol; ■, dieckol; □, triphlorethol A; ▲, eckstolonol. Experiments were performed in triplicate and the data are expressed as mean ± SE.

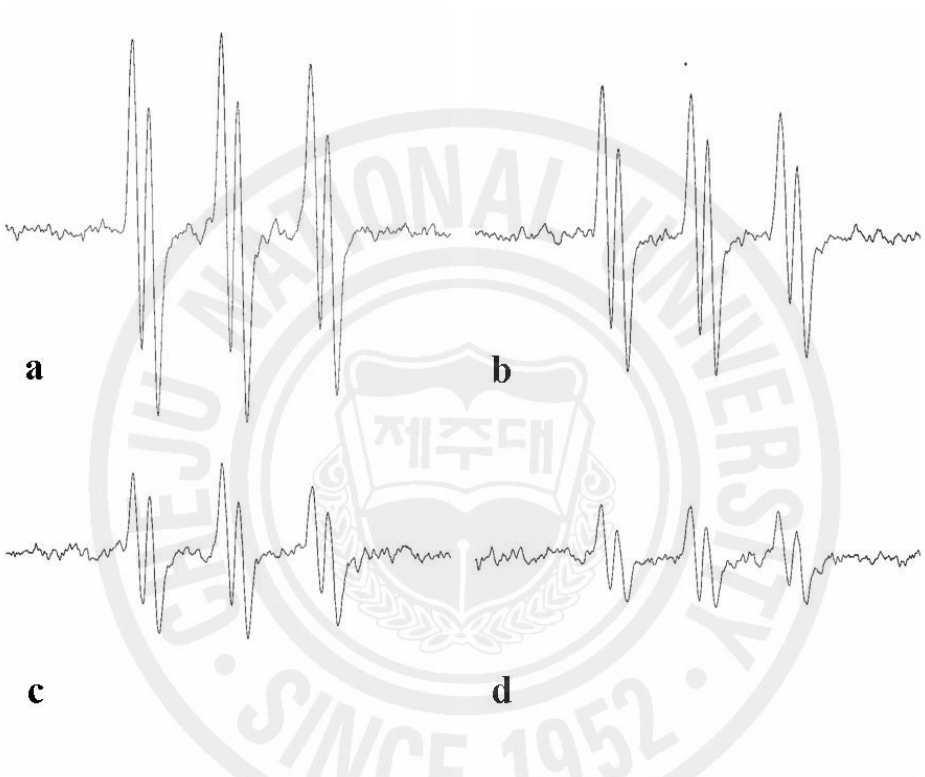

Fig. 4-7A. ESR spectrum obtained during incubation of AAPH with 4-POBN at various concentrations of phloroglucinol isolated from *E. cava*.

a, control; b, 1 μM; c, 10 μM; d, 20 μM.

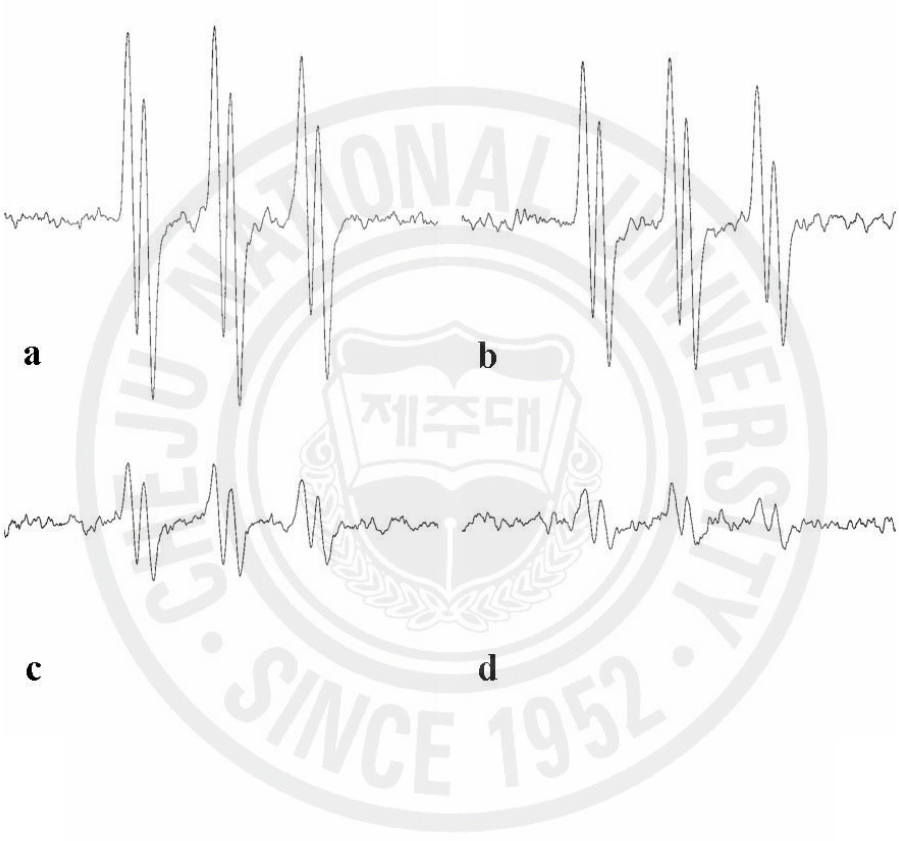

Fig. 4-7B. ESR spectrum obtained during incubation of AAPH with 4-POBN at various concentrations of eckol isolated from *E. cava*.

a, control; b, 1 μM; c, 10 μM; d, 20 μM.

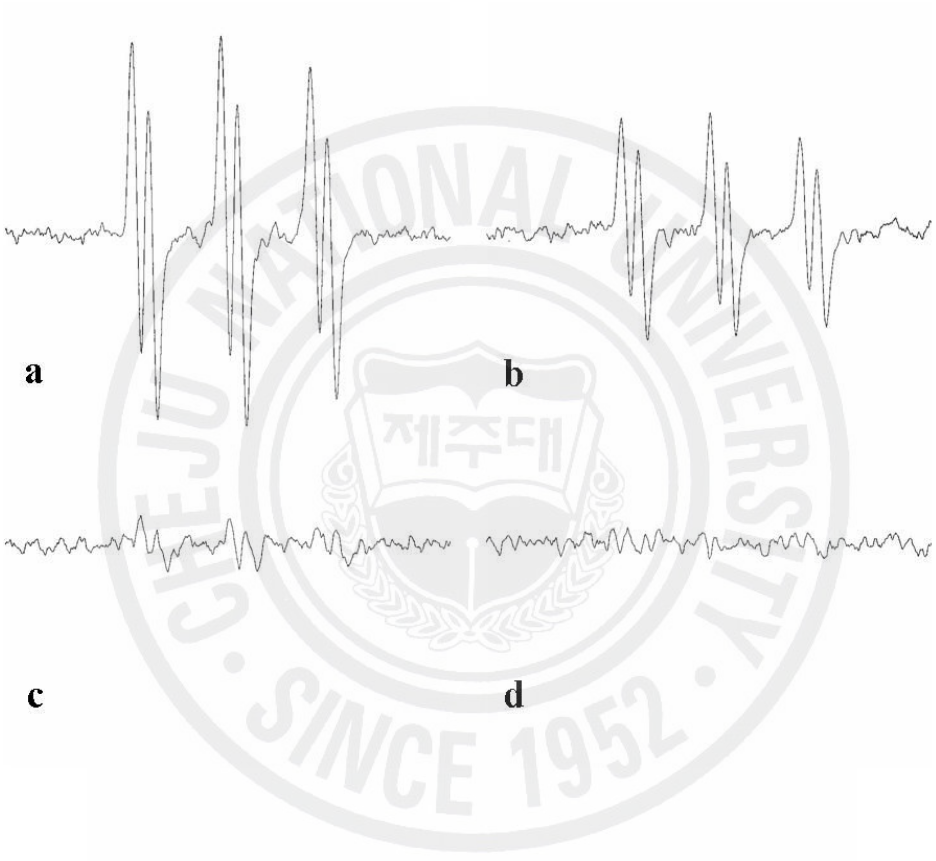

Fig. 4-7C. ESR spectrum obtained during incubation of AAPH with 4-POBN at various concentrations of dieckol isolated from *E. cava*.

a, control; b, 1 μM; c, 10 μM; d, 20 μM.

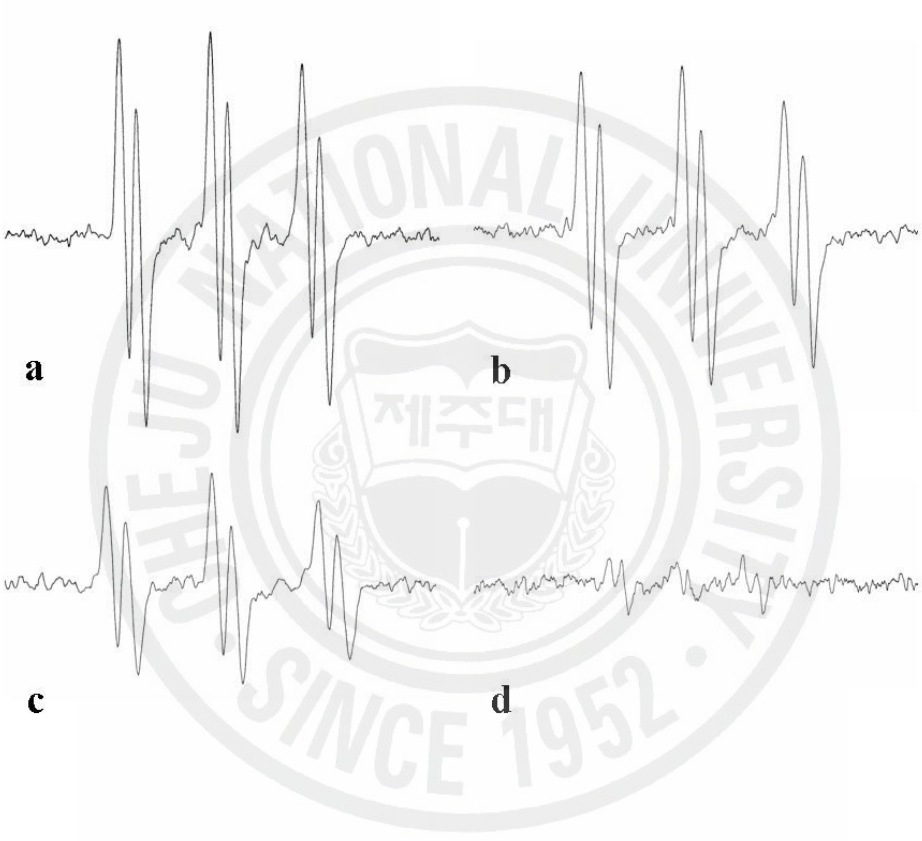

Fig. 4-7D. ESR spectrum obtained during incubation of AAPH with 4-POBN at various concentrations of triphlorethol A isolated from *E. cava*.

a, control; b, 1 μM; c, 10 μM; d, 20 μM.

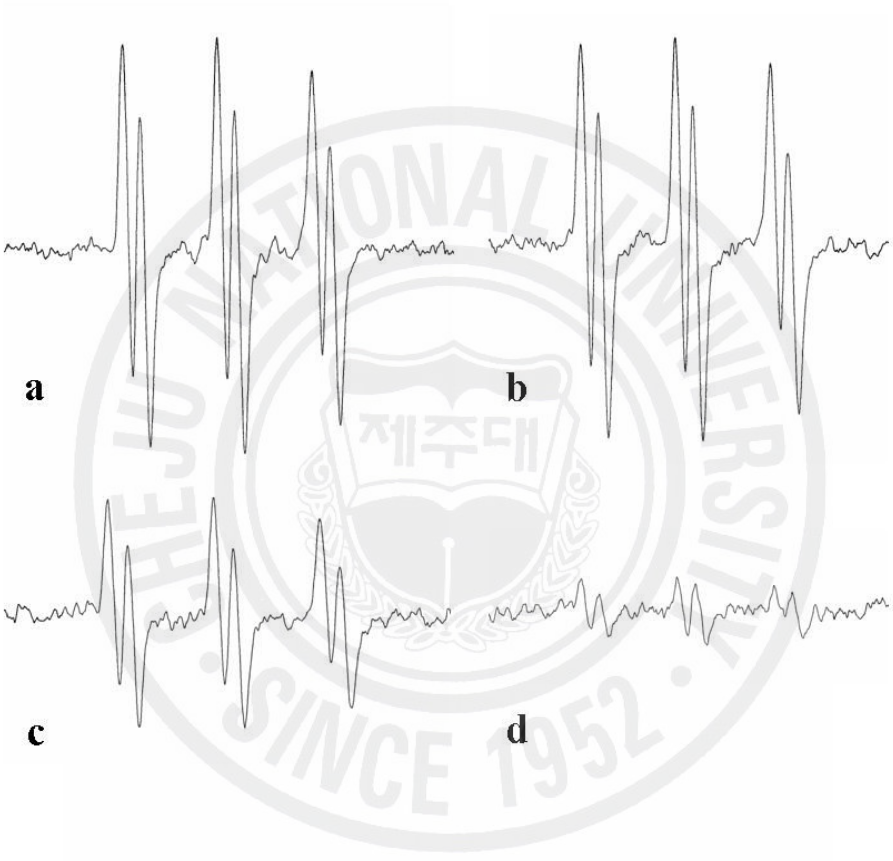

Fig. 4-7E. ESR spectrum obtained during incubation of AAPH with 4-POBN at various concentrations of eckstolonol isolated from *E. cava*.

a, control; b, 1 μM; c, 10 μM; d, 20 μM.

Table 4-6. Scavenging activity of the active compounds isolated from *E. cava* against alkyl radical

	IC_{50} (μM)
Phloroglucinol	**12.42**
Eckol	**6.83**
Dieckol	**2.60**
Triphlorethol A	**5.34**
Eckstolonol	**6.52**
Ascorbic acid	**19.26**

Hydroxyl radicals are the major reactive oxygen species, which are generated by Fenton reaction ($Fe^{2+} + H_2O_2 \rightarrow Fe^{3+} + {}^{-}OH + {}^{\cdot}OH$) and are trapped by DMPO, forming a spin adduct that can be detected by the ESR system. We therefore also examined whether phlorotannins can scavenge hydroxyl radicals generated by this reaction. The ability of the phlorotannins isolated from *E. cava* to scavenge hydroxyl radical was shown in **Fig. 4-8**. Scavenging activity of **17**, **18**, and **19** against hydroxyl recorded 73.58, 75.34, and 77.31% at 120 μM, whereas **15** and **16** showed 68.43 and 92.90% at 500 μM, respectively. In addition, **17**, **18**, and **19** showed 45.03, 63.47, and 61.58% of scavenging activity at even 60 μM, and those compounds exhibited more effective than those of commercial antioxidant (**Table 4-7**). The decrease of the amount of DMPO-OH adduct was expressed by ESR signals after the addition of phlorotannins and the values were dose-dependent manners (**Fig. 4-9**). The hydroxyl radical is the most reactive radical species and capable of damaging almost every molecule found in living cells (Castro and Freeman, 2001). Thus, due to high reactivity of hydroxyl radicals they are more likely to be scavenged by direct reactions with other surrounding molecules before attacking the target molecule. Therefore, the present study used the ESR technique, which could easily detect the amount of hydroxyl radical. From this result, **17**, **18**, and **19** might be used to potential hydroxyl radical scavengers.

Phlorotannin compounds, which are present in brown algae, are polymers of phloroglucinol. As mentioned in some reports associated with antioxidative cpapcity of brown algae, phlorotannins are potential antioxidant compounds. It has been reported that Nakai et al. (2006) isolated bifuhalol oligomer, a kind of phlorotannin from *S. ringgoldianum*, the bifuhalol oligomer exhibited strong superoxide anion radical scavenging activity (IC_{50}=1 μg/ml). Kim et al. (2004) also isolated phlorotannins such

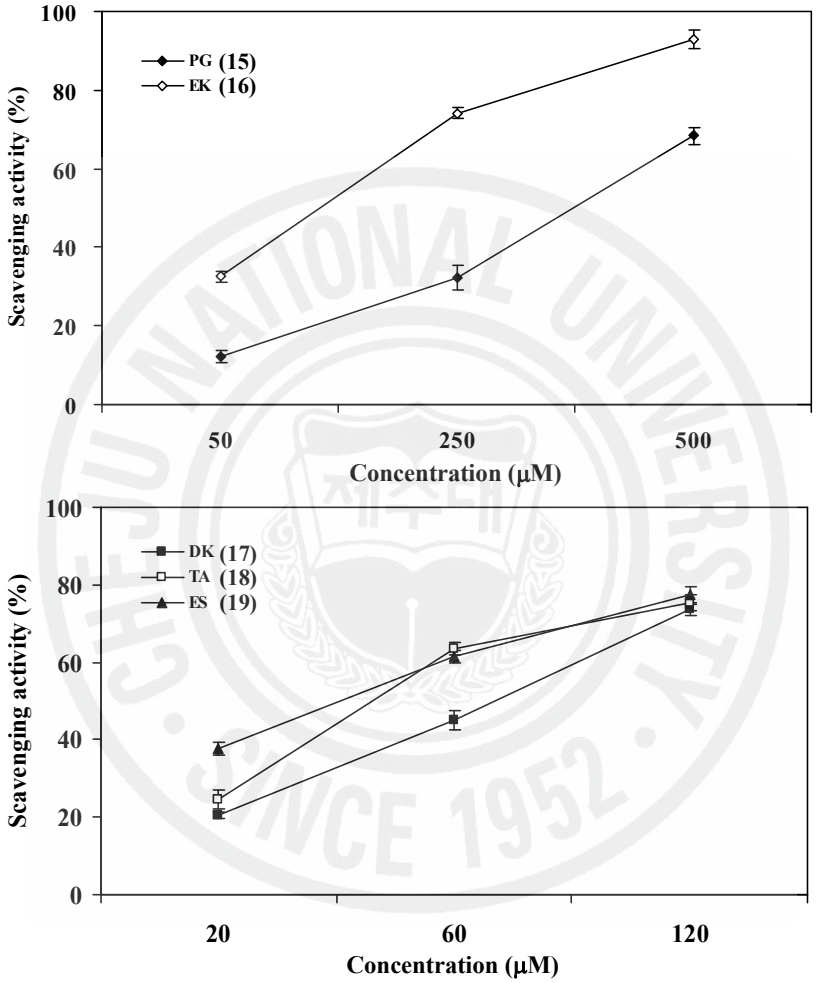

Fig. 4-8. Hydroxyl radical scavenging activity of the active compounds isolated from *E. cava*. ◆, phloroglucinol; ◇, eckol; ■, dieckol; □, triphlorethol A; ▲, eckstolonol. Experiments were performed in triplicate and the data are expressed as mean ± SE.

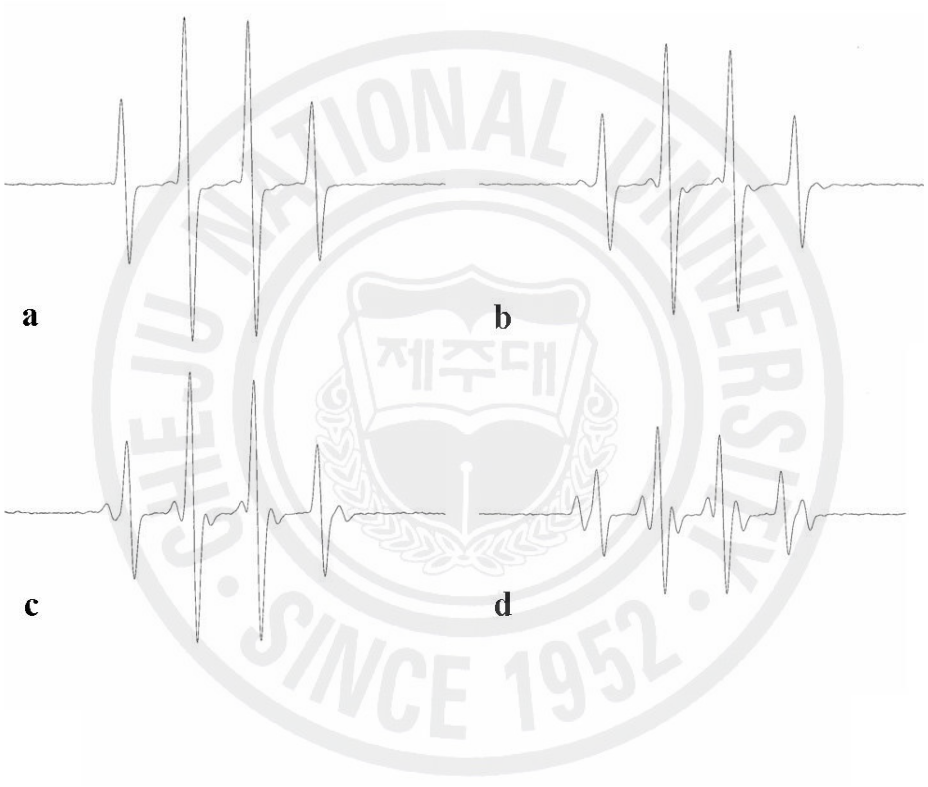

Fig. 4-9A. ESR spectrum obtained in Fenton reaction system at various concentrations of phloroglucinol isolated from *E. cava*.

a, control; b, 50 μM; c, 250 μM; d, 500 μM.

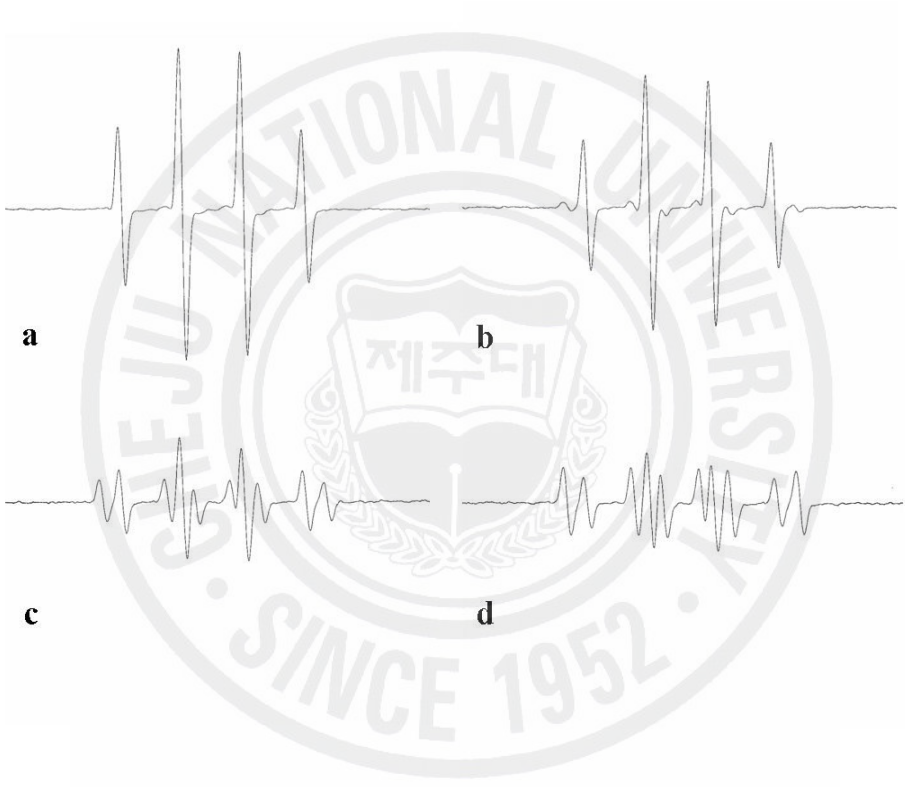

Fig. 4-9B. ESR spectrum obtained in Fenton reaction system at various concentrations of eckol isolated from *E. cava*.

a, control; b, 50 μM; c, 250 μM; d, 500 μM.

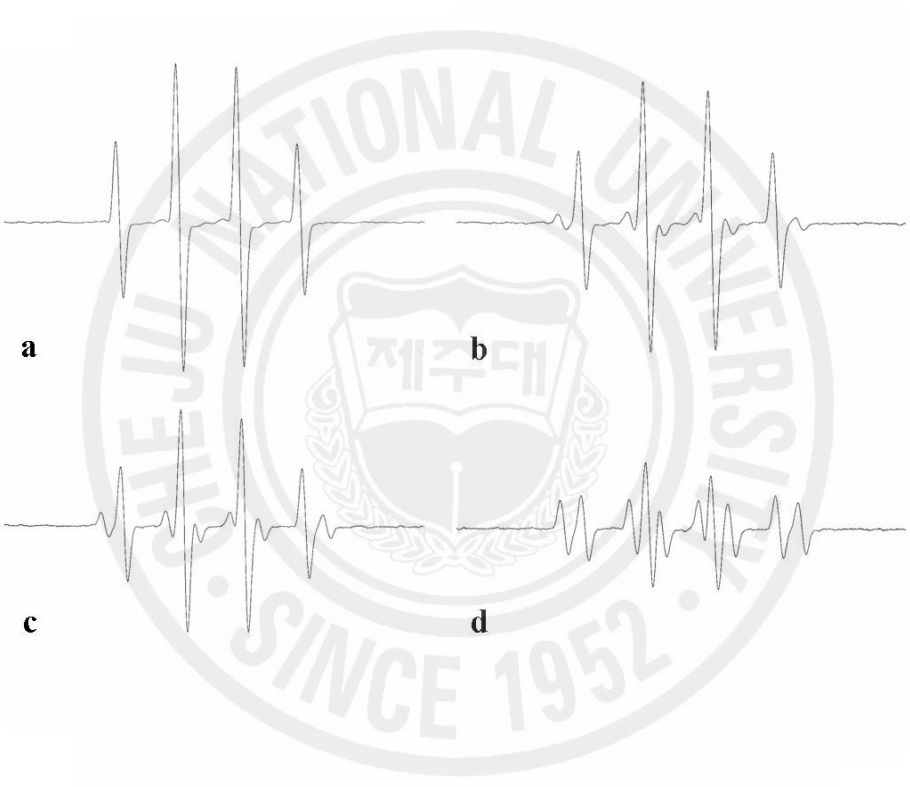

Fig. 4-9C. ESR spectrum obtained in Fenton reaction system at various concentrations of dieckol isolated from *E. cava*.

a, control; b, 20 μM; c, 60 μM; d, 120 μM.

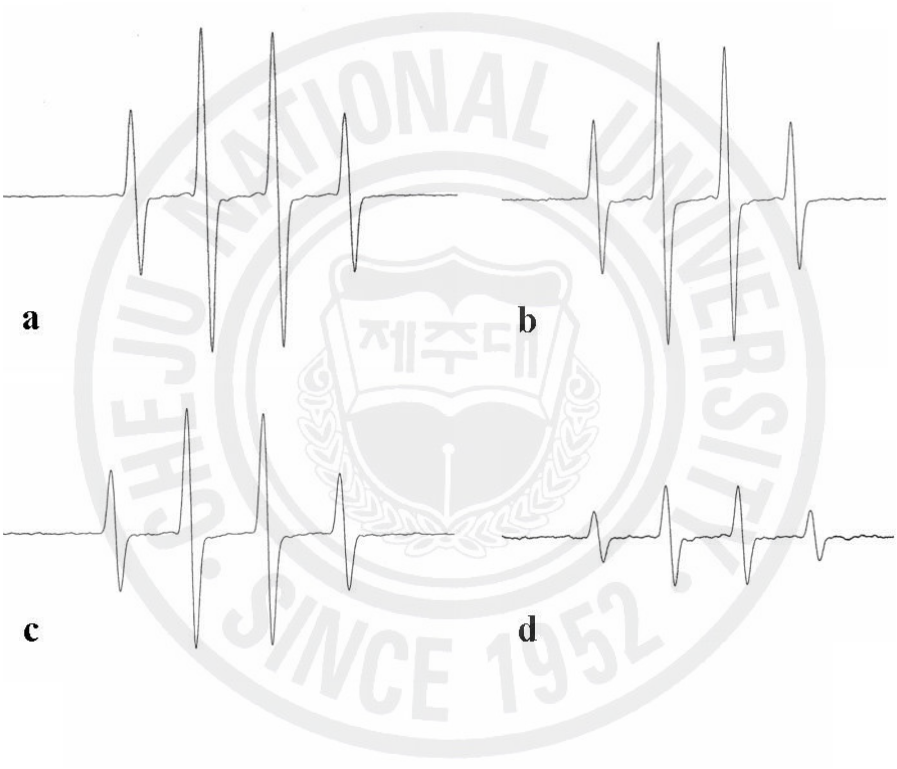

Fig. 4-9D. ESR spectrum obtained in Fenton reaction system at various concentrations of triphlorethol A isolated from *E. cava*.

a, control; b, 20 μM; c, 60 μM; d, 120 μM.

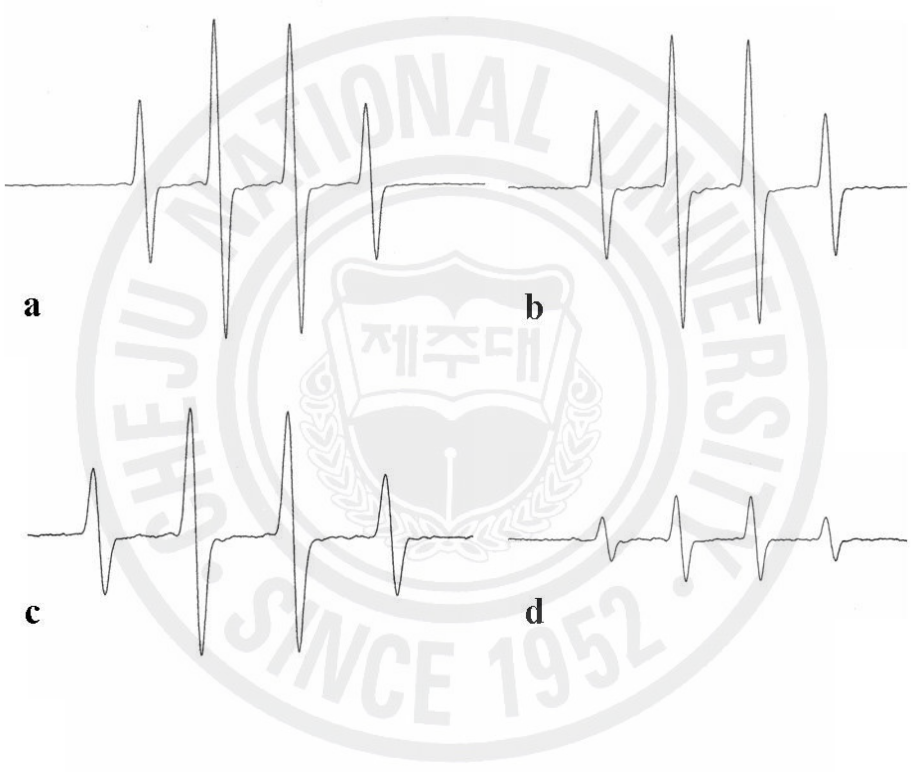

Fig. 4-9E. ESR spectrum obtained in Fenton reaction system at various concentrations of eckstolonol isolated from *E. cava*.

a, control; b, 20 μM; c, 60 μM; d, 120 μM.

Table 4-7. Scavenging activity of the active compounds isolated from *E. cava* against hydroxyl radical

	IC_{50} (μM)
Phloroglucinol	**373.90**
Eckol	**110.32**
Dieckol	**68.12**
Triphlorethol A	**47.24**
Eckstolonol	**28.43**
Ascorbic acid	**69.75**

as eckol, dieckol, 6-6' bieckol, and phlorofucofuroeckol A from *E. cava*, the phlorotannins showed potent lipid peroxidation inhibitory effect with the IC_{50} values of 70, 51, 56, and 80 μg/ml, respectively. In this study, we investigated the abilities of five phlorotannins isolated from *E. cava* to scavenge DPPH, alkyl, and hydroxyl radicals via ESR technique, which is the most direct method to detect highly reactive free radicals. According to these results, we identified that the phlorotannins have profound antioxidant activities for scavenging free radicals such as DPPH, alkyl, and hydroxyl radicals.

Hydrogen peroxide (H_2O_2) is an oxidant belongs to reactive oxygen species (ROS) but does not have a radical. H_2O_2 as a molecule is weakly reactive, but the single bond between the two oxygen atoms is easily broken, so that is readily fragments into a hydrogen and a hydroperoxyl radical or into two hydroxyl radicals. Hence, the measurement of H_2O_2 scavenging activity can be one of the useful methods determining the ability of antioxidants to decrease the level of prooxidants such as H_2O_2 (Pazdzioch-Czochra and Widensk, 2002). Scavenging activity of each compound against H_2O_2 was illustrated in **Fig. 4-10**. It was observed that **16**, **17**, **18**, and **19** scavenged 65.34, 76.76, 74.59, and 57.49% of H_2O_2 at 100 μM, respectively, while **15** exhibited 68.31% H_2O_2 scavenging activity at 500 μM. In addition, **16**, **17**, **18**, and **19** showed higher or similar scavenging activity on H_2O_2 than the commercial antioxidant BHA (**Table 4-8**). The potential H_2O_2 scavenging activity of the phlorotannins could be beneficial in minimizing or retarding the adverse effects of H_2O_2. Moreover, H_2O_2 is a prooxidant which serves as a starting material for the production of harmful hydroxyl radical and non free radical species like singlet oxygen. Hydroxyl radical is the most reactive among reactive oxygen species and the cell-damaging action of hydroxyl radical is the strongest among free radical. Therefore, H_2O_2 scavenging activity of the phlorotannins

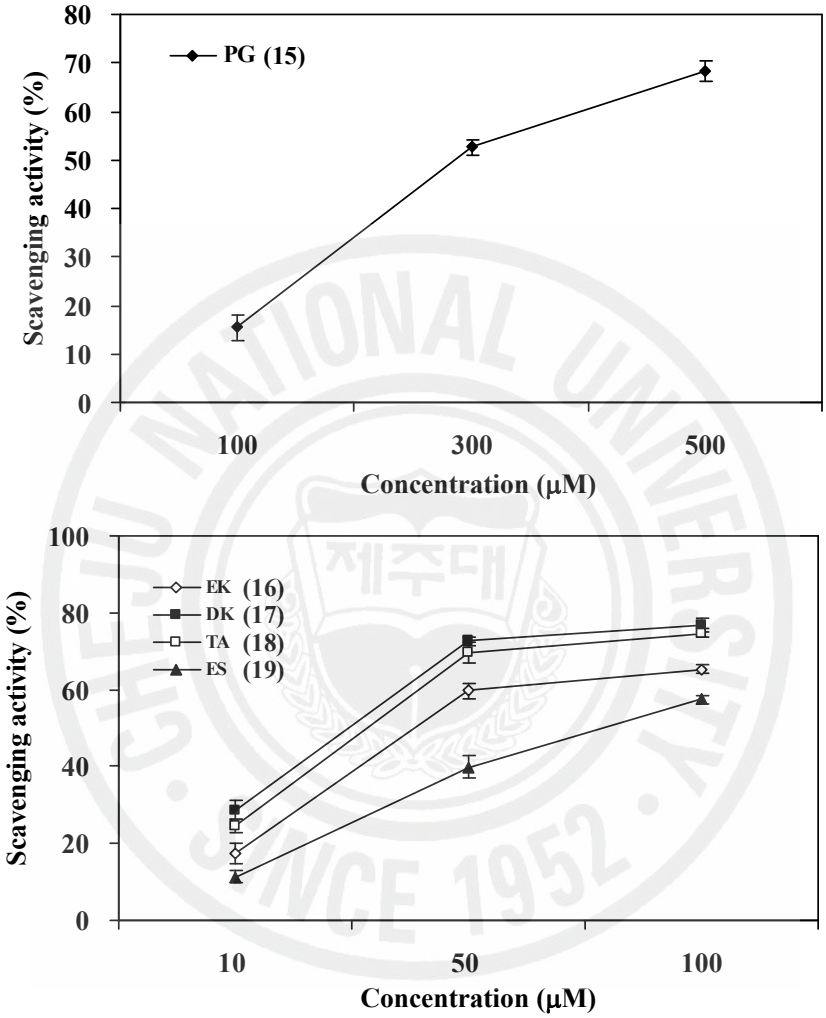

Fig. 4-10. Hydrogen peroxide scavenging activity of the active compounds isolated from *E. cava*. ◆, phloroglucinol; ◇, eckol; ■, dieckol; □, triphlorethol A; ▲, eckstolonol. Experiments were performed in triplicate and the data are expressed as mean ± SE.

Table 4-8. Scavenging activity of the active compounds isolated from *E. cava* against hydrogen peroxide

	IC_{50}(μM)
Phloroglucinol	**302.66**
Eckol	**41.59**
Dieckol	**24.46**
Triphlorethol A	**32.88**
Eckstolonol	**79.67**
BHA	**73.92**

isolated from *E. cava* is important as a potential antioxidant that can maintain good health by overcoming complications possible with harmful oxidants.

Many studies have shown that oxidative stress is a major cause of cellular injuries in a variety of human diseases including atherosclerosis, arthritis, muscular dystrophy, and inflammatory disorders. ROS such as hydrogen peroxide, superoxide anion, and hydroxyl radical readily damage to biological molecules, which can ultimately lead to apoptotic or necrotic cell death (Zhang et al., 2007). Thus, removal of excess ROS or suppression of their generation by antioxidants may be effective in preventing oxidative cell death. H_2O_2 has been extensively used as an inducer of oxidative stress *in vitro* model. The exposure of cultured cells to H_2O_2 results in an imbalance in energy metabolism and the deleterious effects of hydroxyl and peroxiyl radicals on membrane lipids and proteins. Therefore, in this study, we investigated the antioxidant effects of the isolated compounds after the administration of H_2O_2 treatment in cell lines. DCFH-DA was used as a probe for ROS measurement. DCFH-DA crosses cell membranes and is hydrolyzed enzymatically by intracellular esterases to nonfluorescent DCFH. In the presence of ROS, DCFH is oxidized to highly fluorescent dichlorofluorescein (DCF). It is well known that H_2O_2 is the principal ROS responsible for the oxidation of DCFH to DCF (LeBel et al., 1992). In the present study, we investigated scavenging activity on intracellular ROS using H_2O_2 in Vero cell lines. As shown in **Fig. 4-11**, the intracellular ROS scavenging activity of **15**, **16**, **17**, **18**, and **19** was expressed as 31.60, 64.92, 58.17, 56.62, and 48.57% at the concentration of 100 μM. Interestingly **17** showed almost 50% of scavenging levels at all the concentrations tested. In IC50 values for scavenging of intracellular ROS, moreover, **17** exhibited more effective than those of the other compounds (**Table 4-9**), and the scavenging activities increased when increasing the compound concentration. To evaluate whether phlorotannins protects from cellular

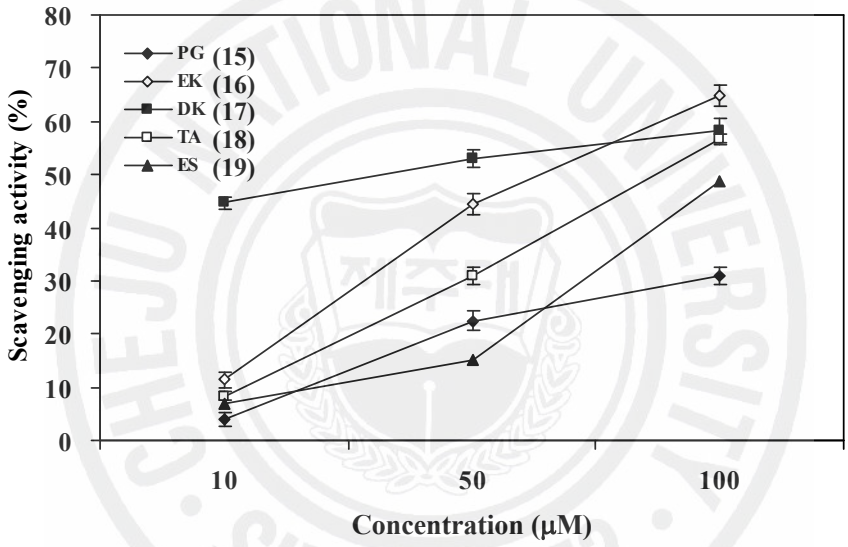

Fig. 4-11. Effect of the active compounds isolated from *E. cava* on scavenging reactive oxygen species. The intracellular reactive oxygen species generated was detected by DCF-DA method. ◆, phloroglucinol; ◇, eckol; ■, dieckol; □, triphlorethol A; ▲, eckstolonol. Experiments were performed in triplicate and the data are expressed as mean ± SE.

Table 4-9. Scavenging activity of the active compounds isolated from *E. cava* against intracellular ROS

	IC_{50} (μM)
Phloroglucinol	**284.51**
Eckol	**69.94**
Dieckol	**40.07**
Triphlorethol A	**87.07**
Eckstolonol	**109.41**

damage induced by H_2O_2, cells were pretreated with phlorotannins for 24 h in the absence or presence of oxidative stress. After then, cell viability was measured by MTT assay. H_2O_2-induced cells recorded 57.82% cell survival rate, whereas treatment of the phlorotannins increased the cell viability (**Fig. 4-12**). Among them, **17**, **18**, and **20** exhibited significant cell survival rates even at 5 μM (78.61, 85.58, and 82.44%, respectively), while all of the tested phlorotannins protected the cells from H_2O_2-induced cytotoxicity in concentration-dependent manners. The protective effect of phlorotannins on DNA damages was also confirmed by comet assay and was presented as tail DNA percent. This assay can reflect different types of DNA damage, such as DNA singe strand breakage, or incomplete DNA repairing and shows high sensitivity in detecting carcinogens (Anderson et al., 1998). H_2O_2 is a well-known genotoxic agent able to induce oxidative DNA damage. H_2O_2 treatment increased the tail moments in the cells versus the control cells. However, the increased tail moments caused by H_2O_2-induced oxidative DNA damage were decreased in the cells treated with phlorotannins. The inhibition activities of **15**, **16**, **17**, **18**, and **19** on DNA damage were 36.42, 60.43, 67.59, 52.41, and 45.37% at the concentrations of 250 μM, respectively, especially, the **17** exhibited higher inhibitory effect at even 100 μM, which values were recorded as 47.75% (**Fig. 4-13**). These results suggest that **17** protect the cell damage induced by oxidative stress.

Melanins play a critical role in the absorption of free radicals and melanogenesis in the skin in a kind of process that produces photoprotective agents against damaging effect of UV. Many cosmetic and pharmaceurical companies have tried to find inhibitor of melanogenesis. The regulation of cellular pigmentation can be controlled at many different stages of melanogenesis. Especially, tyrosinase inhibitors and antioxidants can be used for inhibition of cellular pigmentation since the melanin producing process

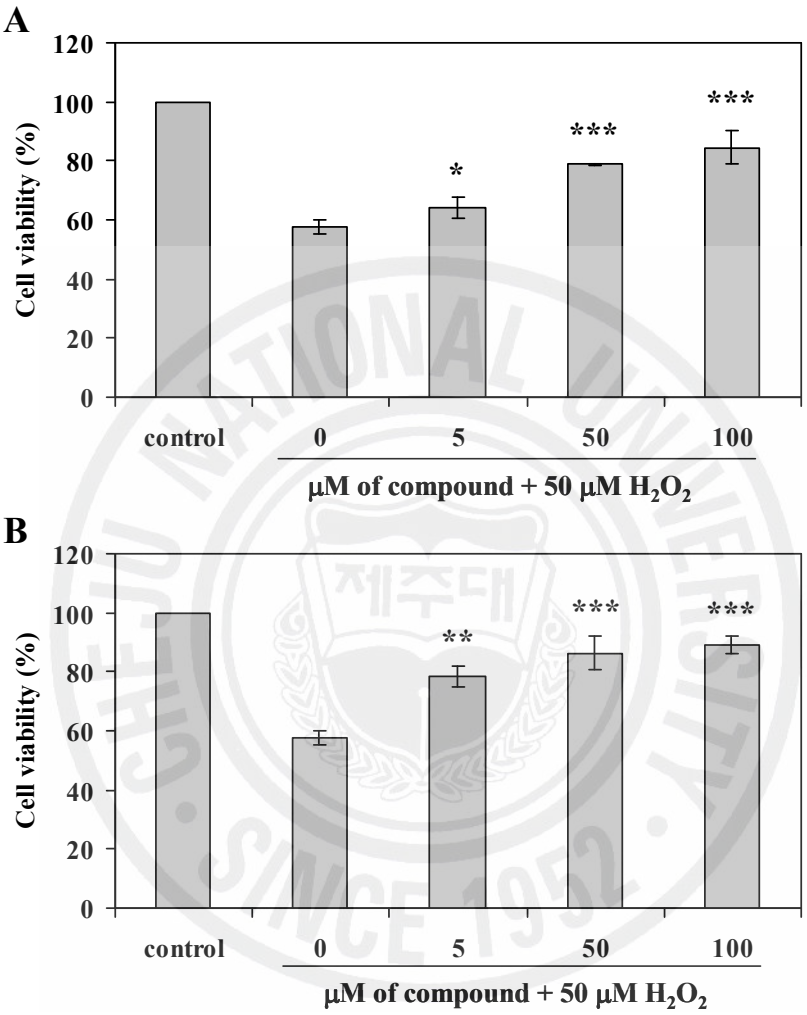

Fig. 4-12. Protective effect of the active compounds isolated from *E. cava* on H_2O_2 induced oxidative damage of vero cells. The viability of vero cells on H_2O_2 treatment was determined by MTT assay. A, phloroglucinol; B, eckol; C, dieckol; D, triphlorethol A; E, eckstolonol. Experiments were performed in triplicate and the data are expressed as mean ± SE. Statistical evaluation was performed to compare the experimental groups and corresponding control groups. *, $p < 0.05$, **, $p < 0.005$, ***, $p < 0.001$

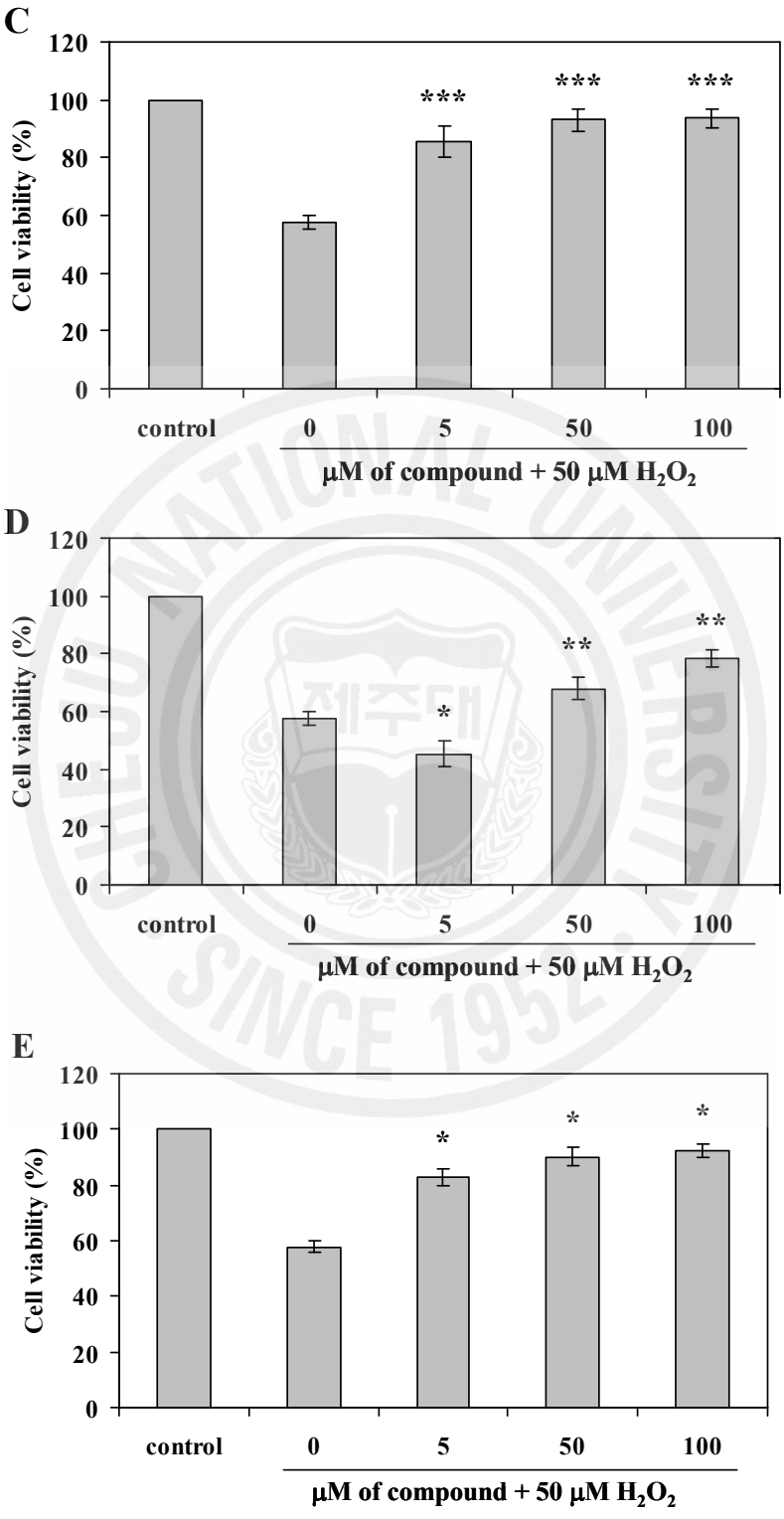

Fig. 4-12. Continued.

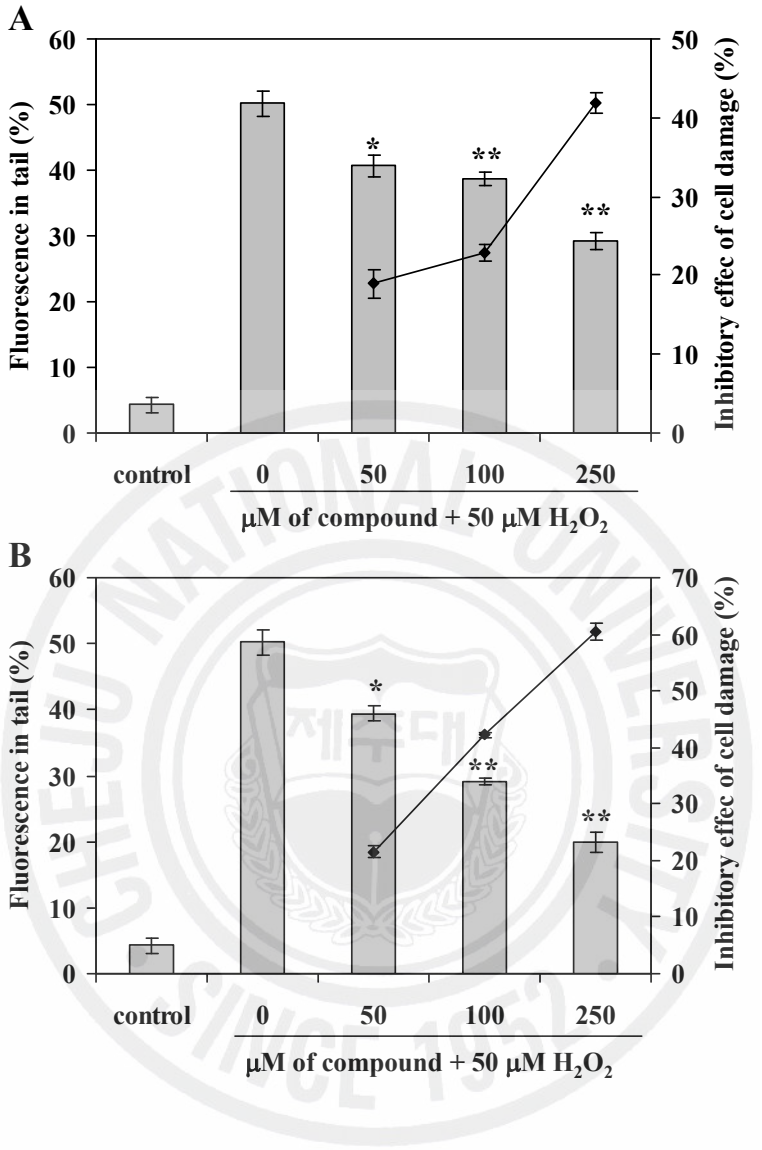

Fig. 4-13. Inhibitory effect of different concentrations of the active compounds isolated from *E. cava* on H_2O_2 induced DNA damages. The damaged cells on H_2O_2 treatment was determined by comet assay. ■, % Fluorescence in tail; ●, Inhibitory effect of cell damage. A, phloroglucinol; B, eckol; C, dieckol; D, triphlorethol A; E, eckstolonol. Experiments were performed in triplicate and the data are expressed as mean ± SE. Statistical evaluation was performed to compare the experimental groups and corresponding control groups. *, $p < 0.005$, **, $p < 0.001$

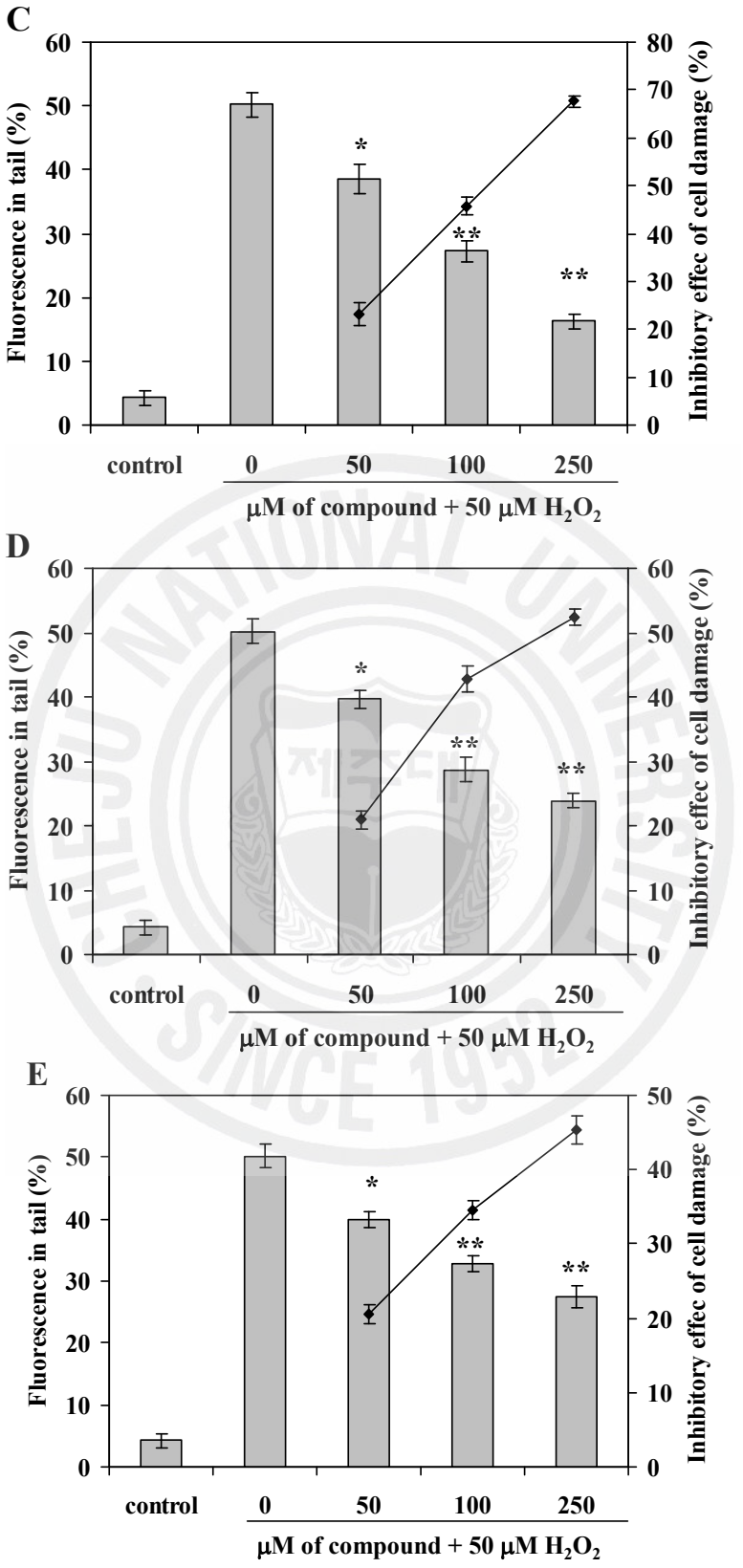

Fig. 4-13. Continued.

involved enzymatic and nonenzymatic oxidation reactions (Lee and Choi, 1999). In this study, the effect of phlorotannins on melanogenesis was examined via inhibitory effect of tyrosinase and melanin synthesis. The inhibition of tyrosinase catalyzed dopachrome formation was evaluated in **Fig. 4-14**. Among the tested phlorotannins, the **17** showed the highest inhibitory effect on tyrosinase as 92.65% at 100 μM, while **16**, **18**, and **19** showed 62.38, 71.85, and 73.52% at 100 μM, respectively, In addition, the **17** showed 88.97% of tyrosinase inhibition even at 50 μM, and the values were better than those of the commercial whitening agent, kojic acid. To evaluate the melanogenesis in cell lines, B16 mouse melanoma cell were used for determination of inhibitory effect of melanin contents. The results with various concentrations of the **15**, **16**, **17**, **18**, and **19** were illustrated in **Fig. 4-15**, and the inhibitory effect was recorded as 42.38, 51.67, 61.78, 48.37, and 47.68% at the concentrations of 250 μM, respectively. Out of the phlorotannins, the **17** possess higher inhibition than the other phlorotannins, but the values were relatively lower than the commercial whitening agents, PTU and retinol (78.64 and 75.34% at 250 μM, respectively). Melanin is an important factor affecting mammalian skin color (Hearing, 2005). The proximal pathway of melanogenesis consists of the enzymatic oxidation of tyrosine or L-DOPA to its corresponding *o*-dopaquinone, a step catalyzed by tyrosinase. After multiple additional biosynthesis steps, further polymerization yields melanin. In the present study, phlorotannins isolated from *I. okamurae* were examined for its ability to inhibit tyrosinase activity and to reduce cellular melanin contents in B16F10 cell lines. From these results, it was deduced that **17** inhibit cellular pigmentation more effectively than the commercial tyrosinase inhibitor (kojic acid) but relatively lower than melanin synthesis inhibitors (PTU and retinol). Although **17** had relatively lower than the commercial whitening agent, it can be applied to whitening materials as a natural compound.

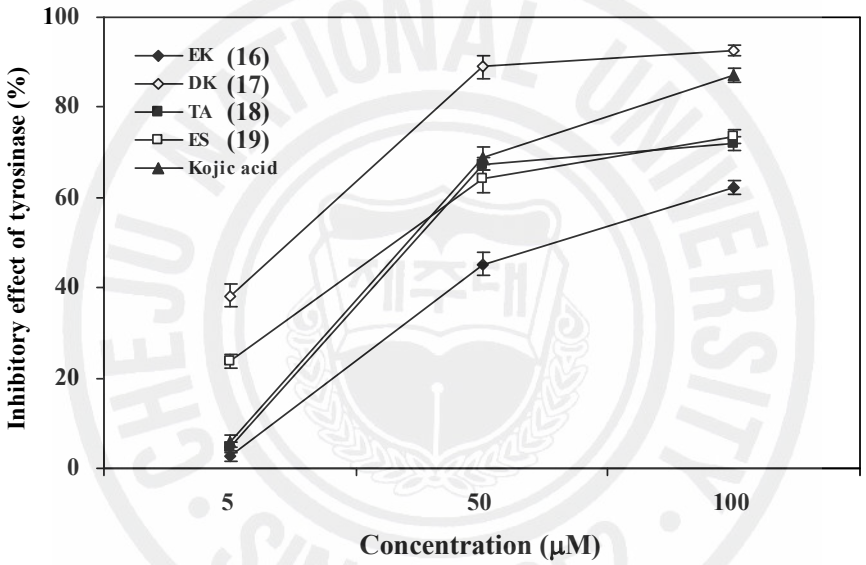

Fig. 4-14. Inhibitory effect of the active compounds isolated from *E. cava* against mushroom tyrosinase. L-tyrosine was used as substrate, and kojic acid and arbutin were used as positive control. Experiments were performed in triplicate and the data are expressed as mean ± SE.

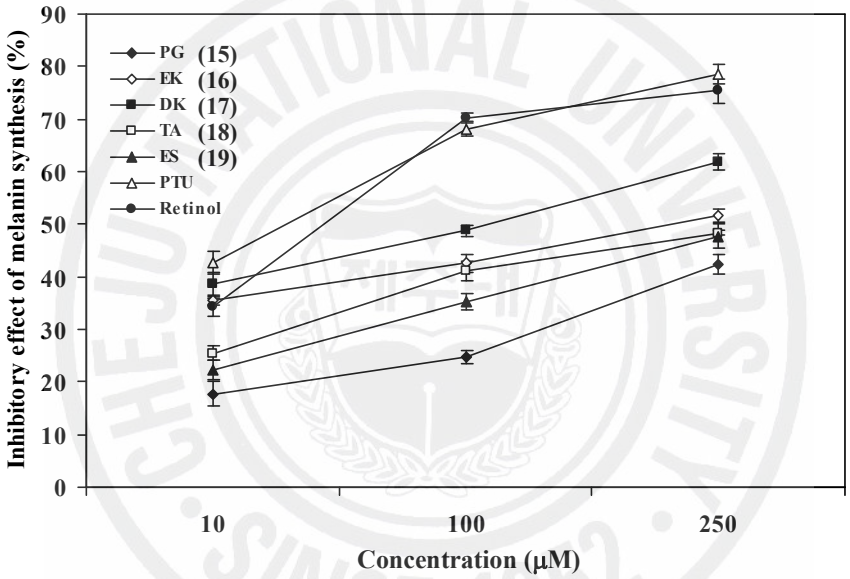

Fig. 4-15. Inhibitory effect of the active compounds isolated from *E. cava* on melanin synthesis. B16F10 melanoma cells were used for this experiment and PTU and retinol were used as positive control. Experiments were performed in triplicate and the data are expressed as mean ± SE.

Exposure to UV-B radiation causes excessive generation of reactive oxygen species in the skin, which contributes to cancer induction, causing oxidative stress in the skin and ultimately damaging DNA (Kvam and Tyrrell, 1997; Scharffetter-Kochanek et al., 1997). The skin possesses an elaborate antioxidant defense system to protect it from oxidative stress, but excessive exposure to reactive oxygen species can shift the prooxidant-antioxidant balance of the skin toward a more oxidative state. The resulting oxidative stress causes many adverse effects and pathological conditions (Ananthaswamy and Kanjilal, 1996; Finkel and Holbrook, 2000). Under these circumstances, regular intake of dietary antioxidants or treatment of the skin with products containing whitening ingredients may be a useful strategy for preventing UV-B induced damage. Therefore, in this study, we report the protective effect of phlorotannins caused by UV-B radiation as antioxidant and whitening purpose. To determine whether the protection afforded to cells by phlorotannins against UV-B induced oxidative cytotoxiciy, cell were pretreated with phlorotannins for 24 h in the absence or presence of oxidative stress, after then, cell viability were measured via MTT assays. In the exposure of 50 mJ/cm^2 of UV-B radiation, there were only 42.21% viable cells as compared to control cells, while various concentrations of phlorotannins prevented cells from UV-B induced damage, restoring cell survival were dose dependent manners (**Fig. 4-16**). Out of theses phlorotannins, the **17** showed significantly increased the cell viability, the cell survival rate were recorded as 50.47, 61.46, and 76.95% at 5, 50, and 100 μM, respectively. These results indicated that **17** have cytoprotective effect against oxidative stress induced by UV-B radiation. To clarify the protective effects of **17** against UV-B radiation, we used a UV absorption assay and UV-B protection test in a mouse model. As shown in **Fig. 4-17**, **17** absorbed a wide range of the UV region, specifically highlighting the absorption spectrum from 280 to

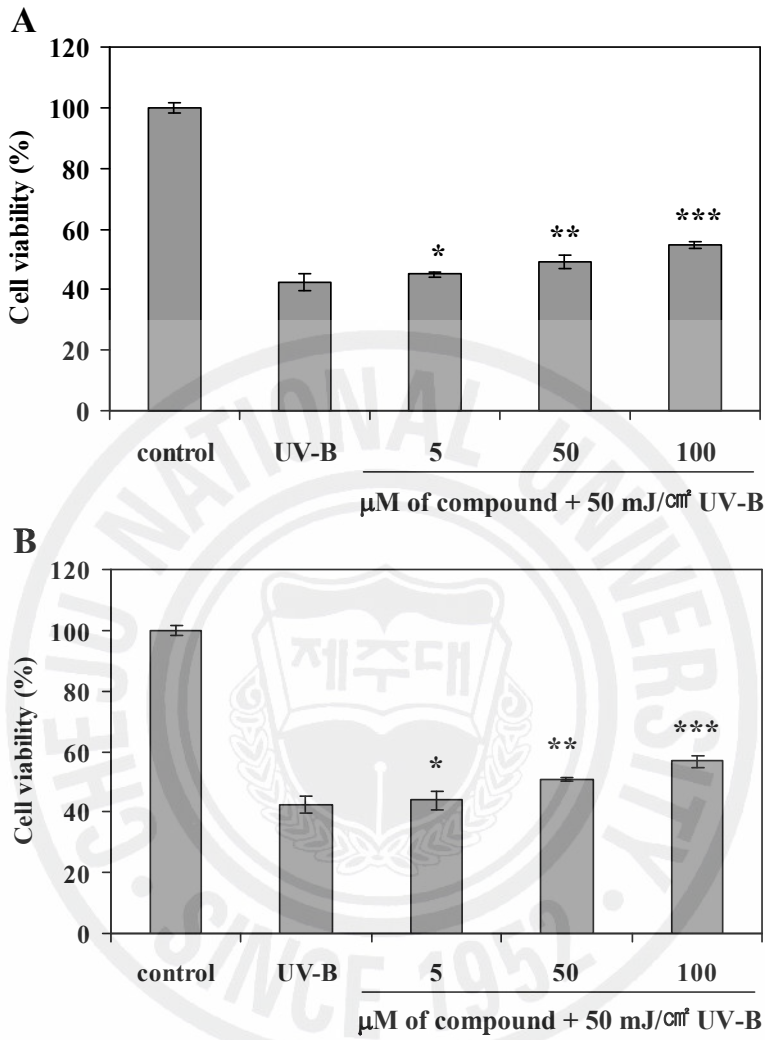

Fig. 4-16. Protective effect of the active compounds isolated from *E. cava* on UV-B radiation-induced cell damage of fibroblasts. The fibroblasts were treated with various concentrations of the active compounds and after 1h later, UV-B radiation at 50 mJ/cm^2 was applied to the cells. The viability of fibroblasts on UV-B radiation was determined by MTT assay. A, phloroglucinol; B, eckol; C, dieckol; D, triphlorethol A; E, eckstolonol. Experiments were performed in triplicate and the data are expressed as mean ± SE. Statistical evaluation was performed to compare the experimental groups and corresponding control groups. *, $p < 0.05$, **, $p < 0.005$, ***, $p < 0.001$

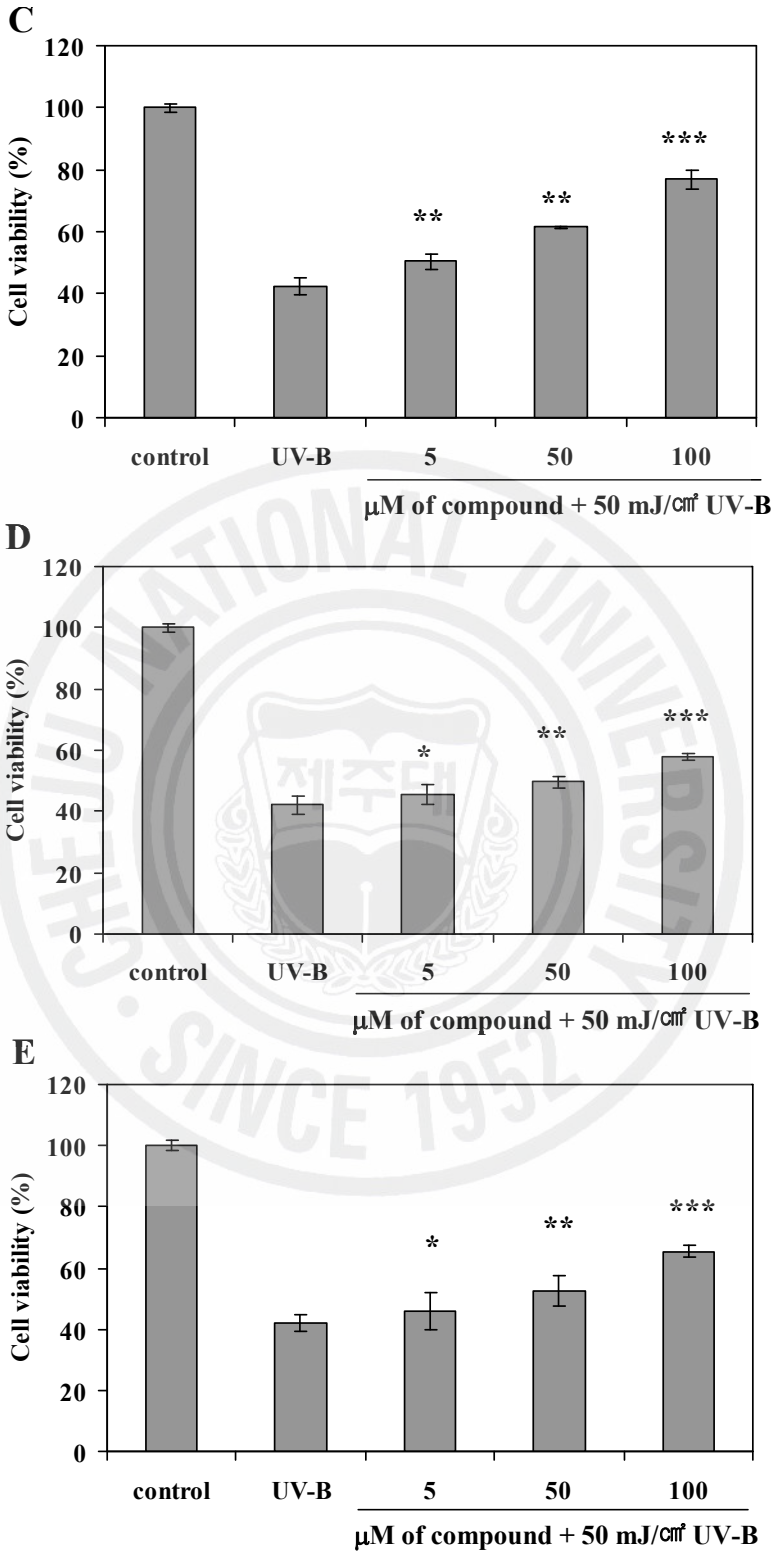

Fig. 4-16. Continued.

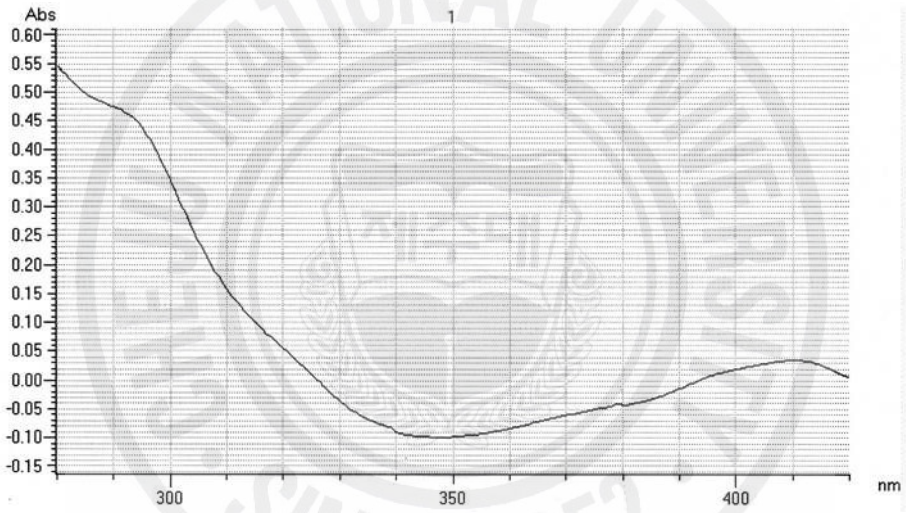

Fig. 4-17. UV absorption spectrum of dieckol isolated from *E. cava*.

320 nm, the UV-B region. This result indicates that **17** possessed potential protective effects against UV-B radiation. Thus, we applied *in vivo* tests to demonstrate the inhibitory effects for erythema and edema. The erythema production rate increased under the tested UV-B radiation intensity, and there were 41.06, 76.95, and 59.52% erythema inhibitory effect observed at 5, 10, and 15 J of radiations, respectively (**Fig.4-18A**). Edema was also examined in hairless mice (**Fig. 4-18B**). The skin expanded as a result of UV-B radiation exposure, but the expansion rate decreased slightly with the treatment of **17**.

Algae have evolved different avoidance mechanisms against oxidative stress and UV-B radiation. By transducing the light signal followed by altered gene expression, they result in synthesis of repair systems, such as UV-B absorbing pigments like flavonoid and related phenolic compounds. Phlorotannins are well known to marine algae polyphenols, which had various biological activities including antioxidant, antitumor, antihypertention, and anti-inflammatory effects. Among them, antioxidant activity related to UV protection is intensively focused due to the currently growing demand from the cosmeceutical industry where they are interested in anti-aging and whitening natural products. Dieckol (**17**), phenolic moiety, is a kind of phlorotannin which consists of six phloroglucinol units and functional hydroxyl groups. Recently studies have demonstrated that the protective effect against oxidative stress induced by ROS and UV radiation is correlated with the number and position of hydrogen- donating hydroxyl groups on the aromatic ring of the phonolic molecules, and is also affected by other factors, such as other H-donating groups (-NH, -SH), etc (Brand-Williams et al., 1995; Rice-Evans et al., 1996; Lien et al., 1999). This study demonstrated that **17** had not only antioxidant effect on oxidative stress but also protective effect against UV-B irradiation. These results indicated that **17** have more functional hydroxyl groups than the other

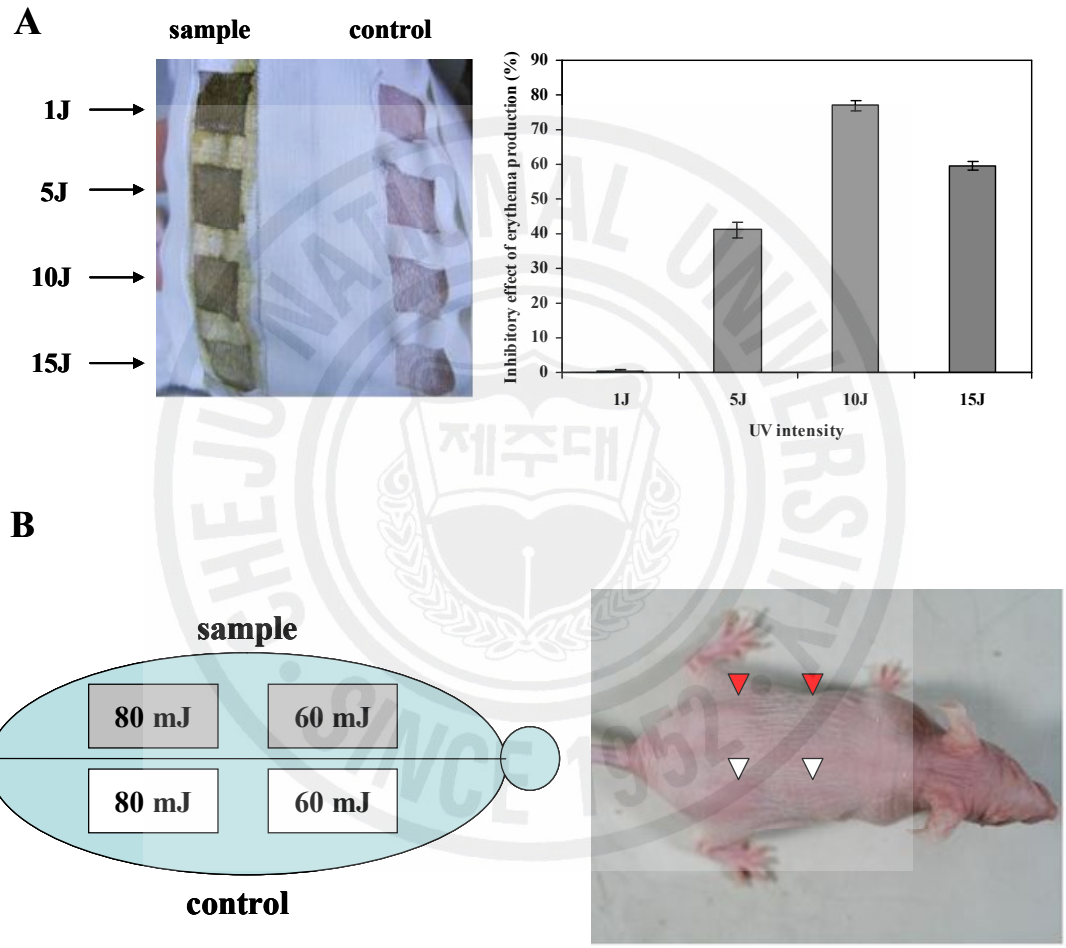

Fig. 4-18. Protective effect of dieckol isolated from *E. cava* on UV-B radiation-induced erythema (A) and edema (B).

tested phlorotannins, therefore, the **17** can easily to applied antioxidant and cosmeceutical industries as natural compound from marine biomass.

SUMMARY

As environmental pollution increases in developed countries, harmful skin damage is increasing by the ultra violet radiation that is emitted due to ozone layer destruction. Skin forms a remarkable protective barrier against the external environment, helping to regulate temperature and fluid balance, keeping out harmful microbes and chemicals, and offering some protection against sunlight. Melanin is the major pigment for color in human skin. It plays a critical role in the absorption of free radicals and melanogenesis in the skin in a kind of process that produces photoprotective agents against damaging UV effects. However, the overproduction of melanin induces serious skin problems including cancer and pigmentary disorders. Hence, many cosmetic and pharmaceutical companies have tried to find melanogenesis inhibitors and UV protection agents. Recently, several researchers have reported on antioxidants for the cosmetic industry, which has been using natural compounds in products. However, only select compounds can be applied in cosmetics.

Therefore, in this study, we investigated the antioxidant, whitening and UV protective effects of 40 kinds of marine algae, to develop natural functional cosmetic materials. Out of these marine algae, *Sargassum siliquastrum*, *Ishige okamurae*, and *Ecklonia cava* were selected as potential biomass from screening experiments, which included radical scavenging activity and tyrosinase inhibitory effects. *S. siliquastrum* presented 13 types of active compounds related to antioxidant activity. Among them, sargachromanols D, E, and G showed higher DPPH radical scavenging activity than a commercial antioxidant (ascorbic acid), while fucoxanthin exhibited profound effects on ROS and UV-induced cell damage. Diphlorethohydroxycarmalol was isolated from *I.*

okamurae, which showed strong antioxidant and whitening effects. Moreover, diphlorethohydroxycarmalol possessed protective effects against ROS and UV-induced cell damages. *E. cava* also contained active compounds related to antioxidant and whitening effects. Among them, dieckol exhibited profound activities in the performed experiments. From these investigations, dieckol showed strong antioxidant and whitening effects, as well as protective effects against UV radiation in both *in vitro* and *in vivo* experiments. Accordingly, dieckol could be used as functional cosmetic materials derived from natural marine product.

REFERENCES

Adebajo, M. O., Gesser, H. D. 2001. ESR study of alkyl radicals adsorbed on porous Vycor glass I. Build-up of methyl and ethyl radicals. *Appl. Surf. Sci.* **171:** 120-124.

Ahn, C. B., Jeon, Y. J., Kang, D. S., Shin, T. S., Jung, B. M. 2004. Free radical scavenging activity of enzymatic extracts from a brown seaweed *Scytosiphon lomentaria* by electron spin resonance spectrometry. *Food Res. Int.* **37:** 253-258.

Ahn, G. N., Kim, K. N., Cha, S. H., Song, C. B., Lee, J., Heo, M. S., Yeo, I. K., Lee, N. H., Jee, Y. H., Kim, J. S., Heu, M. S., Jeon, Y. J. 2007. Antioxidant activities of phlorotannins purified from *Ecklonia cava* on free radical scavenging using ESR and H_2O_2-mediated DNA damage. *Eur. Food Res. Technol.* **226:** 71-79.

Ananthaswamy, H. N., Kanjilal, S. 1996. Oncogenes and tumor suppressor genes in photocarcinogenesis. *Photochem. Photobiol.* **63:** 428-432.

Anderson, D., Yu, T. W., Mcgregor, D. B. 1998. Comet assay responses as indictors of carcinogen exposure. *Mutagenesis* **13:** 539-555.

Antonella, D. L., Vincenzo, M. 2003. Effectiveness of caffeic acid as an anti-oxidant for cod liver oil. *Int. J. Food Sci. Technol.* **38:** 475–480.

Argolo, A. C. C., Sant'Ana, A. E. G., Pletsch, M., Coelho, L. C. B. B. 2004. Antioxidant activity of leaf extracts from *Bauhinia monandra*. *Bioresource Technol.* **95:** 229-233.

Aruoma, O. I. 1998. Free radicals, oxidative stress, and antioxidants in human health and disease. *J. Am. Oil Chem. Soc.* **75:** 199-212.

Athukorala, Y., Jeon, Y. J. 2005. Screening for angiotensin 1-converting enzyme inhibitory activity of *Ecklonia cava*. *J. Food Sci. Nutr.* **10:** 134-139.

Aust, S. D., Chignell, C. F., Bray, T. M., Kalyanaraman, B., Mason, R. P., 1993. Free radicals in toxicology. *Toxicol. Appl. Pharm.* **120:** 168–178.

Bagchi, D., Bagchi, M., Stohs, S. J., Das, D. K., Ray, S. D., Kuszynski, C. A., Joshi, S. S., Pruess, H. G. 2000. Free radicals and grape seed proanthocyanidin extract: importance in human health and disease prevention. *Toxicology* **148:** 187-197.

Baurin, N., Arnoult, E., Scior, T., Do, Q. T., Bernard, P. 2002. Preliminary screening of some tropical plants for anti-tyrosinase activity. *J. Ethnopharmacol.* **82:** 155-158.

Betii, C., Davini, T., Giannessi, L., Loprieno, N., Barale, R. 1995. Comparative studies by comet test and SCE analysis in human lymphlcytes from 200 healthy subfects. *Mutat. Res.* **307:** 201-207.

Black, H. S., deGruijl, F. R., Forbes, P. D., Cleaver, J. E., Ananthaswamy, H. N., deFabo, E. C., Ullrich, S. E., Tyrrell, R. M. 1997. Photocarcinogenesis: an overview. *J. Photochem. Photobiol. B.* **40:** 29-47.

Blunt, J. W., Copp, B. R., Munro, M. H. G., Northcote, P. T., Prinsep, M. R. 2006. Marine natural products. *Nat. Prod. Rep.* **23:** 26-78.

Brand-Williams, W., Cuvelier, M. E., Berset, C. 1995. Use of a free radical method to evaluate antioxidant activity. *Lebensmwiss. A-Tchnol.* **28:** 25-30.

Cadet, J., Berger, M., Douki, T., Ravanat, J. L. Spinelli, S. 1997. Effects of UV and visible radiation on DNA final base damage. *Biol. Chem.* **378:** 1275-1286.

Castro, L., Freeman, B. A. 2001. Reactive oxygen species in human health and disease. *Nutrition* **170:** 161-165.

Choi, J. S., Lee, W. K., Cho, Y. J., Kim, D. S., Kim, A., Chung, H. Y., Jung, J. H., Im, K. S., Choi, W. C., Choi, H. D., Son, B. W. 2000. Bioactive carotenoids, Fucoxanthin as chemotaxonomic marker and antioxidative agent from the marine bacillariophycean microalga *Hantzschia marina*. *Nat. Prod. Sci.* **6:** 122-125.

Chung, S. K., Osawa, T., Kawakishi, S. 1997. Hydroxyl radical scavenging effects of spices and scavengers from Brown Mustard (*Brassica nigra*). *Biosci. Biotech. Bioch.* **61:** 118-123.

Dapkevicius, A., Venskutonis, R., van Beek, T. A., Linssen, J. P. H. 1998. Antioxidant activity of extracts obtained by different isolation procedures from some aromatic herbs grown in Lithuania. *J. Sci. Food Agric.* **77:** 140-146.

Dawes, C. J. 1998. Marine Botany. John Wiley & Sons, Inc., New York, p. 480.

Dooley, T. P. 1997. Topical skin depigmentation agents: current products and discovery of novel inhibitors of melanogenesis. *J. Dermatol. Treat.* **8:** 275-279.

Dorman, H. J., Kosar, M., Kahlos, K., Holm, Y., Hiltunen, R. 2003. Antioxidant properties and composition of aqueous extracts from Mentha species, hybrids, varieties and cultivars. *J. Agric. Food Chem.* **51:** 4563-4569.

Edwards, P. D., Bernstein, P. R. 1994. Synthetic inhibitors of elastase. *Med. Res. Rev.* **14:** 127-194.

Ekerot, L., Ohlsson, K. 1984. Interactions of granulocyte proteases with inhibitors in rheumatoid arthritis. *Adv. Exp. Med. Biol.* **167:** 335-344.

Emerit, I. 1992. Free radicals and aging of the skin. *EXS.* **62:** 328-341.

Farag, R. S., El-Baroty, G. S., Basuny, A. M. 2003. The influence of phenolic extracts obtained from the olive plant (cvs. Picual and Kronakii), on the stability of sunflower oil. *Int. J. Food Sci. Technol.* **38:** 81–87.

Finkel, T., Holbrook, N. J. 2000. Oxidants, oxidative stress and the biology of ageing. *Nature* **408:** 239-247.

Frlich, I., Riederer, P. 1995. Free radical mechanisms in dementia of Alzheimer type and the potential for antioxidative treatment. *Drug Res.* **45:** 443–449.

Fukuyama, Y., Kodama, M., Miura, I., Kinzyo, Z., Kido, M., Mori, H., Nakayama, Y.,

Takahashi, M. 1989. Structure of an anti-plasmin inhibitor, eckol, isolated from the brown alga *Ecklonia kurome* OKAMURA and inhibitory activities of its derivatives on plasma plasmin inhibitors. *Chem. Pharm. Bull.* **37:** 349-353.

Gange, R. W. 1988. Comparison of pigment responses in human skin to UVB and UVA radiation, In: Bagnara, J. T. (ed.). Advances in Pigment Cell Research. *Prog. Clin. Biol. Res.* Vol. 256, Alan R. Liss, New York, 475-485.

Gonzalez, M. C., Serrano, A., Zafra-Polo, M. C., Cores, D. 1995. Polycerasoidin and polycerasoidol, two new prenylated benzopyran derivatives from *Polyalthia cerasoides*. *J. Nat. Prod.* **58:** 1278-1284.

Gorinstein, S., Moncheva, S., Toledo, F., Arancibia-Avila, P., Trakhtenberg, S., Gorinstein, A., Goshev, I., Namiesnik, J. 2006. Relationship between seawater pollution and qualitative changes in the extracted proteins from mussels *Mytilus galloprovincialis*. *Sci. Total Environ.* **364:** 251-259.

Gschwind, M., Huber, G. 1995. Apoptotic cell death induced by β-amyloid 1-42 peptide is cell type dependent. *J. Neurochem.* **65:** 292-300.

Guarneri, B., Vaccaro, M., Moretti, G., Valenti, A., Guarneri, F., Morganti, P. 2000. Photoaging and free radicals: correlation between skin biochemical properties and plasmatic levels of skin oxidative species and antioxidant compounds. *J. Appl. Cosmetol.* **18:** 65-71.

Guo, Q., Zhao, B., Shen, S., Hou, J., Hu, J., Xin, W. 1999. ESR study on the structure-antioxidant activity relationship of tea catechins and their epimers. *Biochim. Biophy. Acta* **1427:** 13-23.

Halliwell, B., Gutteridge, J. M. C. 1999. Antioxidant defenses. In: Free radicals in biology and medicine, 3rd ed. pp. 105-159. Oxford Science Publications, Oxford, UK.

Haslam, E. 1989. Plant polyphenols: Vegetable tannins revisited. Cambridge, UK: Cambridge University Press.

Hearing, V. J. 2005. Biogenesis of pigment granules: a sensitive way to regulate melanocyte function. *J. Dermatol. Sci.* **37:** 3-14.

Heo, S. J., Cha, S. H., Lee, K. W., Jeon, Y. J. 2006. Antioxidant activities of red algae from Jeju Island. *Algae* **21:** 149-156.

Heo, S. J., Kim, J. P., Jung, W. K., Lee, N. H., Kang, H. S., Jun, E. M., Park, S. H., Kang, S. M., Lee, Y. J., Park, P. J., Jeon, Y. J. 2008. Identification of chemical structure and free radical scavenging activity of diphlorethohydroxycarmalol isolated from brown alga, *Ishige okamurae*. *J. Micobiol. Biotechnol.* In press.

Heo, S. J., Pak, E. J., Lee, K. W., Jeon, Y. J. 2005. Antioxidant activities of enzymatic extracts from brown seaweeds. *Bioresource Technol.* **96:** 1613-1623.

Heo, S. J., Park, P. J., Park, E. J., Kim, S. K., Jeon, Y. J. 2005. Antioxidant activity of enzymatic extracts from a brown seaweed *Ecklonia cava* by electron spin resonance spectrometry and comet assay. *Eur. Food Res. Technol.* **221:** 41-47.

Hiramoto, K., Johkoh, H., Sako, K. I., Kikugawa, K. 1993. DNA breaking activity of the carbon-centered radical generated from 2,2'-azobis(2-amidinopropane) hydrochloride (AAPH). *Free Radical Res. Commun.* **19:** 323-332.

Hosokawa, M., Kudo, M., Maeda, H., Kohno, H., Tanaka, T., Miyashita, K. 2004. Fucoxanthin induces apoptosis and enhances the antiproliferative effect on the PPARγ ligand, troglitazone, on colon cancer cells. *Biochim. Biophys. Acta* **1675:** 113-119.

Huang, X., Dai, J., Fournier, J., Ali, A. M., Zhang, Q., Frenkel, K. 2002. Ferrous ion autoxidation and its chelation in iron-loaded human liver HepG2 cells. *Free Radical Biol. Med.* **32:** 84-92.

Hwang, H., Chen, T., Nines, R. G., Shin, H. C., Stoner, G. D. 2006. Photochemopreventiion of UVB-induced skin carcinogenesis in SKH-1 mice by brown algae polyphenols. *Int. J. Cancer* **119:** 2742-2749.

Iwashima, M., Mori, J., Ting, X., Matsunaga, T., Hayashi, K., Shinoda, D., Saito, H., Sankawa, U., Hayashi, T. 2005. Antioxidant and antiviral activities of plastoquinones from the brown alga *Sargassum micracanthum*, and a new chromene derivative converted from the plastoquinones. *Biol. Pharm. Bull.* **28:** 374-377.

Jang, K. H., Lee, B. H., Choi, B. W., Lee, H. S., Shin, J. 2005. Chromenes from the brown alga *Sargassum siliquastrum*. *J. Nat. Prod.* **68:** 716-723.

Jensen, A. 1993. Present and future needs for alga and algal products. *Hydrobiology* **260/261:** 15-21.

Jones, K., Hughes, J., Hong, M., Jia, Q., Orndorff, S. 2002. Modulation of melanogenesis by aloesin: a competitive inhibitor of tyrosinase. *Pigement Cell Res.* **15:** 335-340.

Jorgensen, L. V., Madsen, H. L., Thomsen, M. K., Dragsted, L. O., Skibsted, L. H. 1999. Regulation of Phenolic antioxidants from phenoxyl radicals: An ESR and electrochemical study of antioxidant hierarchy. *Free Radical Res.* **30:** 207-220.

Juhlin, L. 1997. Hyaluronan in skin. *J. Int. Med.* **242:** 61-66.

Kang, H. S., Chung, H. Y., Jung, H. A., Son, B. W., Choi, J. S. 2003. A new phlorotannins from the brown alga *Ecklonia stolonifera*. *Chem. Pharm. Bull.* **51:** 1012–1014.

Kang, K. A., Lee, K. H., Chae, S., Zhang, R., Jung, M. S., Ham, Y. M., Baik, J. S., Lee, N. H., Hyun, J. W. 2006. Cytoprotective effect of phloroglucinol on oxidative stress induced cell damage via caltalase activation. *J. Cell. Biochem.* **97:** 609-620.

Kang, K. A., Lee, K. H., Chae, S., Zhang, R., Jung, M. S., Lee, Y., Kim, S. Y., Kim, H. S., Joo, H. G., Park, J. W., Ham, Y. M., Lee, N. H., Hyun, J. W. 2005. Eckol isolated from *Ecklonia cava* attenuates oxidative stress induced cell damage in lung fibroblast cells. *FEBS Lett.* **579:** 6295-6304.

Kang, K., Hwang, H. J., Hong, D. H., Park, Y., Kim, S. H., Lee, B. H., Shin, H. C. 2004. Antioxidant and anti-inflammatory activities of ventol, a phlorotannin-rich natural agent derived from *Ecklonia cava*, and its effect on proteoglycan degradation in cartilage explant culture. *Res. Commun. Mol. Pathol. Parmacol.* **115-116:** 77-95.

Kappus, H. 1991. Lipid peroxidation: mechanism and biological relevance. In: Free radicals and food additives, pp. 59-75. Taylor & Francis, London, UK.

Karawita, R., Siriwardhana, N., Lee, K. W., Heo, M. S., Yeo, I. K., Lee, Y. D., Jeon, Y. J. 2005. Reactive oxygen species scavenging, metal chelation, reducing power and lipid peroxidation inhibition properties of different solvent fractions from *Hizikia fusiformis*. *Eur. Food Res. Technol.* **220:** 363-371.

Kikuchi, T., Mori, Y., Yokoi, T., Nakazawa, S., Kuroda, H., Masada, Y., Kitamura, K., Kuriyama, K. 1983. Structure and absolute configuration of sargatriol, a new isoprenoid chromenol from a brown alga, *Sargassum tortile* C. Agardh. *Chem. Pharm. Bull.* **31:** 106-113.

Kim, J. A., Lee, J. M., Shin, D. B., Lee, N. H. 2004. The antioxidant activity and tyrosinase inhibitory activity of phloro-tannins in *Ecklonia cava*. *Food Sci. Biotechnol.* **13:** 476-480.

Kim, Y. J., Uyama, H. 2005. Tyrosinase inhibitors from natural and synthetic sources: structure, inhibition mechanism and perspective for the future. *Cell. Mol. Life Sci.* **62:** 1707-1723.

Kotake-Nara, E., Asai, A., Nagao, A. 2005. Neoxanthin and fucoxanthin induce

apoptosis in PC-3 human prostate cancer cells. *Cancer letters* **220:** 75-84.

Kuda, T., Tsunekawa, M., Goto, H., Araki, Y. 2005. Antioxidant properties of four edible algae harvested in the Noto Peninsula, Japan. *J. Food Comp. Anal.* **18:** 625-633.

Kusumi, T., Shibata, Y., Ishitsuka, M., Kinoshita, T., Kakisawa, H. 1979. Structures of new plastoquinones from the brown alga *Sargassum serratifolium*. *Chem. Lett.* **8:** 277-278.

Kvam, E., Tyrrell, R. M. 1997. Induction of oxidative DNA base damage in human skin cells by UV and near visible radiation. *Carcinogenesis* **18:** 2379-2384.

LeBel, C. P., Ischiopoulos, H., Bondy, S. C. 1992. Evaluation of the probe 2', 7'-dichlorofluorescin as an indicator of reactive oxygen species formation and oxidative stress. *Chem. Res. Toxicol.* **5:** 227-231.

Lee, J. H., Kim, N. D., Choi, J. S., Kim, Y. J., Heo, M. Y., Lim, S. Y. Park, K. Y. 1998. Inhibitory effects of the methanolic extract of an edible brown alga, *Ecklonia stolonifera* and its component, phloroglucinol on benzo(a)pyrene or N-methyl N-nitrosourea clastogenicity *in vitro* (Mouse micronucleus test). *Nat. Prod. Sci.* **4:** 105-114.

Lee, K. K., Choi, J. D. 1999. The effects of *Areca catechu* L extract on anti-inflammation and anti-melanogenesis. *Int. J. Cos. Sci.* **21:** 275-284.

Lee, S. K., Mbwambo, Z. H., Chung, H., Luyengi, L., Gamez, E. J., Mehta, R. G., Kinghorn, A. D., Pezzuto, J. M. 1998. Evaluation of the antioxidant potential of natural products. *Comb. Chem. High Throughput Screen.* **1:** 35-46.

Lewis, J. G., Stanley, N. F., Guist, G. G. 1988. In: Lembi, C. A., Waaland, J. R. (Eds.). Algae and Human Affairs. Cambridge University Press, New York, PP. 205-236.

Liaeen-Jensen, S. 1978. Marine carotenoids. In Marine Natural Products, *Chemical and*

Biochemical Perspective Vol. 2; Scheuer, P. J., Ed.; Academic Press: New York, pp. 1-73.

Liaeen-Jensen, S. 1998. Carotenoids in chemosystematics. In Carotenoids, Vol. 3, *Biosynthesis and Metabolism*; Britton, G., Liaaen-Jensen, S., Pfander, H., Eds.; Birkhauser: Basel, Switzerland, pp. 217-247.

Lien, E. J., Ren, S. J., Bui, H. Y. H., Wang, R. B. 1999. Quantitative structure-activity relationship analysis of phenolic antioxidants. *Free Radical Bio. Med.* **26:** 285-294.

Lizard, G., Fournel, S., Genestier, L., Dhedin, N., Chaput, C., Flacher, M., Mutin, M., Panaye G., Revillard, J. P. 1995. Kinetics of plasma membrane and mitochondrial alterations in the cells undergoing apoptosis. *Cytometry* **21:** 275-283.

Lopez-Torres, M., Thiele, J. J., Shindo, Y., Han, D., Packer, L. 1998. Topical application of alpha-tocopherol modulates the antioxidant network and diminishes ultrabiolet-induced oxidative damage in murine skin. *Br. J. Dermatol.* **138:** 207-215.

Lupo, M. P. 2001. Antioxidants and vitamins in cosmetics. *Clin. Dermatol.* **19:** 467-473.

Maeda, H., Hosokawa, M., Sashima, T. Funayama, K., Miyashita, K. 2005. Fucoxanthin from edible seaweed, *Undaria pinnatifida*, shows antiobesity effect through UCP1 expression in white adipose tissues. *Biochem. Biophys. Res. Commum.* **332:** 392-371.

Manuskiatti, W., Maibach, H. I. 1996. Hyaluronic acid and skin: wound healing and aging. *Int. J. Dermatol.* **35:** 539-544.

Maurya, D. K., Devasagayam, T. P. A., Nair, C. K. K. 2006. Some novel approaches for radioprotection and the beneficial effect of natural products. *Indian J. Exp. Biol.* **44:** 93-114.

May, G. S., Furberg, C. D., Eberlein, K. A., Barbara, J. G. 1983. Secondary prevention after myocardial infarction: a review of short-term acute phase trials. *Prog.*

Cardiovasc. Dis. **25:** 335-359.

Mayer, A. M. S., Hamann, M. T. 2004. Marine pharmacology in 2000: marine compounds with antibacterial, anticoagulant, antifungal, anti-inflammatory, antimalarial, antiplatelet, antiprotozoal, anti-tuberculosis, and antiviral activities; affecting the cardiovascular, immune and nervous systems and other miscellaneous mechanisms of action. *Mar. Biotechnol.* **6:** 37-52.

Mayer, A. M. S., Hamann, M. T. 2005. Marine pharmacology in 2001-2002: marine compounds with anthelmintic, antibacterial, anticoagulant, antidiabetic, antifungal, anti-inflammatory, antimalarial, antiplatelet, antiprotozoal, anti-tuberculosis, and antiviral activities; affecting the cardiovascular, immune and nervous systems and other miscellaneous mechanisms of action. *Comp. Biochem. Physiol. C.* **140:** 265-286.

Mori, J., Iwashima, M., Wakasugi, H., Saito, H., Matsunaga, T., Ogasawara, M., Takahashi, S., Suzuki, H., Hayashi, T. 2005. New plastoquinones isolated from the brown alga, *Sargassum micracanthum*. *Chem. Parm. Bull.* **53:** 1159-1163.

Mosmann, T. 1983. Rapid colorimetric assay for cellular growth and survival: application to proliferation and cytotoxicity assays. *J. Immunol. Methods* **65:** 55-63.

Müller, H. E. 1985. Detection of hydrogen peroxide produced by microorganism on ABTS-peroxidase medium. *Zentralbl Bakteriol. Mikrobio. Hyg.* **259:** 151-158.

Nagai, T., Yukimoto, T. 2003. Preparation and functional properties of beverages made from sea algae. *Food Chem.* **81:** 327-332.

Nagayama, K., Iwamura, Y., Shibata, T., Hirayama, I., Nakamura, T. 2002. Bactericidal activity of phlorotannins from the brown alga *Ecklonia kurome*. *J. Antimicrob. Chemother.* **50:** 889-893.

Nahas, R., Abatis, D., Anagnostopoulou, M. A., Kefalas, P., Vagias, C., Roussis, V. 2007.

Radical-scavenging activity of Aegean Sea marine algae. *Food Chem.* **102:** 577-581.

Naito, Y. 2002. Neutrophil-dependent oxidative stress in gastrointestinal inflammation. In: Yoshikawa, T. (Ed), Oxidative stress and digestive disease. Kager, Basel, pp. 24-40.

Nakagawa, T., Momohara, S., Fujita, K., Kodama, T., Yamada, H., Nagai, Y. 1995. Serine proteinase in articular cartilage, subchondral bone marrow and synovial fluid in human osteoarthritis and rheumatoid arthritis. *Biomed. Res.* **16:** 11-20.

Nakai, M., Kageyama, N., Nakahara, K., Miki, W. 2006. Phlorotannins as radical scavengers from the extract of *Sargassum ringgoldianum*. *Mar. Biotechnol.* **8:** 409-414.

Nanjo, F., Goto, K., Seto, R., Suzuki, M., Sakai, M., Hara, Y. 1996. Scavenging effects of tea catechins and their derivatives on 1,1-diphenyl-2-picrylydrazyl radical. *Free Radical Bio. Med.* **21:** 895-902.

Nishino, H. 1995. Cancer chemoprevention by natural carotenoids and their related compounds. *J. Cell. Biochem. Suppl.* **22:** 231-235.

Nishino, H. 1998. Cancer prevention by carotenoids. *Mutat. Res.* **402:** 159-163.

Nisizawa, K., Noda, H., Kikuchi, R., Watamaba, T. 1987. The main seaweed foods in Japan. *Hydrobiol.* **151/152:** 5–29.

Noda, H. 1993. Health benefits and nutritional properties of Nori. *J. Appl. Phycol.* **5:** 255-258.

Ohkatsu, Y., Matsuura, T., Yamato, M. 2003. A phenolic antioxidant trapping both alkyl and peroxy radicals. *Polym. Degrad. Stabil.* **81:** 151-156.

Okuzumi, J., Takahashi, T., Yamane, T., Kitao, Y., Inagake, M., Ohya, K., Nishino, H., Tanaka, Y. 1993. Inhibitory effects of fucoxanthin, a natural carotenoid, on *N*-

ethyl-*N*'-nitro-*N*-nitrosoguanidine-induced mouse duodenal carcinogenesis. *Cancer Lett.* **68:** 159-168.

Olive, P. L., Banath, J. P., Durand, R. E. 1990. Heterogeneity in radiation-induced DNA damage and repair in tumor and normal cells measured using the "Comet" assay. *Radiat. Res.* **122:** 86-94.

Oohusa, T. 1993. Recent trend in Nori products and market in Asia. *J. Appl. Phycol.* **5:** 155-159.

Palermo, J. A., Gros, E. G., Seldes, A. M. 1991. Carotenoids from three red algae of the Corallinaceae. *Phytochem.* **30:** 2983-2986.

Park, K. E., Kim, Y. A., Jung, H. A., Lee, H. J., Ahn, J. W., Lee, B. J., Seo, Y. 2004. Three norisoprenoids from the brown alga *Sargassum thunbergii*. *J. Kor. Chem. Soc.* **48:** 394-398.

Park, P. J., Heo, S. J., Park, E. J., Kim, S. K., Byun, H. G., Jeon, B. T., Jeon, Y. J. 2005. Reactive oxygen scavenging effect of enzymatic extracts from *Sargassum thunbergii*. *J. Agric. Food Chem.* **53:** 6666-6672.

Park, P. J., Shahidi, F., Jeon, Y. J. 2004. Antioxidant activities of enzymatic extracts from an edible seaweed *Sargassum horneri* using ESR spectrometry. *J Food Lipids* **11:** 15-27.

Pazdzioch-Czochra, M., Widenska, A. 2002. Spectrometric determination of hydrogen peroxide scavenging activity. *Anal. Chimica Acta* **452:** 177-184.

Pettit, G. R., Herald, C. L., Ode, R. H., Brown, P., Gust, D. J., Mechel, C. 1980. The isolation of loliolide from an Indian Ocean opisthobranch mollusk. *J. Nat. Prod.* **43:** 752-755.

Plaza, M., Cifuentes, A., Ibáñez, E. 2007. In the search of new functional food ingredients from algae. *Trends Food Sci. Tech.* In press.

Podda, M., Traber, M. G., Weber, C., Lan, L. J., Packer, L. 1992. UV-irradiation depletes antioxidants and causes oxidative damage in a model of human skin. *Photochem. Photobiol.* **56:** 357-363.

Polivka, T., Sundström, V. 2004. Ultrafast dynamics of carotenoid excited states-from solution to natural and artificial systems. *Chem. Rev.* **104:** 2021-2071.

Portanova, J. P., Zhang, Y., Anderson, G. D., Hauser, S. D., Masferrer, J. L., Seibert, K., Gregory, S. A., Isakson, P. C. 1996. Selective neutralization of prostaglandin E2 blocks inflammation, hyperalgesia and interleukin-6 production *in vivo*. *J. Exp. Med.* **184:** 883-891.

Potin, P., Bouarab, K., Kupper, F., Kloareg, B. 1999. Oligosaccharide recognition signals and defence reactions in marine plant-microbe interactions. *Curr. Poin. Microbiol.* **2:** 276-283.

Powers, J. C., Odake, S., Oleksyszyn, J., Hori, H., Ueda, T., Boduszek, B., Kam, C. M. 1993. Proteases – structures, mechanism and inhibitors. *Agents Actions Suppl.* **42:** 3-18.

Rao, A. V., Agarwal, S. 1998. Effect of diet and smoking on serum lycopene and lipid peroxidation. *Nurt. Res.* **18:** 713-721.

Re, R., Pellegrini, N., Proteggente, A., Pannala, A., Yang, M., Rice-Evans, C. 1999. Antioxidant activity applying an improved ABTS radical cation decolorization assay. *Free Rad. Biol. Med.* **26:** 1231-1237.

Rice-Evans, C. A., Miller, N. J., Paganga, G. 1996. Structure-antioxidant activity relationships of flavonoids and phenolic acids. *Free Radical Bio. Med.* **20:** 933-956.

Rice-Evans, C. A., Muller, N. J., Bolwell, P. G., BramLey, P. M., Pridham, J. B. 1995. The relative antioxidant activities of plant-derived polyphenolic flavonoids. *Free Radical Res.* **22:** 375-383.

Ricketts, E., Calvin, J. 1962. *Between pacific tides*. 3rd et. Revised by Hedgpeth, J. Stanford, California: Stanford University Press. Smith, G. M. 1944. *Marine algae of the monterey peninsula*. Stanford, California: Stanford University Press.

Rittié, L., Fisher, G. J. 2002. UV-light-induced signal cascades and skin aging. *Ageing Res. Rev.* **1:** 705-720.

Rosen, G. M., Rauckman, E. J. 1984. Spin trapping of superoxide and hydroxyl radicals. In L. Packer (Ed.), Methods in enzymology. Orlando, FL: Academic Press; pp. 198-209.

Ruberto, G., Baratta, M. T., Biondi, D. M., Amico, V. 2001. Antioxidant activity of extracts of the marine algal genus Cystoseira in a micellar model system. *J. Appl. Phycol.* **13:** 403-407.

Sánchez-Ferrer, A., Rodríguez-López, J. N., García-Cánovas, F., García-Carmona, F. 1995. Tyrosinase: a comprehensive review of its mechanism. *Biochim. Biophys. Acta* **1247:** 1-11.

Santos, M. S., Gaziano, J., Leka, L. S., Bertha, A. A., Hennekens, C. H., Meydani, S. N. 1998. β-Carotene-induced enhancement of natural killer cell activity in elderly men: an investigation on the role of citokines. *Am. J. Nutr.* **68:** 164-170.

Sato, A., Shindo, T., Kasanuki, N., Hasegawa, K. 1989. Antioxidant metabolites from the tunicate *Amaroucium multiplicatum*. *J. Nat. Prod.* **52:** 975-981.

Scharffetter-Kochanek, K., Wlaschek, M., Brenneisen, P., Schauen, M., Blaudschun, R., Wenk, F. 1997. UV-induced reactive oxygen species in photo-carcinogenesis and photoaging. *Biol. Chem.* **378:** 1247-1257.

Schwarz, K., Bertelsen, G., Nissen, L. R., Gardner, P. T., Heinonen, M. I., Hopia, A., Huynh-Ba, T., Lambelet, P., McPhail, D., Skibsted, L. H., Tijburg, L. 2001. Investigation of plant extracts for the protection of processed foods against lipid

oxidation. Comparison of antioxidant assays based on radical scavenging. Lipid oxidation and analysis of the principal antioxidant compounds. *Eur. Food Res. Technol.* **212:** 319–328.

Senthilmohan, S. T., Zhang, J., Stanley, R. A. 2003. Effects of flavonoid extract enzogenol with vitamin C on protein oxidation and DNA damage in older human subfects. *Nutr. Res.* **23:** 1999-1210.

Seo, S. Y., Sharma, V. K., Sharma, N. 2003. Mushroom tyrosinase: recent prospects. *J. Agric. Food Chem.* **51:** 2837-2853.

Shapiro, S. D. 2002. Proteinases in chronic obstructive pulmonary disease. *Biochem. Soc. Trans.* **30:** 98-102.

Shibata, T., Fujimoto, K., Nagayama, K., Yamaguchi, K., Nakamura, T. 2002. Inhibitory activity of brown algal phlorotannins against hyaluronidase. *Int. J. Food. Sci. Technol.* **37:** 703-709.

Shimidzu, N., Goto, M., Miki, W. 1996. Carotenoid as singlet oxygen quenchers in marine organisms. *Fish. Sci.* **62:** 134-137.

Singh, I. P., Bharate, S. B. 2006. Phloroglucinol compounds of natural origin. *Nat. Prod. Rep.* **23:** 558-591.

Singh, N. P. 2000. Microgels for estimation of DNA strand breaks, DNA protein cross links and apoptosis. *Mutat. Res.* **455:** 111-127.

Singh, N. P., Graham, M. M., Singh, V., Khan, A. 1995. Induction of DNA single-strand breaks in human lymphocytes by low doses of γ-rays. *Int. Radiat. Biol.* **68:** 563-569.

Skjak-Braek, G., Martinsen, A. 1991. In: Guiry, M. D., Blunden, G. (Eds.). Seaweed Resources in Europe: Uses and Potential. John Wiley & Sons, pp. 219-256.

Smit, A. J. 2004. Medicinal and pharmaceutical uses of seaweed natural products: a

review. *J. Appl. Phycol.* **16:** 245-262.

Solomons, N. W., Bulux, J. 1994. Plant sources of pro-vitamin A and human nutriture. *Nutr. Rev.* **51:** 199-204.

Sørensen, M., Jensen, B. R., Poulsen, H. E., Deng, X., Tygstrup, N., Dalhoff, K., Loft, S. 2001. Effects of a Brussels sprouts extract on oxidative DNA damage and metabolishing enzymes in rat liver. *Food Chem. Toxicol.* **39:** 533-540.

Stohs, S. J. 1995. The role of free radicals in toxicity and disease. *J. Basic Clin. Physiol. Pharm.* **6:** 205–228.

Sugiura, Y., Matsuda, K., Yamada, Y., Nishikawa, M., Shioya, K., Katsuzaki, H., Imai, K., Amano, H. 2006. Isolation of a new anti-allergic phlorotannin, phlorofucofuroeckol-B, from an edible brown alga, *Eisenia arborea*. *Biosci. Biotechnol. Biochem.* **70:** 2807-2811.

Tang, S., Sheehan, D., Buckely, D. J., Morrissey, P. A., Kerry, J. P. 2001. Anti-oxidant activity of added tea catechins on lipid oxidation of raw minced red meat, poultry and fish muscle. *Int. J. Food Sci. Technol.* **36:** 685–692.

Tepe, B, Sokmen, A. 2007. Screening of the antioxidative properties and total phenolic contents of three endemic Tanacetum subspecies from Turkish flora. *Bioresource Technol.* **98:** 3076-3079.

Thiele, J. J., Podda, M., Packer, L. 1997. Tropospheric ozone and emerging environmental stress to skin. *Biol. Chem.* **378:** 1299-1305.

Tranggono, R. I. S. 2000. The influence of SPA products treatment for skin-care. *J. Appl. Cosmetol.* **18:** 177-184.

Tsuboi, T., Kondoh, H., Hiratsuka, J., Mishima, Y. 1998. Enhanced melanogenesis induced by tyrosinase gene-transfer increases boron-uptake and killing effect of boron neutron capture therapy for amelanotic melanoma. *Pigm.Cell Res.* **11:** 275-

282.

Tsuchiya, N., Sato, A., Haruyama, H., Watanabe, T., Iijima, Y. 1998. Nahocols and isonahocols, endothelin antagonists from the brown alga, *Sargassum autumnale*. *Phycochem.* **48:** 1003-1011.

Vanni, A., Gastaldi, D., Giunata, G. 1990. Kinetic investigations on the double enzymatic activity of the tyrosinase mushroom. *Annali. di Chimica.* **80:** 35-60.

Velioglu, Y. S., Mazza, G., Gao, L., Oomah, B. D. 1998. Antioxidant activity and total phenolic in selected fruits, vegetables and grain products. *J. Agric. Food Chem.* **46:** 4113-4117.

Wang, G., Chen, K., Chen, L., Hu, C., Zhang, D., Liu, Y. 2007. The involvement of the antioxidant system in protection of desert cyanobacterium *Nostoc* sp. against UV-B radiation and the effects of exogenous antioxidant. *Ecotox. Environ. Safe.* In press.

Watts, R. J., Bottenberg, B. C., Hess, T. F., Jensen, M. D., Teel, A. L. 1999. Role of reductants in the enhanced desorption and transformation of chloroaliphatic compounds by modified Fenton's reactions. *Environ. Sci. Technol.* **33:** 3432-3437.

Wei, H., Zhang, X., Zhao, J. F., Wang, Z. Y., Bickers, D., Lebwohl, M. 1999. Scavenging of hydrogen peroxide and inhibition of ultraviolet light-induced oxidative DNA damage by aqueous extracts from green and black teas. *Free Radic. Biol. Med.* **26:** 1427-1435.

Wiedow, O., Schröder, J. M., Gregory, H., Young, J. A., Christophers, E. 1990. Elafin: an elastase-specific inhibitor of human skin. Purification, characterization, and complete amino acid sequence. *J. Biol. Chem.* **265:** 14791-14795.

Wu, J. J., Dutson, T. R., Carpenter, Z. L. 1981. Effect of post-mortem time and temperature on the release of lysosomal enzymes and their possible effects on bovine connective tissue components of the muscle. *J. Food Sci.* **46:** 1132-1135.

Yan, X., Chuda, Y., Suzuki, M., Nagata, T. 1999. Fucoxanthin as the major antioxidant in *Hijikia fusiformis*, a common edible seaweed. *Biosci. Biotechnol. Biochem.* **63:** 605-607.

Yan, X., Li, X., Zhou, C., Fan, X. 1996. Prevention of fish oil rancidity by phlorotannins from *Sargassum kjellmanianum*. *J. Appl. Phycol.* **8:** 201-203.

Yan, Z. Y., Guon, G. X., Zhang, W. Q., Lin, Z. F. 1994. Elastolytic activity from *Flavobacterium odoratum*. Microbial screening and cultivation, enzyme production and purification. *Process Biochem.* **29:** 427-436.

Yuan, Y. V., Bone, D. E., Carrington, M. F. 2005. Antioxdant activity of dulse (*Palmaria palmata*) extract evaluated in vitro. *Food Chem.* **91:** 485-494.

Zhang, L., Yu, H., Sun, Y., Lin, X., Bhen, B., Tan, C., Cao, G., Wang, Z. 2007. Protective effects of salidroside on hydrogen peroxide-induced apoptosis in SH-SY5Y human neuroblastoma cells. *Eur. J. Pharmacol.* **564:** 18-25.

Zhou, K., Laux, J. J., Yu, L. 2004. Comparison of Swiss red wheat grain and fractions for their antioxidant properties. *J. Agric. Food Chem.* **52:** 1118-1123.

Zhu, Q. Y., Hackman, R. M., Ensunsa, J. L., Holt, R. R., Keen, C. L. 2002. Antioxidative activities of oolong tea. *J. Agric. Food Chem.* **50:** 6929-6934.

ACKNOWLEDGEMENT

작은 씨앗으로부터 대지를 푸르게 수놓을 생명들이 탄생하듯 작지만 꾸준한 내 노력의 결실이 드디어 박사학위논문이라는 결과물로서 이렇게 놓여지게 되었습니다. 이것은 결코 나 혼자만의 노력이 아닌 많은 분들의 도움으로 이루어낸 산물이기에 이 자리를 빌어 감사의 말씀을 드리고자 합니다. 먼저 수 많은 시간 동안 험난한 시련과 장애물이 내 앞을 가로막을 때마다 스승이자 인생의 선배로서 격려와 조언을 아끼지 않으시고 내 삶의 방향을 바로 잡아주신 전유진 교수님께 진심으로 감사 드립니다. 또한 바쁘신 가운데서도 논문의 틀을 바로 잡아주시고 심사를 해 주신 이기완 교수님, 김수현 교수님, 이제희 교수님, 지영흔 교수님과 끊임없는 관심으로 좋은 논문을 쓸 수 있게 채찍질 해 주신 송춘복 교수님, 허문수 교수님, 여인규 교수님, 하진환교수님께 진심으로 감사 드립니다.

1년 이라는 연수기간 동안 새로운 분야에 도전하는 저에게 많은 배움을 주시고 새로운 깨달음을 주신 한국생명공학연구원 유익동 박사님, 김종평 박사님, 윤봉식 박사님, 이인경 박사님, 김영숙 박사님께 감사 드리고, 세세한 부분까지 관심을 갖고 연구실 생활과 실험을 할 수 있게 도와준 강학수, 박순혜, 전은미, 유남희, 정진영, 장윤우, 허진우, 류인자 선생님, 김영희 선생님, 추수진, 조성민 등 모든 대사체 기능연구센터 구성원들에게도 고마운 마음을 전합니다.

또한 가장 가까이에서 서로에게 힘을 북돋아주며 든든한 버팀목이 되어 주었던 해양생물자원이용공학연구실 김원석 선배님, 양현필 선배님, 김길남, 차선희, 안긴내, 이승홍, 강성명, 고석천, 신우석, 한선영, 김아름다슬, Rona, Yasantha, Mahinda, 관련 실험에 큰 도움을 주셨던 정민호 교수님, 인생의

선배로서 많은 조언과 도움을 주신 정원교 선배님, 진창남 선배님, 강도형 선배님, 박경일 선배님, 강상균 선배님, 양병규 선배님, 이치훈 선배님, 강현실 후배님, 내가 기쁠 때나 슬플 때나 항상 믿음을 갖고 나를 지켜봐 준 나의 친우 오영빈, 문영건, 오철홍, 양문휴, 고범석, 현인석, 김태윤, 한우진, 김경찬, 강영란, 김지연, 때론 친구처럼 때론 동생처럼 나에게 용기를 주던 김만철, 오상규 후배님들께도 깊은 감사를 드립니다.

그리고 오늘의 제가 있기까지 지극한 사랑과 보살핌으로 한 남자로서 우뚝 서게 도와주신 사랑하는 부모님과, 추운 날도 마다 않으시고 절에 다니시면서 사위 잘되라고 불공도 들여주시고 항상 정진하라는 좋은 말을 아끼시지 않는 장인어른과 장모님, 하나밖에 없는 든든한 동생 수용이, 그리고 나를 믿고 도와주신 모든 가족들에게도 감사의 마음을 전합니다.

마지막으로 항상 나의 곁에서 힘들 때 다독여주고, 기쁠 때 더 기뻐해 주면서 나에게 용기를 주고, 연구에 몰두할 수 있도록 헌신의 사랑을 주는 사랑하는 나의 아내 강지연에게 고맙다는 말과 함께 진심 어린 사랑을 드립니다.